

When do spectral gradient updates help in deep learning?

Damek Davis*

Dmitriy Drusvyatskiy†

Abstract

Spectral gradient methods, such as the recently popularized Muon optimizer, are a promising alternative to standard Euclidean gradient descent for training deep neural networks and transformers, but it is still unclear in which regimes they are expected to perform better. We propose a simple layerwise condition that predicts when a spectral update yields a larger decrease in the loss than a Euclidean gradient step. This condition compares, for each parameter block, the squared nuclear-to-Frobenius ratio of the gradient to the stable rank of the incoming activations. To understand when this condition may be satisfied, we first prove that post-activation matrices have low stable rank at Gaussian initialization in random feature regression, feedforward networks, and transformer blocks. In spiked random feature models we then show that, after a short burn-in, the Euclidean gradient’s nuclear-to-Frobenius ratio grows with the data dimension while the stable rank of the activations remains bounded, so the predicted advantage of spectral updates scales with dimension. We validate these predictions in synthetic regression experiments and in NanoGPT-scale language model training, where we find that intermediate activations have low-stable-rank throughout training and the corresponding gradients maintain large nuclear-to-Frobenius ratios. Together, these results identify conditions for spectral gradient methods, such as Muon, to be effective in training deep networks and transformers.

1 Introduction

Modern deep neural networks are almost always trained with first-order methods, most prominently stochastic gradient descent (SGD) and its adaptive variants such as **Adam** [32], **RMSprop** [51], and **AdaGrad** [16]. These algorithms can be viewed as Euclidean gradient descent equipped with inexpensive preconditioners, typically diagonal rescalings or structured approximations such as Kronecker-factored schemes (**K-FAC** [38], **Shampoo** [19]). Despite differences in their per-iteration cost, they share a common design principle: one follows the Euclidean gradient that is adjusted by a preconditioner derived from past gradients or curvature information. A complementary line of work takes a different viewpoint and modifies the *geometry* of the update itself by operating on the spectrum of layerwise gradient matrices. The spectral gradient descent method (**SpecGD** [9]) replaces the raw gradient with its polar factor, thus moving in a direction with the same singular vectors but unit singular values and step length given by the nuclear norm. The recently proposed optimizer **MUON** [28] implements a momentum-based variant of this spectral update, and has been observed to match or surpass variants of **Adam** [32] in large-language-model pretraining. Motivated by these empirical findings, we ask the following question.

*Department of Statistics and Data Science, The Wharton School, University of Pennsylvania; www.damekdavis.com. Research of Davis supported by NSF DMS award 2047637.

†Halıcıoğlu Data Science Institute (HDSI), University of California San Diego, La Jolla, CA, sites.google.com/view/dmitriy-drusvyatskiy. Research of Drusvyatskiy was supported by NSF DMS-2306322, NSF DMS-2023166, and AFOSR FA9550-24-1-0092 awards.

In what regimes should one expect spectral updates to outperform standard Euclidean gradient methods for training deep neural networks and transformers?

The explanation we propose is based on a simple but prevalent structural property of the post-activation matrices. We show experimentally and theoretically that the *post-activation matrices in intermediate layers of deep neural networks tend to have stable rank bounded by a small numerical constant that is independent of the ambient dimension*. This low stable rank reflects a strong degeneracy of the learned representations and, in particular, implies an ill-conditioned optimization landscape when viewed through the Euclidean lens. Spectral updates, such as **SpecGD**, which align with the singular vector directions and depend only on spectral and nuclear norms, are naturally adapted to this regime. We make this precise in a sequence of toy and semi-realistic settings, where the advantage of spectral over Euclidean updates can be quantified directly in terms of the stable rank of post-activation matrices. Our goal is not to analyze MUON in all of its practical details, but rather to understand why its underlying spectral update rule is well suited to the low-stable-rank structure that arises when training modern neural networks.

At a technical level, our results are organized around a one-step comparison of Euclidean and spectral updates acting on a single matrix block. Let W be any matrix parameter that multiplies an incoming activation matrix A (for example, a layer weight acting on the post-activations from the previous layer), and let $G = \nabla_W \mathcal{L}(W)$ denote the corresponding block of the gradient. A simple argument (carried out in Section 1.2 and extended in Section 1.2.1) shows that for a variety of models (random features, MLPs, and transformers) the guaranteed decrease in the loss after one Euclidean gradient step and one spectral step can be bounded as

$$\Delta_{\text{GD}} \asymp \frac{\|G\|_F^2}{\|A\|_{\text{op}}^2} \quad \text{and} \quad \Delta_{\text{Spec}} \asymp \frac{\|G\|_*^2}{\|A\|_F^2}.$$

Therefore, spectral descent is favored whenever

$$\frac{\|G\|_*^2}{\|G\|_F^2} \geq \frac{\|A\|_F^2}{\|A\|_{\text{op}}^2}. \quad (1.1)$$

The right-hand side is precisely the stable rank $\text{st}(A) := \|A\|_F^2/\|A\|_{\text{op}}^2$ of the incoming features, while the left-hand side measures how spread out the singular values of the gradient are; we will refer to this ratio as the *nuclear rank* of G and denote it by

$$\text{nr}(G) := \frac{\|G\|_*^2}{\|G\|_F^2}.$$

In terms of these quantities, the ratio of the one-step descent guarantees is $\frac{\Delta_{\text{Spec}}}{\Delta_{\text{GD}}} \asymp \frac{\text{nr}(G)}{\text{st}(A)}$. In particular, when $\text{st}(A)$ is $O(1)$ and $\text{nr}(G)$ grows with the dimension—as we prove in random-feature models after a short-burn-in and observe empirically in realistic networks—the predicted speedup of spectral over Euclidean updates is itself dimension-dependent (and in our examples linear in d), matching the large early-time advantage we see for spectral methods in practice.

In a multilayer network, the parameters naturally decompose into matrix blocks W_ℓ with gradients G_ℓ that interact with post-activations $A_{\ell-1}$. The same one-step comparison then yields a *layerwise* condition

$$\text{nr}(G_\ell) \geq \text{st}(A_{\ell-1}), \quad (1.2)$$

which identifies when a blockwise spectral update on W_ℓ is favored over a Euclidean one. For standard MLPs, $A_{\ell-1}$ is simply the usual post-activation of the previous layer, so the inequality

compares a gradient-based quantity $\text{nr}(G_\ell)$ to the stable rank of the propagated data seen by that layer. In Section 1.2.1 we show that the same blockwise condition continues to hold for a broad class of layered architectures, including transformers. In that setting, the relevant $A_{\ell-1}$ is the normalized or MLP activation feeding each projection (for example the RMS-normalized hidden states entering W_Q, W_K, W_V , or the MLP post-activations entering W_2). The upshot is a simple rule of thumb: spectral updates are most advantageous on those blocks whose incoming features have low-stable-rank and whose gradients have large nuclear rank $\text{nr}(G_\ell)$.¹

Beyond this one-step picture, we also show that the nuclear-rank advantage of spectral updates is not a purely transient phenomenon. In spiked random-feature regression models, the gradient nuclear rank becomes large after a short burn-in period and then remains high along a macroscopic window of gradient-descent iterations. More precisely, in both realizable and teacher-student variants we prove that after a short $O(\log d)$ burn-in period there is a window of $\Theta(d)$ iterations on which $\text{nr}(\nabla \mathcal{L}(W_t)) = \Omega(d)$ and, for any fixed $\varepsilon > 0$, a longer window of $\Theta(d \log d)$ iterations on which $\text{nr}(\nabla \mathcal{L}(W_t)) \geq d^{1-\varepsilon}$ (Theorem 6.6 and Corollary 6.12). In the same models, Euclidean gradient descent needs $\Theta(d \log(d/\delta))$ steps to reach relative error $\delta \in (0, 1)$, so for any fixed target accuracy this $\Theta(d \log d)$ window represents a constant fraction of the training time. Thus, if we were to restart a spectral method such as `SpecGD` or `MUON` from any point in this window, its one-step improvement over Euclidean gradient descent would itself be dimension-dependent.

The rest of this introductory section describes our results in more detail. The reader may find code to reproduce our experiments at <https://github.com/damek/specgd/>.

1.1 Post-activation matrices have low-stable rank.

The layerwise criterion (1.2) compares the gradient nuclear rank $\text{nr}(G_\ell)$ to the stable rank of the incoming activations. To understand when this criterion is activated in realistic architectures, we need structural control on the matrices that propagate through the network. Our main conclusion is that, at Gaussian initialization, the matrices feeding the internal (two-dimensional) weight blocks of standard MLPs and decoder-only transformers typically have stable rank bounded by a small numerical constant, independent of width and (for transformers) sequence length. The argument has the following two components:

- (i) two base cases explaining how low-stable-rank representations arise in the first place, namely through (a) mean-induced spikes and (b) token-indicator/embedding structure;
- (ii) a propagation calculus showing how the stable rank evolves as data propagates through standard network blocks.

(1a) Mean-spike inducing activations. Call a pointwise activation σ *mean-spike inducing* (MSI) if, for a Gaussian input $\gamma \sim \mathcal{N}(0, 1)$, the mean is nonzero and the second moment is finite:

$$m_1 := \mathbb{E}[\sigma(\gamma)] \neq 0 \quad \text{and} \quad m_2 := \mathbb{E}[\sigma(\gamma)^2] < \infty.$$

This property is generic for non-centered activations used in practice (e.g. ReLU). Our first main theorem (Theorem 2.6) shows that, for any fixed input matrix X and Gaussian weights W , the post-activation matrix $A = \sigma(WX)$ has stable rank controlled by the one-dimensional moment ratio m_2/m_1^2 up to a slack $(1 \pm \varepsilon)$. For the concrete example of ReLU this ratio is π .

¹Similar gradient nuclear ranks also appear implicitly or explicitly in convergence analyses of spectral optimizers such as `MUON` and `Scion` [42, 47]; our focus here is to relate this ratio to the *stable rank of the propagated data* and to show that the resulting inequality is naturally activated in realistic networks.

Why does a nonzero mean force a spectral spike? To see this, let $a_1^\top, \dots, a_k^\top \in \mathbf{R}^n$ denote the rows of the post-activation matrix $A \in \mathbf{R}^{k \times n}$. It is straightforward to see that the row Gram matrix trivially satisfies

$$\frac{1}{d} A^\top A \succeq \bar{a} \bar{a}^\top,$$

where $\bar{a} := \frac{1}{d} \sum_{i=1}^k a_i$ is the row mean. Thus, we obtain the estimate

$$\text{st}(A) = \frac{\|A\|_F^2}{\|A\|_{\text{op}}^2} \leq \frac{(1/d)\|A\|_F^2}{\|\bar{a}\|_2^2}.$$

We later show that the numerator and denominator separately concentrate, so we may bound the ratio by the population counterpart. Writing x_t for the t 'th column of X and $w \sim \mathcal{N}(0, I)$, the population counterparts are

$$\mathbb{E}\left[\frac{1}{k}\|A\|_F^2\right] = \sum_{t=1}^n \mathbb{E}[\sigma(\langle w, x_t \rangle)^2] \quad \text{and} \quad \mathbb{E}\|\bar{a}\|_2^2 = \sum_{t=1}^n \mathbb{E}[\sigma(\langle w, x_t \rangle)]^2.$$

For p -homogeneous σ , we have $\mathbb{E}[\sigma(\langle w, x_t \rangle)] = m_1 \|x_t\|_2^p$ and $\mathbb{E}[\sigma(\langle w, x_t \rangle)^2] = m_2 \|x_t\|_2^{2p}$, so the ratio above simplifies to m_2/m_1^2 . A slightly more involved arguments yield a similar conclusion for all the common non-homogeneous and non-centered functions used in practice (Theorem 2.6). Iterating this one-layer statement yields an $O(1)$ stable-rank bound for *every* hidden-layer post-activation matrix in an MLP with an MSI activation function at Gaussian initialization (Corollary 4.1).

(1b) Token-indicator matrices as a pervasive low-stable-rank input. For transformers, low stable rank already appears at the input. Let $H \in \mathbf{R}^{V \times n}$ be the token-indicator matrix for a length- n token sequence: the t 'th column is the one-hot vector for token i_t . Writing p_{\max} for the empirical frequency of the most common token in the sequence, a direct calculation gives

$$\text{st}(H) = \frac{1}{p_{\max}},$$

so the stable rank of the token-indicator matrix is the inverse frequency of the most common token. In natural language corpora, token frequencies are heavy-tailed (Zipf-type behavior), so p_{\max} is not extremely small and $\text{st}(H)$ is modest. Section 2.3 shows that a Gaussian embedding layer maps this indicator structure to an embedding matrix whose stable rank is controlled (up to constants) by the same p_{\max} , and combining this base case with the propagation rules in part (2) below yields width- and sequence-length-independent stable-rank bounds for the RMS-normalized hidden states and MLP activations throughout a randomly initialized transformer (see Corollary 5.2). As an illustration, Figure 10 tracks, in a NanoGPT training run, the stable rank of the token-indicator matrix and of the embedding activations throughout training.

(2) Stable-rank propagation through network blocks. The base cases (1a) and (1b) above explain why low-stable-rank structure can arise either from the activation nonlinearity (mean spikes) or from the input representation (token indicators/embeddings). To pass from these base cases to full architectures—especially transformers, where each block contains normalization, attention mixing, residual updates, and (possibly gated) MLPs—we develop a “calculus” showing that stable rank remains small as the data is propagated through standard building blocks. These results are proved in Section 3; Table 1 informally summarizes the form of the bounds that we obtain. In particular, at Gaussian initialization these rules show that the stable rank of the representations entering each internal weight block is controlled by the stable rank of the upstream representation, rather than inflating with width or sequence length.

Block	Stable rank	Assumptions
Linear map	$\text{st}(WX) \lesssim \text{st}(X)$	—
Pointwise nonlinearity	$\text{st}(\sigma(WX)) \lesssim \text{st}(X)$	$ \mathbb{E}\sigma'(g) > 0$
Residual connection	$\text{st}(X + WH) \lesssim \min\{\text{st}(X), \text{st}(H)\}$	$\ X\ _F \asymp \ H\ _F$
RMSNorm	$\text{st}\left(\begin{bmatrix} \frac{x_1}{\ x_1\ _2} & \cdots & \frac{x_n}{\ x_n\ _2} \end{bmatrix}\right) \lesssim \text{st}(X)$	nearly const. column norms
Gating	$\text{st}(\sigma(VZ) \odot WX) \lesssim \text{st}(X)$	nearly const. column norms, $ \mathbb{E}\sigma(g) > 0$

Table 1: Stable-rank propagation rules for common network operations at Gaussian initialization; precise statements and constants appear in Section 3.

Empirical results. Although our sharpest guarantees apply at initialization, the same low-stable-rank structure persists empirically well into training. In a synthetic sparse-regression experiment (training a three layer neural network on the target $f(x) = x_1x_2x_3$), Figure 1 shows that hidden-layer post-activations have stable rank far below the ambient dimension throughout training. In a NanoGPT-scale language model run, Figure 2 shows that MLP post-activations across all blocks maintain low stable rank, and the embedding/token-indicator behavior is illustrated in Figure 10. RMS-normalized hidden states feeding attention and MLP projections exhibit the same behavior; see Figure 6.

Taken together, these results indicate that, already at initialization, the activation matrices A entering most internal weight blocks are typically low-stable-rank. We now examine how this degeneracy interacts with Euclidean and spectral updates in a simple, yet representative, random-feature regression model.

1.2 Impact of post-activation degeneracy on training algorithms

Low-stable-rank post-activations have a pronounced impact on the behavior of first-order training algorithms. We first make this precise in the random-feature regression model:

$$\min_{W \in \mathbb{R}^{m \times k}} \mathcal{L}(W) := \frac{1}{2n} \|WA - Y\|_F^2. \quad (1.3)$$

We will think about W as the ℓ 'th layer weight matrix to be trained and A is the post-activation matrix of the propagated data from the previous layers. The random feature model is a standard and analytically tractable simplification of neural networks; see for example [12, 14, 43–45].

Now being a quadratic, the function \mathcal{L} may be rewritten as a Taylor-expansion:

$$\mathcal{L}(W + U) = \mathcal{L}(W) + \langle \nabla \mathcal{L}(W), U \rangle + \frac{1}{2n} \|UA\|_F^2. \quad (1.4)$$

The usual starting point for first-order algorithms is based on the majorization principle: one upper-bounds the pure quadratic term $\|UA\|_F^2$ in (1.4) by a function that decouples U from the data A . The update direction of the algorithm is then obtained by minimizing this simple upper model over U . Euclidean gradient descent (GD) and spectral gradient descent (SpecGD) proposed in [9] utilize the following two approximations, respectively:²

$$\frac{1}{n} \|UA\|_F^2 \leq \underbrace{\frac{1}{n} \|A\|_{\text{op}}^2}_{=: L_F} \cdot \|U\|_F^2 \quad \text{and} \quad \frac{1}{n} \|UA\|_F^2 \leq \underbrace{\frac{1}{n} \|A\|_F^2}_{=: L_{\text{op}}} \cdot \|U\|_{\text{op}}^2. \quad (1.5)$$

²Note that both of these inequalities are tight for some matrix U .

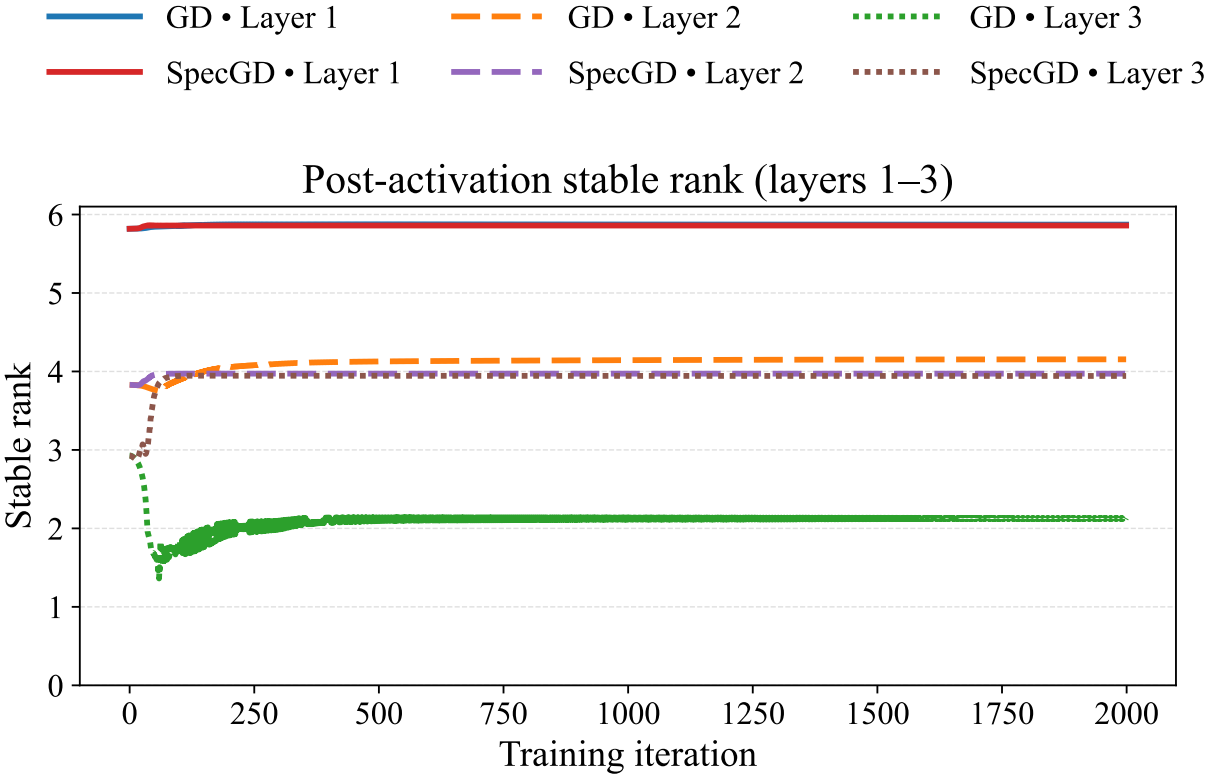


Figure 1: We generate $n = 512$ random gaussian vectors of dimension $d = 128$ and use target y which is the product of the first 3 coordinates. We then train a 4 layer feedforward neural network, with activation function $\sigma(t) = \max\{0, t\}^2$, mapping from input space \mathbb{R}^d to \mathbb{R} as follows: $\mathbb{R}^d \rightarrow \mathbb{R}^{4d} \rightarrow \mathbb{R}^{4d} \rightarrow \mathbb{R}^{4d} \rightarrow \mathbb{R}$. We start at the standard pytorch random initialization and run full batch algorithms: Gradient Descent and a Spectral descent method (only on layers 2 and 3, while layer 1 and 4 simply take Euclidean gradient steps; see Section 1.2.1 for a justification of this choice) and observe the stable ranks of the activation matrices. We note that the maximum possible stable rank of such matrices is 256.

Thus **GD** and **SpecGD** impose the (Euclidean) Frobenius norm and the (non-Euclidean) operator norm on the domain, respectively. Combining (1.4) with each of the inequalities (1.5) and minimizing in U yields the explicit updates for **GD** and **SpecGD**, respectively:

$$W_{\text{GD}} := W - \frac{1}{L_F} \nabla \mathcal{L}(W) \quad \text{and} \quad W_{\text{SD}} = W - \frac{\|\nabla \mathcal{L}(W)\|_*}{L_{\text{op}}} \text{polar}(\nabla \mathcal{L}(W)).$$

Here, the polar of the matrix is the product of the left and right orthogonal factors appearing in its singular value decomposition. **MUON** is a variant of **SpecGD**, where the polar is approximated by the Newton-Schulz algorithm, and one further incorporates momentum. Now the guaranteed function decrease achieved by **GD** and **SpecGD** is fully determined by the dual norm of the gradient:

$$\mathcal{L}(W) - \mathcal{L}(W_{\text{GD}}) \geq \frac{1}{2L_F} \|\nabla \mathcal{L}(W)\|_F^2 \quad \text{and} \quad \mathcal{L}(W) - \mathcal{L}(W_{\text{SD}}) \geq \frac{1}{2L_{\text{op}}} \|\nabla \mathcal{L}(W)\|_*^2.$$

Comparing the two bounds, we see that **SpecGD** promises more descent than **GD** whenever

$$\text{nr}(\nabla \mathcal{L}(W)) \geq \text{st}(A), \tag{1.6}$$

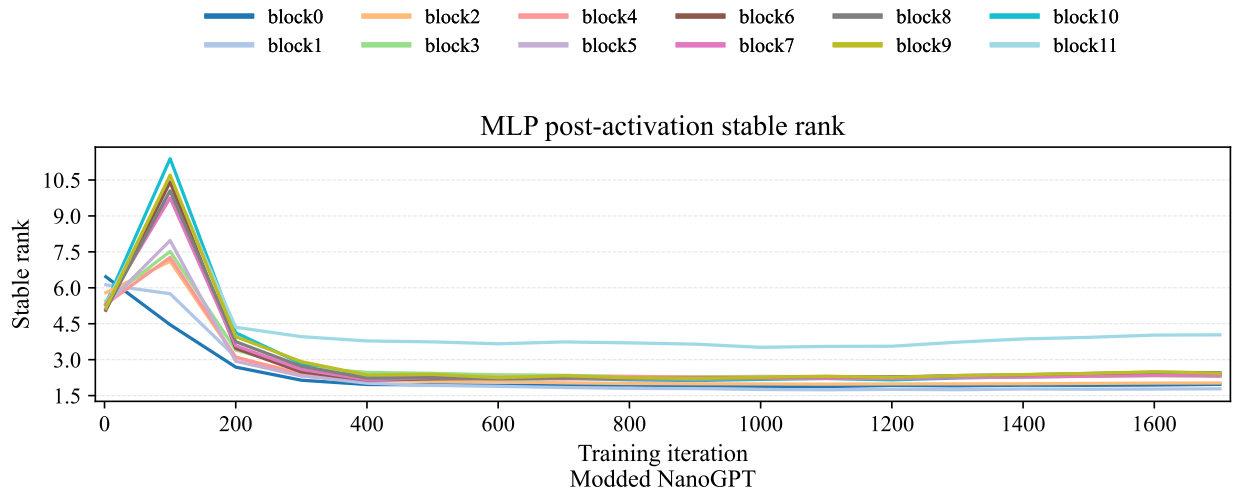


Figure 2: Stable rank of MLP post activations while running a particular snapshot (specifically [27]) of the modded-NanoGPT repo [30]. We also include the July 18th snapshot of the architecture at the time of training in Section 28. We note that the maximal rank of any activation matrix in this plot is 3072. Thus, the the stable rank of the post-activations are far below their maximal value.

When the stable rank of the post-activation $\text{st}(A)$ is constant (independent of dimension), one expects that (1.6) will hold, since the ratio on the left-side can scale with the dimension.

As a numerical illustration (Figure 3), we compare the performance of GD and SpecGD on random feature regression corresponding to training second layer weights, namely $A_1 = \sigma(W_1 X)$, where $W_1 \in \mathbb{R}^{100 \times 50}$ and $X \in \mathbb{R}^{100 \times 50}$ have iid standard Gaussian entries and $\sigma(t) = \max\{0, t\}$ is the ReLU activation function applied coordinatewise. It is clear from the figure that (i) equation (1.6) holds along both GD and SpecGD trajectories and (ii) SpecGD significantly outperforms GD as expected.

The argument we presented above is particularly clean for least squares, but it can be generalized much further. As a first example, we stay within the random feature model and consider a smooth loss f on WA for which the gradient ∇f is L -Lipschitz. Note that we can think of W as a fixed layer within a network, keeping the rest of the weights frozen, and A would be the previous layers post-activations. Now, define $\mathcal{L}(W) := f(WA)$ and note that

$$\mathcal{L}(W + U) \leq \mathcal{L}(W) + \langle \nabla \mathcal{L}(W), U \rangle + \frac{L}{2} \|UA\|_F^2. \quad (1.7)$$

Then, as before, we may bound $\|UA\|_F^2$ by $\|A\|_{\text{op}}^2 \|U\|_F^2$ or $\|A\|_F^2 \|U\|_{\text{op}}^2$, and minimize the two constructed bounds in the variable U . This gives us GD and SpecGD, respectively:

$$W_{\text{GD}} := W - \frac{1}{L_F \cdot L} \nabla \mathcal{L}(W) \quad \text{and} \quad W_{\text{SD}} = W - \frac{\|\nabla \mathcal{L}(W)\|_*}{L_{\text{op}} \cdot L} \text{polar}(\nabla \mathcal{L}(W)),$$

Plugging in the update in (1.7), we find

$$\mathcal{L}(W) - \mathcal{L}(W_{\text{GD}}) \geq \frac{1}{2L_F \cdot L} \|\nabla \mathcal{L}(W)\|_F^2 \quad \text{and} \quad \mathcal{L}(W) - \mathcal{L}(W_{\text{SD}}) \geq \frac{1}{2L_{\text{op}} \cdot L} \|\nabla \mathcal{L}(W)\|_*^2.$$

Thus, descent promised by SpecGD is again greater than that promised by GD whenever (1.6) holds.

Although the random feature model is idealized, the derived conclusions appear to hold more generally. For example, in Figure 20 we build on the sparse regression setting of Figure 1, plotting

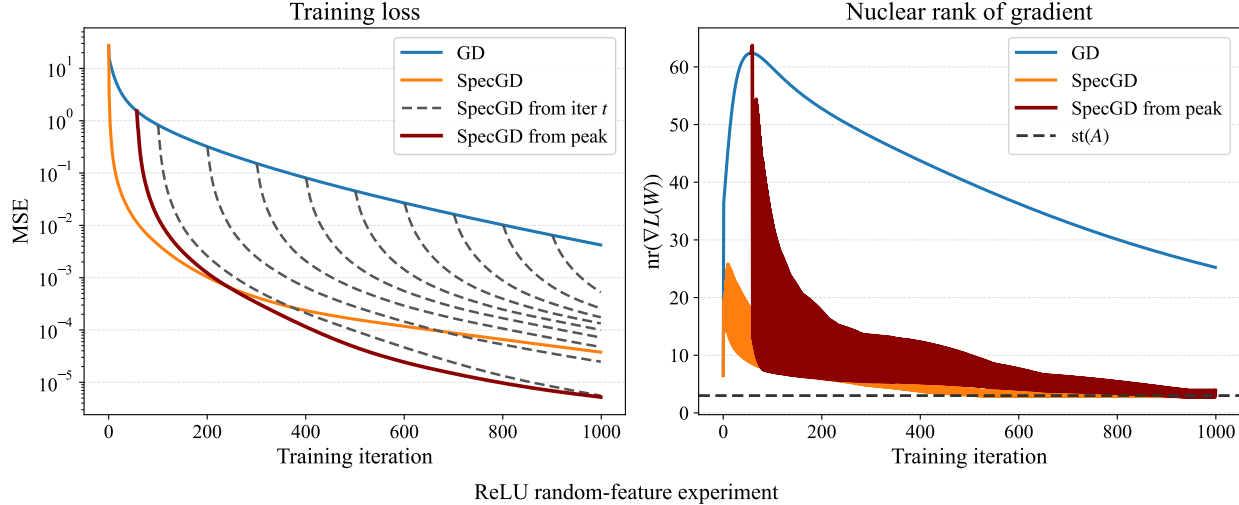


Figure 3: Comparison of gradient descent (GD) and spectral gradient descent (SpecGD) on the random feature model $\min_W \mathcal{L}(W) = \frac{1}{2n} \|WA - Y\|_F^2$ with $W \in \mathbb{R}^{100 \times 100}$. The ground truth matrix $W_{\sharp} \in \mathbb{R}^{100 \times 100}$ is drawn with iid standard Gaussian entries. The data matrix is generated by $A = \sigma(W_1 X)$, where $W_1 \in \mathbb{R}^{100 \times 50}$ and $X \in \mathbb{R}^{100 \times 400}$ have iid standard Gaussian entries and $\sigma(t) = \max\{0, t\}$ is the ReLU activation function applied coordinatewise. The target matrix $Y = W_{\sharp} A$ is generated from a ground truth matrix $W_{\sharp} \in \mathbb{R}^{100 \times 100}$ that has iid standard Gaussian entries. Both methods are initialized at the all-zeros matrix. Left: supoptimality gap in function value along the GD (solid blue) and SpecGD (solid gold) iterations. The dashed curves plot the suboptimality gap if we were to initialize SpecGD at the current GD step, plotted every 100 iterations. The superior performance of SpecGD is clear from the figure. Right: nuclear rank $\text{nr}(\nabla \mathcal{L}(W))$ of the gradient along the GD and SpecGD iterations initialized at the all-zeros matrix; the black dashed line signifies the level $\text{st}(A)$, above which SpecGD is superior to GD. The nuclear rank $\text{nr}(\nabla \mathcal{L}(W))$ can be large (with (1.6) holding) along the trajectories.

the performance of GD and SpecGD, along with the nuclear rank $\text{nr}(\nabla \mathcal{L}(W))$. SpecGD exhibits significantly better performance than GD, especially early on in training when the nuclear ranks of the gradients are large. Further, building on Figure 2, we plot in Figure 5 the ratio $\text{nr}(\nabla \mathcal{L}(W))$ for the MLP layers when training the NanoGPT model. We observe that this ratio can indeed be large along the trajectory, thereby suggesting a significant advantage of MUON/SpecGD over GD.

Implementing spectral updates such as SpecGD/Muon in large distributed runs is nontrivial because the relevant gradient (or momentum) matrices are typically sharded across devices; in Appendix E we analyze a shardwise alternative that applies the polar-factor map independently to each local shard (incurring no incremental communication) and derive the corresponding analogue of the nuclear-rank versus stable-rank condition.

1.2.1 Multiple layers and transformer blocks

The discussion so far has treated a single matrix block W acting on a post-activation matrix A , and has shown that whenever the incoming features have low stable rank and the gradient has large nuclear rank, a spectral update on W enjoys a strictly better one-step guarantee than its Euclidean counterpart. In practice, however, we train *all* layers of a deep architecture simultaneously, and the parameters interact through a highly coupled nonlinearity. To understand when spectral methods

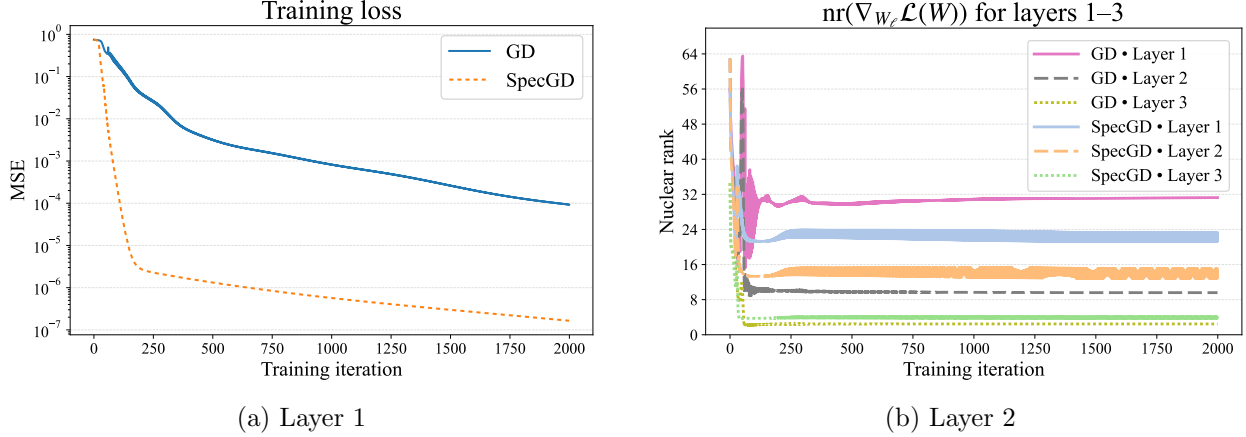


Figure 4: The training loss and gradient nuclear rank associated to the sparse regression problem in Figure 1. We see that the training loss for **SpecGD** decreases significantly faster than for **GD** during the initial phase of training, when the nuclear rank of the gradient is large. The maximum possible nuclear rank at layer 1 is 128, while for layers 2 and 3, it is 256.

are still favored in this setting, we abstract the architecture into a general layered model and study the full Hessian of the composite loss.

In Section 7 we formalize this viewpoint. We fix preactivation matrices $X_\ell(W) = W_\ell A_{\ell-1}(W)$ at each layer and let the activations $A_\ell(W)$ be obtained from $(X_1(W), \dots, X_\ell(W))$ through a twice differentiable map Φ_ℓ . The outer loss f is defined on the collection of preactivations (X_1, \dots, X_L) , and the training objective is $\mathcal{L}(W) := f(X_1(W), \dots, X_L(W))$. In this setting we show that the Hessian of \mathcal{L} is controlled by a feature-based term plus a smaller parameter-dependent term:

$$\langle \Delta W, \nabla^2 \mathcal{L}(W) \Delta W \rangle \leq C_F(W) \sum_{\ell=1}^L \|\Delta W_\ell A_{\ell-1}(W)\|_F^2 + C_{\text{op}}(W) \sum_{\ell=1}^L \|\Delta W_\ell\|_{\text{op}}^2,$$

for all perturbations $\Delta W = (\Delta W_1, \dots, \Delta W_L)$ and some finite constants $C_F(W)$ and $C_{\text{op}}(W)$ depending smoothly on the current iterate. For the standard $1/n$ -averaged losses we consider (squared loss, cross-entropy), $C_F(W)$ scales like $O(1/n)$, so the feature-based curvature constants inherit the usual $1/n$ dependence on the batch size. Both $C_F(W)$ and $C_{\text{op}}(W)$ are otherwise dimension-free in the sense that they depend only on the network architecture, depth, and current weight operator norms, and not on width or sequence length.³

Applying Taylor’s theorem with remainder, we may therefore write,

$$\mathcal{L}(W + \Delta W) = \mathcal{L}(W) + \sum_{\ell=1}^L \langle G_\ell(W), \Delta W_\ell \rangle + \frac{1}{2} \langle \Delta W, \nabla^2 \mathcal{L}(W) \Delta W \rangle + R(\Delta W), \quad (1.8)$$

where $G_\ell(W) := \nabla_{W_\ell} \mathcal{L}(W)$ and $R(\Delta W) = o(\|\Delta W\|_F)$ collects higher order terms. Combining the Hessian bound with the basic norm inequalities

$$\|\Delta W_\ell A_{\ell-1}\|_F \leq \|A_{\ell-1}\|_{\text{op}} \|\Delta W_\ell\|_F, \quad \|\Delta W_\ell A_{\ell-1}\|_F \leq \|A_{\ell-1}\|_F \|\Delta W_\ell\|_{\text{op}},$$

³For simplicity, we state our Hessian bounds with a single feature term $\sum_\ell \|\Delta W_\ell A_{\ell-1}\|_F^2$ and a single parameter term $\sum_\ell \|\Delta W_\ell\|_{\text{op}}^2$. All of our arguments, most importantly the layerwise criterion comparing $\text{nr}(G_\ell)$ to $\text{st}(A_{\ell-1})$, continue to hold if one instead uses blockwise curvature weights $C_{\ell,F}(W)$ in front of $\|\Delta W_\ell A_{\ell-1}\|_F^2$ and $C_{\ell,\text{op}}(W)$ in front of $\|\Delta W_\ell\|_{\text{op}}^2$. This refinement only rescales the natural step sizes $L_\ell^F, L_\ell^{\text{op}}$ for each block and does not affect the nuclear-versus-stable-rank comparison.

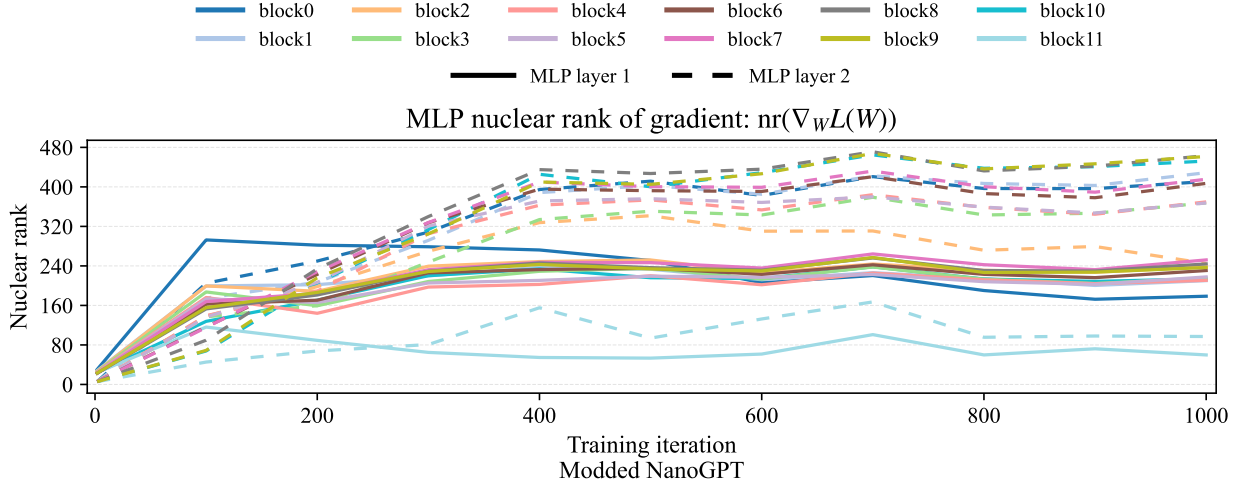


Figure 5: Modded NanoGPT MLP gradient nuclear ranks.

we obtain feature-based blockwise curvature coefficients

$$L_\ell^F(W) := C_F(W) \|A_{\ell-1}(W)\|_{\text{op}}^2, \quad L_\ell^{\text{op}}(W) := C_F(W) \|A_{\ell-1}(W)\|_F^2.$$

Their ratio is exactly the stable rank of the incoming features:

$$\frac{L_\ell^{\text{op}}(W)}{L_\ell^F(W)} = \frac{\|A_{\ell-1}(W)\|_F^2}{\|A_{\ell-1}(W)\|_{\text{op}}^2} = \text{st}(A_{\ell-1}(W)).$$

These feature-based constants suggest natural blockwise step sizes. In the layered analysis of Section 7 (see in particular Section 7.4), we proceed as follows. For each block ℓ we fix two descent directions:

$$\text{GD direction: } -G_\ell(W), \quad \text{spectral direction: } -\text{polar}(G_\ell(W)),$$

and then choose scalar step sizes along these directions that minimize the quadratic upper bound in the Taylor model (1.8) under the mixed Hessian bound. This produces two full updates: a Euclidean update W^{GD} and a mixed spectral update W^{Spec} which applies spectral steps on blocks in $\mathcal{S} \subseteq [L]$ and Euclidean steps on the remaining blocks.

Section 7.4 shows that the spectral update has at least as much predicted decrease as the Euclidean update yet again when the nuclear-rank versus stable-rank inequality holds:

$$\text{nr}(G_\ell(W)) \geq \text{st}(A_{\ell-1}(W)). \quad (1.9)$$

Thus, already at the level of the layered quadratic model, we recover the same criterion as in the random-feature setting: spectral updates are favored on those blocks whose incoming activations $A_{\ell-1}(W)$ have low stable rank while their gradients $G_\ell(W)$ have high nuclear rank.

For fully connected networks this picture is particularly transparent. The matrices $A_{\ell-1}$ are precisely the layerwise post-activations introduced in (4.1). Section 2 shows that when the activation are mean spike indusing, the stable rank $\text{st}(A_{\ell-1})$ is bounded by a numerical constant for all internal layers at initialization, while the input $A_0 = X$ need not have any such structure. In this regime, the constants L_ℓ^{op} and L_ℓ^F differ only by a fixed factor for $2 \leq \ell \leq L-1$, but may be very different at the input and output layers. Our implementation of **SpecGD** therefore uses the spectral step with step size $\|G_\ell\|_* / L_\ell^{\text{op}}$ on all internal weight matrices, and keeps the first and last

layers on standard Euclidean steps with step size $1/L_\ell^F$. In other words, we apply spectral updates exactly where the incoming post-activations are empirically low-stable-rank, and retain Euclidean updates where the features (raw inputs or task-specific heads) are not guaranteed to be degenerate.

Transformers require a slightly more detailed bookkeeping, because the matrices which appear multiplying a given weight are composites of several operations: normalization, attention, residual connections and MLPs. Nevertheless, the layered formalism and the seminorm $\sum_\ell \|\Delta W_\ell A_{\ell-1}\|_F^2$ apply unchanged once we view each transformer block as built from linear maps W_ℓ composed with smooth activation maps Φ_ℓ . For concreteness, we write formulas for a single decoder block acting on a sequence representation $X \in \mathbb{R}^{d_{\text{model}} \times T}$ (hidden dimension d_{model} , sequence length T), and we suppress masking, multiple-heads, and positional encodings (e.g. RoPE) from the notation, though we include them in Section 5. The single-head attention sublayer can be written as

$$\begin{aligned} A^{\text{rms}} &= \text{RMSNorm}(X), \\ Q &= W_Q A^{\text{rms}}, \quad K = W_K A^{\text{rms}}, \quad V = W_V A^{\text{rms}}, \\ P &= \text{softmax}(d_{\text{model}}^{-1/2} K^\top Q), \\ H &= VP, \\ X^{\text{att}} &= X + W_O H, \end{aligned}$$

where W_Q, W_K, W_V, W_O are the attention weight matrices and d_{embed} is the embedding dimension. The MLP sublayer then takes the form

$$\begin{aligned} A_{\text{mlp}}^{\text{rms}} &= \text{RMSNorm}(X^{\text{att}}), \\ B &= \sigma(W_1 A_{\text{mlp}}^{\text{rms}}), \\ X^+ &= X^{\text{att}} + W_2 B, \end{aligned}$$

where σ is a pointwise nonlinearity (e.g. GELU) and W_1, W_2 are the MLP weights. At the end of the network, a language-modeling head applies an RMS normalization followed by a linear map

$$A_{\text{final}}^{\text{rms}} = \text{RMSNorm}(X^+), \quad Z = W_{\text{lm}} A_{\text{final}}^{\text{rms}},$$

producing logits Z over the vocabulary.

In this block-level description, each trainable matrix appears exactly in the affine form $X_\ell = W_\ell A_{\ell-1}$ required by our layered model. The corresponding incoming features $A_{\ell-1}$ are:

$$A_{\ell-1} \in \{A^{\text{rms}}, A_{\text{mlp}}^{\text{rms}}, B, H, A_{\text{final}}^{\text{rms}}\},$$

depending on whether W_ℓ is one of $W_Q, W_K, W_V, W_O, W_1, W_2, W_{\text{lm}}$. For simplicity we have written RMSNorm as parameter-free, but in practice each normalization can carry a learned weight vector $\gamma \in \mathbf{R}^{d_{\text{model}}}$ acting elementwise as $x \mapsto \gamma \circ \frac{x}{\|x\|_{\text{rms}}}$. In our notation these weights can be treated as additional diagonal blocks $W_{\text{rms}} := \text{Diag}(\gamma)$ acting on the parameter-free RMS-normalized activations \tilde{A}^{rms} , so that $A^{\text{rms}} = W_{\text{rms}} \tilde{A}^{\text{rms}}$ and the affine form $X_\ell = W_\ell A_{\ell-1}$ continues to hold. The corresponding updates are slightly different. Indeed, on diagonal blocks spectral updates reduce to a sign-type update in the gain. We discuss this in more detail in Appendix 7.5. Note that the modded-NanoGPT repo [27] does not train the RMSNorm parameter, and instead uses fixed weight $\gamma = \mathbf{1}$.

Our measurements in Figure 2 (MLP post-activations B) and in Figure 6 (RMS activations $A^{\text{rms}}, A_{\text{mlp}}^{\text{rms}}, A_{\text{final}}^{\text{rms}}$) show that the RMS-normalized activations $A^{\text{rms}}, A_{\text{mlp}}^{\text{rms}}, A_{\text{final}}^{\text{rms}}$ and the MLP post-activations B all have low stable rank throughout training. For the attention output features H we may further write

$$H = VP = W_V A^{\text{rms}} P,$$

so that for perturbations of the output projection W_O we have

$$\Delta W_O H = \Delta W_O W_V A^{\text{rms}} P.$$

Here the RMS-normalized activations A^{rms} sit *between* two linear operators, but submultiplicativity still isolates their contribution:

$$\|\Delta W_O H\|_F = \|\Delta W_O W_V A^{\text{rms}} P\|_F \leq \|\Delta W_O\|_{\text{op}} \|W_V\|_{\text{op}} \|A^{\text{rms}}\|_F \|P\|_{\text{op}}.$$

More generally, each seminorm term $\|\Delta W_\ell A_{\ell-1}\|_F$ associated with a transformer block can be written as a product of the form

$$\Delta W_\ell A_{\ell-1} = \Delta W_\ell M_{\ell,\text{left}} \tilde{A}_{\ell-1} M_{\ell,\text{right}},$$

where $\tilde{A}_{\ell-1}$ is one of the low-stable-rank matrices A^{rms} , $A^{\text{rms}}_{\text{mlp}}$, B , $A^{\text{rms}}_{\text{final}}$, and $M_{\ell,\text{left}}$, $M_{\ell,\text{right}}$ are fixed linear maps (products of attention projections, residual additions, or the attention kernel P). Using

$$\|\Delta W_\ell A_{\ell-1}\|_F = \|\Delta W_\ell M_{\ell,\text{left}} \tilde{A}_{\ell-1} M_{\ell,\text{right}}\|_F \leq \|\Delta W_\ell\|_{\text{op}} \|M_{\ell,\text{left}}\|_{\text{op}} \|M_{\ell,\text{right}}\|_{\text{op}} \|\tilde{A}_{\ell-1}\|_F,$$

we see that the curvature constants relevant for block ℓ scale with $\|\tilde{A}_{\ell-1}\|_F^2$, and the ratio $L_\ell^{\text{op}}/L_\ell^{\text{F}}$ is again governed by the stable rank of these RMS and MLP activations.

To make the connection between gradient nuclear ranks and the upstream feature matrices completely explicit, it is useful to summarize, for each parameter block, which activation matrix enters the condition (1.9). Table 2 records the correspondence we will use in our experiments.

Parameters W_ℓ	Activation in (1.9) (for W_ℓ)
W_Q	A^{rms}
W_K	A^{rms}
W_V	A^{rms}
W_O	A^{rms} (via $H = W_V A^{\text{rms}} P$)
W_1	$A^{\text{rms}}_{\text{mlp}}$
W_2	B
W_{lm}	$A^{\text{rms}}_{\text{final}}$
Embedding	X (moderate stable-rank guarantee)

Table 2: For each parameter block W_ℓ , the activation matrix whose stable rank appears on the right-hand side of (1.9). The corresponding left-hand side is always the gradient nuclear rank $\text{nr}(G_\ell)$ for that same block.

Figures 5, 6, 7, 8, and 9 illustrate how these quantities behave in a NanoGPT run. The plots in Figure 5 show that the gradient nuclear ranks for the MLP weights remain consistently large along training, while Figures 2 and 6 demonstrate that both the MLP post-activations B and the RMS-normalized activations A^{rms} , $A^{\text{rms}}_{\text{mlp}}$, $A^{\text{rms}}_{\text{final}}$ have stable rank bounded by a small numerical constant. Thus, for these blocks, the inequality (1.9) is strongly activated, and the simple GD-based model predicts a clear advantage for spectral-style updates. This is consistent with the convergence bounds presented in [42], where improvements over Euclidean methods are also driven by large nuclear-to-Frobenius ratios.

Figures 8 and 9 shows a similar behavior for the attention weights: the gradient nuclear ranks for W_Q , W_K , W_O are typically large and W_V is more modestly sized, while their reference activations in Table 2 are the low-stable-rank RMS features of Figure 6. In contrast, Figure 7 reveals a different

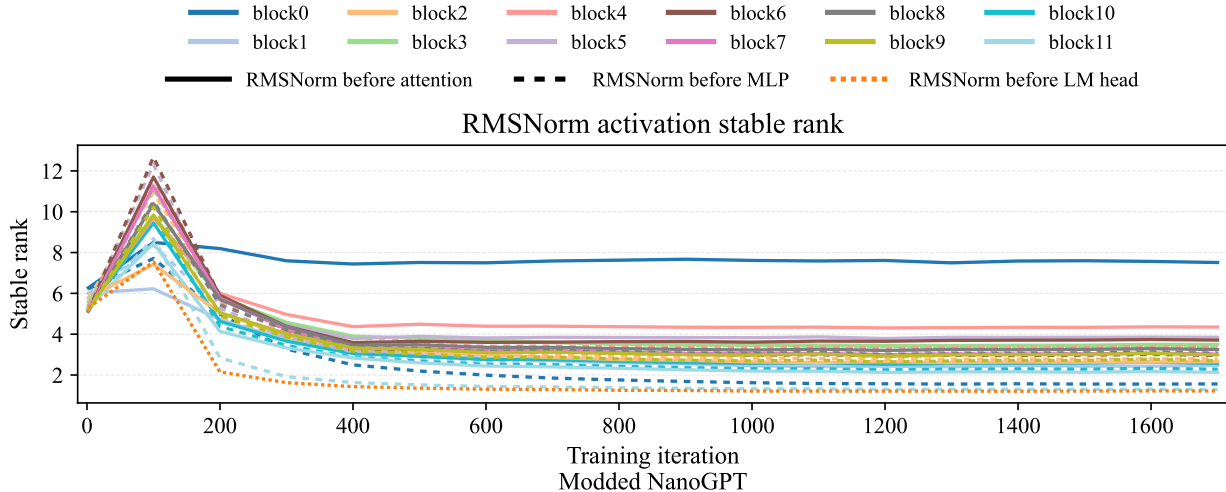


Figure 6: Stable rank of RMS-normalized activations A^{rms} , $A_{\text{mlp}}^{\text{rms}}$, $A_{\text{final}}^{\text{rms}}$.

picture for the input embedding weights and the language-model head. The embedding matrix multiplies a raw token-indicator matrix whose stable rank hovers around 26 (see section 2.3 for more on this), which is modestly low relative to the ambient dimension but noticeably larger than the stable ranks of the internal post-activations; the nuclear rank of the embedding gradient grows from roughly 100 to 400 over the course of training (Figure 10). Thus the ratio $\text{nr}(G_{\text{emb}})/\text{st}(X)$ is only moderately larger than one and much smaller than the corresponding ratios for the hidden MLP and attention blocks, so our condition (1.9) predicts a milder advantage for spectral updates on the embedding matrix. This matches our empirical experience with the NanoGPT: applying MUON-style spectral updates to the input embedding in the Modded-NanoGPT run changes training and validation curves only slightly (not shown). From the viewpoint of [42], a more natural geometry for the embedding block is the $\ell_1 \rightarrow \ell_2$ operator norm, since the input tokens are one-hot vectors of ℓ_1 -norm one; in that setting the relevant Lipschitz constants are controlled by the maximum column norm of the embedding matrix rather than its spectral norm, and the stable-rank heuristic is replaced by an ℓ_1 -based argument. We do not pursue this alternative geometry here.

To sum up, all matrix-valued weights interior to the the transformer blocks—the attention projections and MLP matrices—see incoming features that are effectively low-stable-rank in the sense relevant for the Hessian bound, and their gradient nuclear ranks are typically large. For these blocks the inequality (1.9) is strongly activated, and spectral updates have a clear structural advantage over Euclidean ones. The input embedding weight matrix, by contrast, multiplies raw token indicators and lies only marginally in this regime, while the language-model head sits in an intermediate regime where the same inequality holds but with a much smaller margin. The resulting picture is consistent with current practice: the modded-NanoGPT repository applies spectral updates (implemented via MUON) to all 2D weight blocks inside the transformer, while keeping both the token embedding and the language-model head on AdamW-style updates. Moreover, Section 5 shows that, at initialization, the transformer activations that feed these blocks have stable rank bounded by numerical constants independent of width and sequence length, uniformly for the MLP post-activations, and growing at most quadratically with the layer index for the remaining RMS-normalized and hidden states. In view of the momentum-based implementation of MUON and the different effective geometry of AdamW, our comparison should be read as a geometric heuristic instead of a precise hyperparameter recommendation: the nuclear-rank versus stable-rank condition

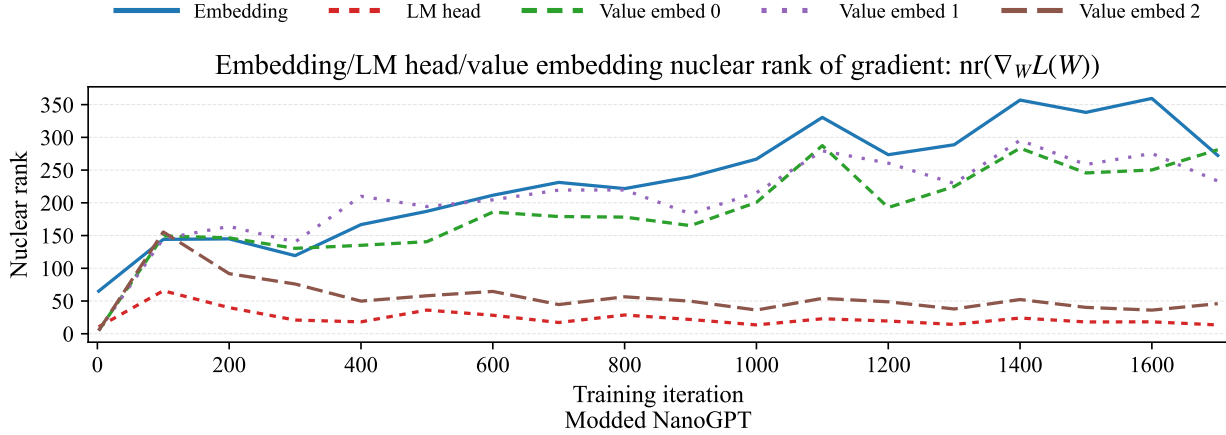


Figure 7: Gradient nuclear ranks for the token embedding and language-model head parameters in the same NanoGPT run. The mean ratio for the LM head over the last 1000 steps is approximately 42.68.

explains why spectral geometry is well matched to the internal layers of MLPs and transformers, even though our one-step comparison is carried out for Euclidean gradient descent instead of AdamW.

1.3 When do we expect the nuclear rank of the gradient to be large?

So far, we have primarily focused on understanding when the stable rank of the post-activation matrices is small. On the other hand, in order for the spectral updates to be superior to Euclidean gradient updates according to the rule (1.9), the nuclear rank of the gradient should be large. Naively, one may think that the low stable rank of the post-activation matrix may inadvertently translate into a low nuclear rank of the gradient, thereby nullifying our thesis. On the contrary, in Section 6 we show that in the representative model of random feature regression (1.3) both in the realizable and student-teacher set-ups, the nuclear rank of the gradient is expected to be large through training. More precisely, consider running the Euclidean gradient method on the problem (1.3) initialized with the all-zero matrix W_0 and with stepsize $\eta > 0$. Let W_t be the resulting weight matrices generated across the iterations. We show that if the activation function σ is mean-spike inducing (or more generally if AA^\top follows a spiked model), the following are true.

- When using a nearly maximal stepsize of the form $\eta = \frac{1}{c + \|A\|_{\text{op}}^2}$ for $c > 0$, the weight matrix W_1 generated by a single step has nuclear rank that scales with the dimension $\text{nr}(\nabla \mathcal{L}(W_1)) \gtrsim d$.
- When using a more realistic stepsize $\eta = \frac{1}{C\|A\|_{\text{op}}^2}$ for $C > 1$, after a short $O(\log d)$ burn-in period there is a window of $\Theta(d)$ iterations on which $\text{nr}(\nabla \mathcal{L}(W_t)) = \Omega(d)$ and, for any fixed $\varepsilon > 0$, a longer window of $\Theta(d \log d)$ iterations on which $\text{nr}(\nabla \mathcal{L}(W_t)) \geq d^{1-\varepsilon}$ (Theorem 6.6 and Corollary 6.12).

In the same models, Euclidean gradient descent needs $\Theta(d \log(d/\delta))$ steps to reach relative error $\delta \in (0, 1)$, so for any target accuracy this $\Theta(d \log d)$ window represents a constant fraction of the training time. Thus, if we were to restart SpecGD from any point in this window, its one-step improvement over Euclidean gradient descent would be dimension-dependent. Notice that these

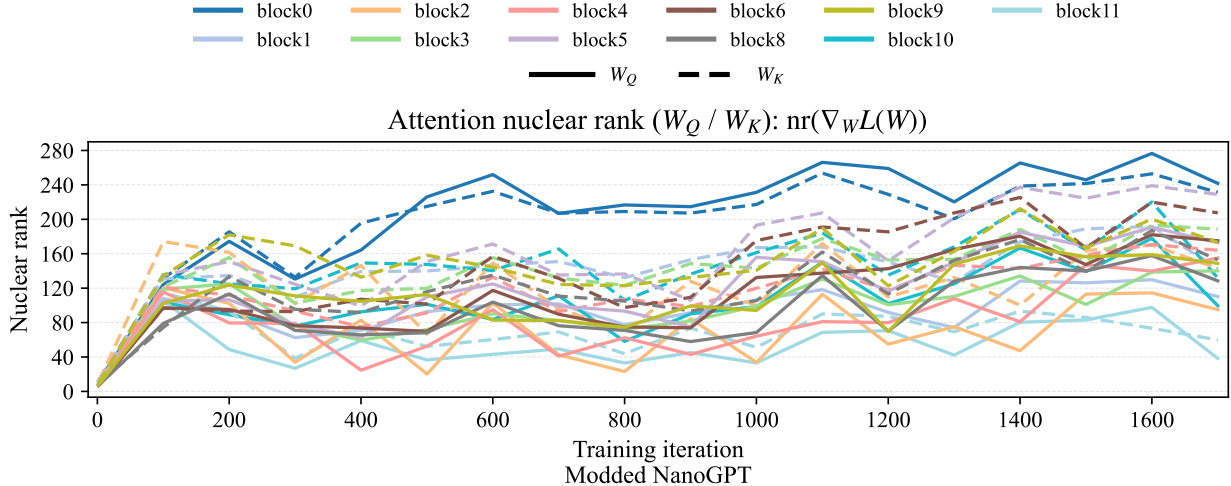


Figure 8: Gradient nuclear ranks for the attention parameters W_Q, W_K in the same NanoGPT run.

results are consistent with the nuclear ranks plotted in our experiments on random feature regression (Figures 3) and the MLP layer in modded NanoGPT (Figure 5), wherein the gradient nuclear rank starts off low but quickly increases through training.

1.4 When are spectral updates less helpful?

Given the discussion thus far the reader might conclude that spectral updates are always preferred to Euclidean ones. This is not the case. The random-feature model with *centered activations*, already provides a simple counterexample in which the nuclear-rank condition (1.6) fails and spectral updates are *slower* than Euclidean ones.

To demonstrate, we repeat the experiment from Figure 3, keeping the same dimensions, data distribution, and ground-truth matrix W_{\sharp} , but replacing ReLU with a SwiGLU activation; the result is summarized in Figure 11. Concretely, in this variant the random-feature matrix is

$$A = \text{SwiGLU}(W_1 X, W_2 X) := \text{SiLU}(W_1 X) \circ (W_2 X),$$

where $W_1, W_2 \in \mathbf{R}^{k \times d}$ are independent Gaussian weight matrices, the Hadamard product \circ is taken coordinatewise, and

$$\text{SiLU}(t) := t \cdot (1 + e^{-t})^{-1}$$

is the usual Swish/SiLU nonlinearity applied elementwise. Thus each feature coordinate is of the form

$$a_{ij} = \text{SiLU}((W_1 X)_{ij})(W_2 X)_{ij},$$

in contrast to the ReLU experiment where $A = \sigma(W_1 X)$ depends on a single weight matrix. We will refer to such activations of the form $\phi(W_1 X) \circ (W_2 X)$ as *gated activations*. In particular, in the Gaussian setup above each feature row is (exactly) centered: $\mathbb{E}[a] = 0$.

In Figure 3 (ReLU features), the post-activation matrices A are empirically low-stable-rank. As explained in Section 2.2, non-centered activations such as ReLU produce a large rank-one contribution to the second moment: equivalently, $(1/k)A^T A$ develops a spike aligned with the mean row vector $\mathbb{E}a$. This spike dominates the spectrum and keeps $\text{st}(A)$ bounded by a numerical constant even as the width grows. Gated activations like SwiGLU behave differently. Here $\mathbb{E}a = 0$,

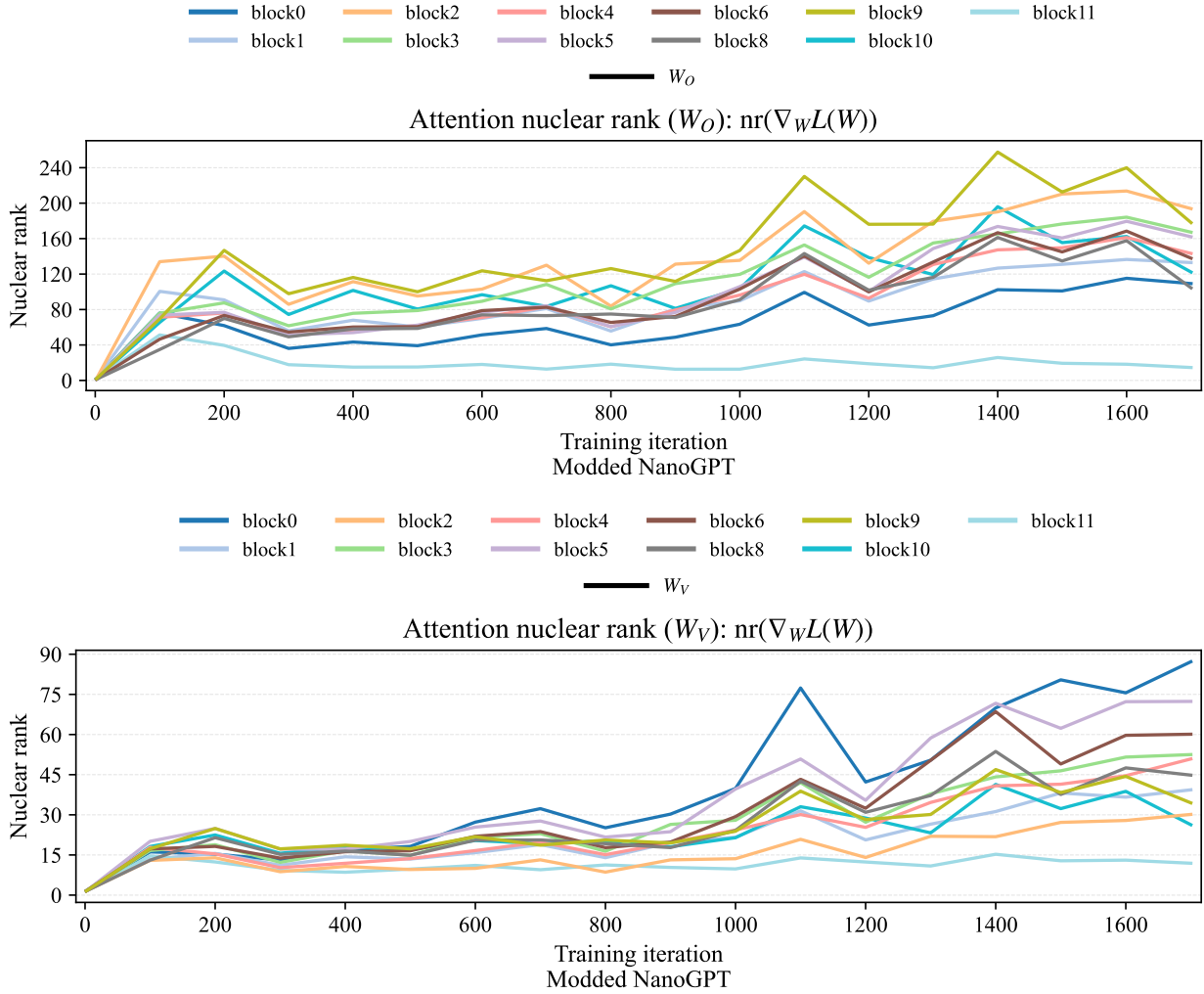


Figure 9: Gradient nuclear ranks for the attention parameters W_O, W_V in the same NanoGPT run.

so the mean-induced spike in $A^\top A$ is absent. The resulting Gram matrix has a more isotropic spectrum, and the stable rank $\text{st}(A)$ now grows proportionally with the width instead of remaining $O(1)$, while the nuclear rank $\text{nr}(\nabla \mathcal{L}(W))$ of the gradient remains modest. In the Gaussian random-feature experiment considered here this means that $A^\top A$ has essentially no spike at initialization: its spectrum is bulk-only. For data that already carry a low-rank spike, such as the embedding/token-indicator input of a transformer at initialization (see Section 2.3), centered activations are known to propagate that *informative* spike, as in the nonlinear spiked-covariance and conjugate-kernel analyses discussed in Section 1.5 [2, 57]; what they avoid is exactly the large, uninformative mean-induced spike that drives the low-stable-rank regime in our ReLU examples.

In this experiment the inequality

$$\text{nr}(\nabla \mathcal{L}(W)) \geq \text{st}(A)$$

is violated: the right-hand panel of Figure 11 shows the nuclear-rank curves dipping below the dashed stable-rank level. The one-step comparison in (1.6) therefore predicts that gradient descent should outperform spectral descent, and the left-hand panel confirms this prediction: GD reaches a much smaller objective value in far fewer iterations than **SpecGD**.

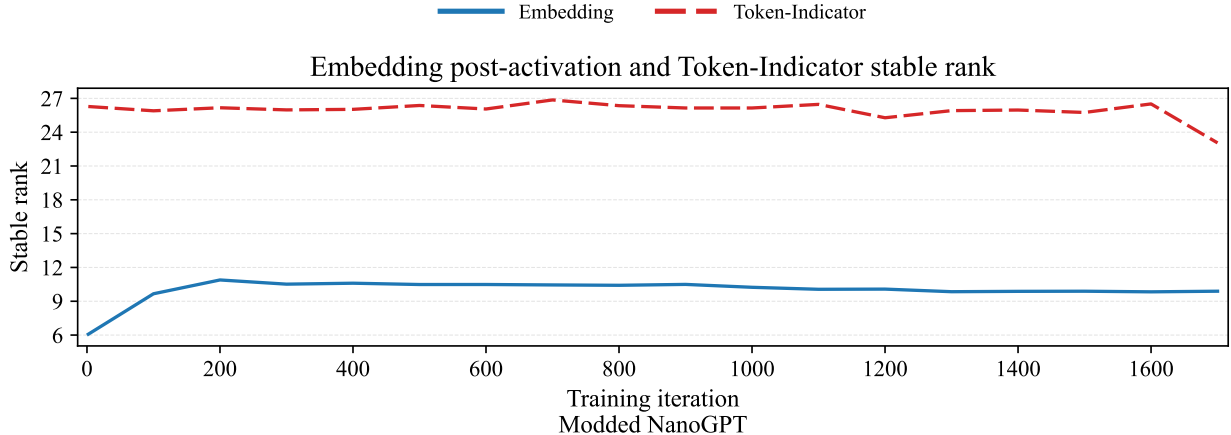


Figure 10: Embeddings matrix post-activation and Token-Indicator stable rank throughout training. See Section 2.3 for more on these matrices.

In Appendix A, we also repeat the sparse regression experiment of Figure 1 with a SwiGLU activation. There we see that SpecGD can still perform well at small batch sizes, where the post-activations remain moderately low-stable-rank, but that its advantage is quickly lost as the batch size (and hence the stable rank) increases.

For transformers, however, this toy counterexample does not preclude low-stable-rank internal features. In Appendix B, we repeat the modded-NanoGPT diagnostics with a SwiGLU MLP, finding that the internal activations remain low-stable-rank (though typically larger than in the squared-ReLU run) and the corresponding gradient nuclear ranks remain large. This is consistent with the results of Section 5: even in the nonMSI/gated regime, low stable rank is already present at the input through the token-indicator/embedding structure (Section 2.3) and is then preserved through attention and MLP blocks by the propagation bounds, yielding width- and sequence-length-independent stable-rank control at initialization.

Method	Non-gated MLP	Gated MLP
All Adam	3.9242	3.8837
Muon(W_{out} only)	3.7023	3.7843
Muon(All Attn, MLP)	3.5654	3.5125

Table 3: Validation loss at $10k$ training steps for the MLP ablations of Wang et al. [56]. The model is a 160M-parameter NanoGPT-style decoder-only transformer trained on FineWeb, with columns corresponding to standard (non-gated) and gated MLP variants as in Eqns. (3.2)–(3.3) of [56]. In the gated case, the MLP uses a gated activation of the form $\phi(W_{\text{in}}h) \circ (W_{\text{gate}}h)$ feeding W_{out} .

As a point of comparison, Table 3 summarizes the MLP ablations reported by Wang et al. [56]. For the non-gated MLP, switching only W_{out} from Adam to Muon reduces the validation loss from 3.9242 (All Adam) to 3.7023, while full Muon on all attention and MLP weights reaches 3.5654; thus about 62% of the total improvement from Adam to full Muon is already captured by changing W_{out} alone. In the gated MLP, the corresponding losses are 3.8837 (All Adam), 3.7843 (Muon on W_{out} only), and 3.5125 (Muon on all attention and MLP weights), so the change on W_{out} accounts for only about 27% of the full gain. One plausible interpretation, in light of the SwiGLU random-

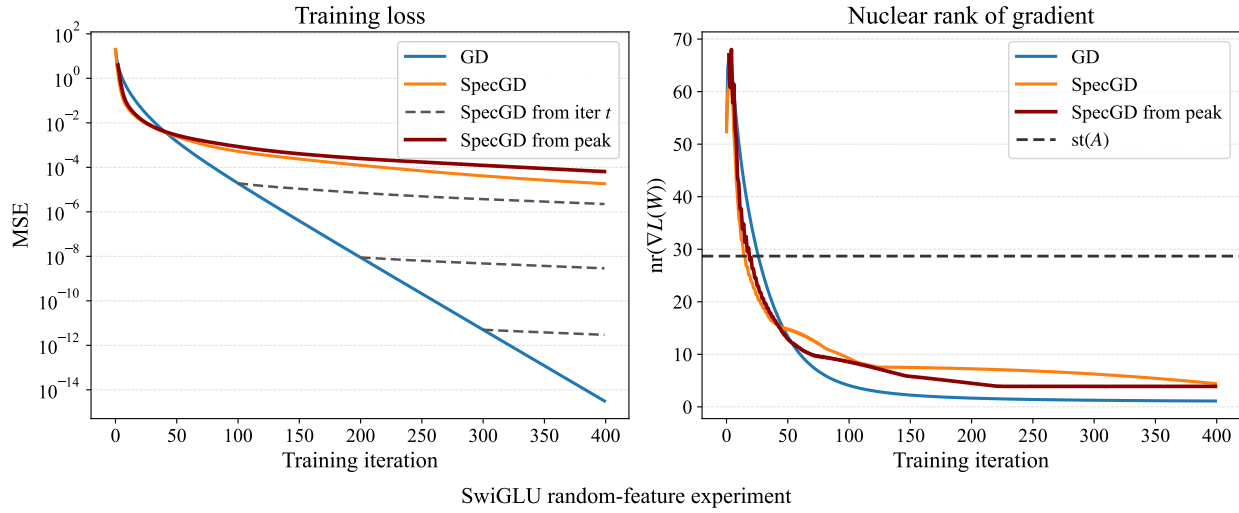


Figure 11: **A cautionary tale.** Random-feature regression with SwiGLU features $A = \text{SwiGLU}(W_1 X, W_2 X) = \text{SiLU}(W_1 X) \circ (W_2 X)$, in the same setup as Figure 3 but with the ReLU nonlinearity replaced by SwiGLU. *Left:* objective gap $\mathcal{L}(W) - \min \mathcal{L}$ along gradient descent (GD, solid blue) and spectral gradient descent (SpecGD, solid orange). Unlike the ReLU experiment in Figure 3, here SpecGD is *slower* than GD. *Right:* nuclear rank $\text{nr}(\nabla \mathcal{L}(W))$ of the gradient (solid curves) together with the stable rank $\text{st}(A)$ of the post-activations (black dashed line). Because SwiGLU yields centered post-activations at Gaussian initialization, the mean-induced spike is absent and $\text{st}(A)$ scales with width. The inequality $\text{nr}(\nabla \mathcal{L}(W)) \gtrsim \text{st}(A)$ is more easily violated during training, and the one-step guarantees from Section 1.2 predict that Euclidean updates should outperform spectral ones.

feature example above, is that gated activations produce more nearly centered, higher-stable-rank post-activations feeding W_{out} , which makes Euclidean updates on that block better conditioned and leaves less room for a spectral update to help. A detailed verification of this mechanism in large transformers would require additional ablations and lies beyond our scope here.

1.5 Related literature

We briefly discuss work on (i) spectral and norm-constrained optimizers such as **SpecGD**, **Muon**, and **Scion**, and (ii) empirical and theoretical studies of low-rank structure in gradients and activations. We focus only on results that are relevant to the structural phenomena studied in this paper.

Spectral and norm-constrained optimizers. Preconditioned Spectral Descent (PSD) and Stochastic Spectral Descent (SSD) were among the first optimizers to use spectral geometry for training deep models. Carlson et al. formulate non-Euclidean gradient descent in general Schatten norms and show that for objectives built from log-sum-exp terms (including RBMs, feedforward networks, and CNNs), the loss admits a tighter majorization bound in the Schatten- ∞ norm than in the Frobenius norm; this motivates steepest descent in the spectral norm rather than the Euclidean norm [8, 10]. Their analysis is entirely in terms of norm-dependent Lipschitz constants and matrix updates; they do not study nuclear ranks ratios of the gradient, nor connect the choice of geometry to the stable rank of the propagated data.

Muon [28] applies a similar spectral update—implemented with a Newton–Schulz approximation

to the polar factor—to the hidden layers of modern architectures and has shown strong empirical performance for NanoGPT-scale models and other large-scale training tasks. Related work by Bernstein and collaborators has advocated norm-aware training via “modular norms” and “modular duality,” helping to popularize spectral and operator-norm updates in large-scale settings and providing practical Newton–Schulz-based orthogonalization routines used in **Muon** implementations [3, 4, 35]. A recent convergence analysis of **Muon** by Shen et al. [47] is particularly close in spirit to our work. In a general nonconvex setting, they derive iteration-complexity bounds for **Muon** and GD under various smoothness assumptions and identify two key quantities: a Hessian-based ratio J_t/L_t , and the gradient nuclear ranks $\text{nr}(\nabla f(W_t))$. Their central condition (Eq. (4) in [47]) is

$$\frac{J_t}{L_t} \lesssim \frac{\|\nabla f(W_t)\|_*^2}{\|\nabla f(W_t)\|_F^2}, \quad (1.10)$$

and they show that when (1.10) holds along the trajectory, **Muon** enjoys better convergence guarantees than GD for reaching a nuclear-norm stationary point. They also empirically track J_t , L_t , and the gradient nuclear ranks during GD and **Muon** training of a small MLP, and observe that (1.10) holds in the early and middle phases of training, consistent with **Muon**’s speedup.

Our analysis is complementary. We derive a *layerwise* inequality for **SpecGD** versus GD that has the same gradient ratio on the right-hand side as Shen et al. (1.10), but replaces the Hessian ratio J_t/L_t by the *stable rank* of the post-activation matrices:

$$\text{st}(A^{\ell-1}) \lesssim \text{nr}(\nabla_{W_\ell} \mathcal{L}(W))$$

We do not claim that it is conceptually novel that the nuclear rank of the gradient controls when spectral updates are better than Euclidean updates—this is already implicit in PSD/SSD and explicit in the convergence bounds for **Muon** and related methods. Our contribution is to show that, in the setting of random-feature regression, deep neural networks, and transformers, the *left-hand side* of this inequality is naturally small (post-activations have low stable rank), while the *right-hand side* can be large (gradient nuclear rank is dimension-dependent), both theoretically (after a few GD steps in random-feature models) and empirically (in NanoGPT-scale training). This provides a concrete, data-driven explanation for the regimes where spectral updates outperform GD.

The **Scion** optimizer of Pethick et al. [42] builds a general framework of stochastic conditional gradient (LMO-based) methods with norm constraints, in which **Muon** is one special case and **Scion** corresponds to using operator norms (e.g., spectral and ℓ_∞ norms) for different layers. Their convergence guarantees are stated in terms of the dual norm of the gradient, $\|\nabla f(x)\|_*$, under L -smoothness in the corresponding primal norm, and in the spectral case this dual norm is exactly the nuclear norm. Thus their rates naturally control $\mathbb{E}\|\nabla f(x)\|_*$, while classical GD rates control $\mathbb{E}\|\nabla f(x)\|_F$. To compare these guarantees, one must again relate nuclear and Frobenius norms of the gradient, i.e., consider $\|\nabla f(x)\|_*/\|\nabla f(x)\|_F$. Pethick et al. focus on the algorithmic framework, norm choices, and hyperparameter transfer, and do not attempt to characterize when this ratio is large in neural networks.

Relation to nonlinear spiked covariance and conjugate kernel work. Our perspective is complementary to recent analyses of nonlinear spiked covariance matrices and conjugate kernels [2, 57]. There, the goal is to understand how a finite number of *informative* spikes in the input data propagate through random networks or how nonlinearity and non-Gaussianity affect the edge of the spectrum, and for this reason the activations (and weights) are explicitly centered to suppress large, non-informative outliers. Earlier work by Pennington and Worah [41] analyzes the same one-layer Gram matrix $M = \frac{1}{m}YY^\top$ with $Y = f(WX)$ in a proportional random matrix limit and derives

an explicit characterization of its limiting spectral density in terms of two Gaussian functionals of the activation; like [2, 57], they work with centered nonlinearities and focus on the bulk spectrum rather than on stable rank or mean-induced spikes. By contrast, we work with the non-centered activations used in practice (e.g. ReLU), for which even isotropic inputs generate mean-induced spikes in the post-activation covariances at every hidden layer. These spikes need not carry task-relevant signal, but they force the activation matrices to be intrinsically low-stable-rank, and it is precisely this degenerate geometry that makes spectral updates more effective than Euclidean ones in the regimes we study.

Low-rank structure in gradients and activations. There is a substantial literature documenting low-dimensional or low-rank structure in the gradients and representations of deep networks. Gur-Ari et al. [20] showed that during training, gradients quickly concentrate in a low-dimensional subspace spanned by the top Hessian eigenvectors—a “tiny subspace” whose dimension is often comparable to the number of classes [20]. This is a statement about *gradient subspace* dimension rather than nuclear rank, but it supports the general picture that most of the optimization geometry is captured by a small number of directions. More recent work in large-scale training leverages this low-rank structure explicitly: the GaLore algorithm [60] performs gradient low-rank projection to reduce optimizer memory while preserving pretraining performance, and reports empirical evidence that gradients of large language models admit very low-rank approximations; Sonthalia et al. [48] analyze low-rank gradients in two-layer networks in a spiked data model, proving that the gradient spectrum is sharply concentrated and identifying parameter and data regimes where gradient rank is small.

Huh et al. [24] empirically observe that the Gram matrix of the final-layer embeddings of deep networks has low effective rank (Observation 3.1 and 3.2), both at initialization and after training, and conjecture that deeper networks are biased toward lower effective-rank embeddings. In our notation, their Gram matrices are constructed from the columns of the post-activation matrix A_L , and effective rank is a soft-rank functional of the same spectrum as the stable rank $\text{st}(A_L)$. Our results are consistent with these observations and extend them in two directions: (i) we work with the stable rank $\text{st}(A_\ell)$ of the layerwise post-activation matrices, which is a closely related notion of effective dimensionality of the embeddings, and show theoretically in several random-feature and quadratic-activation models that $\text{st}(A_\ell)$ is bounded by a numerical constant independent of the layer width; and (ii) we verify empirically in realistic MLP and NanoGPT models that this low-stable-rank property holds across *all* intermediate layers, not only for the final embedding, and that it persists along the optimization trajectory. While we are mainly interested here in the stable rank, our results immediately imply that the “effective rank” in the sense of [24] is of order $\log(d)$.

A complementary line of work seeks to *remove* the kind of low-rank degeneracy we study by introducing normalization layers such as batch normalization [25]. For example, Daneshmand et al. [13] show that in deep *linear* networks (i.e., without nonlinear activations), batch normalization provably prevents rank collapse: the (soft) rank of the hidden activations remains of order d at all depths, whereas in the unnormalized case the representations become effectively rank one as depth grows. This line of work is complementary to ours: rather than modifying the architecture to avoid degeneracy, we take the activation matrices as they arise in standard, non-normalized networks with non-centered nonlinearities, and analyze how their low-stable-rank, spiked covariance structure influences optimization and favors spectral updates over Euclidean ones.

Finally, a parallel line of work examines the spectral structure of the Hessian itself and reports a similar “bulk + spikes” picture: Sagun et al. [46] and Papyan [40] find that deep networks have a large bulk of near-zero eigenvalues with a small number of large outliers, while Ghorbani et

al. [18] show that these outliers appear rapidly during training and that the gradient concentrates in their eigenspaces. Our stable-rank perspective is consistent with this broader view of degenerate curvature, but focuses on the propagated data matrices that directly enter the layerwise Lipschitz constants relevant for spectral versus Euclidean updates.

Organization. Section 2 gives two base cases for low-stable-rank representations: mean-induced spikes for non-centered activations and low-stable-rank token indicators/embeddings in transformers. Section 3 develops propagation rules showing that stable rank (and the column-norm regularity needed for RMSNorm) is preserved, up to explicit factors, by the atomic operations appearing in transformer blocks, and packages these rules into attention- and MLP-sublayer bounds. Sections 4 and 5 iterate these one-layer inputs to control stable rank throughout deep MLPs and decoder-only transformers at Gaussian initialization, with a regime split between mean-spike-inducing and nonMSI/gated activations. Turning to the optimization criterion, Section 6 analyzes spiked random-feature regression models and shows that gradient descent quickly produces gradients with dimension-dependent nuclear rank, thereby activating the inequality (1.6) on a macroscopic window of iterates. Finally, Section 7 introduces a general layered model, proves a mixed Hessian bound, and derives a one-step descent comparison for mixed Euclidean/spectral updates that reduces blockwise gains to the same nuclear-rank versus stable-rank condition. The appendices contain additional experiments (e.g., SwiGLU in Appendix A) and supporting concentration and linear-algebra lemmas.

2 Low-stable-rank activations: mean spikes and token-embeddings

This section identifies two sources of low-stable-rank matrices that arise naturally in the settings of this paper, and that will serve as base cases for later arguments. First, post-activation matrices for common non-centered activations, such as ReLU, have low-stable rank due to a large mean-induced spike. Second, for transformers, the input token-indicator matrix and the initial token embeddings are low-stable-rank whenever a single token (e.g., “the”) makes up at least a constant fraction of the sequence.

These results complement those of the upcoming Section 3, which show that stable rank propagates through common network operations with small inflation. Then in Sections 4 and 5 we apply the results of this section and Section 3 to conclude that all relevant post-activation matrices in MLPs and transformers have low stable rank.

2.1 Concentration of the stable rank.

A recurring object in this paper is an *activation matrix with i.i.d. feature columns*:

$$Z_n = [F(x_1), \dots, F(x_n)] \in \mathbf{R}^{d \times n}, \quad (2.1)$$

where x_1, \dots, x_n are i.i.d. and $F : \mathbf{R}^p \rightarrow \mathbf{R}^d$ is a fixed measurable map with $0 < \mathbb{E}\|F(x_1)\|_2^2 < \infty$. In the neural network setting, F is the composition of linear maps and a pointwise activation, and the canonical model is

$$Z_n = \sigma(WX), \quad X = [x_1, \dots, x_n],$$

with σ applied entrywise. Depending on the model, randomness may enter through the data or through the weights: if the columns of X are random and W is fixed, then Z_n has i.i.d. columns; if W is random and X is fixed, then Z_n has i.i.d. rows. Since $\text{st}(Z) = \text{st}(Z^\top)$, we may treat both situations using the same i.i.d.-column setup.

Henceforth, we write $Z_n = [z_1, \dots, z_n] \in \mathbf{R}^{d \times n}$ where z_1, \dots, z_n are i.i.d. copies of a random vector $z \in \mathbf{R}^d$ with $0 < \mathbb{E}\|z\|_2^2 < \infty$. Define the empirical and population second moment matrices, respectively:

$$M_n := \frac{1}{n} Z_n Z_n^\top = \frac{1}{n} \sum_{i=1}^n z_i z_i^\top \quad \text{and} \quad M := \mathbb{E}[zz^\top].$$

For a positive semidefinite matrix B , let $\text{er}(B) := \text{tr}(B)/\|B\|_{\text{op}}$ denote its *effective rank*. Since $\text{tr}(M_n) = \frac{1}{n} \|Z_n\|_F^2$ and $\|M_n\|_{\text{op}} = \frac{1}{n} \|Z_n\|_{\text{op}}^2$, we have the identity

$$\text{st}(Z_n) = \frac{\|Z_n\|_F^2}{\|Z_n\|_{\text{op}}^2} = \frac{\text{tr}(M_n)}{\|M_n\|_{\text{op}}} = \text{er}(M_n). \quad (2.2)$$

Thus, stable-rank control for Z_n reduces to effective-rank control for M_n . Since M is deterministic and typically easier to analyze than M_n , it is natural to first understand $\text{er}(M)$ and then transfer to $\text{er}(M_n)$ with reasonably high probability. Reassuringly, the next lemma records the asymptotic consistency of the estimator $\text{er}(M_n)$.

Lemma 2.1 (Consistency of the stable rank). *Let $Z_n = [z_1, \dots, z_n]$ have i.i.d. columns distributed as z with $0 < \mathbb{E}\|z\|_2^2 < \infty$, and let $M = \mathbb{E}[zz^\top]$. Then*

$$\text{st}(Z_n) \xrightarrow{\text{a.s.}} \text{er}(M) \quad \text{as } n \rightarrow \infty.$$

Proof. By the strong law of large numbers applied entrywise, $M_n \rightarrow M$ almost surely. Since $\text{tr}(M) = \mathbb{E}\|z\|_2^2 > 0$, we have $\|M\|_{\text{op}} > 0$. On the same event, $\|M_n\|_{\text{op}} \rightarrow \|M\|_{\text{op}}$ and $\text{tr}(M_n) \rightarrow \text{tr}(M)$, hence $\text{tr}(M_n)/\|M_n\|_{\text{op}} \rightarrow \text{tr}(M)/\|M\|_{\text{op}}$. Using (2.2) completes the proof. \square

Next, we aim to obtain finite sample guarantees. Since we are primarily interested in upper bounding $\text{er}(M_n)$, an upper-bound on the ratio $\text{er}(M_n)/\text{er}(M)$ suffices. Such a one-sided bound holds under very mild assumptions. In particular, a small-ball condition suffices to obtain a result of this form with constant probability; this is the content of the following theorem.

Theorem 2.2 (Constant probability from a small-ball condition). *Suppose there exists a unit vector $u_\star \in \mathbf{R}^d$ and constants $p_0 \in (0, 1)$ and $c_0 > 0$ satisfying the small-ball condition*

$$\mathbb{P}(\langle z, u_\star \rangle^2 \geq c_0 \|M\|_{\text{op}}) \geq p_0. \quad (2.3)$$

Then for any $c \in (0, \frac{1}{2})$, as long as $n \geq \frac{8}{p_0} \log \frac{1}{c}$, the upper bound

$$\text{st}(Z_n) = \text{er}(M_n) \leq \frac{2}{p_0 c_0} \cdot \text{er}(M), \quad (2.4)$$

holds with probability at least $1 - 2c$.

Proof. Since $\mathbb{E}\text{tr}(M_n) = \text{tr}(M)$, Markov's inequality implies

$$\mathbb{P}(\text{tr}(M_n) > c^{-1} \text{tr}(M)) \leq c.$$

Next, we estimate

$$\|M_n\|_{\text{op}} \geq u_\star^\top M_n u_\star = \frac{1}{n} \sum_{i=1}^n \langle z_i, u_\star \rangle^2.$$

Let $I_i := \mathbf{1}_{\{\langle z_i, u_\star \rangle^2 \geq c_0 \|M\|_{\text{op}}\}}$, so that $\mathbb{E}I_i \geq p_0$ by (2.3). Chernoff's inequality yields

$$\mathbb{P}\left(\sum_{i=1}^n I_i \leq \frac{p_0 n}{2}\right) \leq \exp\left(-\frac{p_0 n}{8}\right).$$

On the event $\{\sum_{i=1}^n I_i \geq p_0 n/2\}$, we have

$$\|M_n\|_{\text{op}} \geq \frac{1}{n} \sum_{i=1}^n \langle z_i, u_{\star} \rangle^2 \geq \frac{p_0 n}{2} \cdot \frac{c_0 \|M\|_{\text{op}}}{n} = \frac{p_0 c_0}{2} \|M\|_{\text{op}}.$$

Combining this lower bound on $\|M_n\|_{\text{op}}$ with $\text{tr}(M_n) \leq c^{-1} \text{tr}(M)$ yields (2.4). Finally, if $n \geq \frac{8}{p_0} \log \frac{1}{c}$, then $\exp(-p_0 n/8) \leq c$, so a union bound gives probability at least $1 - 2c$. \square

Although Theorem 2.2 holds under a very weak small-ball condition, it has a limitation. Namely, the probability of (2.4) not holding scales the right side of (2.4) multiplicatively. The following theorem shows that this limitation can be removed under light tail assumptions.

Theorem 2.3 (High probability upper-bound on the stable rank). *Suppose that there for some values $\theta, \phi > 0$ and $K, L > 0$ the light-tail conditions hold:*

$$\langle z - \mathbb{E}z, u \rangle_{\psi_{\theta}} \leq K \|u\|_2 \quad \forall u \in \mathbf{R}^d \quad \text{and} \quad \|\|z\|_2^2 - \mathbb{E}\|z\|_2^2\|_{\psi_{\phi}} \leq L.$$

Then there exists a constant c , depending only on θ and ϕ , such that for any $\varepsilon \in (0, 1)$ the estimate

$$\text{er}(M_n) \leq \frac{1 + \varepsilon}{1 - \varepsilon} \cdot \text{er}(M),$$

holds with probability at least

$$1 - 6 \exp \left(-c \min \left\{ \frac{n\varepsilon^2 \|M\|_{\text{op}}^2}{K^4}, \frac{n\varepsilon^2 \|M\|_{\text{op}}}{K^2}, \frac{n\varepsilon^2 \text{tr}(M)^2}{L^2}, n^{1 \wedge \frac{\theta}{2}} \left(\frac{\varepsilon \|M\|_{\text{op}}}{K^2} \right)^{\theta/2}, n^{1 \wedge \theta} \left(\frac{\varepsilon \sqrt{\|M\|_{\text{op}}}}{K} \right)^{\theta}, n^{1 \wedge \phi} \left(\frac{\varepsilon \text{tr}(M)}{L} \right)^{\phi} \right\} \right).$$

Proof. First, Theorem C.3 in the appendix directly implies $\|M_n\|_{\text{op}} \geq (1 - \varepsilon) \|M\|_{\text{op}}$ with probability at least

$$1 - 2 \exp \left(-c \left(\frac{n\varepsilon^2 \|M\|_{\text{op}}^2}{K^4} \wedge n^{1 \wedge \frac{\theta}{2}} \left(\frac{\varepsilon \|M\|_{\text{op}}}{K^2} \right)^{\theta/2} \right) \right) - 2 \exp \left(-c \left(\frac{n\varepsilon^2 \|M\|_{\text{op}}}{K^2} \wedge n^{1 \wedge \theta} \left(\frac{\varepsilon \sqrt{\|M\|_{\text{op}}}}{K} \right)^{\theta} \right) \right).$$

for some numerical constant c depending only on θ . Next, we upper bound the trace of M_n . To this end, we write

$$\text{tr}(M_n) - \text{tr}(M) = \frac{1}{n} \sum_{i=1}^n (\|z_i\|_2^2 - \mathbb{E}\|z\|_2^2).$$

Bernstein's inequality [34, Theorem 3.1] then implies $\text{tr}(M_n) \leq (1 + \varepsilon) \text{tr}(M)$ with probability

$$1 - 2 \exp \left(-c \left(\frac{n\varepsilon^2 \text{tr}(M)^2}{L^2} \wedge n^{1 \wedge \phi} \left(\frac{\varepsilon \text{tr}(M)}{L} \right)^{\phi} \right) \right),$$

which completes the proof. \square

With the concentration results in mind, we can focus on estimating the effective rank of M and then transfer back to M_n using the results we have obtained. With this in mind, we now isolate two sources of low stable ranks in post-activation matrices: mean-induced spikes (Section 2.2) and token embedding in transformers (Section 2.3).

2.2 Mean spikes

The quantity $\text{er}(M)$ is small whenever $\text{tr}(M)$ is moderate and $\|M\|_{\text{op}}$ is large. By linearity, we have

$$\text{tr}(M) = \mathbb{E} \text{tr}(zz^\top) = \mathbb{E} \|z\|_2^2. \quad (2.5)$$

If the mean $\mu := \mathbb{E}z$ is nonzero, we can estimate

$$M = \mathbb{E}[zz^\top] = \mu\mu^\top + \text{Cov}(z) \succeq \mu\mu^\top,$$

and therefore $\|M\|_{\text{op}} \geq \|\mu\|_2^2$. Consequently, we deduce

$$\text{er}(M) = \frac{\mathbb{E}\|z\|_2^2}{\|M\|_{\text{op}}} \leq \frac{\mathbb{E}\|z\|_2^2}{\|\mathbb{E}z\|_2^2}. \quad (2.6)$$

We call the ratio on the right the *(population) noise-to-signal ratio* of z :

$$\text{NSR}(z) := \frac{\mathbb{E}\|z\|_2^2}{\|\mathbb{E}z\|_2^2} \quad (\mathbb{E}z \neq 0).$$

Thus, whenever the squared norm of the mean is comparable to the second moment, the effective rank of M is small. Now, the population NSR can be approximated by its empirical counterpart. Namely, define

$$\hat{\mu} := \frac{1}{n} \sum_{i=1}^n z_i, \quad \hat{m}_2 := \frac{1}{n} \sum_{i=1}^n \|z_i\|_2^2, \quad \widehat{\text{NSR}}(Z) := \frac{\hat{m}_2}{\|\hat{\mu}\|_2^2}.$$

Then the same argument as leading to (2.6) shows

$$\text{st}(Z_n) \leq \widehat{\text{NSR}}(Z_n).$$

Reassuringly, under mild light tail assumptions, $\widehat{\text{NSR}}(Z_n)$ and $\text{NSR}(z)$ are indeed close, as the following lemma shows. We will use the usual Orlicz quasi-norm $\|z\|_{\psi_\theta}$ of a random vector z for $\theta > 0$. Namely, $\|z\|_{\psi_\theta}$ is the infimum over all values $\sigma \geq 0$ satisfying $\mathbb{E} \exp(|z/\sigma|^\theta) \leq 2$.

Lemma 2.4 (Consistency of the Empirical NSR). *Let $z \in \mathbf{R}^d$ be a random vector with mean $\mu := \mathbb{E}z \neq 0$ and finite second moment $m_2 := \mathbb{E}\|z\|_2^2$. Fix parameters $\theta, \phi > 0$ and constants $K, L > 0$ such that*

$$\|\langle z - \mu, u \rangle\|_{\psi_\theta} \leq K\|u\|_2 \quad \text{for all } u \in \mathbf{R}^d, \quad \text{and} \quad \|\|z\|_2^2 - \mathbb{E}\|z\|_2^2\|_{\psi_\phi} \leq L.$$

Let z_1, \dots, z_n be iid copies of z , and define the empirical mean and the second moment:

$$\hat{\mu} = \frac{1}{n} \sum_{i=1}^n z_i, \quad \hat{m}_2 = \frac{1}{n} \sum_{i=1}^n \|z_i\|_2^2.$$

Then there exist constants $c_1 = c_1(\theta) > 0$ and $c_2 = c_2(\phi) > 0$ such that for any $0 < \varepsilon_1 \leq 1$ and $0 < \varepsilon_2 < 1$, the estimate

$$\frac{\hat{m}_2}{\|\hat{\mu}\|_2^2} \leq \frac{1 + \varepsilon_1}{(1 - \varepsilon_2)^2} \cdot \frac{m_2}{\|\mu\|_2^2}$$

holds with probability at least

$$1 - 2 \exp \left(-c_1 \min \left\{ n \varepsilon_2^2 \frac{\|\mu\|_2^2}{K^2}, n^{1 \wedge \theta} \varepsilon_2^\theta \frac{\|\mu\|_2^\theta}{K^\theta} \right\} \right) - 2 \exp \left(-c_2 \min \left\{ n \varepsilon_1^2 \frac{m_2^2}{L^2}, n^{1 \wedge \phi} \varepsilon_1^\phi \frac{m_2^\phi}{L^\phi} \right\} \right).$$

In particular, in this event the estimate holds:

$$\text{st}(Z) \leq \frac{1 + \varepsilon_1}{(1 - \varepsilon_2)^2} \text{NSR}(z).$$

Proof. We first control the empirical mean. Let $u_\star := \mu/\|\mu\|_2$ be the unit vector in the direction of μ , and write

$$\hat{\mu} - \mu = \frac{1}{n} \sum_{i=1}^n (z_i - \mu).$$

Then $X_i := \langle z_i - \mu, u_\star \rangle$ are iid mean-zero random variables with $\|X_i\|_{\psi_\theta} \leq K$. A Bernstein-type inequality [34, Theorem 3.1] for ψ_θ random variables yields for all $t > 0$ the estimate

$$\mathbb{P}\left(\left|\frac{1}{n} \sum_{i=1}^n X_i\right| \geq t\right) \leq 2 \exp\left(-c \min\left\{n \frac{t^2}{K^2}, n^{1 \wedge \theta} \left(\frac{t}{K}\right)^\theta\right\}\right)$$

for a numerical constant $c > 0$. Setting $t = \varepsilon_2 \|\mu\|_2$ and using the estimate

$$\|\hat{\mu}\|_2 \geq \langle \hat{\mu}, u_\star \rangle = \|\mu\|_2 + \langle \hat{\mu} - \mu, u_\star \rangle,$$

we obtain

$$\mathbb{P}(\|\hat{\mu}\|_2 \leq (1 - \varepsilon_2) \|\mu\|_2) \leq 2 \exp\left(-c_1 \min\left\{n \varepsilon_2^2 \frac{\|\mu\|_2^2}{K^2}, n^{1 \wedge \theta} \varepsilon_2^\theta \frac{\|\mu\|_2^\theta}{K^\theta}\right\}\right), \quad (2.7)$$

for a numerical constant $c_1 > 0$.

We next control the empirical second moment. Define $Y_i := \|z_i\|_2^2 - m_2$. By assumption $\|Y_i\|_{\psi_\phi} \leq L$, so Y_i are iid centered ψ_ϕ random variables with parameter L . The same Bernstein-type inequality [34, Theorem 3.1] yields that for all $t > 0$,

$$\mathbb{P}\left(\left|\frac{1}{n} \sum_{i=1}^n Y_i\right| \geq t\right) \leq 2 \exp\left(-c_2 \min\left\{n \frac{t^2}{L^2}, n^{1 \wedge \phi} \left(\frac{t}{L}\right)^\phi\right\}\right),$$

for a numerical constant $c_2 > 0$. Substituting $t = \varepsilon_1 m_2$ yields

$$\mathbb{P}(\hat{m}_2 > (1 + \varepsilon_1) m_2) \leq 2 \exp\left(-c_2 \min\left\{n \varepsilon_1^2 \frac{m_2^2}{L^2}, n^{1 \wedge \phi} \varepsilon_1^\phi \frac{m_2^\phi}{L^\phi}\right\}\right). \quad (2.8)$$

Combining (2.7) and (2.8) and taking a union bound over the two events completes the proof. \square

2.2.1 Bounding the effective rank for random data: polynomial maps

We are now ready to establish our first main result. Namely, we will bound $\text{er}(M)$ for *squares of polynomial functions applied to Gaussian inputs*. This covers, for example, a single layer $Z_n = \sigma_{\text{sq}}(WX)$ with a quadratic activation $\sigma_{\text{sq}}(t) := t^2$ and when the columns of X are i.i.d. Gaussian, and more generally, deeper layers of the form $Z_n = \sigma_{\text{sq}}(W[F(x_1), \dots, F(x_n)])$ where the coordinate functions of F are polynomials. Our strategy is to show that the population NSR is small and then pass to the empirical counterpart using Theorem 2.2 and the Paley-Zygmund inequality.

Theorem 2.5 (Stable rank for polynomial-square features under Gaussian data). *Let $x_1, \dots, x_n \in \mathbf{R}^p$ be iid Gaussian, and let $f_1, \dots, f_d : \mathbf{R}^p \rightarrow \mathbf{R}$ be polynomials of degree at most $q \geq 1$. Define the feature map*

$$F(x) := (f_1(x)^2, \dots, f_d(x)^2) \in \mathbf{R}^d, \quad Z_n := [F(x_1), \dots, F(x_n)] \in \mathbf{R}^{d \times n}.$$

Then for any $c \in (0, \frac{1}{2})$, as long as $n \geq 18 \cdot 3^{4q} \log \frac{1}{c}$, the bound

$$\text{st}(Z_n) \leq \frac{27}{2c} \cdot 3^{6q}$$

holds with probability at least $1 - 2c$.

Proof. Set $z := F(x) \in \mathbf{R}^d$ for a single Gaussian draw x , and set $M = \mathbb{E}[zz^\top]$. If $\mathbb{E}\|z\|_2^2 = 0$ then $Z_n = 0$ almost surely and the claim is trivial, so assume $\mathbb{E}\|z\|_2^2 > 0$. Since at least one f_j is not identically zero, we have $\mathbb{E}[f_j(x)^2] > 0$ for that j , hence $\mathbb{E}z \neq 0$ and $\text{NSR}(z)$ is well-defined.

We aim to apply Theorem 2.2. To this end, we first verify the small ball condition (2.3). Let u_\star be a top-eigenvector of M and set $g(x) := \langle F(x), u_\star \rangle$. Then $\mathbb{E}[g(x)^2] = \|M\|_{\text{op}}$ and g is a polynomial of degree at most $2q$. Using Gaussian hypercontractivity [37, Chapter 3.2], we deduce

$$\mathbb{E}[g(x)^4] \leq 3^{4q} (\mathbb{E}[g(x)^2])^2.$$

Therefore, the Paley–Zygmund inequality gives

$$\mathbb{P}\left(g(x)^2 \geq \frac{1}{3} \mathbb{E}[g(x)^2]\right) \geq \left(1 - \frac{1}{3}\right)^2 \frac{(\mathbb{E}[g(x)^2])^2}{\mathbb{E}[g(x)^4]} \geq \frac{4}{9} \cdot 3^{-4q}.$$

Thus the small ball condition (2.3) holds with $c_0 = 1/3$ and $p_0 = \frac{4}{9} 3^{-4q}$. With these constants, Theorem 2.2 shows that in the regime $n \geq \frac{8}{p_0} \log \frac{1}{c} = 18 \cdot 3^{4q} \log \frac{1}{c}$, with probability at least $1 - 2c$, we have

$$\text{st}(Z_n) \leq \frac{2}{p_0 c_0 c} \text{er}(M) = \frac{27}{2c} \cdot 3^{4q} \text{er}(M). \quad (2.9)$$

It remains to upper bound $\text{er}(M)$. To this end, since $\mathbb{E}z \neq 0$, equation (2.6) implies $\text{er}(M) \leq \text{NSR}(z)$. Writing $z = (z_1, \dots, z_d)$ with $z_j = f_j(x)^2$, we have

$$\text{NSR}(z) = \frac{\mathbb{E}\|z\|_2^2}{\|\mathbb{E}z\|_2^2} = \frac{\sum_{j=1}^d \mathbb{E}[z_j^2]}{\sum_{j=1}^d (\mathbb{E}z_j)^2} \leq \max_{1 \leq j \leq d} \frac{\mathbb{E}[z_j^2]}{(\mathbb{E}z_j)^2} = \max_{1 \leq j \leq d} \frac{\mathbb{E}[f_j(x)^4]}{(\mathbb{E}[f_j(x)^2])^2}.$$

Each f_j has degree at most q , so hypercontractivity gives $\mathbb{E}[f_j(x)^4] \leq 3^{2q} (\mathbb{E}[f_j(x)^2])^2$, and hence $\text{er}(M) \leq \text{NSR}(z) \leq 3^{2q}$. Substituting this into (2.9) yields

$$\text{st}(Z_n) \leq \frac{27}{2c} \cdot 3^{4q} \cdot 3^{2q} = \frac{27}{2c} \cdot 3^{6q},$$

on the same event, completing the proof. \square

In particular, for a depth L feedforward neural network with quadratic activation functions σ_{sq} in each layer, Theorem 2.5 shows that with fixed weight matrices W_1, \dots, W_L and random Gaussian data X , the stable rank of the final post-activation matrix A^L is bounded by $\text{st}(A^L) \leq \frac{27}{2c} 3^{3 \cdot 2^L}$ with probability at least $1 - 2c$.

Theorem 2.5 gives a dimension-free stable-rank bound in a random-data regime, but only with constant probability and with a dependence that is exponential in the polynomial degree (hence doubly exponential in the depth for quadratic compositions). We now turn to the random-weights regime, where we obtain bounds for general activations.

2.2.2 Bounding the stable rank with random weights: polynomial-growth activations

We now return to the canonical post-activation matrix $A = \sigma(WX)$ with random weights W and fixed input X . In this regime the *rows* of A are iid; we therefore apply the iid-column bounds in Lemma 2.4 to A^\top , using the equality $\text{st}(A) = \text{st}(A^\top)$. The remaining work is to express the population NSR of $\sigma(X^\top w)$ (with Gaussian w) in terms of one-dimensional Gaussian moments of

σ over the range of nonzero column norms of X . To this end, let $\gamma \sim \mathcal{N}(0, 1)$. For $0 < a \leq b < \infty$ and $q > 0$, define the two quantities:

$$s_\sigma(a, b) := \sup_{s \in [a, b]} \frac{\mathbb{E}[\sigma(s\gamma)^2]}{(\mathbb{E}[\sigma(s\gamma)])^2} \quad \text{and} \quad \kappa_{\sigma, q}(a, b) := \inf_{s \in [a, b]} \frac{|\mathbb{E}[\sigma(s\gamma)]|}{s^q}.$$

Note that these quantities simplify drastically for the important case of q -homogeneous activations, meaning those satisfying $\sigma(\alpha t) = \alpha^q \sigma(t)$ for all $t \in \mathbf{R}$, $\alpha \geq 0$. For such functions, both $s_\sigma(a, b)$ and $\kappa_{\sigma, q}(a, b)$ are independent of a and b and reduce to $s_\sigma(a, b) = \frac{\mathbb{E}\sigma(\gamma)^2}{(\mathbb{E}\sigma(\gamma))^2}$ and $\kappa_{\sigma, q}(a, b) = |\mathbb{E}\sigma(\gamma)|$.

The following theorem estimates the stable rank of $A = \sigma(WX)$; without loss of generality, we assume that none of the columns of X are the zero vector since zero columns can simply be deleted.

Theorem 2.6 (Gaussian weights yield low stable rank). *Fix a matrix $X = [x_1, \dots, x_n] \in \mathbf{R}^{d \times n}$ with nonzero columns and let $W \in \mathbf{R}^{m \times d}$ have iid entries $\mathcal{N}(0, \frac{1}{d})$. Define the post-activation matrix $A = \sigma(WX) \in \mathbf{R}^{m \times n}$, where $\sigma : \mathbf{R} \rightarrow \mathbf{R}$ satisfies $\sigma(0) = 0$ and the polynomial growth bound*

$$|\sigma(t)| \leq L_\sigma |t|^p \quad \text{for all } t \in \mathbf{R},$$

for some $p \geq 1$ and $L_\sigma < \infty$. Set

$$a := \frac{1}{\sqrt{d}} \min_{1 \leq t \leq n} \|x_t\|_2, \quad b := \frac{1}{\sqrt{d}} \max_{1 \leq t \leq n} \|x_t\|_2.$$

Fix a constant $q > 0$ satisfying $\kappa_{\sigma, q}(a, b) > 0$ and define the scale ratio

$$r_{p, q} := \frac{L_\sigma}{\kappa_{\sigma, q}(a, b)} \cdot \sup_{s \in [a, b]} s^{p-q}.$$

Then there exists a constant $c = c(p) > 0$ such that for any $0 < \varepsilon_1 \leq 1$ and $0 < \varepsilon_2 < 1$, with probability at least

$$1 - 2 \exp\left(-c \min\left\{m \varepsilon_2^2 r_{p, q}^{-2}, m^{1 \wedge \frac{2}{p}} \varepsilon_2^{2/p} r_{p, q}^{-2/p}\right\}\right) - 2 \exp\left(-c \min\left\{m \varepsilon_1^2 r_{p, q}^{-4}, m^{1 \wedge \frac{1}{p}} \varepsilon_1^{1/p} r_{p, q}^{-2/p}\right\}\right),$$

we have

$$\text{st}(A) \leq \frac{1 + \varepsilon_1}{(1 - \varepsilon_2)^2} s_\sigma(a, b).$$

Proof. Write the rows of W as $w_1^\top, \dots, w_m^\top$. Since $\text{st}(A) = \text{st}(A^\top)$ and

$$A^\top = [\sigma(X^\top w_1), \dots, \sigma(X^\top w_m)] \in \mathbf{R}^{n \times m},$$

the columns of A^\top are iid copies of $z := \sigma(X^\top w) \in \mathbf{R}^n$ with $w \sim \mathcal{N}(0, \frac{1}{d} I_d)$.

Applying Lemma 2.4 with sample size m yields the estimate

$$\text{st}(A) = \text{st}(A^\top) \leq \frac{1 + \varepsilon_1}{(1 - \varepsilon_2)^2} \text{NSR}(z),$$

with probability

$$1 - 2 \exp\left(-c_1 \min\left\{m \varepsilon_2^2 \frac{\|\mu\|_2^2}{K^2}, m^{1 \wedge \theta} \varepsilon_2^\theta \frac{\|\mu\|_2^\theta}{K^\theta}\right\}\right) - 2 \exp\left(-c_2 \min\left\{m \varepsilon_1^2 \frac{m_2^2}{L^2}, m^{1 \wedge \phi} \varepsilon_1^\phi \frac{m_2^\phi}{L^\phi}\right\}\right). \quad (2.10)$$

It remains now to estimate $\text{NSR}(z)$, $\|\mu\|_2^2$, K , θ , ϕ , which we do in order. Observe $g_t := \langle w, x_t \rangle \sim \mathcal{N}(0, s_t^2)$ with $s_t = \frac{1}{\sqrt{d}} \|x_t\|_2 \in [a, b]$. Therefore, we deduce

$$\text{NSR}(z) = \frac{\sum_t \mathbb{E}[\sigma(g_t)^2]}{\sum_t (\mathbb{E}[\sigma(g_t)])^2} = \frac{\sum_t \mathbb{E}[\sigma(s_t \gamma)^2]}{\sum_t (\mathbb{E}[\sigma(s_t \gamma)])^2} \leq \max_t \frac{\mathbb{E}[\sigma(s_t \gamma)^2]}{(\mathbb{E}[\sigma(s_t \gamma)])^2} \leq s_\sigma(a, b),$$

where γ is a standard Gaussian.

Next, noting $\kappa_{\sigma, q}(a, b) > 0$ and $s_t \in [a, b]$, we have $|\mathbb{E}[\sigma(g_t)]| \geq \kappa_{\sigma, q}(a, b) s_t^q$ for all t , and therefore

$$\|\mu\|_2^2 = \sum_t (\mathbb{E}[\sigma(g_t)])^2 \geq \kappa_{\sigma, q}(a, b)^2 \sum_t s_t^{2q}. \quad (2.11)$$

In order to bound the tail growth, we use only the polynomial growth bound $|\sigma(t)| \leq L_\sigma |t|^p$. Namely, for any $u \in \mathbf{R}^n$, using $|x - \mathbb{E}x| \leq |x| + \mathbb{E}|x|$ we have

$$|\langle z - \mu, u \rangle| = \left| \sum_t u_t (\sigma(g_t) - \mathbb{E}\sigma(g_t)) \right| \leq \sum_t |u_t| |\sigma(g_t)| + \sum_t |u_t| \mathbb{E}|\sigma(g_t)|.$$

Using $|\sigma(t)| \leq L_\sigma |t|^p$ and Cauchy–Schwarz, we deduce

$$\sum_t |u_t| |\sigma(g_t)| \leq L_\sigma \sum_t |u_t| |g_t|^p \leq L_\sigma \|u\|_2 \left(\sum_t |g_t|^{2p} \right)^{1/2}.$$

Moreover, since $\mathbb{E}|\sigma(g_t)| \leq L_\sigma \mathbb{E}|g_t|^p = L_\sigma s_t^p \mathbb{E}|\gamma|^p$, another application of Cauchy–Schwarz gives

$$\sum_t |u_t| \mathbb{E}|\sigma(g_t)| \leq \|u\|_2 \left(\sum_t (\mathbb{E}|\sigma(g_t)|)^2 \right)^{1/2} \leq C_p L_\sigma \|u\|_2 \left(\sum_t s_t^{2p} \right)^{1/2},$$

for some constant C_p that depends only on p . To bound the $\psi_{2/p}$ norm of $(\sum_t |g_t|^{2p})^{1/2}$, set $a_t := |g_t|^p$ and $X := (\sum_t a_t^2)^{1/2}$. Fixing $r \geq 2$, the Minkowski's inequality in $L_{r/2}$ implies

$$\|X\|_{L_r}^2 = \left\| \sum_t a_t^2 \right\|_{L_{r/2}} \leq \sum_t \|a_t^2\|_{L_{r/2}} = \sum_t \|a_t\|_{L_r}^2,$$

and hence

$$\|X\|_{L_r} \leq \left(\sum_t \|a_t\|_{L_r}^2 \right)^{1/2}.$$

For $1 \leq r \leq 2$, by monotonicity of L_r norms we have $\|X\|_{L_r} \leq \|X\|_{L_2}$, and the same bound follows from the case $r = 2$. Since $g_t \sim \mathcal{N}(0, s_t^2)$, we have $\|a_t\|_{L_r} = \|g_t\|_{L_r} = \|g_t\|_{L_{pr}}^p \leq C_p r^{p/2} s_t^p$, for some constant C_p depending only on p . Therefore, for all $r \geq 1$, we obtain

$$\|X\|_{L_r} \leq C_p r^{p/2} \left(\sum_t s_t^{2p} \right)^{1/2}.$$

By the standard equivalence between moment growth and Orlicz norms (with constants depending only on p), we have

$$\|X\|_{\psi_{2/p}} \leq C_p \left(\sum_t s_t^{2p} \right)^{1/2}.$$

Combining the bounds above yields

$$\|\langle z - \mu, u \rangle\|_{\psi_{2/p}} \leq C_p L_\sigma \left(\sum_t s_t^{2p} \right)^{1/2} \|u\|_2.$$

This verifies the first hypothesis of Lemma 2.4 with $\theta = 2/p$ and $K \leq C_p L_\sigma \left(\sum_t s_t^{2p} \right)^{1/2}$.

For the second hypothesis, define $Y := \|z\|_2^2 - \mathbb{E}\|z\|_2^2 = \sum_t (\sigma(g_t)^2 - \mathbb{E}\sigma(g_t)^2)$. For any $r \geq 1$, Minkowski's inequality gives

$$\|Y\|_{L_r} \leq \sum_t \|\sigma(g_t)^2 - \mathbb{E}\sigma(g_t)^2\|_{L_r} \leq 2 \sum_t \|\sigma(g_t)^2\|_{L_r}.$$

Using $|\sigma(t)| \leq L_\sigma |t|^p$ and $g_t \sim \mathcal{N}(0, s_t^2)$, we have

$$\|\sigma(g_t)^2\|_{L_r} \leq L_\sigma^2 \|g_t\|_{L_r}^{2p} = L_\sigma^2 \|g_t\|_{L_{2pr}}^{2p} \leq C_p L_\sigma^2 r^p s_t^{2p}.$$

Therefore $\|Y\|_{L_r} \leq C_p L_\sigma^2 r^p \sum_t s_t^{2p}$, and by the standard equivalence between moment growth and Orlicz norms (with constants depending only on p), we obtain

$$\|\|z\|_2^2 - \mathbb{E}\|z\|_2^2\|_{\psi_{1/p}} = \|Y\|_{\psi_{1/p}} \leq C_p L_\sigma^2 \sum_t s_t^{2p}.$$

This verifies the second hypothesis of Lemma 2.4 with $\phi = 1/p$ and $L \leq C_p L_\sigma^2 \sum_t s_t^{2p}$.

Finally, since $s_t \in [a, b]$ for all t , we have $s_t^{2p} \leq (\sup_{s \in [a, b]} s^{p-q})^2 s_t^{2q}$ and hence

$$\sum_t s_t^{2p} \leq \left(\sup_{s \in [a, b]} s^{p-q} \right)^2 \sum_t s_t^{2q}.$$

Combining this with (2.11) and $m_2 \geq \|\mu\|_2^2$ shows that

$$\frac{\|\mu\|_2^2}{K^2} \geq c r_{p,q}^{-2}, \quad \frac{m_2^2}{L^2} \geq c r_{p,q}^{-4}, \quad \frac{m_2^{1/p}}{L^{1/p}} \geq c r_{p,q}^{-2/p}, \quad \frac{\|\mu\|_2^{2/p}}{K^{2/p}} \geq c r_{p,q}^{-2/p},$$

for a constant $c > 0$ depending only on p . Substituting these bounds into (2.10) yields the stated probability bound. \square

As a concrete illustration, Table 4 instantiates Theorem 2.6 for a number of common activation functions.

Theorem 2.6 becomes particularly simple for q -homogeneous functions.

Corollary 2.7 (Gaussian weights yield low stable rank, the case of q -homogeneous functions). *Fix a matrix $X = [x_1, \dots, x_n] \in \mathbf{R}^{d \times n}$ with nonzero columns and let $W \in \mathbf{R}^{m \times d}$ have iid entries $\mathcal{N}(0, \frac{1}{d})$. Define the post-activation matrix $A = \sigma(WX) \in \mathbf{R}^{m \times n}$, where $\sigma : \mathbf{R} \rightarrow \mathbf{R}$ satisfies $\sigma(0) = 0$, is q -homogeneous for some $q \geq 1$, and has nonzero mean $\mu_\sigma := \mathbb{E}[\sigma(\gamma)] \neq 0$ with respect to the standard gaussian γ . Then there exists a constant $c > 0$, which depends only on q , $\sigma(1)$, $\sigma(-1)$, μ_σ such that for any $0 < \varepsilon_1 \leq 1$ and $0 < \varepsilon_2 < 1$, with probability at least*

$$1 - 2 \exp \left(-c \min \left\{ m \varepsilon_2^2, m^{1 \wedge \frac{2}{q}} \varepsilon_2^{2/q} \right\} \right) - 2 \exp \left(-c \min \left\{ m \varepsilon_1^2, m^{1 \wedge \frac{1}{q}} \varepsilon_1^{1/q} \right\} \right),$$

we have

$$\text{st}(A) \leq \frac{1 + \varepsilon_1}{(1 - \varepsilon_2)^2} \frac{\mathbb{E}[\sigma(\gamma)^2]}{(\mathbb{E}[\sigma(\gamma)])^2},$$

Activation $\sigma(t)$	(p, q)	$s_\sigma(a, b)$	Upper bound on $r_{p,q}(a, b)$
Absolute value $ t $	$(1, 1)$	$\frac{\pi}{2}$	$\sqrt{\frac{\pi}{2}}$
ReLU t_+	$(1, 1)$	π	$\sqrt{2\pi}$
Leaky ReLU $\alpha t \mathbf{1}_{\{t \geq 0\}} + \beta t \mathbf{1}_{\{t < 0\}}$ ($\alpha > \beta$)	$(1, 1)$	$\frac{\pi(\alpha^2 + \beta^2)}{(\alpha - \beta)^2}$	$\sqrt{2\pi} \frac{\max\{ \alpha , \beta \}}{\alpha - \beta}$
Squared ReLU $(t_+)^2$	$(2, 2)$	6	2
Quadratic t^2	$(2, 2)$	3	1
GELU $t \Phi(t)$	$(1, 1)$	$s_\sigma(a, b) \leq 2\pi \left(1 + \frac{1}{a^2}\right) \left(1 + \frac{1}{\sqrt{2\pi e}}\right) \frac{\sqrt{2\pi(1 + a^2)}}{a}$	

Table 4: The pairs (p, q) correspond to the growth bound $|\sigma(t)| \leq L_\sigma |t|^p$ and the mean lower bound $\kappa_{\sigma,q}(a, b) > 0$. For homogeneous activations in the table, $s_\sigma(a, b)$ and $r_{p,q}(a, b)$ are scale-invariant. For GELU, the mean scales like s^2 as $s \downarrow 0$, so $s_\sigma(a, b)$ grows as a^{-2} and $r_{1,1}(a, b)$ grows as a^{-1} .

2.3 Token indicator matrices and Gaussian embeddings

We next establish a base case for transformers. We prove that the token-indicator matrix of a fixed sequence has stable rank exactly $1/p_{\max}$, where p_{\max} is the empirical frequency of the most common token; in typical corpora this is a small number due to heavy-tailed token frequencies. We then show that a Gaussian embedding layer maps this indicator structure to an embedding matrix whose stable rank is controlled by the same p_{\max} up to a constant factor.

Let (i_1, \dots, i_n) be a sequence of tokens with $i_t \in \{1, \dots, V\}$, and let $H \in \mathbf{R}^{V \times n}$ denote the matrix whose t -th column h_t is the standard basis vector with a single 1 in position i_t and zeros elsewhere. For each token $j \in \{1, \dots, V\}$, define

$$c_j := |\{t : i_t = j\}| \quad \text{and} \quad p_j := \frac{c_j}{n},$$

and set

$$p_{\max} := \max_{1 \leq j \leq V} p_j.$$

Then HH^\top is the diagonal matrix with entries c_1, \dots, c_V and therefore

$$\|H\|_{\text{op}}^2 = \lambda_{\max}(HH^\top) = \max_{1 \leq j \leq V} c_j = np_{\max}.$$

On the other hand, $\|H\|_F^2$ simply counts the number of nonzero entries of H , which is n , and therefore

$$\text{st}(H) = \frac{\|H\|_F^2}{\|H\|_{\text{op}}^2} = \frac{n}{np_{\max}} = \frac{1}{p_{\max}}. \quad (2.12)$$

Thus the stable rank of the raw token-indicator matrix is exactly the inverse of the empirical frequency of the most common token. In the NanoGPT experiment of Figure 10, we saw that $\text{st}(H) \approx 26$ throughout training, and hence $p_{\max} \approx 1/26$. That this ratio is low is not so surprising. Indeed, this is consistent with a Zipf-type law $p_j \propto j^{-s}$ over a vocabulary of size $V = 50,257$, for which the observed p_{\max} corresponds to an exponent $s \approx 0.86$.

We now turn to the embedding matrix. Let $E \in \mathbf{R}^{d \times V}$ denote the embedding matrix, whose columns e_1, \dots, e_V are sampled independently from $\mathcal{N}(0, I_d)$. For the fixed sequence of n tokens (i_1, \dots, i_n) we form the embedded data matrix

$$X = [x_1, \dots, x_n] \in \mathbf{R}^{d \times n}, \quad x_t := e_{i_t}.$$

Recall that c_j and p_j denote the empirical counts and frequencies of token j , and $p_{\max} := \max_j p_j$.

Lemma 2.8 (Token embeddings have low stable rank). *Then there exists a universal constants $C > 0$ such that for any $\varepsilon \in (0, 1)$ we have*

$$\mathbb{P}\left(\text{st}(X) \leq \frac{1+\varepsilon}{1-\varepsilon} \frac{1}{p_{\max}}\right) \geq 1 - 4 \exp(-C\varepsilon^2 d).$$

Proof. Define the set of distinct tokens and its cardinality, respectively:

$$S := \{j : c_j > 0\} \quad \text{and} \quad m := |S|$$

Note that we may write

$$XX^\top = \sum_{j \in S} c_j e_j e_j^\top, \quad \text{tr}(XX^\top) = \sum_{j \in S} c_j \|e_j\|_2^2.$$

Let $j_\star \in S$ attain the maximum count $c_{j_\star} = np_{\max}$. Since $XX^\top \geq c_{j_\star} e_{j_\star} e_{j_\star}^\top$, we have

$$\|X\|_{\text{op}}^2 = \lambda_{\max}(XX^\top) \geq c_{j_\star} \|e_{j_\star}\|_2^2.$$

Consequently, we have

$$\text{st}(X) = \frac{\text{tr}(XX^\top)}{\lambda_{\max}(XX^\top)} \leq \frac{\sum_{j \in S} c_j \|e_j\|_2^2}{c_{j_\star} \|e_{j_\star}\|_2^2}. \quad (2.13)$$

We control the numerator and denominator in (2.13) on a high-probability event.

Beginning with the denominator in (2.13), we observe that the standard χ^2 lower tail bound (e.g. [55, Theorem 3.1.1]) implies

$$\mathbb{P}(\|e_{j_\star}\|_2^2 < (1-\varepsilon)d) \leq 2 \exp(-C\varepsilon^2 d), \quad (2.14)$$

for a universal constant $C > 0$. Moving on to the numerator in (2.13), define

$$T := \text{tr}(XX^\top) = \sum_{j \in S} c_j \|e_j\|_2^2.$$

Note that the triangle inequality for the sub-exponential norm implies $\|e_j\|_2^2 - d\|_{\psi_1} \lesssim d$. Note moreover $\mathbb{E}[T] = d \sum_{j \in S} c_j = dn$. Therefore, Bernstein's inequality [55, Corollary 2.9.2] ensures

$$\mathbb{P}(T > (1+\varepsilon)dn) = \mathbb{P}\left(\sum_{j \in S} c_j (\|e_j\|_2^2 - d) > \varepsilon dn\right) \leq 2 \exp\left(-C\left(\frac{\varepsilon^2 n^2}{\sum_{j \in S} c_j^2} \wedge \frac{\varepsilon}{p_{\max}}\right)\right) \quad (2.15)$$

for some numerical constant C . Since $\sum_{j \in S} c_j^2 \leq c_{j_\star} \cdot \sum_{j \in S} c_j = (np_{\max})n = n^2 p_{\max}$, we have $n^2 / \sum_{j \in S} c_j^2 \geq 1/p_{\max} \geq 1$, and therefore the right side of (2.15) is bounded by $2 \exp(-C\varepsilon^2 d)$. Taking a union bound over the two events and continuing with (2.13), we deduce that with probability at least $1 - 4 \exp(-C\varepsilon^2 d)$, we have $\text{st}(X) \leq \frac{(1+\varepsilon)dn}{(1-\varepsilon)c_{j_\star}d} = \frac{1+\varepsilon}{1-\varepsilon} \frac{1}{p_{\max}}$ as claimed. \square

Thus, under the Gaussian embedding model, the activations entering the *first* transformer block already have low stable rank whenever the empirical token distribution is not too uniform (equivalently, whenever p_{\max} is not too small). In particular, if p_{\max} is bounded below by a numerical constant, then both X and A^{rms} have stable rank $O(1)$ at initialization. Interestingly, even though $1/p_{\max}$ is an exact formula for $\text{st}(H)$, we see from Figure 10 that the bound $\text{st}(E) \leq 1/p_{\max}$ is generally loose.

3 Propagation of the stable rank

In the previous section, we showed that a nonzero mean of the activation function (e.g. ReLU) typically forces the post-activation matrix to have a low stable rank. In this section, we prove propagation bounds at Gaussian initialization for the standard building blocks used in transformer blocks (pointwise nonlinearities, residual connections, gating, and RMSNorm): the stable rank of the output is controlled by the stable ranks of the matrices entering the operation, up to explicit factors. We first establish these bounds for the individual (atomic) operations, and then package them into layerwise bounds for attention and MLP sublayers.

Since the propagation results for the RMSNorm depend on per-column ℓ_2 norms, we also record the column-norm regularity needed to apply it under iteration. As shown earlier for transformer input sequences (see Section 2.3), the embedding layer already produces a data matrix with a low stable rank. Iterating the rules proved here, we conclude in Section 5 that the propagated data matrices inside the transformer tend to have low stable rank as well.

3.1 Atomic operations

We first analyze a series of atomic operations that roughly preserve low-stable rank structure. In order to streamline the reading, we provide in the following table a glossary of the main theorems in the section.

Linear activation	Nonlinear activation	Residual connection	RMSnorm	Gating
Theorem 3.1	Theorem 3.4	Theorem 3.5	Theorem 3.2	Theorem 3.8

3.1.1 Linear layer

We begin by analyzing the stable rank of the post-activation matrix of a linear layer. This is the content of the following theorem.

Theorem 3.1 (Linear activation). *Let $W \in \mathbf{R}^{k \times d}$ have iid Gaussian entries $\mathcal{N}(0, \frac{1}{d})$ and fix a matrix $X \in \mathbf{R}^{d \times n}$. Then there exists a constant $c > 0$ such that for any $\varepsilon \in (0, 1)$ we have*

$$(1 - \varepsilon) \frac{1}{d} \|X\|_F^2 \leq \frac{1}{k} \|WX\|_F^2 \leq (1 + \varepsilon) \frac{1}{d} \|X\|_F^2, \quad (3.1)$$

$$(1 - \varepsilon) \frac{1}{d} \|X\|_{\text{op}}^2 \leq \frac{1}{k} \|WX\|_{\text{op}}^2 \quad (3.2)$$

with probability at least $1 - 4 \exp(-c\varepsilon^2 k)$. Consequently, in this event the estimate holds:

$$\text{st}(WX) \leq \frac{1 + \varepsilon}{1 - \varepsilon} \cdot \text{st}(X).$$

Proof. Forming a singular value decomposition of X , and using orthogonal invariance of Gaussian matrices we see that the singular values of WX have the same distribution as those of $W\Sigma$, where Σ is the diagonal matrix with the singular values $\{s_i\}_{i=1}^d$ of X on the diagonal. Now we may write

$$\|W\Sigma\|_F^2 - \frac{k}{d}\|X\|_F^2 = \sum_{i=1}^d s_i^2 (\|w_i\|_2^2 - \frac{k}{d}),$$

where w_i are the columns of W . Classically, we have the sub-exponential bound $\|\|w_i\|_2^2 - \frac{k}{d}\|_{\psi_1} \lesssim \frac{1}{d}$; see e.g. [55, Theorem 3.1.1]. Therefore, Bernstein's inequality [55, Theorem 2.8.2] yields for any $t \geq 0$ the estimate:

$$\mathbb{P}(|\|W\Sigma\|_F^2 - \frac{k}{d}\|X\|_F^2| \geq t) \leq 2 \exp\left(-c \cdot \min\left(\frac{d^2 t^2}{\sum_{i=1}^d s_i^4}, \frac{dt}{\max_i s_i^2}\right)\right).$$

Setting $t = \varepsilon \frac{k}{d} \|X\|_F^2$ and noting that $\|s\|_2^4/\|s\|_4^4 \geq \|s\|_2^2/\|s\|_\infty^2$ completes the proof of (3.1).

Now clearly, we have $\|W\Sigma\|_{\text{op}}^2 \geq s_1^2 \|w_1\|_2^2$, where s_1 is the maximal singular value of X and $w_1 \sim \mathcal{N}(0, \frac{1}{d} I_k)$ is the first column of W . Taking into account concentration of the norm [55, Theorem 3.1.1], we deduce that with probability at least $1 - \exp(-ck\varepsilon^2)$, we have $\|w_1\|_2^2 \geq (1 - \varepsilon) \frac{k}{d}$, which completes the proof. \square

3.1.2 RMSNorm layer

Next, we analyze the propagation of the stable rank through an RMSNorm block, which rescales all the columns in the data matrix $X \in \mathbf{R}^{d \times n}$ to have ℓ_2 -norm \sqrt{d} .

Theorem 3.2 (RMSNorm). *Let $X = [x_1, \dots, x_n] \in \mathbf{R}^{d \times n}$ be a deterministic matrix whose columns satisfy*

$$L \leq \|x_t\|_2 \leq U \quad \text{for all } t = 1, \dots, n,$$

for some values $0 < L \leq U < \infty$. Define the matrix

$$A^{\text{rms}} := \text{RMSNorm}(X) \quad \text{with columns} \quad a_t := \sqrt{d} \frac{x_t}{\|x_t\|_2}.$$

Then the estimate holds:

$$\text{st}(A^{\text{rms}}) \leq \frac{U}{L} \text{st}(X).$$

Proof. Let D be the diagonal matrix with diagonal entries $D_{tt} := \sqrt{d}/\|x_t\|_2$, so that we may write $A^{\text{rms}} = XD$. The bounds on column norms imply

$$\sqrt{\frac{d}{U}} \leq D_{tt} \leq \sqrt{\frac{d}{L}} \quad \text{for all } t.$$

Setting $s_{\min} := \sqrt{\frac{d}{U}}$ and $s_{\max} := \sqrt{\frac{d}{L}}$ we therefore deduce

$$s_{\min} \|X\|_{\text{op}} \leq \|A^{\text{rms}}\|_{\text{op}} \leq s_{\max} \|X\|_{\text{op}}.$$

On the other hand, we have

$$\|A^{\text{rms}}\|_F^2 = \sum_{t=1}^n \|a_t\|_2^2 = nd.$$

Combining these facts and using the estimate $\|X\|_F^2 \geq nL$ yields

$$\text{st}(A^{\text{rms}}) = \frac{\|A^{\text{rms}}\|_F^2}{\|A^{\text{rms}}\|_{\text{op}}^2} \leq \frac{nd}{s_{\min}^2 \|X\|_{\text{op}}^2} = \frac{U}{d} \frac{nd}{\|X\|_{\text{op}}^2} \leq \frac{U}{L} \frac{\|X\|_F^2}{\|X\|_{\text{op}}^2} = \frac{U}{L} \text{st}(X),$$

which completes the proof. \square

3.1.3 Pointwise nonlinear layer

Next, we consider stable rank propagation through a nonlinear activation function σ that is square integrable under Gaussian measure. This assumption allows us to expand the activation function in the Hermite basis. Namely, letting $h_k: \mathbf{R} \rightarrow \mathbf{R}$ be the orthonormal Hermite polynomials on \mathbf{R} , we define the coefficients:

$$\hat{\sigma}_k(s) := \mathbb{E}_\gamma[\sigma(s\gamma)h_k(\gamma)],$$

where $\gamma \sim \mathcal{N}(0, 1)$ is a standard normal. Equivalently, using Stein's lemma we may interpret Hermite coefficients as average derivatives:

$$\hat{\sigma}_k(s) = \frac{s^k}{\sqrt{k}} \cdot \mathbb{E}_\gamma \sigma^{(k)}(s\gamma),$$

as long as σ is k -times weakly differentiable and polynomially bounded. We will need the following lemma that expresses $k(x, x') = \mathbb{E}_g[\sigma(\langle x, g \rangle)\sigma(\langle x', g \rangle)]$, with $g \sim \mathcal{N}(0, \frac{1}{d}I_d)$ in a Hermite series. The proof follows by standard techniques, but we include it for completeness.

Lemma 3.3 (Kernel Hermite expansion). *Consider a function $\sigma: \mathbf{R} \rightarrow \mathbf{R}$ that is square integrable with respect to the Gaussian measure and define the kernel function $k(x, x') = \mathbb{E}_g[\sigma(\langle x, g \rangle)\sigma(\langle x', g \rangle)]$, where the expectation is taken with respect to $g \sim \mathcal{N}(0, \frac{1}{d}I_d)$. Then we may write*

$$k(x, x') = \sum_{k=0}^{\infty} \hat{\sigma}_k \left(\frac{\|x\|_2}{\sqrt{d}} \right) \hat{\sigma}_k \left(\frac{\|x'\|_2}{\sqrt{d}} \right) \left(\frac{\langle x, x' \rangle}{\|x\|_2 \cdot \|x'\|_2} \right)^k.$$

Proof. Let $s := \|x\|_2/\sqrt{d}$ and $s' := \|x'\|_2/\sqrt{d}$. Define $U := \langle x, g \rangle/s$ and $V := \langle x', g \rangle/s'$. Then (U, V) is jointly Gaussian with $\mathbb{E}[U^2] = \mathbb{E}[V^2] = 1$ and correlation $\rho = \mathbb{E}[UV] = \frac{\langle x, x' \rangle}{\|x\|_2 \|x'\|_2}$. Hence

$$k(x, x') = \mathbb{E}[\sigma(\langle x, g \rangle)\sigma(\langle x', g \rangle)] = \mathbb{E}[\sigma(sU)\sigma(s'V)].$$

We now expand the function $\gamma \mapsto \sigma(s\gamma)$ in a Hermite basis (see e.g. [39, Prop. 11.30]):

$$\sigma(s\gamma) = \sum_{k \geq 0} \hat{\sigma}_k(s) h_k(\gamma), \quad \text{where} \quad \hat{\sigma}_k(s) := \mathbb{E}_\gamma[\sigma(s\gamma)h_k(\gamma)].$$

Hence, we obtain the expression

$$k(x, x') = \sum_{k, \ell \geq 0} \hat{\sigma}_k(s) \hat{\sigma}_\ell(s') \mathbb{E}[h_k(U)h_\ell(V)].$$

For ρ -correlated standard Gaussians (U, V) , the Hermite polynomials satisfy $\mathbb{E}[h_k(U)h_\ell(V)] = \rho^k \mathbf{1}_{k=\ell}$ (see [39, Prop. 11.31]), which completes the proof. \square

We are now ready to establish stable rank propagation through a nonlinear activation. The only assumptions we make on σ is that $|\sigma(t)| \leq |t|$ for all $t \in \mathbf{R}$ and that the first Hermite coefficient $\hat{\sigma}_1 \left(\frac{\|x_i\|}{\sqrt{d}} \right)$ is nonzero, where x_i are the columns of the data matrix. Concretely, for the ReLU activation function a quick computation shows $s^{-1}\hat{\sigma}_1(s) = \frac{1}{2}$ for any s and therefore we may set $p = 1/2$ in (3.3). Similar computations for other common activation functions appear in Table 5.

Activation $\sigma(t)$	$s^{-1}\hat{\sigma}_1(s)$
Linear t	1
ReLU $\max(0, t)$	$\frac{1}{2}$
Leaky ReLU $\max(t, \alpha t)$	$\frac{1+\alpha}{2}$
Exact GELU $t \Phi(t)$	$\frac{1}{2}$
HardTanh $\text{clip}(t, -1, 1)$	$2\Phi(1/s) - 1$
$\tanh(t)$	$\mathbb{E}[\text{sech}^2(s\gamma)]$
Softsign $t(1 + t ^{-1})$	$\mathbb{E}[(1 + s\gamma)^{-2}]$
SiLU $t(1 + e^{-t})^{-1}$	$\frac{1}{2}$

Table 5: Values of $s^{-1}\hat{\sigma}_1(s) = \mathbb{E}[\sigma'(s\gamma)]$ for common activation functions, where $\gamma \sim \mathcal{N}(0, 1)$ and Φ denotes the standard normal CDF.

Theorem 3.4 (Nonlinear activation). *Consider a matrix $W \in \mathbf{R}^{k \times d}$ with iid Gaussian entries $\mathcal{N}(0, \frac{1}{d})$ and let $X \in \mathbf{R}^{d \times n}$ be an arbitrary matrix with columns $x_i \in \mathbf{R}^k$. Let $\sigma: \mathbf{R} \rightarrow \mathbf{R}$ be a function satisfying $|\sigma(t)| \leq |t|$ for all $t \in \mathbf{R}$ and whose first Hermite coefficient satisfies*

$$p := \min_{i=1, \dots, n} \frac{d}{\|x_i\|_2^2} \cdot \hat{\sigma}_1^2 \left(\frac{\|x_i\|_2}{\sqrt{d}} \right) > 0. \quad (3.3)$$

Then there exists a constant $c > 0$ such that for any $\varepsilon \in (0, 1)$ we have

$$(1 - \varepsilon) \frac{p}{d} \|X\|_F^2 \leq \frac{1}{k} \|\sigma(WX)\|_F^2 \leq (1 + \varepsilon) \frac{1}{d} \|X\|_F^2, \quad (3.4)$$

$$(1 - \varepsilon) \frac{p}{d} \|X\|_{\text{op}}^2 \leq \frac{1}{k} \|\sigma(WX)\|_{\text{op}}^2, \quad (3.5)$$

with probability at least $1 - 8 \exp(-c\varepsilon^2 p^2 k)$. Consequently, in this event the estimate holds:

$$\text{st}(\sigma(WX)) \leq \frac{1 + \varepsilon}{1 - \varepsilon} \cdot \frac{1}{p} \cdot \text{st}(X).$$

Proof. First, taking into account that $|\sigma(t)| \leq |t|$ for all t , we deduce

$$\|\sigma(WX)\|_F^2 \leq \|WX\|_F^2.$$

Therefore Lemma 3.1 shows that with probability at least $1 - 2 \exp(-c\varepsilon^2 k)$ we have $\frac{1}{k} \|\sigma(WX)\|_F^2 \leq (1 + \varepsilon) \frac{1}{d} \|X\|_F^2$, thereby establishing the right side of (3.4).

Define now the matrix

$$M_k := \frac{1}{k} \sigma(WX)^\top \sigma(WX) = \frac{1}{k} \sum_{i=1}^k \sigma(X^\top w_i) \sigma(X^\top w_i)^\top,$$

where w_i^\top are the rows of W . We first analyze the expectation of M_k . To this end, define $z := \sigma(X^\top w)$ where $w \sim \mathcal{N}(0, \frac{1}{d} I_d)$, and set $M := \mathbb{E}zz^\top = \mathbb{E}[M_k]$. Note that the ij entry of M is simply $\mathbb{E}_w \sigma(\langle x_i, w \rangle) \sigma(\langle x_j, w \rangle)$ where x_i and x_j are the i 'th and j 'th columns of X , respectively. Therefore, applying Lemma 3.3 entrywise, we may write

$$M = \sum_{q=0}^{\infty} \hat{\Sigma}_q \left(\frac{1}{d} X^\top X \right)^{\odot q} \hat{\Sigma}_q,$$

where $\odot q$ denotes a q -fold Hadamard product and $\hat{\Sigma}_q$ is a diagonal matrix with diagonal entries $\hat{\sigma}_q(\frac{\|x_i\|_2}{\sqrt{d}}) \cdot \frac{d^{q/2}}{\|x_i\|_2^q}$. Since the Hadamard product of positive semidefinite matrices is positive semidefinite (Schur product theorem [5, Sec. 1.2]), every summand on the right side is positive. Dropping all but the term $q = 1$ we obtain the lower bound in PSD order

$$M \succeq \frac{p}{d} X^\top X. \quad (3.6)$$

Therefore we obtain the two lower bounds, $\|M\|_{\text{op}} \geq \frac{p}{d} \cdot \|X\|_{\text{op}}^2$ and $\text{tr}(M) \geq \frac{p}{d} \cdot \|X\|_F^2$. We now argue using concentration that the operator norm of M_k can not be much smaller than the operator norm of M . Indeed, since σ is 1-Lipschitz, Gaussian concentration [55, Theorem 5.2.3] shows that the vector $z - \mathbb{E}[z]$ is sub-Gaussian with parameter $K = C\|X\|_{\text{op}}/\sqrt{d}$ for some constant C . Therefore, applying Lemma C.3 we deduce $\|M_k\|_{\text{op}} \geq (1 - \varepsilon)\|M\|_{\text{op}}$ with probability at least

$$1 - 2 \exp\left(-ck\left(\frac{\varepsilon^2 d^2 \|M\|_{\text{op}}^2}{\|X\|_{\text{op}}^4} \wedge \frac{d\varepsilon\|M\|_{\text{op}}}{\|X\|_{\text{op}}^2}\right)\right) - 2 \exp\left(-\frac{ck\varepsilon^2 d\|M\|_{\text{op}}}{\|X\|_{\text{op}}^2}\right).$$

Using (3.6), we deduce that this probability can be lower bounded by $1 - 4 \exp(-ck\varepsilon^2(p \wedge p^2))$. Thus in this event, the claimed estimate (3.5) holds.

Finally, we argue that the trace of M_k can not be much smaller than the trace of M . To see this, write $z = \sigma(X^\top w)$ and $z_i = \sigma(X^\top w_i)$ and let x_j denote the j 'th row to X . Then, we may write $\text{tr}(M_k) - \text{tr}(M) = \frac{1}{k} \sum_{i=1}^k \|z_i\|_2^2 - \mathbb{E}\|z\|_2^2$. Since σ is 1-Lipschitz with $\sigma(0) = 0$, we have $(z_i)_j^2 = \sigma(x_j^\top w_i)^2 \leq (x_j^\top w_i)^2$. Therefore we deduce

$$\|(z_i)_j^2\|_{\psi_1} \leq \|(x_j^\top w_i)^2\|_{\psi_1} = \|x_j^\top w_i\|_{\psi_2}^2 = \frac{\|x_j\|_2^2}{d},$$

where the first equality follows from [55, Lemma 2.8.5] and the second equality from the fact that $x_j^\top w_i$ is a centered Gaussian with variance $\frac{\|x_j\|_2^2}{d}$. Using the triangle inequality we deduce that $\|z_i\|_2^2$ is sub-Gaussian with parameter $\|X\|_F^2/d$. The centering lemma [55, Exercise 2.44] therefore implies $\|\|z_i\|_2^2 - \mathbb{E}\|z_i\|_2^2\|_{\psi_1} \lesssim \|X\|_F^2/d$. Applying Bernstein's inequality [53, Theorem 2.9.1], we therefore deduce for any $\varepsilon > 0$ the estimate:

$$\mathbb{P}(|\text{tr}(M_k) - \text{tr}(M)| \geq \varepsilon \text{tr}(M)) \leq 2 \exp\left(-c\left(\frac{kd^2\varepsilon^2 \text{tr}(M)^2}{\|X\|_F^4} \wedge \frac{kd\varepsilon \text{tr}(M)}{\|X\|_F^2}\right)\right)$$

Taking into account as we have seen that $\text{tr}(M) \geq \frac{p}{d}\|X\|_F^2$ and $p < 1$ due to the standing growth assumption on σ , the right side is bounded by $2 \exp(-ck\varepsilon^2 p^2)$. Taking a union bound over all the encountered events completes the proof of (3.4) and (3.5). Within these events, we then compute

$$\text{st}(\sigma(WX)) \leq \frac{\|M_k\|_F}{\|M_k\|_{\text{op}}} \leq \frac{(1 + \varepsilon)\frac{1}{d}\|X\|_F^2}{(1 - \varepsilon)\frac{p}{d}\|X\|_{\text{op}}^2} = \frac{1 + \varepsilon}{1 - \varepsilon} \cdot \frac{1}{p} \cdot \text{st}(X),$$

as we had to show. \square

3.1.4 Residual connections

Next, we establish stable rank propagation through residual skip connections.

Theorem 3.5 (Residual skip connection). *Let $X \in \mathbf{R}^{d \times n}$ and $H \in \mathbf{R}^{k \times n}$ be fixed matrices and let $W \in \mathbf{R}^{d \times k}$ have iid Gaussian entries $\mathcal{N}(0, \frac{1}{k})$. Then there exists a constant $c > 0$ such that for every $\varepsilon \in (0, 1)$, the estimate*

$$\text{st}(X + WH) \leq \frac{1 + \varepsilon}{1 - \varepsilon} \cdot \frac{\frac{1}{d} \|X\|_F^2 + \frac{1}{k} \|H\|_F^2}{\max \left\{ \frac{1}{d} \|X\|_{\text{op}}^2, \frac{1}{k} \|H\|_{\text{op}}^2 \right\}}. \quad (3.7)$$

holds with probability at least $1 - 10 \exp(-c\varepsilon^2 d)$.

Proof. Define the matrix $G := WH$. We bound the Frobenius and operator norms of $X + G$ separately, beginning with the former. To this end, we compute

$$\|X + G\|_F^2 = \|X\|_F^2 + \|G\|_F^2 + 2\langle X, G \rangle.$$

Using Lemma 3.1, we see that the estimate $\|G\|_F^2 \leq (1 + \frac{\varepsilon}{2}) \frac{d}{k} \|H\|_F^2$ holds with probability at least $1 - 4 \exp(-c\varepsilon^2 d)$. Let us bound the last term

$$\langle X, G \rangle = \text{tr}(W H X^\top) = \sum_{i,j} W_{ij} (H X^\top)_{ji}.$$

Note that the square sum of coefficients is simply $\sum_{i,j} (H X^\top)_{ji}^2 = \|H X^\top\|_F^2$. Therefore Hoeffding's inequality [55, Theorem 2.7.3] shows that for any $\varepsilon > 0$ the estimate $|\langle X, G \rangle| \leq \varepsilon \sqrt{\frac{d}{k}} \|H X^\top\|_F$ holds with probability at least $1 - 2 \exp(-cd\varepsilon^2)$. Using submultiplicativity of the Frobenius norm and Young's inequality, we further estimate

$$\sqrt{\frac{d}{k}} \|H X^\top\|_F \leq \sqrt{\frac{d}{k}} \|H\|_F \cdot \|X\|_F \leq \frac{d}{2k} \|H\|_F^2 + \frac{1}{2} \|X\|_F^2.$$

Thus in this event, we have the estimate

$$\|X + G\|_F^2 \leq (1 + \varepsilon) (\|X\|_F^2 + \frac{d}{k} \|H\|_F^2).$$

Next, we lower bound the operator norm $\|X + G\|_{\text{op}}$ by $\|X\|_{\text{op}}$ and $\|H\|_{\text{op}}$. To this end, fix a unit vector v . Then expanding the square we compute

$$\|(X + G)v\|_2^2 = \|Xv + Gv\|_2^2 = \|Xv\|_2^2 + \|g\|_2^2 + 2\langle Xv, g \rangle \quad (3.8)$$

where we set $g := Gv = WHv \sim \mathcal{N}(0, \frac{\|Hv\|_2^2}{k} I_d)$. Hoeffding's inequality shows that for any $t > 0$ we have $|\langle Xv, g \rangle| \leq t \sqrt{\frac{d}{k}} \|Xv\|_2 \|Hv\|_2$ with probability at least $1 - 2 \exp(-cdt^2)$. Concentration of the norm in turn shows that for any $\varepsilon \in (0, 1)$ we have $\|g\|_2 - \sqrt{\frac{d}{k}} \|Hv\|_2 \leq \varepsilon \sqrt{\frac{d}{k}} \|Hv\|_2$ with probability at least $1 - 2 \exp(-cd\varepsilon^2)$.

Case I: Lower-bounding with $\|X\|_{\text{op}}$. Suppose now that the unit vector v satisfies $\|Xv\|_2 = \|X\|_{\text{op}}$. Then setting $t = \varepsilon(1 - \varepsilon)^2$, we deduce

$$\begin{aligned} \|g\|_2^2 + 2\langle Xv, g \rangle &\geq (1 - \varepsilon)^2 \frac{d}{k} \|Hv\|_2^2 - 2t \sqrt{\frac{d}{k}} \|Hv\|_2 \|X\|_{\text{op}} \\ &\geq (1 - \varepsilon)^2 \frac{d}{k} \|Hv\|_2^2 - t \frac{d}{k} \|Hv\|_2^2 - t \|X\|_{\text{op}}^2 \\ &\geq -t \|X\|_{\text{op}}^2, \end{aligned}$$

where the second to last inequality follows from Young's inequality. Thus in this event we have

$$\|(X + G)v\|_2^2 \geq (1 - \varepsilon(1 - \varepsilon)^2)\|X\|_{\text{op}}^2.$$

Clearly $(1 - \varepsilon)^2$ can be treated as a constant and absorbed into ε .

Case II: Lower-bounding with $\|H\|_{\text{op}}$. Suppose now that the unit vector v satisfies $\|Hv\|_2 = \|H\|_{\text{op}}$. Then using Young's inequality, we deduce

$$\|Xv\|_2^2 + 2\langle Xv, g \rangle \geq \|Xv\|_2^2 - 2t\sqrt{\frac{d}{k}}\|Hv\|_2\|Xv\|_2 \geq -t^2\frac{d}{k}\|Hv\|_2^2.$$

Consequently, we have

$$\|(X + G)v\|_2^2 = \|g\|_2^2 + \|Xv\|_2^2 + 2\langle Xv, g \rangle \geq ((1 - \varepsilon)^2 - t^2)\frac{d}{k}\|Hv\|_2^2.$$

Using the inequality $(1 - \varepsilon)^2 - t \geq 1 - 2\varepsilon - t$ and replacing t and ε by $\varepsilon/3$ completes the proof. \square

Residual connections preserve column norms. In Section 5 we will apply the blockwise calculus rules from this subsection to control the stable rank of activations inside a transformer at Gaussian initialization. Several of those bounds, most notably RMSNorm (Theorem 3.2), require uniform control of the column norms of the matrices entering a block, not just their stable rank. Thus we must understand how column norms change when we pass through a residual connection. At initialization, a typical residual update has the form $x_t \mapsto x_t + Wh_t$, where W is a Gaussian matrix. The following lemma records the needed fact: uniformly over columns, $\frac{1}{d}\|x_t + Wh_t\|_2^2$ concentrates around $\frac{1}{d}\|x_t\|_2^2 + \frac{1}{k}\|h_t\|_2^2$, ensuring that the column-norm regularity required by the subsequent stable-rank bounds is preserved under such residual updates.

Lemma 3.6 (Residual connection and column norms). *Let $X = [x_1, \dots, x_n] \in \mathbf{R}^{d \times n}$ and $H = [h_1, \dots, h_n] \in \mathbf{R}^{k \times n}$ be deterministic and let $W \in \mathbf{R}^{d \times k}$ have iid entries $\mathcal{N}(0, \frac{1}{k})$. Then for any $\varepsilon \in (0, 1)$, with probability at least $1 - Cn \exp(-c\varepsilon^2 d)$, simultaneously for all $t = 1, \dots, n$ we have*

$$(1 - \varepsilon)\left(\frac{1}{d}\|x_t\|_2^2 + \frac{1}{k}\|h_t\|_2^2\right) \leq \frac{1}{d}\|x_t + Wh_t\|_2^2 \leq (1 + \varepsilon)\left(\frac{1}{d}\|x_t\|_2^2 + \frac{1}{k}\|h_t\|_2^2\right).$$

Proof. Fix t and set $\sigma_t^2 := \|h_t\|_2^2/k$. Then $g_t := Wh_t$ follows the law $\mathcal{N}(0, \sigma_t^2 I_d)$, and therefore we may write $g_t = \sigma_t z$ with $z \sim \mathcal{N}(0, I_d)$ and $\|g_t\|_2^2 = \sigma_t^2 \|z\|_2^2$. The standard χ^2 tail bound implies

$$\mathbb{P}\left(\|z\|_2^2 - d \geq \frac{\varepsilon}{4}d\right) \leq 2 \exp(-c\varepsilon^2 d),$$

and hence on this event we have

$$(1 - \frac{\varepsilon}{4})\sigma_t^2 d \leq \|g_t\|_2^2 \leq (1 + \frac{\varepsilon}{4})\sigma_t^2 d. \quad (3.9)$$

Now assume that $x_t \neq 0$; otherwise, the result follows from (3.9).

Note that $\langle x_t, g_t \rangle$ is Gaussian with mean 0 and variance $\sigma_t^2 \|x_t\|_2^2$, and therefore

$$\mathbb{P}\left(|2\langle x_t, g_t \rangle| \geq \frac{\varepsilon}{2}(\|x_t\|_2^2 + \sigma_t^2 d)\right) \leq 2 \exp\left(-c\varepsilon^2 \frac{(\|x_t\|_2^2 + \sigma_t^2 d)^2}{\sigma_t^2 \|x_t\|_2^2}\right) \leq 2 \exp(-c\varepsilon^2 d),$$

where the last inequality follows from the algebraic identity $(\|x_t\|_2^2 + \sigma_t^2 d)^2 / (\sigma_t^2 \|x_t\|_2^2) \geq d$.

On the intersection of these two events, we deduce that the quantity

$$\|x_t + g_t\|_2^2 = \|x_t\|_2^2 + \|g_t\|_2^2 + 2\langle x_t, g_t \rangle$$

lies between

$$\|x_t\|_2^2 + (1 - \frac{\varepsilon}{4})\sigma_t^2 d - \frac{\varepsilon}{2}(\|x_t\|_2^2 + \sigma_t^2 d) \quad \text{and} \quad \|x_t\|_2^2 + (1 + \frac{\varepsilon}{4})\sigma_t^2 d + \frac{\varepsilon}{2}(\|x_t\|_2^2 + \sigma_t^2 d),$$

which are respectively bounded below by $(1 - \varepsilon)(\|x_t\|_2^2 + \sigma_t^2 d)$ and above by $(1 + \varepsilon)(\|x_t\|_2^2 + \sigma_t^2 d)$ for $\varepsilon \in (0, 1)$. Since $\sigma_t^2 d = (d/k)\|h_t\|_2^2$, this proves the desired inequality for the fixed t . Finally, the failure probability for a fixed t is at most $C \exp(-c\varepsilon^2 d)$, and a union bound over $t = 1, \dots, n$ yields the stated probability $1 - Cne^{-c\varepsilon^2 d}$ after adjusting constants. \square

3.1.5 Gated nonlinear layer

The final building block we will consider is the gating transformation, which has the form

$$X_{\text{gate}} := \sigma(VZ) \odot WX$$

for fixed data matrices X and Z and random weight matrices V and W . Here, \odot denotes the Hadamard product. The key to establishing propagation of the stable rank through the gating block is the following theorem, which states that under reasonable conditions the operator norm and trace of a matrix of the form $\sum_{i=1}^k (a_i a_i^\top) \odot H$ is well distributed among the summands.

Theorem 3.7 (Dispersion of operator norm and trace). *Consider a positive semidefinite matrix $H \in \mathbb{R}^{n \times n}$ and a sequence of random vectors $a_1, \dots, a_k \in \mathbb{R}^n$. Define now the matrices*

$$X_i := (a_i a_i^\top) \odot H \in \mathbb{R}^{n \times n} \quad \text{and their sum} \quad S := \sum_{i=1}^k X_i.$$

We suppose that a_i are iid realizations of the vector $a = \sigma(Z^\top v)$ where $v \sim N(0, \frac{1}{d}I_d)$ and $Z = [z_1, \dots, z_n] \in \mathbb{R}^{d \times n}$ is a fixed matrix. We suppose moreover that $\sigma: \mathbf{R} \rightarrow \mathbf{R}$ is an activation function that is 1-Lipschitz with $\sigma(0) = 0$. Then the following are true.

1. **(Trace dispersion)** Suppose that the diagonal entries of H satisfy

$$L \leq H_{jj} \leq U \quad \text{for all } j = 1, \dots, n,$$

for some values $0 < L \leq U < \infty$. Suppose moreover that the first Hermite coefficient is nonzero:

$$p := \min_{i=1, \dots, n} \frac{d}{\|z_i\|_2^2} \cdot \hat{\sigma}_1^2 \left(\frac{\|z_i\|_2}{\sqrt{d}} \right) > 0. \quad (3.10)$$

Then for any constant $q > 0$, there exist constants $c, C < \infty$ such that the estimate

$$\frac{\text{tr}(S)}{\max_{1 \leq i \leq k} \text{tr}(X_i)} \geq \frac{cL}{U} \frac{kp}{\log k}$$

holds with probability at least $1 - \exp(-Cp^2 k) - k^{-q}$.

2. (Operator norm dispersion) Suppose that the columns z_j of Z satisfy

$$L \leq \|z_j\|_2^2 \leq U \quad \text{for all } j = 1, \dots, n,$$

for some values $0 < L \leq U < \infty$. Suppose moreover that for some numerical constant $\kappa > 0$ we have $\left| \mathbb{E}_{g \sim \mathcal{N}(0, s^2)} \sigma(g) \right| \geq \kappa s$ for all $s \in [\sqrt{L/d}, \sqrt{U/d}]$. Then for any constant $q > 0$, there exist constants $c, C < \infty$ such that the estimate

$$\frac{\|S\|_{\text{op}}}{\max_{1 \leq i \leq k} \|X_i\|_{\text{op}}} \geq \frac{cd}{\log(kn)} \cdot \frac{k}{d} \cdot \frac{L}{U},$$

holds with probability at least $1 - \exp\left(-Ck\frac{L^2}{U^2}\right) - \frac{1}{(nk)^q}$.

Proof. We first dispense with the Trace Dispersion claim, which is straightforward. Define the matrix $A = \sigma(Z^\top V)$ where the columns v_i of $V \in \mathbf{R}^{d \times k}$ are Gaussian $N(0, \frac{1}{d}I_d)$. Thus a_i are the columns of A . Summing the diagonal entries of X_i and using the upper and lower bounds on the diagonal entries of H directly yields the estimates:

$$\begin{aligned} L\|a_i\|_2^2 &\leq \text{tr}(X_i) \leq U\|a_i\|_2^2 \quad \forall i = 1, \dots, n, \\ L\|A\|_F^2 &\leq \text{tr}(S) \leq U\|A\|_F^2. \end{aligned}$$

We first lower bound $\|A\|_F^2$. To this end, Theorem 3.4 (equation (3.4)) shows that there exist constant c_1, c_2 such that

$$\mathbb{P}\left(\|A\|_F^2 \geq c_1 p \frac{k}{d} \|Z\|_F^2\right) \geq 1 - 8 \exp(-c_2 p^2 k).$$

Let us next upper bound the maximal row norms $\max_i \|a_i\|_2$. Since σ is 1-Lipschitz and satisfies $\sigma(0) = 0$, we have $\|a_i\|_2^2 \leq \|Z^\top v_i\|_2^2$. The Hanson-Wright inequality [55, Exercise 6.13] together with monotonicity of the subgaussian norm then implies

$$\left\| \|a_i\|_2 - \frac{1}{\sqrt{d}} \|Z\|_F \right\|_{\psi_2} \lesssim \frac{1}{\sqrt{d}} \|Z\|_{\text{op}}.$$

Therefore, for any $t \geq 0$ we have

$$\mathbb{P}\left(\|a_i\|_2 \geq \frac{1+t}{\sqrt{d}} \|Z\|_F\right) \leq \exp(-ct^2).$$

Taking a union bound over $i = 1, \dots, k$, we deduce

$$\mathbb{P}\left(\max_{i=1, \dots, k} \|a_i\|_2 \geq \frac{1+t}{\sqrt{d}} \|Z\|_F\right) \leq \exp(\log(k) - ct^2).$$

With the choice $t^2 = \frac{q+1}{c} \log(k)$, we deduce that there is a constant $C > 0$ such that

$$\mathbb{P}\left(\max_{i=1, \dots, k} \|a_i\|_2 \leq C \sqrt{\frac{\log(k)}{d}} \cdot \|Z\|_F\right) \geq 1 - \frac{1}{k^q}.$$

Summarizing, we have established that there exist constants $c, C > 0$ such that the estimate

$$\frac{\text{tr}(S)}{\max_{1 \leq i \leq k} \text{tr}(X_i)} \geq \frac{cL}{U} \cdot \frac{\frac{pk}{d} \|Z\|_F^2}{\frac{\log(k)}{d} \|Z\|_F^2} = \frac{cL}{U} \frac{pk}{\log k}$$

holds with probability at least $1 - 8 \exp(-Cp^2k) - k^{-q}$.

The remainder of the proof focuses on establishing dispersion of the operator norm. For any vector $a \in \mathbb{R}^n$, define the diagonal matrix $D_a := \text{Diag}(a) \in \mathbb{R}^{n \times n}$. Then clearly equality holds:

$$(aa^\top) \odot H = D_a H D_a. \quad (3.11)$$

Upper bound on $\|X_i\|_{\text{op}}$. Using (3.11) and submultiplicativity, we deduce

$$\|X_i\|_{\text{op}} = \|D_{a_i} H D_{a_i}\|_{\text{op}} \leq \|D_{a_i}\|_{\text{op}}^2 \|H\|_{\text{op}} = \|a_i\|_\infty^2 \|H\|_{\text{op}}.$$

Fix indices (i, j) . Since $v_i \sim \mathcal{N}(0, \frac{1}{d} I_d)$, we have $v_i^\top z_j \sim \mathcal{N}(0, \|z_j\|_2^2/d)$. Since σ is 1-Lipschitz with $\sigma(0) = 0$, the entry $(a_i)_j = \sigma(v_i^\top z_j)$ satisfies

$$\mathbb{P}(|(a_i)_j| \geq t) \leq \mathbb{P}(|v_i^\top z_j| \geq t) \leq 2 \exp\left(-\frac{dt^2}{2\|z_j\|_2^2}\right) \leq 2 \exp\left(-\frac{dt^2}{2U}\right),$$

for any $t \geq 0$. Taking a union bound over all kn pairs (i, j) yields

$$\mathbb{P}\left(\max_{1 \leq i \leq k} \|a_i\|_\infty \geq t\right) \leq \exp\left(\log(2kn) - \frac{dt^2}{2U}\right).$$

With the choice $t^2 = (q+1)\frac{2U}{d} \log(2kn)$, the right-hand side is at most $\frac{1}{(kn)^q}$. Thus with probability at least $1 - \frac{1}{(kn)^q}$, we have

$$\max_{1 \leq i \leq k} \|X_i\|_{\text{op}} \leq \|H\|_{\text{op}} \max_{1 \leq i \leq k} \|a_i\|_\infty^2 \leq \frac{2(q+1)U}{d} \|H\|_{\text{op}} \log(2kn). \quad (3.12)$$

Deterministic lower-bound on $\|S\|_{\text{op}}$. Define $\lambda := \|H\|_{\text{op}}$ and let $u \in \mathbb{R}^n$ be a unit top eigenvector of H , that is $Hu = \lambda u$. In particular, we clearly have $H \geq \lambda uu^\top$. We compute

$$\begin{aligned} \|S\|_{\text{op}} &\geq u^\top S u = \sum_{i=1}^k u^\top D_{a_i} H D_{a_i} u = \sum_{i=1}^k (D_{a_i} u)^\top H (D_{a_i} u) \\ &\geq \lambda \sum_{i=1}^k (D_{a_i} u)^\top (uu^\top) (D_{a_i} u) = \lambda \sum_{i=1}^k \underbrace{(u^\top D_{a_i} u)^2}_{=: T_i}. \end{aligned} \quad (3.13)$$

A lower bound on $\mathbb{E}T_i$ via the mean outer product. Let $v \sim \mathcal{N}(0, \frac{1}{d} I_d)$ and set $a := \sigma(Z^\top v) \in \mathbb{R}^n$. Observe that each coordinate a_j has the form $a_j = \sigma(z_j^\top v) \sim \sigma(s\gamma)$ where $s = \sqrt{\|z_j\|_2^2/d}$ and $\gamma \sim \mathcal{N}(0, 1)$. The assumption that for some numerical constant $\kappa > 0$ we have $\left| \mathbb{E}_{g \sim \mathcal{N}(0, s^2)} \sigma(g) \right| \geq \kappa s$ for all $s \in [\sqrt{L/d}, \sqrt{U/d}]$ therefore ensures that the mean $\mu := \mathbb{E}[a]$ satisfies $\mu_j \geq \kappa \sqrt{\frac{L}{d}}$ for all j .

Define the kernel matrix $K := \mathbb{E}[aa^\top] \in \mathbb{R}^{n \times n}$ and observe the estimate

$$K = \mathbb{E}[aa^\top] = \text{Cov}(a) + \mu\mu^\top \geq \mu\mu^\top. \quad (3.14)$$

Define now the weights $w_j := u_j^2$, which clearly satisfy $w_j \geq 0$ and $\sum_j w_j = 1$. Observe that T_i have the same distribution as $T := (w^\top a)^2$. Therefore, we deduce

$$\mathbb{E}[T] = \mathbb{E}(w^\top a)^2 = w^\top K w \geq (w^\top \mu)^2 \geq \min_j \mu_j^2 \gtrsim \frac{L}{d}, \quad (3.15)$$

where the second inequality follows from the fact that the weight vector $\{w_j\}_j$ lies on the simplex.

Concentration of $\sum_{i=1}^k T_i$ below its mean. We will now show that $T - \mathbb{E}T$ is subexponential with parameter $\asymp U/d$. To see this, write $v = g/\sqrt{d}$ with $g \sim \mathcal{N}(0, I_d)$ and define

$$f(g) := w^\top a = \sum_{j=1}^n w_j \sigma\left(\frac{1}{\sqrt{d}} g^\top z_j\right).$$

Since σ is 1-Lipschitz, for any $g, g' \in \mathbb{R}^d$, we have

$$|f(g) - f(g')| \leq \frac{1}{\sqrt{d}} \sum_{j=1}^n w_j |(g - g')^\top z_j| \leq \frac{\|g - g'\|_2}{\sqrt{d}} \sum_{j=1}^n w_j \|z_j\|_2 \leq \sqrt{\frac{U}{d}} \|g - g'\|_2,$$

Thus f is $\sqrt{\frac{U}{d}}$ -Lipschitz. By Gaussian concentration for Lipschitz functions [55, Theorem 5.2.3], the random variable $Y := f(g) = w^\top a$ satisfies

$$\|Y - \mathbb{E}Y\|_{\psi_2} \lesssim \sqrt{\frac{U}{d}}. \quad (3.16)$$

Therefore we deduce

$$\|(Y - \mathbb{E}Y)^2 - \mathbb{E}(Y - \mathbb{E}Y)^2\|_{\psi_1} \lesssim \|(Y - \mathbb{E}Y)^2\|_{\psi_1} \asymp \|Y - \mathbb{E}Y\|_{\psi_2}^2 \lesssim \frac{U}{d},$$

where the first inequality follows from the centering lemma [55, Exercise 2.44] while the equality follows from [55, Lemma 2.8.5]. Moreover, expanding the squares on the left and isolating the cross term gives

$$\|(Y - \mathbb{E}Y)^2 - \mathbb{E}(Y - \mathbb{E}Y)^2\|_{\psi_1} \geq \|Y^2 - \mathbb{E}Y^2\|_{\psi_1} - 2 \underbrace{|\mathbb{E}Y|}_{\lesssim \|\mu\|_\infty} \cdot \underbrace{\|(Y - \mathbb{E}Y)\|_{\psi_1}}_{\lesssim \sqrt{\frac{U}{d}}}.$$

Thus, we have arrived at

$$\|T - \mathbb{E}T\|_{\psi_1} = \|Y^2 - \mathbb{E}Y^2\|_{\psi_1} \lesssim \frac{U}{d} + \sqrt{\frac{U}{d}} \cdot \|\mu\|_\infty \lesssim \frac{U}{d},$$

where we use the bound that $\|\mu\|_\infty \lesssim \sqrt{U/d}$. Applying the Bernstein inequality [55, Theorem 2.9.1] we deduce for any $s \geq 0$ the estimate $\sum_{i=1}^k T_i \geq k \cdot \mathbb{E}T - s$ holds with probability at least

$$1 - \exp\left(-c\left(\frac{d^2 s^2}{kU^2} \wedge \frac{ds}{U}\right)\right).$$

Recall that from (3.15) we further have the lower bound $\mathbb{E}T \geq \frac{CL}{d}$ for some numerical constant C . Therefore setting $s = \frac{kCL}{2d}$, the estimate $\sum_{i=1}^k T_i \geq \frac{kCL}{2d}$ holds with probability at least $1 - \exp\left(-C'k\frac{L^2}{U^2}\right)$. In this event, returning to (3.13), we have

$$\|S\|_{\text{op}} \geq CL \frac{k}{d} \|H\|_{\text{op}}.$$

Therefore, taking a union bound with the event which ensured (3.12), we deduce that the estimate

$$\frac{\|S\|_{\text{op}}}{\max_{1 \leq i \leq k} \|X_i\|_{\text{op}}} \gtrsim \frac{d}{\log(kn)} \cdot \frac{k}{d} \cdot \frac{L}{U},$$

holds with probability at least $1 - \exp\left(-C'k \frac{L^2}{U^2}\right) - \frac{1}{(nk)^q}$. This completes the proof. \square

Armed with Theorem 3.7 we can now establish propagation of the stable rank for the gating block, induced by a nonlinear activation with a nonzero mean (e.g. ReLU).

Theorem 3.8 (Gating). *Consider the matrix*

$$Q = \sigma(VZ) \odot WX$$

where $Z \in \mathbf{R}^{d_1 \times n}$ and $X \in \mathbf{R}^{d_2 \times n}$ are fixed and $V \in \mathbf{R}^{k \times d_1}$ and $W \in \mathbf{R}^{k \times d_2}$ have iid Gaussian entries, $\mathcal{N}(0, \frac{1}{d_1})$ and $\mathcal{N}(0, \frac{1}{d_2})$ respectively. Suppose moreover that we are in the proportionate regime $k \asymp d_1$. Suppose that the column norms of X and Z satisfy

$$L \leq \|x_i\|_2^2 \leq U \quad \text{and} \quad L \leq \|z_i\|_2^2 \leq U \quad \forall i \in [n].$$

Suppose moreover that the activation function σ is 1-Lipschitz with $\sigma(0) = 0$ and that for some numerical constants $p, \kappa > 0$ we have

$$\left| \mathbb{E}_{g \sim \mathcal{N}(0, s^2)} \sigma(g) \right| \geq \kappa s \quad \text{and} \quad \hat{\sigma}_1(s) \geq \sqrt{p} \cdot s \quad \forall s \in [\sqrt{L/d_1}, \sqrt{U/d_1}].$$

Then for any constant $q > 0$, there exist constants $c, C < \infty$ such that the estimate

$$\text{st}(Q) \leq \frac{(1 + \varepsilon)^2}{(1 - \varepsilon)^3} \cdot \frac{U^2}{L^2} \cdot \kappa^{-2} \cdot \text{st}(X)$$

holds with probability at least $1 - C \left(\exp\left(-c\varepsilon^2 \frac{k}{\log^2(k)}\right) - \exp\left(-c\varepsilon^2 k \frac{L^2}{U^2}\right) - k^{-q} \right)$.

Proof. We proceed by analyzing the gram matrix of Q by first conditioning on V . Setting the notation, define the matrices $A := \sigma(VZ)$ and $B := WX$, let q_j^\top denote the j 'th rows of Q , and define the matrices

$$S := Q^\top Q = \sum_{j=1}^k q_j q_j^\top, \quad M_j := \mathbb{E}[q_j q_j^\top \mid V], \quad M := \mathbb{E}[S \mid V].$$

Let us first compute $q_j q_j^\top$ and M_j in terms of the rows b_j^\top and w_j^\top of B and W , respectively. To this end, observe that equality $q_j^\top = a_j^\top \odot (w_j^\top X)$ holds and therefore we may write the outer product

$$q_j^\top q_j = a_j a_j^\top \odot (X^\top w_j w_j^\top X).$$

In particular, taking the expectation with respect to W and with V fixed, we deduce the equalities:

$$M_j = \frac{1}{d_2} (a_j a_j^\top) \odot (X^\top X) \quad \text{and} \quad M = \frac{1}{d_2} (A^\top A) \odot (X^\top X)$$

Thus conditioned on V , the vectors q_j are independent mean-zero Gaussian with covariance M_j .

We will now show that the effective rank of S is not much larger than the effective rank of M with high probability over the pair (V, W) . We do so by estimating the operator norm and trace, in order. Fix a constant $\varepsilon \in (0, 1)$ and define the event

$$\mathcal{E}_1 = \{\|S\|_{\text{op}} \geq (1 - \varepsilon)\|M\|_{\text{op}}\}.$$

Observe that q_j is a mean-zero Gaussian random vector with covariance M_j . Therefore, we now apply Theorem C.2 with $K_j = 1$ and with V fixed. We thus deduce that there exists a constant $c > 0$ (independent of ε) such that

$$\mathbb{P}(\mathcal{E}_1^c \mid V) \leq \exp\left(-c \min\left\{\frac{\varepsilon^2 \|M\|_{\text{op}}^2}{\sum_{j=1}^k \|M_j\|_{\text{op}}^2}, \frac{\varepsilon \|M\|_{\text{op}}}{\max_{1 \leq j \leq k} \|M_j\|_{\text{op}}}\right\}\right). \quad (3.17)$$

Now applying Theorem 3.7 we see that for any constant $q > 0$, there exist constants $c, C < \infty$ such that the estimate

$$\frac{\|M\|_{\text{op}}}{\max_{1 \leq j \leq k} \|M_j\|_{\text{op}}} \geq \frac{cd_2}{\log(kn)} \cdot \frac{k}{d_2} \cdot \frac{L}{U},$$

holds with probability at least $1 - \exp\left(-Ck \frac{L^2}{U^2}\right) - \frac{1}{(nk)^q}$. Within this event, which we denote by \mathcal{E}_2 , the right-side of (3.17) is bounded by $\omega := \exp\left(-\frac{c'\varepsilon^2 k}{\log^2(kn)}\right)$ for some numerical constant $c' < \infty$, which follows by upper bounding the sum by the k times the maximum. Thus the probability of the complementary event \mathcal{E}_1 can be lower bounded as

$$\begin{aligned} \mathbb{P}[\mathcal{E}_1^c] &= \mathbb{E}[\mathbb{P}(\mathcal{E}_1^c \mid V)] = \mathbb{E}[\mathbb{P}(\mathcal{E}_1^c \mid V)\mathbf{1}_{\mathcal{E}_2}] + \mathbb{E}[\mathbb{P}(\mathcal{E}_1^c \mid V)\mathbf{1}_{\mathcal{E}_2^c}] \\ &\leq \omega + \mathbb{P}(\mathcal{E}_2^c) \\ &\leq \exp\left(-\frac{c'\varepsilon^2 k}{\log^2(kn)}\right) + \exp\left(-Ck \frac{L^2}{U^2}\right) + \frac{1}{(nk)^q}. \end{aligned} \quad (3.18)$$

Next, we estimate the trace of S . To this end, fix $\varepsilon > 0$ and define the event

$$\mathcal{F}_1 = \{\text{tr}(S) \leq (1 + \varepsilon)\text{tr}(M)\}.$$

We now apply Theorem C.1 with $K_j = 1$ and with V fixed. We thus deduce that there exists a constant $c > 0$ (independent of ε) such that

$$\mathbb{P}(\mathcal{F}_1^c \mid V) \leq 2 \exp\left(-c \left(\frac{\varepsilon^2 \text{tr}(M)^2}{\sum_{i=1}^n \text{tr}(M_i)^2} \wedge \frac{\varepsilon \text{tr}(M)}{\max_{i=1, \dots, k} \text{tr}(M_i)}\right)\right) \quad (3.19)$$

Trace dispersion of Theorem 3.7 guarantees

$$\frac{\text{tr}(M)}{\max_{1 \leq i \leq k} \text{tr}(M_i)} \geq \frac{cL}{U} \frac{k}{\log k}$$

holds with probability at least $1 - 2n \exp(-Ck) - k^{-q}$. Within this event, the right side of (3.19) is bounded by $\exp\left(-\frac{c'\varepsilon^2 k}{\log^2(k)}\right)$. A completely analogous argument to (3.18) shows that

$$\mathbb{P}[\mathcal{F}_1^c] \leq \exp\left(-\frac{c'\varepsilon^2 k}{\log^2(k)}\right) + 2n \exp(-Ck) + k^{-q}.$$

It remains now to estimate $\text{tr}(M)$ and $\|M\|_{\text{op}}$. Clearly, we have

$$\text{tr}(M) \leq \frac{U}{d_2} \|A\|_F^2.$$

Since σ is 1-Lipschitz with $\sigma(0) = 0$, we have $\|A\|_F^2 \leq \|VZ\|_F^2$. Using Theorem 3.1 the estimate $\|VZ\|_F^2 \leq (1 + \varepsilon) \frac{k}{d_1} \|Z\|_F^2$ holds with probability at least $1 - 2 \exp(-C\varepsilon^2 k)$.

Next, we lower-bound the operator norm $\|M\|_{\text{op}}$. To this end, define $\mu = \mathbb{E}[a]$. Fix j and note that $(a_i)_j = \sigma(v_i^\top z_j)$, where conditional on z_j we have $v_i^\top z_j \sim \mathcal{N}(0, \|z_j\|_2^2/d)$ and $\|z_j\|_2^2 \leq U$. Hence $\|v_i^\top z_j\|_{\psi_2} \leq \|z_j\|_2/\sqrt{d} \leq \sqrt{U/d}$. Since σ is 1-Lipschitz with $\sigma(0) = 0$, we have $|\sigma(t)| \leq |t|$, and therefore $\|(a_i)_j\|_{\psi_2} \leq \sqrt{U/d}$, and moreover $\|(a_i)_j - \mu_j\|_{\psi_2} \leq 2\sqrt{U/d}$. Thus, the sub-Gaussian Hoeffding bound yields

$$\mathbb{P}(|\hat{\mu}_j - \mu_j| \geq \varepsilon |\mu_j|) \leq 2 \exp\left(-c\varepsilon^2 k \frac{\mu_j^2}{U/d}\right).$$

Using the assumption $|\mu_j| = |\mathbb{E}\sigma(v^\top z_j)| \geq \kappa\sqrt{\|z_j\|_2^2/d} \geq \kappa\sqrt{L/d}$, we get

$$|\hat{\mu}_j - \mu_j| \leq \varepsilon |\mu_j|$$

with probability at least $1 - 2 \exp(-c\varepsilon^2 k \kappa^2 L/U)$. Taking a union bound over $j = 1, \dots, n$ we deduce $\sup_j |\hat{\mu}_j - \mu_j| \leq \varepsilon |\mu_j|$ with probability at least $1 - 2n \exp(-c\varepsilon^2 k \kappa^2 L/U)$. Using the elementary observation $\frac{1}{k} A^T A \geq \hat{\mu} \hat{\mu}^\top$, we may now estimate

$$\frac{d_2}{k} \cdot M = (\frac{1}{k} A^T A) \odot (X^\top X) \geq (\hat{\mu} \hat{\mu}^\top) \odot (X^\top X) = \text{Diag}(\hat{\mu}) X^\top X \text{Diag}(\hat{\mu}) \geq (1 - \varepsilon)^2 \min_j \mu_j^2 \cdot X^\top X.$$

Therefore we deduce

$$\|M\|_{\text{op}} \geq \frac{(1 - \varepsilon)^2 k}{d_2} \min_j \mu_j^2 \|X\|_{\text{op}}^2 \geq \frac{(1 - \varepsilon)^2 L \kappa^2}{d_1 d_2} \|X\|_{\text{op}}^2,$$

where the last inequality follows from the assumption that $\left| \mathbb{E}_{g \sim \mathcal{N}(0, s^2)} \sigma(g) \right| \geq \kappa s$ for all $s \in [\sqrt{L/d_1}, \sqrt{U/d_1}]$.

Therefore, in the intersection of the considered events we have

$$\text{st}(Q) \leq \frac{1 + \varepsilon}{1 - \varepsilon} \cdot \text{er}(M) \leq \frac{1 + \varepsilon}{1 - \varepsilon} \cdot \frac{(1 + \varepsilon) k U \|Z\|_F^2 / (d_1 d_2)}{(1 - \varepsilon)^2 k L \kappa^2 \|X\|_{\text{op}}^2 / (d_1 d_2)} \leq \frac{(1 + \varepsilon)^2}{(1 - \varepsilon)^3} \cdot \frac{U^2}{L^2} \cdot \kappa^{-2} \cdot \text{st}(X),$$

where the last inequality uses the relation $\|Z\|_F^2 \leq nU$ and $\|X\|_F^2 \geq nL$. The proof is complete. \square

Column norm bounds for Gated activations. Finally, we bound the column norms of gated activations. This lemma will be used in conjunction with Lemma 3.6 to control the evolution of column norms throughout the transformer architecture.

Lemma 3.9 (Gated column norms). *Fix a vector $a \in \mathbf{R}^d$ satisfying $\|a\|_2^2 = d$ and a function $\sigma: \mathbf{R} \rightarrow \mathbf{R}$ that 1-Lipschitz with $\sigma(0) = 0$ and a second moment $m_2 := \mathbb{E}[\sigma(\gamma)^2]$ for $\gamma \sim \mathcal{N}(0, 1)$ that is bounded from above and below by a positive numerical constant. Let $w^{\text{in}}, w^{\text{gate}} \in \mathbf{R}^d$ be independent random vectors with iid entries $\mathcal{N}(0, \frac{1}{d})$. Define*

$$z := \langle w^{\text{in}}, a \rangle, \quad h := \langle w^{\text{gate}}, a \rangle, \quad y := \sigma(z) h.$$

Define now the vector $b := (y_1, \dots, y_k) \in \mathbf{R}^k$ where y_i are iid copies of y . Then there exists a numerical constant c such that for every $\varepsilon \in (0, 1)$, we have

$$\mathbb{P}(\|b\|_2^2 \leq (1 + \varepsilon)^2 m_2 k) \geq 1 - 4 \exp(-c\varepsilon^2 k) - 2k \exp\left(-\frac{1}{2} k^{1/3}\right) - 2 \exp\left(-c\varepsilon^2 (1 - \varepsilon) m_2 k^{2/3}\right).$$

Proof. Let $(z_i, h_i)_{i=1}^k$ be iid with $z_i, h_i \sim \mathcal{N}(0, 1)$ and set $y_i = \sigma(z_i)h_i$. Define $s_i := \sigma(z_i)^2$ and

$$S := \sum_{i=1}^k s_i, \quad T := \sum_{i=1}^k s_i(h_i^2 - 1).$$

Then clearly, we may write $\|b\|_2^2 = \sum_{i=1}^k s_i h_i^2 = S + T$. Conditional on $(s_i)_{i=1}^k$, the random variables $h_i^2 - 1$ are independent, mean zero, and sub-exponential with a constant parameter $C > 0$. Bernstein's inequality therefore yields a numerical $c_0 > 0$ such that, for every $u > 0$, it holds:

$$\mathbb{P}(T \geq u \mid (s_i)_{i=1}^k) \leq \exp\left(-c_0 \min\left\{\frac{u^2}{\sum_{i=1}^k s_i^2}, \frac{u}{\max_{i \leq k} s_i}\right\}\right).$$

Setting $u := \varepsilon S$ and noting $\sum_{i=1}^k s_i^2 \leq (\max_{i \leq k} s_i) \sum_{i=1}^k s_i = (\max_i s_i) S$, we deduce

$$\min\left\{\frac{u^2}{\sum_{i=1}^k s_i^2}, \frac{u}{\max_{i \leq k} s_i}\right\} \geq \min\left\{\frac{\varepsilon^2 S^2}{(\max_i s_i) S}, \frac{\varepsilon S}{\max_i s_i}\right\} = \frac{\varepsilon^2 S}{\max_i s_i},$$

and hence

$$\mathbb{P}(T \geq \varepsilon S \mid (s_i)_{i=1}^k) \leq \exp\left(-c_0 \varepsilon^2 \frac{S}{\max_i s_i}\right). \quad (3.20)$$

Define the events

$$\mathcal{E} := \{T \geq \varepsilon S\}, \quad \mathcal{E}_{\text{sum}} := \{(1 - \varepsilon)m_2 k \leq S \leq (1 + \varepsilon)m_2 k\}, \quad \mathcal{E}_{\text{max}} := \{\max_{i \leq k} s_i \leq k^{1/3}\}.$$

Then we compute

$$\begin{aligned} \mathbb{P}[\mathcal{E}] &= \mathbb{E}[\mathbb{P}(\mathcal{E} \mid (s_i)_{i=1}^k)] = \mathbb{E}[\mathbb{P}(\mathcal{E} \mid (s_i)_{i=1}^k)) \mathbf{1}_{\mathcal{E}_{\text{sum}} \cap \mathcal{E}_{\text{max}}}] + \mathbb{E}[\mathbb{P}(\mathcal{E} \mid (s_i)_{i=1}^k)) \mathbf{1}_{(\mathcal{E}_{\text{sum}} \cap \mathcal{E}_{\text{max}})^c}] \\ &\leq \exp(-c_0 \varepsilon^2 (1 - \varepsilon)m_2 k^{2/3}) + \mathbb{P}(\mathcal{E}_{\text{sum}}^c) + \mathbb{P}(\mathcal{E}_{\text{max}}^c), \end{aligned} \quad (3.21)$$

where the last inequality follows from (3.20) and a union bound over the two events $\mathcal{E}_{\text{sum}}^c$ and $\mathcal{E}_{\text{max}}^c$.

We now bound $\mathbb{P}(\mathcal{E}_{\text{sum}}^c)$ and $\mathbb{P}(\mathcal{E}_{\text{max}}^c)$. Since σ is 1-Lipschitz with $\sigma(0) = 0$, we have $|\sigma(t)| \leq |t|$ for all t , and hence $0 \leq s_i \leq z_i^2$. In particular, $s_i - m_2$ is sub-exponential with $\|s_i - m_2\|_{\psi_1} \leq C$ for a numerical constant $C > 0$. Therefore, Bernstein's inequality yields $\mathbb{P}(\mathcal{E}_{\text{sum}}^c) \leq 2 \exp(-c \varepsilon^2 k)$ for a numerical $c > 0$.

For \mathcal{E}_{max} , using $s_i \leq z_i^2$ and the Gaussian tail bound $\mathbb{P}(z_i^2 \geq t) \leq 2 \exp(-t/2)$, we obtain

$$\mathbb{P}(\mathcal{E}_{\text{max}}^c) \leq \mathbb{P}\left(\max_{i \leq k} z_i^2 > k^{1/3}\right) \leq 2k \exp\left(-\frac{1}{2}k^{1/3}\right),$$

where the last inequality follows from a union bound. Substituting these estimates into (3.21) shows that, with probability at least

$$1 - 2 \exp(-c \varepsilon^2 k) - 2k \exp\left(-\frac{1}{2}k^{1/3}\right) - \exp\left(-c_0 \varepsilon^2 (1 - \varepsilon)m_2 k^{2/3}\right),$$

we have $T \leq \varepsilon S$. Taking a further union bound with the event \mathcal{E}_{sum} we further deduce,

$$\|b\|_2^2 = S + T \leq (1 + \varepsilon)S \leq (1 + \varepsilon)^2 m_2 k,$$

which is the claim after adjusting constants in the last term. \square

3.2 Compound operations: attention and MLP layers

In Section 5, we will analyze transformer architectures at Gaussian initialization. Those architectures (see Section 1.2.1) are compositions of two compound sublayers (attention and MLP), each wrapped with RMS normalization and a residual connection. To further iterate transformer blocks in Section 5 using the atomic calculus rules above, we need two layerwise propagation inputs: (a) a uniform column-norm envelope for the matrices entering RMSNorm (since Theorem 3.2 depends on the ratio of maximal to minimal column norm), and (b) control of how the stable rank changes when passing through one attention sublayer and one MLP sublayer.

The next subsubsections provide these packaged bounds by composing the atomic lemmas already proved (RMSNorm, Gaussian linear maps, pointwise nonlinearities, and Gaussian residual connection in Lemma 3.6 and Theorem 3.5). For the attention operation, the proofs use only the fact that the headwise mixing operators are column-stochastic; the resulting bounds are uniform in the number of heads and do not depend on whether masks or positional encodings are used.

For MLP sublayers, we distinguish two activation regimes. In the *mean-spike-inducing* regime (Section 3, Theorem 2.6), a nonzero Gaussian mean introduces a rank-one contribution to the second moment and forces the post-activation matrix to have uniformly low stable rank; this is recorded in Assumption A and used in Lemma 3.12. In the *propagation* regime treated below, the activation does not provide such a uniform reset; instead, the post-activation matrix has stable rank controlled by that of the RMS-normalized input, and we additionally track a uniform upper bound on the column norms needed for the residual connection and subsequent RMSNorm. Two natural examples are gated MLPs and pointwise activations applied to normalized inputs.

Finally, we include one mixture-of-experts calculation as a one-off illustration of the breadth of the calculus rules: under arbitrary routing, stable rank still propagates assuming only $\hat{\sigma}_1(1) > 0$ from Theorem 3.4. We will not return to MoE layers elsewhere in the paper.

3.2.1 Attention layer propagation

We now derive an attention layer estimate by combining the atomic rules already proved: RMS normalization (Theorem 3.2), Gaussian linear maps (Theorem 3.1), and Gaussian residual connections for column norms and stable rank (Lemma 3.6 and Theorem 3.5). The only property of the attention kernels used below is that they act as column-stochastic mixing operators. See the companion Figure 12.

Definition 3.10 (Multi-headed value aggregation map). Fix integers $n_{\text{head}} \geq 1$ and $d \geq 1$ with d divisible by n_{head} , and set $d_{\text{head}} := d/n_{\text{head}}$. Fix matrices $P^{(h)} \in \mathbf{R}^{n \times n}$ for $h \in [n_{\text{head}}]$, each with columns that are probability vectors. Fix matrices $W_O \in \mathbf{R}^{d \times d}$ and $W_V^{(h)} \in \mathbf{R}^{d_{\text{head}} \times d}$ for $h \in [n_{\text{head}}]$. Given any input $X \in \mathbf{R}^{d \times n}$ define

$$A^{\text{rms}} := \text{RMSNorm}(X), \quad Y^{(h)} := A^{\text{rms}} P^{(h)}, \quad H^{(h)} := W_V^{(h)} Y^{(h)} \in \mathbf{R}^{d_{\text{head}} \times n},$$

$$H := \text{Concat}_{h \in [n_{\text{head}}]} H^{(h)} \in \mathbf{R}^{d \times n}, \quad X^{\text{att}} := X + W_O H, \quad A_{\text{mlp}}^{\text{rms}} := \text{RMSNorm}(X^{\text{att}}),$$

and set $\text{MHA}(X) := X^{\text{att}}$.

Where the matrices $P^{(h)}$ come from. In a standard decoder block, $P^{(h)}$ is obtained from the headwise query/key projections $Q^{(h)} = W_Q^{(h)} A^{\text{rms}}$ and $K^{(h)} = W_K^{(h)} A^{\text{rms}}$ via a (masked) softmax:

$$P^{(h)} = \text{softmax}(d_{\text{head}}^{-1/2} (K^{(h)})^\top Q^{(h)}),$$

possibly with positional encodings (RoPE) folded into $Q^{(h)}, K^{(h)}$. For the bounds below we do not use this structure; we only require that each $P^{(h)}$ is column-stochastic. To keep notation light we write $\text{MHA}(X)$, although it depends on all parameters $\{P^{(h)}\}_{h \in [n_{\text{head}}]}$, $\{W_V^{(h)}\}_{h \in [n_{\text{head}}]}$, and W_O .

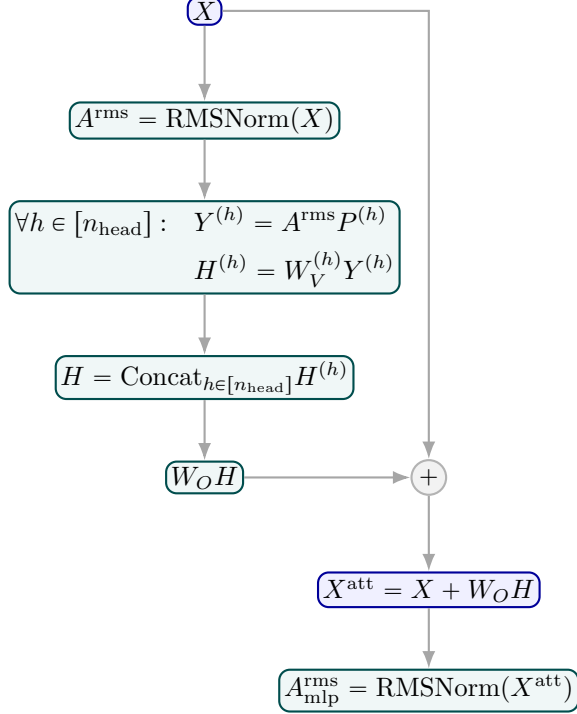


Figure 12: Multi-headed value aggregation sublayer (the attention kernels $P^{(h)}$ are treated as column-stochastic matrices).

Lemma 3.11 (Attention/RMS sublayer bounds). *Fix constants $c_-, c_+ > 0$. Let $X \in \mathbb{R}^{d \times n}$ be a matrix. Suppose the squared column norms of X lie between $c_- d$ and $c_+ d$. We work in the setting of Definition 3.10. Assume that $W_O \in \mathbb{R}^{d \times d}$ and $\{W_V^{(h)} \in \mathbb{R}^{d_{\text{head}} \times d}\}_{h \in [n_{\text{head}}]}$ have iid entries $\mathcal{N}(0, 1/d)$. Fix $\delta \in (0, \frac{1}{4})$. Then there exist numerical constants $c, C > 0$ such that, whenever $d_{\text{head}} \geq C\delta^{-2} \log(nn_{\text{head}})$, the following hold with probability at least $1 - Ce^{-c\delta^2 d_{\text{head}}}$:*

(i) **Column norms of X^{att} .** For all $t = 1, \dots, n$, we have

$$(1 - \delta)c_- d \leq \|x_t^{\text{att}}\|_2^2 \leq (1 + \delta)(c_+ + 1)d.$$

(ii) **Stable ranks.** The matrices $A^{\text{rms}}, X^{\text{att}}, A_{\text{mlp}}^{\text{rms}}$ satisfy

$$\begin{aligned} \text{st}(A^{\text{rms}}) &\leq \frac{c_+}{c_-} \text{st}(X), \\ \text{st}(X^{\text{att}}) &\leq \frac{1 + \delta}{1 - \delta} \left(1 + \frac{2}{c_-}\right) \text{st}(X), \\ \text{st}(A_{\text{mlp}}^{\text{rms}}) &\leq \frac{(1 + \delta)^2}{(1 - \delta)^2} \frac{c_+ + 1}{c_-} \left(1 + \frac{2}{c_-}\right) \text{st}(X). \end{aligned}$$

Proof. Throughou the proof, set $\eta := \delta/4$. We go in order through the operations making up the multi-head attention layer.

RMS normalization of the input. By the column norm assumptions on X , we have $c_-d \leq \|x_t\|_2^2 \leq c_+d$ for all t . Applying Theorem 3.2 with $L = c_-d$ and $U = c_+d$ yields

$$\text{st}(A^{\text{rms}}) \leq \frac{c_+}{c_-} \text{st}(X), \quad \|A^{\text{rms}}\|_F^2 = \sum_{t=1}^n \|a_t\|_2^2 = nd,$$

since each RMS-normalized column satisfies $\|a_t\|_2^2 = d$.

Bounds for $Y^{(h)}$ and $H^{(h)}$; concatenation. Fix a head $h \in [n_{\text{head}}]$ and write $Y^{(h)} = [y_1^{(h)}, \dots, y_n^{(h)}]$. Since each column of $P^{(h)}$ is a probability vector, Jensen's inequality yields

$$\|y_t^{(h)}\|_2^2 = \left\| \sum_{i=1}^n P_{it}^{(h)} a_i \right\|_2^2 \leq \sum_{i=1}^n P_{it}^{(h)} \|a_i\|_2^2 = d, \quad \forall t = 1, \dots, n,$$

and hence $\|Y^{(h)}\|_F^2 \leq nd$.

Condition on $Y^{(h)}$ and let $W_V^{(h)} \in \mathbf{R}^{d_{\text{head}} \times d}$ have iid entries $\mathcal{N}(0, 1/d)$. By Theorem 3.1 (with $k = d_{\text{head}}$ and $\varepsilon = \eta$), with probability at least $1 - 4e^{-c\eta^2 d_{\text{head}}}$, we have

$$\|H^{(h)}\|_F^2 = \|W_V^{(h)} Y^{(h)}\|_F^2 \leq (1 + \eta) \frac{d_{\text{head}}}{d} \|Y^{(h)}\|_F^2 \leq (1 + \eta) n d_{\text{head}}.$$

Applying the same theorem to each column $y_t^{(h)} \in \mathbf{R}^{d \times 1}$ and taking a union bound over $(h, t) \in [n_{\text{head}}] \times [n]$, whenever $d_{\text{head}} \geq C\eta^{-2} \log(nn_{\text{head}})$ we also have with probability at least $1 - Ce^{-c\eta^2 d_{\text{head}}}$, the estimates

$$\|h_t^{(h)}\|_2^2 = \|W_V^{(h)} y_t^{(h)}\|_2^2 \leq (1 + \eta) \frac{d_{\text{head}}}{d} \|y_t^{(h)}\|_2^2 \leq (1 + \eta) d_{\text{head}} \quad \forall (h, t).$$

On this event, we have

$$\|H\|_F^2 = \sum_{h=1}^{n_{\text{head}}} \|H^{(h)}\|_F^2 \leq (1 + \eta) n d, \quad \|h_t\|_2^2 = \sum_{h=1}^{n_{\text{head}}} \|h_t^{(h)}\|_2^2 \leq (1 + \eta) d \quad \forall t.$$

Denote this event by E_V .

Column norms of $X^{\text{att}} = X + W_O H$. Condition on H and let $W_O \in \mathbf{R}^{d \times d}$ have i.i.d. entries $\mathcal{N}(0, 1/d)$, independent of the $\{W_V^{(h)}\}$. Apply Lemma 3.6 with parameter η (here $k = d$): on an event E_O with probability at least $1 - Ce^{-c\eta^2 d}$, simultaneously for all t , we have

$$(1 - \eta)(\|x_t\|_2^2 + \|h_t\|_2^2) \leq \|x_t^{\text{att}}\|_2^2 \leq (1 + \eta)(\|x_t\|_2^2 + \|h_t\|_2^2).$$

On $E_V \cap E_O$, using $c_-d \leq \|x_t\|_2^2$ and $\|h_t\|_2^2 \geq 0$ gives

$$\|x_t^{\text{att}}\|_2^2 \geq (1 - \eta)c_-d \geq (1 - \delta)c_-d.$$

Using $\|x_t\|_2^2 \leq c_+d$ and $\|h_t\|_2^2 \leq (1 + \eta)d$ (from E_V) yields

$$\|x_t^{\text{att}}\|_2^2 \leq (1 + \eta)(c_+d + (1 + \eta)d) \leq (1 + \eta)^2(c_+ + 1)d \leq (1 + \delta)(c_+ + 1)d,$$

since $(1 + \eta)^2 \leq 1 + \delta$ for $\eta = \delta/4$ and $\delta \in (0, 1)$. This proves (i).

Stable rank of X^{att} . Apply Theorem 3.5 (with parameter δ) to $X^{\text{att}} = X + W_O H$:

$$\text{st}(X^{\text{att}}) \leq \frac{1+\delta}{1-\delta} \cdot \frac{\|X\|_F^2 + \|H\|_F^2}{\|X\|_{\text{op}}^2} = \frac{1+\delta}{1-\delta} \left(1 + \frac{\|H\|_F^2}{\|X\|_F^2}\right) \text{st}(X).$$

On E_V we have $\|H\|_F^2 \leq (1+\eta)nd$, while $\|X\|_F^2 = \sum_t \|x_t\|_2^2 \geq nc_-d$, hence $\|H\|_F^2/\|X\|_F^2 \leq (1+\eta)/c_- \leq 2/c_-$. Therefore, we deduce

$$\text{st}(X^{\text{att}}) \leq \frac{1+\delta}{1-\delta} \left(1 + \frac{2}{c_-}\right) \text{st}(X).$$

Stable rank of $A_{\text{mlp}}^{\text{rms}} = \text{RMSNorm}(X^{\text{att}})$. Apply Theorem 3.2 to X^{att} using (i), i.e. with $L = (1-\delta)c_-d$ and $U = (1+\delta)(c_+ + 1)d$:

$$\text{st}(A_{\text{mlp}}^{\text{rms}}) \leq \frac{(1+\delta)(c_+ + 1)}{(1-\delta)c_-} \text{st}(X^{\text{att}}),$$

and substitute the bound on $\text{st}(X^{\text{att}})$.

Probability. With the condition $d_{\text{head}} \geq C\eta^{-2} \log(nn_{\text{head}})$, the event E_V fails with probability at most $Ce^{-c\eta^2 d_{\text{head}}}$ after absorbing the union bound over (h, t) . The event E_O fails with probability at most $Ce^{-c\eta^2 d} \leq Ce^{-c\eta^2 d_{\text{head}}}$, and Theorem 3.5 fails with probability at most $Ce^{-c\delta^2 d} \leq Ce^{-c\delta^2 d_{\text{head}}}$. Since $\eta = \delta/4$, a final union bound (conditionally) yields the stated probability. \square

We next move on to the MLP layer of the transformer. We isolate two cases depending on the weather the activation function is mean-spike-inducing (Section 3.2.2) or is not (Section 3.2.3).

3.2.2 Mean-spike-inducing (MSI) MLP layer propagation

This subsection packages the mean-spike-inducing (MSI) MLP sublayer as a composition of the atomic operations already analyzed: RMS normalization (Theorem 3.2), a Gaussian linear map followed by a pointwise activation (captured here by Assumption A), and a Gaussian residual update (Lemma 3.6 and Theorem 3.5). We impose the following assumption. For the activations we will use later, Assumption A follows by combining Theorem 2.6 and Theorem 3.4. In particular, for the ReLU activation, one may take $\text{st}_\sigma = 2\pi$, $p_\sigma = 1/2$, and $P(\sigma, d, k, n) = 1 - c \exp(-Ck)$.

Assumption A. The activation function σ is 1-Lipschitz with $\sigma(0) = 0$. For any matrix $X \in \mathbb{R}^{d \times n}$ with equal column norms and any matrix $W \in \mathbb{R}^{k \times d}$ with iid entries $\mathcal{N}(0, \frac{1}{d})$, we have

$$\text{st}(\sigma(WX)) \leq \text{st}_\sigma \quad \text{and} \quad \|\sigma(WX)\|_F^2 \geq \frac{kp_\sigma}{d} \|X\|_F^2$$

with probability at least $P(\sigma, d, k, n)$, where st_σ and p_σ are some numerical constants.

Now, fix dimensions $d, k, n \geq 1$, an activation $\sigma : \mathbf{R} \rightarrow \mathbf{R}$, and weight matrices $W_1 \in \mathbf{R}^{k \times d}$ and $W_2 \in \mathbf{R}^{d \times k}$. For any input $X \in \mathbf{R}^{d \times n}$ define

$$A^{\text{rms}} := \text{RMSNorm}(X), \quad B := \sigma(W_1 A^{\text{rms}}), \quad X^+ := X + W_2 B.$$

See the companion Figure 13. The following theorem analyzes this setup.

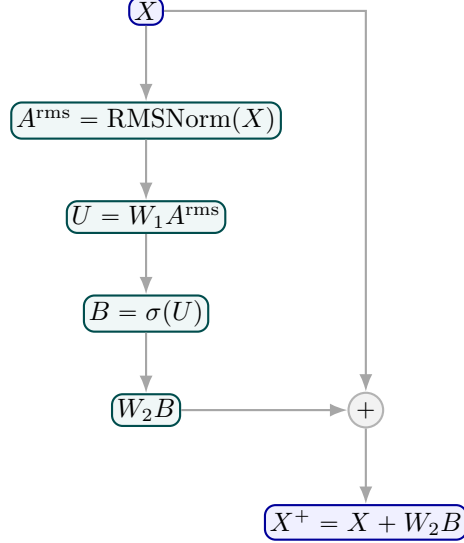


Figure 13: MLP sublayer (RMSNorm, pointwise activation, and residual update).

Lemma 3.12 (Mean-spike-inducing (MSI) MLP sublayer bounds). *Fix constants $c_-, c_+ > 0$. Let $X \in \mathbf{R}^{d \times n}$ be a matrix whose squared column norms lie between $c_- d$ and $c_+ d$. Assume σ satisfies Assumption A. Assume $W_1 \in \mathbf{R}^{k \times d}$ and $W_2 \in \mathbf{R}^{d \times k}$ are independent Gaussian matrices with i.i.d. entries of variance $1/d$ and $1/k$, respectively. Fix $\delta \in (0, \frac{1}{4})$. Then there exist numerical constants $c, C > 0$ such that, whenever $\min\{d, k\} \geq C\delta^{-2} \log n$, the following holds with probability at least*

$$1 - Ce^{-c\delta^2 d} - Ce^{-c\delta^2 k} - (1 - P(\sigma, d, k, n)).$$

(i) **Column norms of X^+ .** For all $t = 1, \dots, n$,

$$(1 - \delta)c_- d \leq \|x_t^+\|_2^2 \leq (1 + \delta)^2(c_+ + 1)d.$$

(ii) **Stable ranks.** We have

$$\text{st}(B) \leq \text{st}_\sigma, \quad \text{st}(X^+) \leq \frac{1 + \delta}{1 - \delta} \left(1 + \frac{c_+}{p_\sigma}\right) \text{st}_\sigma.$$

Proof. Throughout the proof let $\eta := \delta/2$. We work through the MLP layer in order.

Column norms of X^+ . Write $A^{\text{rms}} = [a_1, \dots, a_n]$. By definition of RMSNorm, $\|a_t\|_2^2 = d$ for all t . For each t , define $u_t := W_1 a_t$. Conditional on a_t , we have $u_t \sim \mathcal{N}(0, I_k)$, and since σ is 1-Lipschitz with $\sigma(0) = 0$, we have $|\sigma(u)| \leq |u|$ entrywise and hence

$$\|b_t\|_2^2 \leq \|u_t\|_2^2.$$

A χ^2 tail bound and a union bound over $t = 1, \dots, n$ imply that, whenever $k \geq C\eta^{-2} \log n$, with probability at least $1 - Ce^{-c\eta^2 k}$, we have

$$\|b_t\|_2^2 \leq (1 + \eta)k \quad \text{for all } t. \tag{3.22}$$

Condition on (X, B) and apply Lemma 3.6 with parameter η to $X^+ = X + W_2 B$ (here W_2 has i.i.d. $\mathcal{N}(0, 1/k)$ entries). On an event of probability at least $1 - Ce^{-c\eta^2 d}$ (absorbing the union bound over t using $d \geq C\eta^{-2} \log n$), simultaneously for all t , we deduce

$$(1 - \eta) \left(\|x_t\|_2^2 + \frac{d}{k} \|b_t\|_2^2 \right) \leq \|x_t^+\|_2^2 \leq (1 + \eta) \left(\|x_t\|_2^2 + \frac{d}{k} \|b_t\|_2^2 \right).$$

Using $\|b_t\|_2^2 \geq 0$ and $\|x_t\|_2^2 \geq c_- d$ yields

$$\|x_t^+\|_2^2 \geq (1 - \eta)c_- d \geq (1 - \delta)c_- d.$$

Using $\|x_t\|_2^2 \leq c_+ d$ and (3.22) yields

$$\|x_t^+\|_2^2 \leq (1 + \eta) \left(c_+ d + (1 + \eta)d \right) = (1 + \eta)^2 (c_+ + 1)d \leq (1 + \delta)^2 (c_+ + 1)d,$$

which proves (i).

Stable rank of B . By Assumption A applied to the equal-column-norm matrix A^{rms} and the Gaussian matrix W_1 , on an event E_σ with $\mathbb{P}(E_\sigma) \geq P(\sigma, d, k, n)$ we have

$$\text{st}(B) \leq \text{st}_\sigma, \quad \|B\|_F^2 \geq \frac{kp_\sigma}{d} \|A^{\text{rms}}\|_F^2.$$

Since $\|A^{\text{rms}}\|_F^2 = nd$, this gives $\|B\|_F^2 \geq p_\sigma kn$ on E_σ .

Stable rank of X^+ . Condition on B and apply Theorem 3.5 (with parameter δ) to $X^+ = X + W_2 B$ to get

$$\text{st}(X^+) \leq \frac{1 + \delta}{1 - \delta} \left(\frac{k}{d} \frac{\|X\|_F^2}{\|B\|_{\text{op}}^2} + \text{st}(B) \right).$$

Using $\|X\|_F^2 \leq nc_+ d$ and, on E_σ , the bounds $\text{st}(B) \leq \text{st}_\sigma$ and $\|B\|_{\text{op}}^2 = \|B\|_F^2/\text{st}(B) \geq p_\sigma kn/\text{st}_\sigma$, we obtain

$$\frac{k}{d} \frac{\|X\|_F^2}{\|B\|_{\text{op}}^2} \leq \frac{k}{d} \cdot \frac{nc_+ d}{p_\sigma kn/\text{st}_\sigma} = \frac{\text{st}_\sigma c_+}{p_\sigma}.$$

Therefore, on E_σ , we have

$$\text{st}(X^+) \leq \frac{1 + \delta}{1 - \delta} \left(\frac{\text{st}_\sigma c_+}{p_\sigma} + \text{st}_\sigma \right) = \text{st}_\sigma \frac{1 + \delta}{1 - \delta} \left(1 + \frac{c_+}{p_\sigma} \right),$$

which is (ii).

Probability. Take a union bound (conditionally) over: the column-norm bound (3.22) (probability $\geq 1 - Ce^{-c\eta^2 k}$ after $k \geq C\eta^{-2} \log n$), the residual column-norm event for X^+ (probability $\geq 1 - Ce^{-c\eta^2 d}$ after $d \geq C\eta^{-2} \log n$), the event from Theorem 3.5 (probability $\geq 1 - Ce^{-c\delta^2 d}$), and E_σ (probability $\geq P(\sigma, d, k, n)$). Since $\eta = \delta/2$, this yields the stated probability. \square

3.2.3 MLP layer propagation without mean induced spikes

Unlike the mean-spike-inducing MLP sublayer (Lemma 3.12), here we treat MLP sublayers in which the post-activation matrix does *not* reset to uniformly low stable rank. Instead, stable rank propagates from the RMS-normalized input, and we additionally track a uniform upper bound on the column norms of the intermediate matrix in order to control the subsequent residual update and to re-enter RMSNorm in the next block. We package the two quantitative requirements on the intermediate matrix B into the following assumption.

Assumption B (Propagation interface). Fix $\delta \in (0, 1)$ and dimensions $d, k, n \geq 1$. Let $X \in \mathbf{R}^{d \times n}$ be deterministic and set $A^{\text{rms}} := \text{RMSNorm}(X)$. Let $B = [b_1, \dots, b_n] \in \mathbf{R}^{k \times n}$ be a (possibly random) matrix. We assume there exist constants $C_{\text{PROP}} \geq 1$ and $m_* \geq 0$ and a success probability $P_{\text{PROP}}(\delta) \in [0, 1]$ such that, with probability at least $P_{\text{PROP}}(\delta)$, it holds:

$$\text{st}(B) \leq C_{\text{PROP}} \text{st}(A^{\text{rms}}) \quad \text{and} \quad \|b_t\|_2^2 \leq m_* k \quad \text{for all } t \in [n].$$

There are two natural constructions of B : a gated activation (see Figure 14) and a pointwise activation with $\hat{\sigma}_1(1)^2 > 0$ applied to RMS-normalized inputs. The next lemma verifies that both satisfy Assumption B at Gaussian initialization with explicit constants.

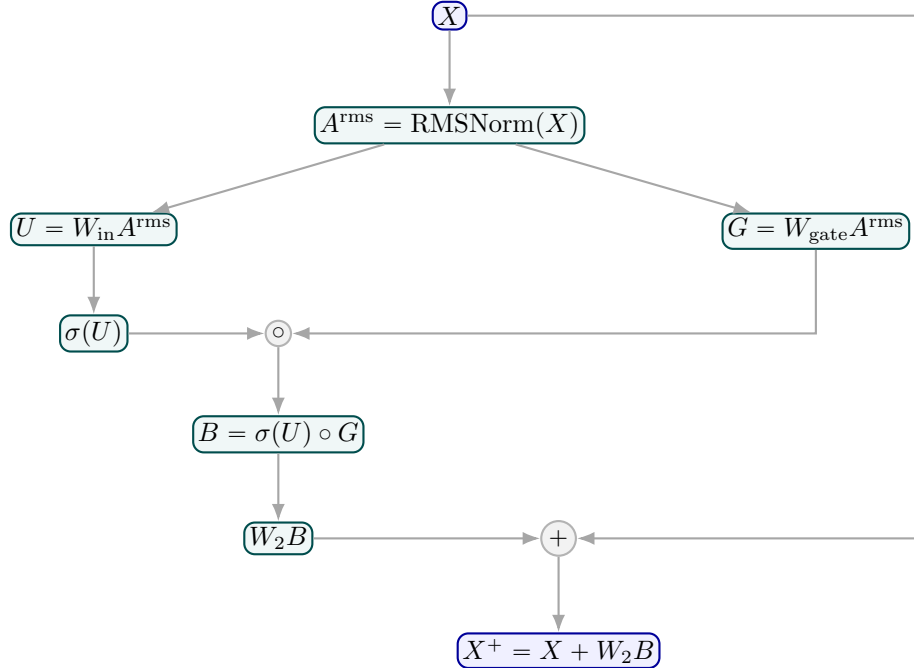


Figure 14: Gated MLP sublayer (two linear maps, pointwise gate, and residual update).

Lemma 3.13 (Gated and Hermite activations satisfy Assumption B). Fix $\delta \in (0, 1)$ and let $A = [a_1, \dots, a_n] \in \mathbf{R}^{d \times n}$ satisfy $\|a_t\|_2^2 = d$ for all $t \in [n]$.

(a) **Gated case.** Assume the setting of Theorem 3.8 (in particular, $k \asymp d$) and set $m_1 = |\mathbb{E}\sigma(\gamma)|$ and $m_2 = \mathbb{E}\sigma(\gamma)^2$ where $\gamma \sim \mathcal{N}(0, 1)$ is a standard Gaussian. Let $W_{\text{in}}, W_{\text{gate}} \in \mathbf{R}^{k \times d}$ be independent with iid entries $\mathcal{N}(0, 1/d)$ and set

$$B := \sigma(W_{\text{in}} A) \circ (W_{\text{gate}} A) \in \mathbf{R}^{k \times n}.$$

Then Assumption B holds (with A^{rms} replaced by A) with

$$C_{\text{PROP}} = \frac{(1+\delta)^2}{(1-\delta)^3} \cdot \frac{1}{m_1^2}, \quad m_* = (1+\delta)m_2,$$

and with probability at least

$$P_{\text{PROP}}(\delta) \geq 1 - n \left(2e^{-c\delta^2 k} + 2ke^{-\frac{1}{2}k^{1/3}} + 2e^{-c\delta^2(1-\delta)m_2 k^{2/3}} \right) - C \exp\left(-c\delta^2 \frac{k}{\log^2 k}\right) - \frac{1}{k^q},$$

for any fixed $q > 0$, with constants c, C depending only on q .

(b) **Hermite case.** Suppose $p := \hat{\sigma}_1(1)^2 > 0$. Let $W_1 \in \mathbf{R}^{k \times d}$ have i.i.d. entries $\mathcal{N}(0, 1/d)$ and set

$$B := \sigma(W_1 A) \in \mathbf{R}^{k \times n}.$$

Then Assumption B holds (with A^{rms} replaced by A) with

$$C_{\text{PROP}} = \frac{1+\delta}{1-\delta} \cdot \frac{1}{p}, \quad m_* = 1+\delta,$$

and with probability at least

$$P_{\text{PROP}}(\delta) \geq 1 - 8 \exp(-c\delta^2 p^2 k) - Cn \exp(-c\delta^2 k).$$

Proof. (a) **Gated case.** For the stable-rank bound, apply Theorem 3.8 with $Z = X = A$, $V = W_{\text{in}}$, $W = W_{\text{gate}}$. Since $\|a_t\|_2^2 = d$ for all t , the parameters in Theorem 3.8 satisfy $L = U = d$ and the mean condition there holds with $\kappa = m_1$, yielding

$$\text{st}(B) \leq \frac{(1+\delta)^2}{(1-\delta)^3} \cdot \frac{1}{m_1^2} \text{st}(A)$$

with the stated probability contribution.

For the column-norm envelope, apply Lemma 3.9 to each column a_t (with parameter $\delta/3$) and take a union bound over $t \in [n]$. Since $(1+\delta/3)^2 \leq 1+\delta$ for $\delta \in (0, 1)$, this gives $\|b_t\|_2^2 \leq (1+\delta)m_2 k$ for all t with the stated probability after adjusting constants.

(b) **simple nonlinear activation case.** Since $\|a_t\|_2^2 = d$, the parameter p in (3.3) for Theorem 3.4 equals $\hat{\sigma}_1(1)^2$. Applying Theorem 3.4 to W_1 and A gives

$$\text{st}(B) \leq \frac{1+\delta}{1-\delta} \cdot \frac{1}{p} \text{st}(A)$$

with probability at least $1 - 8 \exp(-c\delta^2 p^2 k)$.

For the column-norm envelope, fix $t \in [n]$. Since σ is 1-Lipschitz with $\sigma(0) = 0$, we have $|\sigma(u)| \leq |u|$, hence $\|b_t\|_2^2 \leq \|W_1 a_t\|_2^2$. But $W_1 a_t \sim \mathcal{N}(0, I_k)$, so a χ^2 tail bound yields $\mathbb{P}(\|W_1 a_t\|_2^2 > (1+\delta)k) \leq \exp(-c\delta^2 k)$. A union bound over $t \in [n]$ gives the stated probability. \square

We now show how Assumption B feeds into the residual update $X^+ = X + W_2 B$. The only additional hypothesis needed is that B is independent of the Gaussian output matrix W_2 .

Lemma 3.14 (Propagation-activation MLP sublayer bounds). *Fix $\delta \in (0, \frac{1}{4})$ and constants $c_-, c_+ > 0$. Let $X \in \mathbf{R}^{d \times n}$ be a matrix whose squared column norms lie between $c_- d$ and $c_+ d$. Set $A^{\text{rms}} := \text{RMSNorm}(X)$. Let $B = [b_1, \dots, b_n] \in \mathbf{R}^{k \times n}$ be a random matrix satisfying Assumption B (with this δ , constants C_{PROP}, m_* , and success probability $P_{\text{PROP}}(\delta)$). Assume $W_2 \in \mathbf{R}^{d \times k}$ has i.i.d. entries $\mathcal{N}(0, 1/k)$ and is independent of B , and define*

$$X^+ := X + W_2 B.$$

Then there exist numerical constants $c, C > 0$ such that, whenever $d \geq C\delta^{-2} \log n$, the following holds with probability at least

$$1 - Ce^{-c\delta^2 d} - (1 - P_{\text{PROP}}(\delta)).$$

(i) **Column norms of X^+ .** For all $t \in [n]$, it holds:

$$(1 - \delta)c_- d \leq \|x_t^+\|_2^2 \leq (1 + \delta)(c_+ + m_*)d.$$

(ii) **Stable ranks.** On the same event, it holds:

$$\text{st}(B) \leq C_{\text{PROP}} \text{st}(A^{\text{rms}}) \leq \frac{c_+}{c_-} C_{\text{PROP}} \text{st}(X),$$

and

$$\text{st}(X^+) \leq \frac{1 + \delta}{1 - \delta} \left(1 + \frac{m_*}{c_-}\right) \text{st}(X).$$

Proof. Let E_{prop} denote the event in Assumption B, so $\mathbb{P}(E_{\text{prop}}) \geq P_{\text{PROP}}(\delta)$.

Column norms. Condition on (X, B) and apply Lemma 3.6 (with parameter δ) to $X^+ = X + W_2 B$. On an event E_{col} with probability at least $1 - Cn \exp(-c\delta^2 d)$, simultaneously for all $t \in [n]$,

$$(1 - \delta) \left(\|x_t\|_2^2 + \frac{d}{k} \|b_t\|_2^2 \right) \leq \|x_t^+\|_2^2 \leq (1 + \delta) \left(\|x_t\|_2^2 + \frac{d}{k} \|b_t\|_2^2 \right).$$

On $E_{\text{prop}} \cap E_{\text{col}}$, using $\|x_t\|_2^2 \geq c_- d$ gives the lower bound $\|x_t^+\|_2^2 \geq (1 - \delta)c_- d$. Using $\|x_t\|_2^2 \leq c_+ d$ and $\|b_t\|_2^2 \leq m_* k$ from E_{prop} yields

$$\|x_t^+\|_2^2 \leq (1 + \delta) \left(c_+ d + m_* d \right) = (1 + \delta)(c_+ + m_*)d,$$

which proves (i).

Stable ranks. On E_{prop} we have $\text{st}(B) \leq C_{\text{PROP}} \text{st}(A^{\text{rms}})$. Since the squared column norms of X lie between $c_- d$ and $c_+ d$, Theorem 3.2 gives $\text{st}(A^{\text{rms}}) \leq \frac{c_+}{c_-} \text{st}(X)$, proving the displayed bound for $\text{st}(B)$.

For X^+ , condition on B and apply Theorem 3.5 (with parameter δ) to $X^+ = X + W_2 B$. Lower bounding the denominator in (3.7) by $\frac{1}{d} \|X\|_{\text{op}}^2$ yields

$$\text{st}(X^+) \leq \frac{1 + \delta}{1 - \delta} \left(1 + \frac{d}{k} \frac{\|B\|_F^2}{\|X\|_F^2} \right) \text{st}(X).$$

On E_{prop} , we have $\|B\|_F^2 = \sum_{t=1}^n \|b_t\|_2^2 \leq n m_* k$, while $\|X\|_F^2 = \sum_{t=1}^n \|x_t\|_2^2 \geq n c_- d$, so

$$\frac{d}{k} \frac{\|B\|_F^2}{\|X\|_F^2} \leq \frac{m_*}{c_-},$$

which gives the stated bound on $\text{st}(X^+)$.

Probability. By independence of W_2 from B , the residual column-norm event and Theorem 3.5 hold with the same probabilities after conditioning on (X, B) . A union bound gives failure probability at most $(1 - P_{\text{PROP}}(\delta)) + Cne^{-c\delta^2 d} + 10e^{-c\delta^2 d}$. Under $d \geq C\delta^{-2} \log n$, we have $Cne^{-c\delta^2 d} \leq Ce^{-c'\delta^2 d}$ after adjusting constants, which yields the claim. \square

3.2.4 Mixture of Experts layer propagation

We include this final MoE calculation as an illustration of the calculus rules developed above. Unlike the MLP sublayers studied earlier, we will not return to this layer in a later section. Instead, we present this result simply to illustrate that the atomic lemmas already suffice to control propagation through a mixture-of-experts update with *arbitrary* routing: the routing weights enter only through the simplex bound $\sum_e r_{e,t}^2 \leq 1$, while stable-rank control of each expert activation is supplied directly by Theorem 3.4. See the companion Figure 15.

Definition 3.15 (MoE-MLP sublayer map). Fix dimensions $d, k, n, n_{\text{exp}} \geq 1$, an activation $\sigma : \mathbf{R} \rightarrow \mathbf{R}$, expert weight matrices $\{W_1^{(e)}\}_{e \in [n_{\text{exp}}]} \subset \mathbf{R}^{k \times d}$ and $\{W_2^{(e)}\}_{e \in [n_{\text{exp}}]} \subset \mathbf{R}^{d \times k}$, and routing weights $R = (r_{e,t}) \in [0, 1]^{n_{\text{exp}} \times n}$ with $\sum_{e \in [n_{\text{exp}}]} r_{e,t} = 1$ for each $t \in [n]$. Let $D^{(e)} := \text{diag}(r_{e,1}, \dots, r_{e,n})$. For any input $X \in \mathbf{R}^{d \times n}$ define

$$\begin{aligned} A^{\text{rms}} &:= \text{RMSNorm}(X), \\ B^{(e)} &:= \sigma(W_1^{(e)} A^{\text{rms}}) \quad (e \in [n_{\text{exp}}]), \\ X^+ &:= \text{MoE-MLP}(X) := X + \sum_{e \in [n_{\text{exp}}]} W_2^{(e)} B^{(e)} D^{(e)}. \end{aligned}$$

We suppress the dependence of $\text{MoE-MLP}(\cdot)$ on $(\{W_1^{(e)}, W_2^{(e)}\}_{e \in [n_{\text{exp}}]}, \sigma, R)$ in the notation.

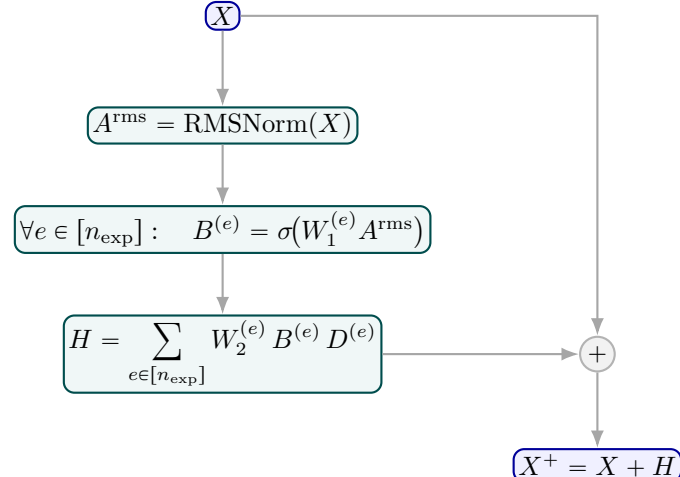


Figure 15: MoE-MLP sublayer (RMSNorm, expert MLPs with routing weights, aggregation, and residual update).

Lemma 3.16 (MoE-MLP sublayer bounds). Fix constants $c_-, c_+ > 0$ and an integer $n_{\text{exp}} \geq 1$. Let $X \in \mathbf{R}^{d \times n}$ be a matrix whose squared column norms lie between $c_- d$ and $c_+ d$. Work in the setting of Definition 3.15. Assume σ is 1-Lipschitz with $\sigma(0) = 0$, and assume $\hat{\sigma}(1)^2 > 0$. Assume

$\{W_1^{(e)}\}_{e \in [n_{\text{exp}}]}$ and $\{W_2^{(e)}\}_{e \in [n_{\text{exp}}]}$ are mutually independent Gaussian matrices with i.i.d. entries of variance $1/d$ and $1/k$, respectively. Fix $\delta \in (0, \frac{1}{4})$. Then there exist numerical constants $c, C > 0$ such that, whenever $\min\{d, k\} \geq C\delta^{-2} \log(n n_{\text{exp}})$, the following holds with probability at least

$$1 - Ce^{-c\delta^2 d} - Ce^{-c\delta^2 k} - 8n_{\text{exp}}e^{-c\delta^2 \hat{\sigma}(1)^4 k}.$$

(i) **Column norms of X^+ .** For all $t \in [n]$,

$$(1 - \delta)c_- d \leq \|x_t^+\|_2^2 \leq (1 + \delta)^2(c_+ + 1)d.$$

(ii) **Stable ranks.** For all $e \in [n_{\text{exp}}]$, it holds:

$$\text{st}(B^{(e)}) \leq \frac{1 + \delta}{1 - \delta} \frac{1}{\hat{\sigma}_1^2(1)} \text{st}(A^{\text{rms}}) \leq \frac{1 + \delta}{1 - \delta} \frac{c_+}{c_-} \frac{1}{\hat{\sigma}_1^2(1)} \text{st}(X),$$

and

$$\text{st}(X^+) \leq \frac{1 + \delta}{1 - \delta} \left(1 + \frac{1 + \delta}{c_-}\right) \text{st}(X).$$

Proof. Let $\eta := \delta/2$.

Column norms of X^+ . Write $A^{\text{rms}} = [a_1, \dots, a_n]$. By definition of RMSNorm, $\|a_t\|_2^2 = d$ for all t . For each expert $e \in [n_{\text{exp}}]$ and token $t \in [n]$, define $u_t^{(e)} := W_1^{(e)} a_t$ and $b_t^{(e)} := \sigma(u_t^{(e)})$. Conditional on a_t , we have $u_t^{(e)} \sim \mathcal{N}(0, I_k)$, and since σ is 1-Lipschitz with $\sigma(0) = 0$, we have $|\sigma(u)| \leq |u|$ entrywise and hence $\|b_t^{(e)}\|_2^2 \leq \|u_t^{(e)}\|_2^2$. A χ^2 tail bound and a union bound over $(e, t) \in [n_{\text{exp}}] \times [n]$ imply that, whenever $k \geq C\eta^{-2} \log(n n_{\text{exp}})$, with probability at least $1 - Ce^{-c\eta^2 k}$,

$$\|b_t^{(e)}\|_2^2 \leq (1 + \eta)k \quad \text{for all } e \in [n_{\text{exp}}], t \in [n]. \quad (3.23)$$

Define the block matrices

$$W_2^{\text{moe}} := \frac{1}{\sqrt{n_{\text{exp}}}} \begin{bmatrix} W_2^{(1)} & \cdots & W_2^{(n_{\text{exp}})} \end{bmatrix} \in \mathbf{R}^{d \times (kn_{\text{exp}})}, \quad B^{\text{moe}} := \begin{bmatrix} \sqrt{n_{\text{exp}}} B^{(1)} D^{(1)} \\ \vdots \\ \sqrt{n_{\text{exp}}} B^{(n_{\text{exp}})} D^{(n_{\text{exp}})} \end{bmatrix} \in \mathbf{R}^{(kn_{\text{exp}}) \times n},$$

so that $X^+ = X + W_2^{\text{moe}} B^{\text{moe}}$. By construction, W_2^{moe} has i.i.d. $\mathcal{N}(0, 1/(kn_{\text{exp}}))$ entries and is independent of (X, B^{moe}) . Write $B^{\text{moe}} = [b_1^{\text{moe}}, \dots, b_n^{\text{moe}}]$. On the event (3.23), for each $t \in [n]$,

$$\|b_t^{\text{moe}}\|_2^2 = n_{\text{exp}} \sum_{e \in [n_{\text{exp}}]} r_{e,t}^2 \|b_t^{(e)}\|_2^2 \leq n_{\text{exp}}(1 + \eta)k \sum_{e \in [n_{\text{exp}}]} r_{e,t}^2 \leq n_{\text{exp}}(1 + \eta)k,$$

since $\sum_e r_{e,t} = 1$ implies $\sum_e r_{e,t}^2 \leq 1$.

Condition on (X, B^{moe}) and apply Lemma 3.6 with parameter η to $X^+ = X + W_2^{\text{moe}} B^{\text{moe}}$. On an event of probability at least $1 - Ce^{-c\eta^2 d}$ (absorbing the union bound over t using $d \geq C\eta^{-2} \log n$), simultaneously for all t ,

$$(1 - \eta) \left(\|x_t\|_2^2 + \frac{d}{kn_{\text{exp}}} \|b_t^{\text{moe}}\|_2^2 \right) \leq \|x_t^+\|_2^2 \leq (1 + \eta) \left(\|x_t\|_2^2 + \frac{d}{kn_{\text{exp}}} \|b_t^{\text{moe}}\|_2^2 \right).$$

Using $\|b_t^{\text{moe}}\|_2^2 \geq 0$ and $\|x_t\|_2^2 \geq c_- d$ yields

$$\|x_t^+\|_2^2 \geq (1 - \eta)c_- d \geq (1 - \delta)c_- d.$$

On (3.23), using $\|x_t\|_2^2 \leq c_+ d$ and $\|b_t^{\text{moe}}\|_2^2 \leq n_{\text{exp}}(1 + \eta)k$ yields

$$\|x_t^+\|_2^2 \leq (1 + \eta) \left(c_+ d + (1 + \eta)k \right) = (1 + \eta)^2(c_+ + 1)d \leq (1 + \delta)^2(c_+ + 1)d,$$

which proves (i).

Stable ranks of $B^{(e)}$. Fix $e \in [n_{\exp}]$ and apply Theorem 3.4 to the Gaussian matrix $W_1^{(e)}$ and the input A^{rms} , with $\varepsilon = \delta$. Since $\|a_t\|_2 = \sqrt{d}$ for all t , the parameter p in (3.3) reduces to $\hat{\sigma}_1^2(1)$, and Theorem 3.4 yields

$$\text{st}(B^{(e)}) \leq \frac{1+\delta}{1-\delta} \frac{1}{\hat{\sigma}_1^2(1)} \text{st}(A^{\text{rms}})$$

with probability at least $1 - 8e^{-c\delta^2 p^2 k}$. A union bound over $e \in [n_{\exp}]$ gives the first inequality in (ii) simultaneously for all experts. The second inequality in (ii) follows from Theorem 3.2, which gives $\text{st}(A^{\text{rms}}) \leq \frac{c_+}{c_-} \text{st}(X)$.

Stable rank of X^+ . Apply Theorem 3.5 (with parameter δ) to $X^+ = X + W_2^{\text{moe}} B^{\text{moe}}$:

$$\text{st}(X^+) \leq \frac{1+\delta}{1-\delta} \cdot \frac{\frac{1}{d} \|X\|_F^2 + \frac{1}{kn_{\exp}} \|B^{\text{moe}}\|_F^2}{\max\{\frac{1}{d} \|X\|_{\text{op}}^2, \frac{1}{kn_{\exp}} \|B^{\text{moe}}\|_{\text{op}}^2\}}.$$

Lower bound the denominator by $\frac{1}{d} \|X\|_{\text{op}}^2$ to obtain

$$\text{st}(X^+) \leq \frac{1+\delta}{1-\delta} \left(1 + \frac{d}{kn_{\exp}} \frac{\|B^{\text{moe}}\|_F^2}{\|X\|_F^2} \right) \text{st}(X), \quad \text{since } \text{st}(X) = \frac{\|X\|_F^2}{\|X\|_{\text{op}}^2}.$$

Using $\|X\|_F^2 = \sum_t \|x_t\|_2^2 \geq nc_- d$ and, on (3.23),

$$\|B^{\text{moe}}\|_F^2 = \sum_{t=1}^n \|b_t^{\text{moe}}\|_2^2 \leq n \cdot n_{\exp} (1 + \eta) k,$$

we obtain

$$\frac{d}{kn_{\exp}} \frac{\|B^{\text{moe}}\|_F^2}{\|X\|_F^2} \leq \frac{d}{kn_{\exp}} \cdot \frac{n \cdot n_{\exp} (1 + \eta) k}{nc_- d} = \frac{1 + \eta}{c_-} \leq \frac{1 + \delta}{c_-},$$

which yields the stated bound on $\text{st}(X^+)$.

Probability. Take a union bound over: the event (3.23) (probability $\geq 1 - Ce^{-c\eta^2 k}$ after $k \geq C\eta^{-2} \log(n_{\exp})$), the residual column-norm event for X^+ (probability $\geq 1 - Ce^{-c\eta^2 d}$ after $d \geq C\eta^{-2} \log n$), the event from Theorem 3.5 (probability $\geq 1 - Ce^{-c\delta^2 d}$), and the n_{\exp} activation events from Theorem 3.4. Since $\eta = \delta/2$, this yields the stated probability after adjusting constants. \square

4 MLPs with Gaussian initialization

We now combine the one-layer results to control the post-activation matrices of a depth- L bias-free MLP at Gaussian initialization (random weights and fixed data). There are two distinct behaviors depending on the activation. If $\mathbb{E}[\sigma(G)] \neq 0$ (mean-spike inducing), then every post-activation matrix has stable rank bounded by a constant depending only on the one-dimensional Gaussian moments of σ ; in particular, stable rank is *reset* at every layer, independently of the stable rank of the input data. If instead the first Hermite coefficient of σ is uniformly nondegenerate, then stable rank propagates through depth and can inflate at most exponentially.

Architecture. Consider a feedforward neural network parametrized by weight matrices W_1, \dots, W_L and a pointwise activation $\sigma: \mathbf{R} \rightarrow \mathbf{R}$ applied entrywise. Let $X \in \mathbf{R}^{d_0 \times n}$ be a data matrix, and define the post-activation matrices by

$$A_0 = X \quad \text{and} \quad A_\ell = \sigma(W_\ell A_{\ell-1}) \quad \forall \ell = 1, \dots, L. \quad (4.1)$$

Unless stated otherwise, we assume that $W_\ell \in \mathbf{R}^{d_\ell \times d_{\ell-1}}$ has iid entries $\mathcal{N}(0, 1/d_{\ell-1})$, and that the matrices $\{W_\ell\}_{\ell=1}^L$ are mutually independent.

Mean-spike inducing activations. Theorem 2.6 bounds $\text{st}(\sigma(WX))$ by a one-dimensional ratio $s_\sigma(a_X, b_X)$ when $\kappa_{\sigma,q}(a_X, b_X) > 0$, i.e., as soon as the Gaussian mean $\mathbb{E}[\sigma(sG)]$ does not vanish on the scale interval induced by the column norms of X and obeys a power- q lower bound there. For homogeneous activations this dependence on (a_X, b_X) disappears, giving input-independent bound.

Corollary 4.1 (All post-activations are low-stable rank with mean-induced spikes). *Assume that σ is p -homogeneous for some $p \geq 1$, satisfies $\sigma(0) = 0$, and the polynomial growth bound*

$$|\sigma(t)| \leq L_\sigma |t|^p \quad \text{for all } t \in \mathbf{R},$$

for some constant $L_\sigma < \infty$. Let $\gamma \sim \mathcal{N}(0, 1)$ be a standard Gaussian and define

$$m_1 := |\mathbb{E}[\sigma(\gamma)]|, \quad m_2 := \mathbb{E}[\sigma(\gamma)^2],$$

and assume $m_1 > 0$. Set $r := L_\sigma/m_1$. Fix $0 < \varepsilon_1 \leq 1$ and $0 < \varepsilon_2 < 1$. Then there exist a constant $c > 0$ that depends only on p , $\sigma(1)$, $\sigma(-1)$, m_1 such that, with probability at least

$$1 - \sum_{\ell=1}^L \left(2 \exp \left(-c \min \{d_\ell \varepsilon_2^2, d_\ell^{1 \wedge \frac{2}{p}} \varepsilon_2^{2/p}\} \right) + 2 \exp \left(-c \min \{d_\ell \varepsilon_1^2, d_\ell^{1 \wedge \frac{1}{p}} \varepsilon_1^{1/p}\} \right) \right),$$

the following holds simultaneously for every $\ell = 1, \dots, L$:

$$\text{st}(A_\ell) \leq \frac{1 + \varepsilon_1}{(1 - \varepsilon_2)^2} \cdot \frac{m_2}{m_1^2}.$$

Proof. This follows immediately by applying Corollary 2.7 conditionally layer by layer. \square

Propagation through nonlinearities. When $\mathbb{E}[\sigma(G)] = 0$, Corollary 4.1 does not apply. In this case we control stable rank using the nondegeneracy of the first Hermite coefficient (Theorem 3.4). For $s > 0$, write $\hat{\sigma}_1(s)$ for the first Hermite coefficient of $\sigma(s\gamma)$ (with $\gamma \sim \mathcal{N}(0, 1)$), and define the uniform Hermite nondegeneracy parameter

$$p_\sigma := \inf_{s>0} \frac{\hat{\sigma}_1(s)^2}{s^2}. \quad (4.2)$$

For activations such as ReLU, leaky ReLU, exact GELU, and SiLU, the ratio $\hat{\sigma}_1(s)/s$ is constant, so p_σ is a positive absolute constant; see Table 5.

Corollary 4.2 (Propagation of stable rank). *Assume that σ is 1-Lipschitz and satisfies $\sigma(0) = 0$, and that $p_\sigma > 0$ as in (4.2). Fix $\varepsilon \in (0, 1)$. Then there exists a numerical constant $c > 0$ such that, with probability at least*

$$1 - \sum_{\ell=1}^L 8 \exp \left(-c \varepsilon^2 p_\sigma^2 d_\ell \right),$$

the following holds simultaneously for every $\ell = 1, \dots, L$:

$$\text{st}(A_\ell) \leq \left(\frac{1+\varepsilon}{1-\varepsilon} \cdot \frac{1}{p_\sigma} \right)^\ell \text{st}(X).$$

Proof. This follows immediately by applying Theorem 3.4 conditionally layer by layer. \square

5 Transformers at Gaussian initialization

In this section we bound the stable rank of the matrices that appear inside an L -layer decoder-only transformer at Gaussian initialization. The input is the embedding matrix $X^{(0)} \in \mathbf{R}^{d \times n}$ for a fixed token sequence. By Section 2.3, the embedding already has low stable rank, governed by the inverse frequency of the most common token. Our goal is to show that this low-stable-rank property persists throughout the network: at every depth we obtain explicit high-probability bounds for the RMS-normalized activations (and, in particular, for $A_{\text{final}}^{\text{rms}} = \text{RMSNorm}(X^{(L)})$).

The proofs follow by an induction over depth, based on the blockwise bounds proved in earlier sections. Two quantities are propagated from layer to layer. First, we maintain control on the ratio of column norms of $X^{(\ell)}$, because the RMSNorm bound (Theorem 3.2) multiplies stable rank by the ratio between maximal and minimal column norms. Second, we propagate stable rank by composing the attention sublayer bound (Lemma 3.11) with an MLP sublayer bound: Lemma 3.12 in the mean-spike-inducing (MSI) case and Lemma 3.14 for activations that propagate stable rank as in Assumption B. The MSI regime yields polynomial (quadratic) growth in depth, while the nonMSI propagation regime yields an exponentially increasing bound.

We work with the layerwise updates recorded in Assumption C. In particular, at each layer and for each head we represent attention by a mixing matrix $P^{(h)} \in \mathbf{R}^{n \times n}$ whose columns are probability vectors. In a standard transformer $P^{(h)}$ is obtained from queries and keys via a softmax (and may incorporate masking, RoPE, etc.); see the discussion surrounding the attention definition. However, all bounds in this section use only column-stochasticity of $P^{(h)}$ together with Gaussian initialization of the *value* and *output* projections. Consequently, we impose no assumptions on the initialization of the query/key maps (or on the particular way $P^{(h)}$ is generated), beyond the measurability/independence conditions recorded in Assumption C.

Assumption C (L -layer transformer at Gaussian initialization). Fix integers $L \geq 1$, $n_{\text{head}} \geq 1$, and $d, k \geq 1$ where d is divisible by n_{head} , and set $d_{\text{head}} := d/n_{\text{head}}$. Let $X^{(0)} \in \mathbf{R}^{d \times n}$ be the (pre-normalization) embedding matrix for a fixed token sequence, constructed from a Gaussian embedding as in Lemma 2.8, with empirical token frequencies $p_j = c_j/n$ and $p_{\max} := \max_j p_j$.

For each depth $\ell \in \{0, \dots, L-1\}$ and head $h \in [n_{\text{head}}]$, let $P^{(h,\ell)} \in \mathbf{R}^{n \times n}$ be a (possibly random) matrix whose columns are probability vectors. Let $W_O^{(h,\ell)} \in \mathbf{R}^{d \times d}$ and $W_V^{(h,\ell)} \in \mathbf{R}^{d_{\text{head}} \times d}$ be weight matrices. Given any block input $X^{(\ell)} \in \mathbf{R}^{d \times n}$ define the attention-sublayer intermediates

$$\begin{aligned} A^{\text{rms},(\ell)} &:= \text{RMSNorm}(X^{(\ell)}), \\ Y^{(h,\ell)} &:= A^{\text{rms},(\ell)} P^{(h,\ell)}, \quad (h \in [n_{\text{head}}]), \\ H^{(h,\ell)} &:= W_V^{(h,\ell)} Y^{(h,\ell)}, \quad (h \in [n_{\text{head}}]), \\ H^{(\ell)} &:= \text{Concat}_{h \in [n_{\text{head}}]} H^{(h,\ell)} \in \mathbf{R}^{d \times n}, \\ X^{\text{att},(\ell)} &:= X^{(\ell)} + W_O^{(\ell)} H^{(\ell)}, \\ A_{\text{mlp}}^{\text{rms},(\ell)} &:= \text{RMSNorm}(X^{\text{att},(\ell)}). \end{aligned}$$

Next define the MLP sublayer output

$$X^{(\ell+1)} := X^{\text{att},(\ell)} + W_2^{(\ell)} B^{(\ell)},$$

where $B^{(\ell)} \in \mathbf{R}^{k \times n}$ is a (possibly random) matrix that is independent of $W_2^{(\ell)}$. Finally, we write $x_t^{(\ell)}$ and $x_t^{\text{att},(\ell)}$ for the t th columns of $X^{(\ell)}$ and $X^{\text{att},(\ell)}$, respectively.

All trainable weight matrices are mutually independent across all layers and are initialized with independent Gaussian entries with variance $1/m$, where m is the input dimension of the map: in particular $(W_O^{(\ell)})_{ij}, (W_V^{(h,\ell)})_{ij} \sim \mathcal{N}(0, 1/d)$ and $(W_2^{(\ell)})_{ij} \sim \mathcal{N}(0, 1/k)$.

The mixing matrices $\{P^{(h,\ell)}\}_{h,\ell}$ may be arbitrary and may depend on all randomness external to the collection of Gaussian weights listed above (including, e.g., query/key projections, masking, RoPE, etc.). The only requirement is that for each fixed (h, ℓ) the matrix $P^{(h,\ell)}$ is independent of $W_O^{(\ell)}$, $\{W_V^{(h',\ell)}\}_{h' \in [n_{\text{head}}]}$, and $W_2^{(\ell)}$.

We now state the stable-rank bounds for the MSI and nonMSI architectures. Before the induction, we record one additional fact about the embedding matrix, complementary to Lemma 2.8. It supplies the uniform column-norm control needed to invoke Theorem 3.2 at depth 0, and to start the column-norm recursion used in both proofs. The proof is standard and we omit it.

Lemma 5.1 (Gaussian embedding column norms). *Fix $\varepsilon \in (0, 1)$. Let $E \in \mathbf{R}^{d \times V}$ have independent columns $e_1, \dots, e_V \sim \mathcal{N}(0, I_d)$. For a fixed token sequence $(i_1, \dots, i_n) \in \{1, \dots, V\}^n$ define*

$$X^{(0)} = [x_1, \dots, x_n] \in \mathbf{R}^{d \times n}, \quad x_t := e_{i_t}.$$

Then there exist numerical constants $c, C > 0$ such that whenever $d \geq C\varepsilon^{-2} \log n$, the estimate

$$(1 - \varepsilon)d \leq \|x_t\|_2^2 \leq (1 + \varepsilon)d \quad \text{for all } t = 1, \dots, n$$

holds with probability at least $1 - Ce^{-c\varepsilon^2 d}$.

5.1 MSI transformer

We first consider the mean-spike-inducing (MSI) regime, in which the MLP post-activations are given by a pointwise activation applied to a Gaussian projection of $A_{\text{mlp}}^{\text{rms},(\ell)}$. The theorem below gives stable-rank bounds for the MLP post-activations and for the RMS-normalized activations at all depths. In particular, the MLP post-activations satisfy $\text{st}(B^{(\ell)}) \leq \text{st}_\sigma$, and the stable ranks of the RMS activations grow at most quadratically in ℓ , with explicit dependence on $\text{st}_\sigma/p_\sigma$.

Theorem 5.2 (Low-stable-rank representations in an L -layer transformer). *Suppose that Assumption C holds. Assume moreover that for each $\ell = 0, \dots, L-1$,*

$$B^{(\ell)} := \sigma(W_1^{(\ell)} A_{\text{mlp}}^{\text{rms},(\ell)}),$$

where σ satisfies Assumption A and the matrices $\{W_1^{(\ell)} \in \mathbf{R}^{k \times d}\}_{\ell=0}^{L-1}$ are mutually independent with i.i.d. entries $\mathcal{N}(0, 1/d)$ and are independent of the randomness in Assumption C. Then there exist numerical constants $c, C > 0$ such that whenever

$$d \geq CL^2 \log(nL), \quad k \geq CL^2 \log(nL),$$

with probability at least

$$1 - CL \exp\left(-c \frac{d}{L^2}\right) - CL \exp\left(-c \frac{k}{L^2}\right) - L(1 - P(\sigma, d, k, n)),$$

the following holds:

(i) **MLP post-activations.** For every $\ell = 0, \dots, L-1$,

$$\text{st}(B^{(\ell)}) \leq \text{st}_\sigma.$$

(ii) **Embedding-layer stable ranks.** We have

$$\text{st}(X^{(0)}) \leq \frac{1.01}{p_{\max}}, \quad \text{st}(A^{\text{rms},(0)}) \leq \frac{1.03}{p_{\max}}, \quad \text{st}(A_{\text{mlp}}^{\text{rms},(0)}) \leq \frac{6.03}{p_{\max}}.$$

(iii) **RMS activations at depth $\ell \geq 1$.** For every $\ell = 1, \dots, L-1$,

$$\begin{aligned} \text{st}(A^{\text{rms},(\ell)}) &\leq 2.1 \text{st}_\sigma(1+\ell) + 4.3 \frac{\text{st}_\sigma}{p_\sigma} \ell(\ell+1), \\ \text{st}(A_{\text{mlp}}^{\text{rms},(\ell)}) &\leq 6.4 \text{st}_\sigma(1+\ell) + 13 \frac{\text{st}_\sigma}{p_\sigma} \ell(\ell+1), \\ \text{st}(A_{\text{final}}^{\text{rms}}) &\leq 2.1 \text{st}_\sigma(1+L) + 4.3 \frac{\text{st}_\sigma}{p_\sigma} L(L+1). \end{aligned}$$

Proof. Set $\delta := \frac{1}{512L}$ and $\varepsilon := \delta$, and write $\alpha := \frac{1+\delta}{1-\delta}$. Let Ω be the event on which Lemmas 2.8 and 5.1 hold with parameter ε , and for every $\ell = 0, \dots, L-1$, Lemmas 3.11 and 3.12 hold with parameter δ at layer ℓ . A union bound yields the stated lower bound on $\mathbb{P}(\Omega)$ after adjusting constants and using $d, k \geq C\delta^{-2} \log(nL)$. Work throughout on Ω .

Embedding layer. Lemma 2.8 yields

$$\text{st}(X^{(0)}) \leq \alpha \frac{1}{p_{\max}}.$$

Lemma 5.1 yields $(1-\varepsilon)d \leq \|x_t^{(0)}\|_2^2 \leq (1+\varepsilon)d$ for all t , hence Theorem 3.2 gives

$$\text{st}(A^{\text{rms},(0)}) \leq \alpha \text{st}(X^{(0)}) \leq \alpha^2 \frac{1}{p_{\max}}.$$

Since $\delta \leq \frac{1}{512}$, we have $\alpha \leq \frac{513}{511} < 1.01$, hence the first two bounds in (ii).

Applying Lemma 3.11(ii) to $X^{(0)}$ with $c_- = 1-\varepsilon$ and $c_+ = 1+\varepsilon$ gives

$$\text{st}(A_{\text{mlp}}^{\text{rms},(0)}) \leq \alpha^2 \frac{2+\varepsilon}{1-\varepsilon} \left(1 + \frac{2}{1-\varepsilon}\right) \text{st}(X^{(0)}).$$

Using $\varepsilon = \delta \leq \frac{1}{512}$ and $\text{st}(X^{(0)}) \leq \alpha/p_{\max}$, a direct bound gives

$$\frac{(1+\delta)^2}{(1-\delta)^2} \cdot \frac{2+\delta}{1-\delta} \cdot \left(1 + \frac{2}{1-\delta}\right) \cdot \alpha \leq \frac{31}{5},$$

which proves the last bound in (ii).

Column-norm control. For each $\ell \geq 0$, define $c_-^{(\ell)}, c_+^{(\ell)}$ by

$$c_-^{(\ell)} d \leq \|x_t^{(\ell)}\|_2^2 \leq c_+^{(\ell)} d \quad \forall t.$$

On Ω , Lemma 5.1 gives $c_-^{(0)} = 1 - \delta$ and $c_+^{(0)} = 1 + \delta$. Lemma 3.11(i) gives

$$(1 - \delta)c_-^{(\ell)} d \leq \|x_t^{\text{att},(\ell)}\|_2^2 \leq (1 + \delta)(c_+^{(\ell)} + 1)d \quad \forall t,$$

and Lemma 3.12(i), applied to $X^{\text{att},(\ell)}$, gives

$$c_-^{(\ell+1)} = (1 - \delta)^2 c_-^{(\ell)}, \quad c_+^{(\ell+1)} = (1 + \delta)^2 \left((1 + \delta)(c_+^{(\ell)} + 1) + 1 \right). \quad (5.1)$$

Hence $c_-^{(\ell)} = (1 - \delta)^{2\ell+1} \geq 1 - (2\ell + 1)\delta \geq \frac{509}{512}$ for all $\ell \leq L$. For the upper envelope, write (5.1) as $c_+^{(\ell+1)} = a c_+^{(\ell)} + b$ with $a = (1 + \delta)^3$ and $b = (1 + \delta)^2(2 + \delta)$. Then

$$c_+^{(\ell)} = a^\ell c_+^{(0)} + b \sum_{j=0}^{\ell-1} a^j \leq a^\ell (c_+^{(0)} + b\ell) \leq a^L ((1 + \delta) + b\ell).$$

Since $\delta L \leq 1/512$, we have $a^L \leq e^{3\delta L} \leq e^{3/512} < 1.01$ and $b \leq (1 + \delta)^2(2 + \delta) \leq 2.01$. Thus, for all $\ell \leq L$,

$$c_+^{(\ell)} \leq 1.03 + 2.03\ell, \quad \text{and hence} \quad c_+^{(\ell)} + 1 \leq 2.03(1 + \ell). \quad (5.2)$$

Stable ranks of $B^{(\ell)}$ and $X^{(\ell)}$. Item (ii) of Lemma 3.12, applied at layer ℓ , yields $\text{st}(B^{(\ell)}) \leq \text{st}_\sigma$, proving (i). Let $s_\ell := \text{st}(X^{(\ell)})$. Lemma 3.12(ii), applied to $X^{\text{att},(\ell)}$ whose upper column-norm parameter is $(1 + \delta)(c_+^{(\ell)} + 1)$, yields

$$s_{\ell+1} \leq \alpha \left(1 + \frac{(1 + \delta)(c_+^{(\ell)} + 1)}{p_\sigma} \right) \text{st}_\sigma.$$

Using $\alpha < 1.01$ and (5.2) gives, for $\ell \leq L$,

$$s_\ell \leq 1.01 \left(1 + \frac{2.04\ell}{p_\sigma} \right) \text{st}_\sigma. \quad (5.3)$$

RMS activations. Fix $\ell \in \{1, \dots, L-1\}$. Theorem 3.2, (5.2), and $c_-^{(\ell)} \geq 509/512$ yield

$$\text{st}(A^{\text{rms},(\ell)}) \leq \frac{c_+^{(\ell)}}{c_-^{(\ell)}} s_\ell \leq \frac{1.03 + 2.03\ell}{509/512} s_\ell \leq 2.05(1 + \ell) s_\ell.$$

Combining with (5.3) gives

$$\text{st}(A^{\text{rms},(\ell)}) \leq 2.05 \cdot 1.01(1 + \ell) \text{st}_\sigma + 2.05 \cdot 1.01 \cdot 2.04 \frac{\ell(\ell+1)}{p_\sigma} \text{st}_\sigma \leq 2.1 \text{st}_\sigma(1 + \ell) + 4.3 \frac{\text{st}_\sigma}{p_\sigma} \ell(\ell+1).$$

For $A_{\text{mlp}}^{\text{rms},(\ell)}$, Lemma 3.11(ii), (5.2), and $c_-^{(\ell)} \geq 509/512$ yield

$$\text{st}(A_{\text{mlp}}^{\text{rms},(\ell)}) \leq \frac{(1 + \delta)^2}{(1 - \delta)^2} \frac{c_+^{(\ell)} + 1}{c_-^{(\ell)}} \left(1 + \frac{2}{c_-^{(\ell)}} \right) s_\ell \leq 6.3(1 + \ell) s_\ell,$$

using $\delta \leq \frac{1}{512}$. Combining with (5.3) gives

$$\text{st}(A_{\text{mlp}}^{\text{rms},(\ell)}) \leq 6.3 \cdot 1.01 (1 + \ell) \text{st}_\sigma + 6.3 \cdot 1.01 \cdot 2.04 \frac{\ell(\ell + 1)}{p_\sigma} \text{st}_\sigma \leq 6.4 \text{st}_\sigma (1 + \ell) + 13 \frac{\text{st}_\sigma}{p_\sigma} \ell(\ell + 1).$$

Finally, applying the same RMSNorm estimate as for $A^{\text{rms},(\ell)}$ to $X^{(L)}$ and using (5.3) with $\ell = L$ yields

$$\text{st}(A_{\text{final}}^{\text{rms}}) \leq 2.1 \text{st}_\sigma (1 + L) + 4.3 \frac{\text{st}_\sigma}{p_\sigma} L(L + 1),$$

thereby completing the proof. \square

5.2 Transformer without mean induced spikes

We now consider the nonMSI propagation regime. In contrast to the MSI case, the MLP sublayer does not reset stable rank, and the hidden-state recursion becomes multiplicative. The theorem below records the resulting exponential-in-depth bounds for the stable ranks of the RMS-normalized activations and the MLP post-activations. Recall that Lemma 3.13 verified Assumption B at Gaussian initialization for two natural classes of such activations: gated MLPs and pointwise activations with $\hat{\sigma}_1(1)^2 > 0$.

Theorem 5.3 (Low-stable-rank representations in an L -layer transformer). *Suppose that Assumption C holds. Assume that for each $\ell = 0, \dots, L-1$ the matrix $B^{(\ell)}$ satisfies Assumption B with $\delta = \frac{1}{512L}$, constants (C_{PROP}, m_*) , and success probability $P_{\text{PROP}}(\frac{1}{512L})$. Set*

$$\rho := 3.1(1 + m_*).$$

Then there exist numerical constants $c, C > 0$ such that whenever

$$d \geq CL^2 \log(nL), \quad k \geq CL^2 \log(nL),$$

with probability at least

$$1 - CL \exp\left(-c \frac{d}{L^2}\right) - L\left(1 - P_{\text{PROP}}\left(\frac{1}{512L}\right)\right),$$

the following holds:

(i) **Embedding-layer stable ranks.** We have

$$\text{st}(X^{(0)}) \leq \frac{1.01}{p_{\max}}, \quad \text{st}(A^{\text{rms},(0)}) \leq \frac{1.03}{p_{\max}}, \quad \text{st}(A_{\text{mlp}}^{\text{rms},(0)}) \leq \frac{6.03}{p_{\max}}.$$

(ii) **Activation stable ranks.** For every $\ell = 0, \dots, L-1$,

$$\begin{aligned} \text{st}(A^{\text{rms},(\ell)}) &\leq \left(1.02 + 1.02(1 + m_*)\ell\right) \frac{1.01}{p_{\max}} \rho^\ell, \\ \text{st}(A_{\text{mlp}}^{\text{rms},(\ell)}) &\leq \left(6.13 + 3.09(1 + m_*)\ell\right) \frac{1.01}{p_{\max}} \rho^\ell, \\ \text{st}(B^{(\ell)}) &\leq C_{\text{PROP}} \left(6.13 + 3.09(1 + m_*)\ell\right) \frac{1.01}{p_{\max}} \rho^\ell, \\ \text{st}(A_{\text{final}}^{\text{rms}}) &\leq \left(1.02 + 1.02(1 + m_*)L\right) \frac{1.01}{p_{\max}} \rho^L. \end{aligned}$$

Proof. Set $\delta := \frac{1}{512L}$ and $\varepsilon := \delta$, and write $\alpha := \frac{1+\delta}{1-\delta}$. Let Ω be the event on which Lemmas 2.8 and 5.1 hold with parameter ε , and for every $\ell = 0, \dots, L-1$, Lemmas 3.11 and 3.14 hold with parameter δ at layer ℓ . A union bound gives the stated lower bound on $\mathbb{P}(\Omega)$ after adjusting constants and using $d, k \geq C\delta^{-2} \log(nL)$. Work throughout on Ω .

Embedding layer. The argument is identical to the MSI case: using Lemmas 2.8, 5.1, and Lemma 3.11 at $\ell = 0$ with $\varepsilon = \delta \leq 1/512$ gives the bounds in (i).

Column-norm control. For each $\ell \geq 0$, define $c_-^{(\ell)}, c_+^{(\ell)}$ by

$$c_-^{(\ell)} d \leq \|x_t^{(\ell)}\|_2^2 \leq c_+^{(\ell)} d \quad \forall t.$$

On Ω , Lemma 5.1 gives $c_-^{(0)} = 1 - \delta$ and $c_+^{(0)} = 1 + \delta$. Lemma 3.11(i) gives

$$(1 - \delta)c_-^{(\ell)} d \leq \|x_t^{\text{att},(\ell)}\|_2^2 \leq (1 + \delta)(c_+^{(\ell)} + 1)d \quad \forall t,$$

and Lemma 3.14(i), applied to $X^{\text{att},(\ell)}$, gives

$$c_-^{(\ell+1)} = (1 - \delta)^2 c_-^{(\ell)}, \quad c_+^{(\ell+1)} = (1 + \delta)((1 + \delta)(c_+^{(\ell)} + 1) + m_*) \quad (5.4)$$

Hence $c_-^{(\ell)} = (1 - \delta)^{2\ell+1} \geq 1 - (2\ell + 1)\delta \geq \frac{509}{512}$ for all $\ell \leq L$. Writing (5.4) as $c_+^{(\ell+1)} = a c_+^{(\ell)} + b$ with $a = (1 + \delta)^2$ and $b = (1 + \delta)((1 + \delta) + m_*)$, we obtain

$$c_+^{(\ell)} \leq a^\ell c_+^{(0)} + b \sum_{j=0}^{\ell-1} a^j \leq a^\ell ((1 + \delta) + b\ell) \leq 1.01 + 1.01(1 + m_*)\ell, \quad \ell \leq L,$$

since $\delta L \leq 1/512$ implies $a^\ell(1 + \delta)^2 < 1.01$

Hidden-state stable rank recursion. Set $s_\ell := \text{st}(X^{(\ell)})$. Lemma 3.11(ii) and $c_-^{(\ell)} \geq 509/512$ imply

$$\text{st}(X^{\text{att},(\ell)}) \leq \alpha \left(1 + \frac{2}{c_-^{(\ell)}}\right) s_\ell \leq 3.03 s_\ell. \quad (5.5)$$

Lemma 3.14(ii), applied to $X^{\text{att},(\ell)}$ whose lower column-norm parameter is $(1 - \delta)c_-^{(\ell)} \geq 0.992$, yields

$$s_{\ell+1} = \text{st}(X^{(\ell+1)}) \leq \alpha \left(1 + \frac{m_*}{(1 - \delta)c_-^{(\ell)}}\right) \text{st}(X^{\text{att},(\ell)}) \leq (1.01 + 1.02 m_*) \text{st}(X^{\text{att},(\ell)}). \quad (5.6)$$

Combining (5.5) and (5.6) gives

$$s_{\ell+1} \leq 3.1(1 + m_*) s_\ell = \rho s_\ell,$$

and iterating yields $s_\ell \leq s_0 \rho^\ell$ for all ℓ . Since $\text{st}(X^{(0)}) \leq 1.01/p_{\max}$ on Ω , we have

$$s_\ell \leq \frac{1.01}{p_{\max}} \rho^\ell \quad \text{for all } \ell = 0, \dots, L. \quad (5.7)$$

Activation stable ranks. For $A^{\text{rms},(\ell)} = \text{RMSNorm}(X^{(\ell)})$, Theorem 3.2 yields

$$\text{st}(A^{\text{rms},(\ell)}) \leq \frac{c_+^{(\ell)}}{c_-^{(\ell)}} s_\ell \leq \left(1.02 + 1.02(1 + m_*)\ell\right) \frac{1.01}{p_{\max}} \rho^\ell,$$

using $c_-^{(\ell)} \geq 509/512$, $c_+^{(\ell)} \leq 1.01 + 1.01(1 + m_*)\ell$, and (5.7). For $A_{\text{mlp}}^{\text{rms},(\ell)} = \text{RMSNorm}(X^{\text{att},(\ell)})$, Lemma 3.11(ii) yields

$$\text{st}(A_{\text{mlp}}^{\text{rms},(\ell)}) \leq \frac{(1 + \delta)^2}{(1 - \delta)^2} \frac{c_+^{(\ell)} + 1}{c_-^{(\ell)}} \left(1 + \frac{2}{c_-^{(\ell)}}\right) s_\ell \leq \left(6.13 + 3.09(1 + m_*)\ell\right) \frac{1.01}{p_{\max}} \rho^\ell,$$

using the same bounds on $c_\pm^{(\ell)}$ and (5.7).

For $B^{(\ell)}$, Lemma 3.14(ii) gives

$$\text{st}(B^{(\ell)}) \leq C_{\text{PROP}} \text{st}(A_{\text{mlp}}^{\text{rms},(\ell)}),$$

and substituting the bound for $\text{st}(A_{\text{mlp}}^{\text{rms},(\ell)})$ yields the claimed inequality for $\text{st}(B^{(\ell)})$.

Finally, $A_{\text{final}}^{\text{rms}} = \text{RMSNorm}(X^{(L)})$ satisfies the same bound as $A^{\text{rms},(L)}$ by Theorem 3.2, giving the last display in (ii). \square

6 Nuclear Rank in random feature models

The layerwise criterion (1.6) shows that spectral updates are most advantageous precisely when the nuclear rank of the gradient is large compared to the stable rank of the incoming activations. At the same time, there is no a priori reason for the gradient nuclear rank to be large early on in training; in fact, we will see that it can be bounded by a numerical constant in simple, yet representative, random-feature models. The goal of this section is to show that a *few* gradient steps are already enough to change this picture entirely leading to a nuclear rank that scales linearly with dimension.

Throughout the section, we consider the quadratic random-feature objective

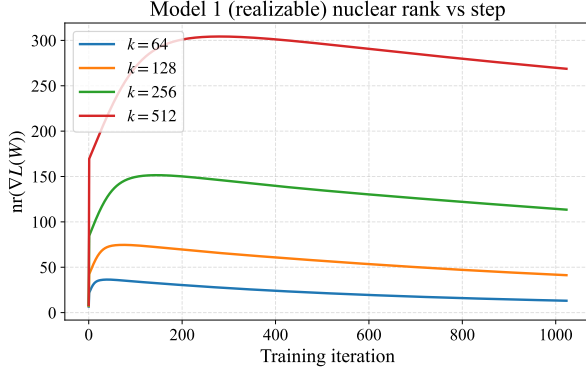
$$\mathcal{L}(W) := \frac{1}{2} \|WA - Y\|_F^2 \quad \text{for} \quad W \in \mathbf{R}^{m \times k},$$

and study two choices of labels Y . In the first model, the “realizable” case, the labels are generated by a ground-truth matrix W_\sharp via $Y = W_\sharp A$, and the Gram matrix $B := AA^\top$ follows the rank-one spike-plus-bulk structure in Assumption D. The main difficulty here is spectral: at initialization the gradient is $-W_\sharp B$ and inherits the poor conditioning of B , so its nuclear rank is small, whereas after a few steps the relevant block becomes $W_\sharp(I - \eta B)^t B$, and we must show that the polynomial $(I - \eta B)^t B$ flattens the spectrum of B : it squeezes the top spike down to constant scale while leaving the bulk eigenvalues at constant scale, so that the nuclear rank of the resulting gradient grows with the feature dimension. In the second model, a teacher–student setup, the labels are generated by a different feature map \bar{A} as $Y = \bar{W} \bar{A}$ with

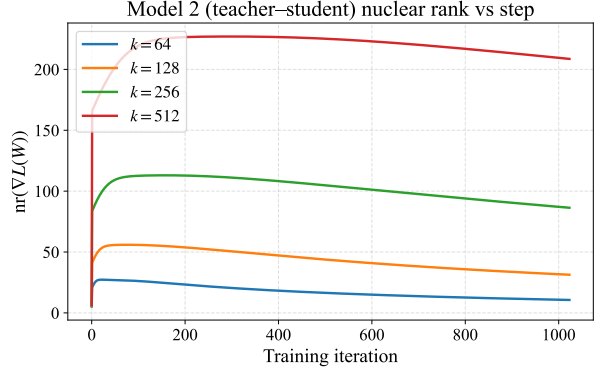
$$A = \sigma(VX), \quad \bar{A} = \sigma(\bar{V}X),$$

so the gradient involves the cross-Gram matrix $\bar{A}A^\top$. Here we work under the spiked assumptions D and F, which encompass both the basic rank-one random-feature setting and its multi-spike extensions, and we show that these models are realized with high probability for ReLU random features with Gaussian inputs and weights: the gradient nuclear rank is $O(1)$ at initialization but becomes dimension-dependent (of order $\Theta(d)$) after a few gradient steps. Moreover, we show that it then remains $\Omega(d)$ over a window of at least $\Theta(d)$ gradient-descent iterates (Theorems 6.6 and 6.11); a refinement of the same arguments yields longer $\Theta(d \log d)$ windows at the cost of a slightly lower nuclear rank, as explained in the subsequent remark.

Before turning to the formal statements, we illustrate these effects numerically in both random-feature models. Figures 16 and 17 show how the gradient nuclear rank evolves over the first few gradient steps and how its first-step value scales with the feature dimension k .



(a) Realizable random-feature model.



(b) Teacher-student random-feature model.

Figure 16: Gradient nuclear rank as a function of the gradient step. We plot $\text{nr}(\nabla_W \mathcal{L}(W_t))$ for several feature dimensions k . Here $n = 2k$ and $d = k/2$. In both the realizable (left) and teacher–student (right) models, the nuclear rank grows rapidly in the first few steps and does so more strongly for larger $k = 2d$, indicating that spectral updates become increasingly advantageous as the feature dimension grows.

Notation. For any $V \in \mathbf{R}^{m \times k}$ we order its singular values as $s_1(V) \geq s_2(V) \geq \dots \geq s_{\min\{k,m\}}(V)$. Similarly, the eigenvalues of any symmetric matrix $B \in \mathbf{R}^{k \times k}$ are $\lambda_1(B) \geq \lambda_2(B) \geq \dots \geq \lambda_k(B)$.

6.1 Random feature model I

In this section, we consider the problem of random feature regression, discussed in Section 1.2 of the introduction. We show two interesting facts that hold under mild assumptions: (1) when initializing at the origin W_0 , the nuclear rank $\text{nr}(\nabla \mathcal{L}(W_0))$ is upper bounded by a numerical constant and (2) after a single gradient step the nuclear rank $\text{nr}(\nabla \mathcal{L}(W_1))$ grows with the dimension. Together these facts show that one can expect the nuclear rank to be large at least early on in training and therefore for spectral descent to outperform the Euclidean gradient method.

Setting the stage, consider the problem

$$\min_{W \in \mathbf{R}^{m \times k}} \mathcal{L}(W) := \frac{1}{2n} \|WA - Y\|_F^2 \quad \text{where} \quad Y = W_{\sharp} A. \quad (6.1)$$

The dimensions of the involved matrices are $W, W_{\sharp} \in \mathbf{R}^{m \times k}$ and $A \in \mathbf{R}^{k \times n}$ and we will be interested in the proportionate regime

$$d \asymp k \quad \text{as} \quad d \rightarrow \infty.$$

We will focus on the setting when the Gram matrix $B := \frac{1}{n} AA^{\top}$ has a “spike+bulk” structure:

Assumption D (Spiked model). Suppose that we may write

$$B = uu^{\top} + \Sigma, \quad (6.2)$$

for some vector $u \in \mathbf{R}^k$ satisfying $\|u\|_2^2 \asymp d$ and a positive definite matrix $\Sigma \in \mathbf{R}^{k \times k}$ satisfying $c_1 I_k \leq \Sigma \leq c_2 I_k$ for some constants $0 < c_1 \leq c_2 < \infty$.

In particular, the rank-one interlacing theorem [21, Chapter 4] implies separation of eigenvalues:

$$\lambda_1(B) \asymp d \quad \text{and} \quad \lambda_i(B) \in [c_1, c_2] \quad \forall i \geq 2.$$

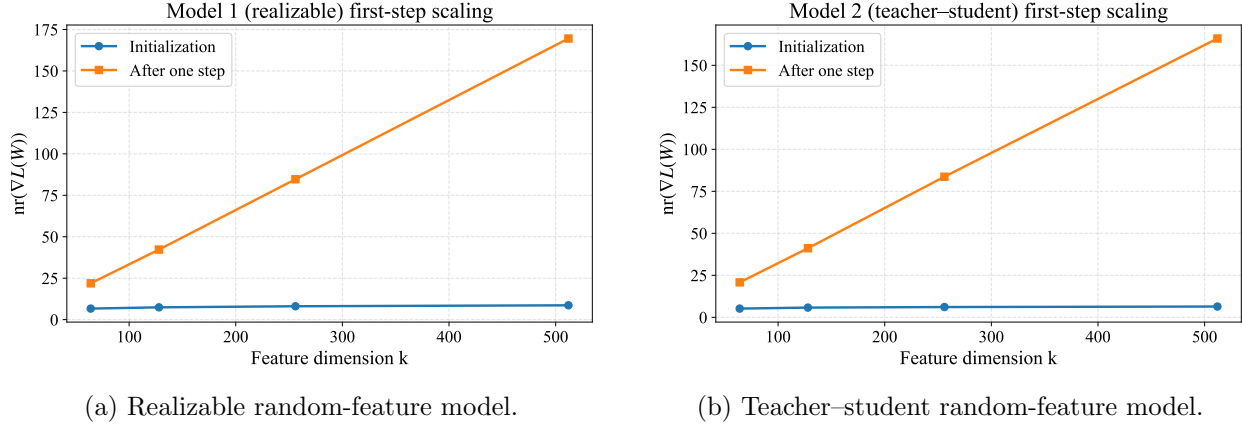


Figure 17: First-step scaling of the gradient nuclear rank with feature dimension. For each feature dimension k we plot the nuclear rank at initialization, $\text{nr}(\nabla_W \mathcal{L}(W_0))$, and after one gradient step, $\text{nr}(\nabla_W \mathcal{L}(W_1))$. Here $n = 2k$ and $d = k/2$. In both the realizable (left) and teacher–student (right) models, the initialization nuclear rank is essentially independent of k , while the post-first-step nuclear rank grows approximately linearly with k . This illustrates the regime captured by our theory: the condition $\text{nr}(\nabla_W \mathcal{L}(W_1)) \gg \text{st}(A)$ is increasingly activated as the feature dimension increases.

Spiked data matrices play an prominent role in random matrix theory [1, 26]. The main example of spiked data matrices for us is the post-activation matrix generated from random data. For the sake of concreteness, we focus on the ReLU activation function, although many other activation functions elicit the same phenomenon.

6.1.1 ReLU post-activation matrices follow the spiked model

Consider the matrix $A = \sigma(VX)$ for some fixed matrix $V \in \mathbf{R}^{k \times d}$ and where $X \in \mathbf{R}^{d \times n}$ is a random matrix with iid standard Gaussian entries $\mathcal{N}(0, 1)$ and σ is the ReLU activation function. We will show that under a mild incoherence condition on the rows of V , the post-activation matrix A indeed follows the spiked model (Assumption D). To see this, we first analyze the expectation of AA^T . Observe that setting $a := \sigma(Vx)$ for a standard Gaussian random vector $x \in \mathbf{R}^d$, we may write

$$\mathbb{E} \left[\frac{1}{n} AA^T \right] = \mathbb{E}[aa^\top] = \mu\mu^\top + \Sigma,$$

where we define

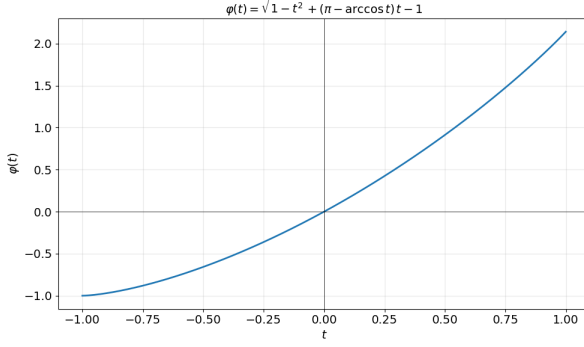
$$\mu := \mathbb{E}[a] \quad \text{and} \quad \Sigma := \text{Cov}(a) = \mathbb{E}(a - \mu)(a - \mu)^\top.$$

A standard computation shows the explicit formulas:

$$\mu = \frac{1}{2\pi} \begin{bmatrix} \|v_1\|_2 & \dots & \|v_k\|_2 \end{bmatrix}^\top \quad \text{and} \quad \Sigma_{ij} = \frac{\|v_i\|_2 \|v_j\|_2}{2\pi} \varphi \left(\frac{\langle v_i, v_j \rangle}{\|v_i\|_2 \|v_j\|_2} \right),$$

where we set $\varphi(t) = (\sqrt{1-t^2} + (\pi - \arccos t) t - 1)$; see Figure 18a for an illustration of φ .

Thus $\mathbb{E}[\frac{1}{n} AA^T]$ has the spike+bulk structure (6.10) with $\|\mu\|_2^2 = \frac{1}{4\pi^2} \|V\|_F^2$. Now in order to estimate the extremal eigenvalues of Σ , we will have to assume that the rows of V have roughly the same norm and are nearly orthogonal—a form of incoherence. This is the content of Theorem 6.2. The proof of Theorem 6.2 relies on the following lemma describing a few standard properties of the Hadamard product. Namely, item 1 is elementary, item 2 appears in [5, Thm. 1.4.1], and item 3 is the Schur product theorem [5, Sec. 1.2].



(a) The reparametrizing function φ

Figure 18: Illustration of φ .

Lemma 6.1 (Properties of Hadamard products). *For any two matrices $Q, P \in \mathbb{R}^{k \times k}$, it holds:*

1. $\|Q \odot P\|_{\text{op}} \leq \max_{ij} |Q_{ij}| \cdot \|P\|_F$
2. $\|Q \odot P\|_{\text{op}} \leq \max_i Q_{ii} \cdot \|P\|_{\text{op}}$ if $Q \geq 0$.
3. $Q \odot P \geq 0$ if $Q \geq 0$ and $P \geq 0$.

Theorem 6.2 (Perfect conditioning of the covariance). *Suppose that the rows v_i of V are incoherent in the following sense: there exist constants $\varepsilon \in (0, 1)$ and $c > 0$ satisfying*

$$1 - \varepsilon \leq \|v_i\|_2^2 \leq 1 + \varepsilon \quad \text{and} \quad \frac{|\langle v_i, v_j \rangle|}{\|v_i\| \|v_j\|} \leq c \sqrt{\frac{\log(k)}{d}} \quad \forall i \neq j. \quad (6.3)$$

Then Σ satisfies the two-sided bound:

$$\left(\frac{1 + \pi^{-1}(1 - \varepsilon)^{-1}}{4} \|V\|_{\text{op}}^2 + \frac{(\pi - 3)(1 + \varepsilon)}{4\pi} + O\left(\frac{k \log^2(k)}{d^2}\right) \right) I_k \geq \Sigma \geq \frac{1}{4} VV^\top + \left(\frac{(\pi - 3)(1 - \varepsilon)}{4\pi} + O\left(\frac{k \log^2(k)}{d^2}\right) \right) I_k. \quad (6.4)$$

Proof. Notice that we may write

$$\Sigma = \frac{1}{2\pi} \Lambda K \Lambda$$

where the entries of K are $K_{ij} = \varphi\left(\frac{\langle v_i, v_j \rangle}{\|v_i\|_2 \|v_j\|_2}\right)$ and Λ is a diagonal matrix with $\Lambda_{ii} = \|v_i\|$. We define $\hat{V} \in \mathbf{R}^{k \times d}$ to be a matrix whose i 'th row is the normalized vector $v_i/\|v_i\|_2$. We will treat K first and deal with Λ at the end of the argument.

The proof proceeds by carefully Taylor expanding φ and treating diagonal and off-diagonal elements separately. First, a quick computation yields the derivatives:

$$\varphi(0) = 0, \quad \varphi'(0) = \frac{\pi}{2}, \quad \varphi''(0) = 1, \quad \varphi^{(3)}(0) = 0, \quad \varphi^{(4)}(0) = 1, \quad \varphi^{(5)}(0) = 0.$$

For any square matrix Q , let $\text{offDiag}(Q)$ denote the matrix obtained by zeroing out the diagonal of Q , that is $\text{offDiag}(Q) = Q - \text{Diag}(Q)$. Using Taylor's theorem with remainder, we may write

$$\text{offDiag}(K) = \frac{\pi}{2} \text{offDiag}(\hat{V} \hat{V}^\top) + \frac{1}{2} \text{offDiag}((\hat{V} \hat{V}^\top)^{\odot 2}) + \frac{1}{4!} D \odot \text{offDiag}((\hat{V} \hat{V}^\top)^{\odot 4}), \quad (6.5)$$

where the entries of D are fourth-order derivatives of φ at some points in the interval $[-\frac{c}{\sqrt{d}}, \frac{c}{\sqrt{d}}]$ and are therefore bounded by some numerical constant. Using Lemma 6.1 (Item 1), we deduce

$$\left\| D \odot \text{offDiag}((\hat{V}\hat{V}^\top)^{\odot 4}) \right\|_{\text{op}} \leq \max_{ij} |D_{ij}| \cdot \left\| \text{offDiag}((\hat{V}\hat{V}^\top)^{\odot 4}) \right\|_F = O(k \log^2(k) d^{-2}),$$

where the last equality follows from the fact that each entry of $\text{offDiag}((\hat{V}\hat{V}^\top)^{\odot 4})$ is bounded by $O(\log^2(k) d^{-2})$. Adding back the diagonal $\text{Diag}(K) = (\pi - 1)I_k$ to (6.5) we therefore obtain

$$K = \frac{\pi}{2}\hat{V}\hat{V}^\top + \frac{1}{2}(\hat{V}\hat{V}^\top)^{\odot 2} + \frac{\pi-3}{2}\pi I_k + E$$

where the error term satisfies $\|E\|_{\text{op}} = O(k \log^2(k) d^{-2})$. Conjugating by Λ and multiplying by $\frac{1}{2\pi}$ yields the expression

$$\Sigma = \frac{1}{4}VV^\top + \frac{1}{4\pi}\Lambda^{-1}(VV^\top)^{\odot 2}\Lambda^{-1} + \frac{\pi-3}{4\pi}\Lambda^2 + \frac{1}{2\pi}E. \quad (6.6)$$

Using Lemma 6.1 (Item 3) we see that $(VV^\top)^{\odot 2}$ is positive semidefinite, and therefore we obtain the claimed lower bound:

$$\Sigma \geq \frac{1}{4}VV^\top + \frac{(\pi-3)(1-\varepsilon)}{4\pi}I_k + \frac{1}{2\pi}E.$$

Conversely, using Lemma 6.1 (Item 2), we see that $\|(VV^\top)^{\odot 2}\|_{\text{op}} \leq \|VV^\top\|_{\text{op}}$ and therefore from (6.6) we deduce

$$\Sigma \leq \left(\frac{1+\pi^{-1}(1-\varepsilon)^{-1}}{4} \|V\|_{\text{op}}^2 + \frac{(\pi-3)(1+\varepsilon)}{4\pi} + O(k \log^2(k) d^{-2}) \right) I_k,$$

which completes the proof. \square

In words, Theorem 6.2 shows that under the incoherence condition (6.3) and in the regime $k/d^2 \rightarrow 0$ as k and d tend to infinity, $\mathbb{E}[nB]$ follows the spiked model (6.10) with $\|u\|_2^2 \asymp \|V\|_F^2$ and Σ satisfying $c_1 \leq \Sigma \leq c_2(1 + \|V\|_{\text{op}}^2)$ where $c_1, c_2 > 0$ are numerical constants. Reassuringly random matrices V with iid Gaussian entries $\mathcal{N}(0, \frac{1}{d}I)$ satisfy the incoherence condition (6.3) and moreover $\|V\|_{\text{op}}$ has order $O(1)$ in the regime $k \asymp d$ while the spike has order $\|\mu\|_2^2 \asymp d$. This is the content of the following lemma; we omit the proof since it is standard.

Lemma 6.3 (Incoherence with random V). *Let $v_1, \dots, v_n \in \mathbb{R}^d$ be independent random vector with $v_i \sim \mathcal{N}(0, \frac{1}{d}I_d)$ and suppose $\frac{\log k}{d} \leq \frac{1}{4}$. Then we have*

$$\mathbb{P} \left(\max_{i \neq j} \left| \frac{\langle v_i, v_j \rangle}{\|v_i\|_2 \|v_j\|_2} \right| \leq 4\sqrt{\frac{\log k}{d}} \quad \text{and} \quad \max_{i \leq k} \left| \|v_i\|_2^2 - 1 \right| \leq 4\sqrt{\frac{\log k}{d}} \right) \geq 1 - \frac{4}{k}. \quad (6.7)$$

Moreover, with probability at least $1 - 4e^{-c\delta^2 d}$ it holds:

$$\|V\|_{\text{op}} \leq \sqrt{\frac{k}{d}} + (1 + \delta) \quad \text{and} \quad (1 - \delta)k \leq \|V\|_F^2 \leq (1 + \delta)k. \quad (6.8)$$

It remains to take into account concentration of $\frac{1}{n}AA^\top$ around its mean in order to deduce that it follows the spiked model. This is the content of the following theorem, which is immediate from standard results on concentration of covariance matrices. In the theorem, we denote the i 'th column of A by a_i .

Theorem 6.4 (Spiked model from Gaussian initialization). *Let $V \in \mathbf{R}^{k \times d}$ have iid Gaussian entries $N(0, \frac{1}{d}I_d)$. Then there exist constants $C_0, C_1, C_2 > 0$ such that in the regime $k \asymp d$ and $n \geq C_0 d$, with probability tending to one as $d \rightarrow \infty$, we may write*

$$\frac{1}{n}AA^\top = \bar{\mu}\bar{\mu}^\top + \bar{\Sigma},$$

where the empirical mean $\bar{\mu} = \frac{1}{n} \sum_{i=1}^n a_i$ and the empirical covariance $\bar{\Sigma} = \frac{1}{n} \sum_{i=1}^n (a_i - \bar{\mu})(a_i - \bar{\mu})^\top$ satisfy $\|\bar{\mu}\|^2 \asymp d$ and $C_1 I \leq \bar{\Sigma} \leq C_2 I$.

Proof. Suppose that the events (6.7) and (6.8) hold, which occurs with probability at least $1 - \frac{4}{k} - 4 \exp(-c\delta^2 d)$. Then Theorem 6.2 implies that the bound (6.4) holds say for $\varepsilon = 1/2$ as long as $d \geq c \log(k)$ for some constant c .

Define the empirical mean $\bar{\mu} = \frac{1}{n} \sum_{i=1}^n a_i$ and the empirical covariance $\bar{\Sigma} = \frac{1}{n} \sum_{i=1}^n (a_i - \bar{\mu})(a_i - \bar{\mu})^\top$ and note the equality:

$$\frac{1}{n}AA^\top = \bar{\mu}\bar{\mu}^\top + \bar{\Sigma}.$$

Note that $\langle a, u \rangle = \langle \sigma(Vx), u \rangle$ is a Lipschitz continuous function of the Gaussian vector x with Lipschitz constant $\|V\|_{\text{op}} \cdot \|u\|_2$. Therefore, Gaussian concentration [55, Theorem 5.2.3] shows:

$$\|\langle a - \mathbb{E}a, u \rangle\|_{\psi_2} \lesssim \underbrace{\|V\|_{\text{op}}}_{\lesssim 1} \|u\|_2 \quad \forall u.$$

Moreover, the minimal eigenvalues of Σ is bounded from below by a constant (6.4) and therefore we may write

$$\|\langle a - \mathbb{E}a, u \rangle\|_{\psi_2} \lesssim \sqrt{\langle \Sigma u, u \rangle} \quad \forall u.$$

Appealing to concentration of covariance matrices [55, Remark 9.2.3], we deduce that there exist universal constants $c, C > 0$ such that for all $u \geq 1$, with probability at least $1 - 2e^{-d}$, it holds:

$$\|\bar{\Sigma} - \Sigma\|_{\text{op}} \lesssim \left(\sqrt{\frac{d}{n}} + \frac{d}{n} \right) \underbrace{\|\Sigma\|_{\text{op}}}_{\lesssim 1}.$$

Appealing to concentration of the mean [22, Theorem 1], we also obtain:

$$\|\bar{\mu} - \mu\|_2 \lesssim \sqrt{\frac{d}{n}},$$

with probability $1 - e^{-d}$. In particular, taking into account (6.8) in this event we may estimate

$$\sqrt{k} - \sqrt{\frac{d}{n}} \lesssim \|\bar{\mu}\|_2 \lesssim \sqrt{k} + \sqrt{\frac{d}{n}},$$

which completes the proof. \square

6.1.2 The nuclear rank at initialization is constant

We now look at the consequences of the spiked model (6.10) on the nuclear rank of the gradient. Namely, consider initializing gradient descent on the problem (6.1) at W_0 . Then taking into account the expression for the gradient

$$\nabla \mathcal{L}(W) = (W - W_\sharp)B \quad \text{with} \quad B := \frac{1}{n}AA^\top,$$

we have

$$\nabla \mathcal{L}(W_0) = -W_{\sharp} B. \quad (6.9)$$

Now suppose that the ground truth matrix W_{\sharp} does not eliminate the spike in the following sense:

$$\|W_{\sharp}\|_{\text{op}} \leq C \quad \text{and} \quad \|W_{\sharp} u\|_2 \geq \kappa \cdot \|u\|_2,$$

where C and κ are numerical constants. This is indeed the case for example if the singular values $s_1(W_{\sharp})$ and $s_k(W_{\sharp})$ are bounded from above and below by a numerical constant or is true with high probability if the entries of $W_{\sharp} \in \mathbf{R}^{m \times k}$ are iid Gaussian $\mathcal{N}(0, \frac{1}{m})$ and $m \gtrsim k$. Then we can estimate the nuclear rank of the gradient as:

$$\sqrt{\text{nr}(W_{\sharp} B)} = \frac{\|W_{\sharp} B\|_*}{\|W_{\sharp} B\|_F} \leq \frac{C\|B\|_*}{\|W_{\sharp} u u^\top\|_F - \|W_{\sharp} \Sigma\|_F} \leq \frac{C\|u\|_2^2 + C\|\Sigma\|_*}{\kappa\|u\|_2^2 - C\|\Sigma\|_F} \lesssim \frac{d}{d - \sqrt{d}} \asymp 1.$$

Thus indeed the nuclear rank of the gradient $\nabla \mathcal{L}(W_0)$ is bounded by a constant.

6.1.3 The nuclear rank after one gradient step scales with dimension.

Let us now analyze what happens after a single gradient step $W_1 = W_0 - \eta \nabla \mathcal{L}(W_0)$. Observe the gradient of the objective function at W_1 is

$$\nabla \mathcal{L}(W_1) = (\eta W_{\sharp} B - W_{\sharp}) B = -W_{\sharp} \underbrace{(I - \eta B) B}_{=: T_{\eta}}.$$

We will now see that although B is a poorly conditioned matrix, T_{η} is perfectly conditioned for any stepsize $\eta = \frac{1}{c + \|B\|_{\text{op}}}$ with constant $c > 0$.

Lemma 6.5 (Nuclear rank after one iteration grows with dimension). *Suppose that Assumption D holds and fix a step-size $\eta = \frac{1}{c + \|B\|_{\text{op}}}$ for any constant $c > 0$. Then the condition number of T_{η} is bounded by a numerical constant in the regime $k \asymp d$ as $d \rightarrow \infty$, and consequently, we have*

$$\text{nr}(\nabla \mathcal{L}(W_1)) \gtrsim \text{nr}(W_{\sharp}).$$

Proof. The eigenvalues of T_{η} have the form $\lambda_i \left(1 - \frac{\lambda_i}{c + \lambda_1}\right)$ where λ_i is the i 'th largest eigenvalue of B . Now clearly, we have $\lambda_1(B) \geq \|u\|_2^2 \asymp d$. Moreover by the rank one interlacing theorem we have

$$\lambda_i(\Sigma) \geq \lambda_{i+1}(B) \geq \lambda_{i+1}(\Sigma) \quad \forall i = 1, \dots, d-1.$$

Consequently, the eigenvalues $\lambda_i(B)$ for $i = 2, \dots, d$ all lie in the interval $[c_1, c_2]$. We therefore deduce for $i \geq 2$ the estimates:

$$1 \lesssim c_1 \left(1 - \frac{c_2}{c + \lambda_1}\right) \leq \lambda_i \left(1 - \frac{\lambda_i}{c + \lambda_1}\right) \leq c_2.$$

Moreover, for $i = 1$ we have $\lambda_1 \left(1 - \frac{\lambda_1}{c + \lambda_1}\right) = \frac{c\lambda_1}{c + \lambda_1} \asymp 1$. Thus T_{η} is bounded by a numerical constant in the regime $k \asymp d$ as $d \rightarrow \infty$. Using the elementary observation $\text{nr}(W_{\sharp} T_{\eta}) \gtrsim \left(\frac{\lambda_k(T_{\eta})}{\lambda_1(T_{\eta})}\right)^2 \text{nr}(W_{\sharp})$ completes the proof. \square

Since typical ground truth matrices W_{\sharp} (e.g. Gaussian) have nuclear rank that grows with dimension, Lemma 6.5 shows that the nuclear rank of $\nabla \mathcal{L}(W_1)$ grows with dimension as well.

6.1.4 Multi-step and Multi-spike

The results in the previous section established that, under a spiked model and for a specific choice of stepsize, the nuclear rank of the gradient is initially small at W_0 and becomes large already at W_1 . There are, however, two serious simplifications in this setup. First, we assumed a stepsize of the form $\eta = 1/(c + \|B\|_{\text{op}})$, whereas in practice it is more natural to consider the choice $\eta = 1/(c\|B\|_{\text{op}})$ with $c \geq 1$. Second, we worked with a single spike uu^\top , while random feature Gram matrices in applications often exhibit multiple prominent directions (e.g, [2, 57]). In this subsection, we show that both of these limitations can be removed simultaneously: under a multi-spiked model and with the more realistic stepsize $\eta = 1/(c\|B\|_{\text{op}})$, the same qualitative conclusions on the growth of nuclear rank continue to hold. The main difference is that the phenomenon no longer occurs at the very first update; instead, after a short burn-in period, gradient descent produces iterates W_t for which $\nabla\mathcal{L}(W_t)$ has large nuclear rank over a long time window.

Assumption E (Multi-spiked model). Suppose that we may write

$$B = S + \Sigma, \quad (6.10)$$

for some symmetric matrices $S, \Sigma \in \mathbf{R}^{k \times k}$ with S having rank $r \in \mathbb{N}$ and satisfying $c_1 d^\ell I_k \leq S \leq c_2 d^u I_k$ and $c_1 I_k \leq \Sigma \leq c_2 I_k$ for some constants $0 < c_1 \leq c_2 < \infty$ and $\ell, u > 0$.

In words, Assumption E asserts that the matrix B can be decomposed into a low-rank “signal” part S and a full-rank, well-conditioned “bulk” part Σ . The matrix S has rank r and eigenvalues that grow polynomially with d , between $c_1 d^\ell$ and $c_2 d^u$, so there are only r directions in feature space along which B is very large. In contrast, Σ has all of its eigenvalues uniformly bounded above and below by numerical constants, so it behaves like a well-conditioned background covariance on the remaining $k - r$ directions. Thus, this assumption generalizes the rank-one spiked model considered earlier: instead of a single prominent direction u , we now allow a low-dimensional subspace of “spiky” directions with substantially larger eigenvalues than the bulk. The parameters ℓ and u control how quickly the spike eigenvalues can grow, while a small rank r ensures that the spiky subspace remains negligible in dimension compared to the overall ambient dimension.

We now turn to the dynamics of gradient descent with stepsize η , given by

$$W_{t+1} = W_t - \eta \nabla\mathcal{L}(W_t) = W_t - \eta(W_t - W_\sharp)B.$$

Recall that we initialize the algorithm at the all zero-matrix W_0 . Introducing the error matrix $E_t := W_t - W_\sharp$, this recursion becomes

$$E_{t+1} = E_t(I - \eta B) = E_0(I - \eta B)^t.$$

Substituting this into the expression for the gradient, we obtain the convenient expression

$$\nabla\mathcal{L}(W_t) = (W_t - W_\sharp)B = -W_\sharp \underbrace{(I - \eta B)^t B}_{=: T_{\eta, t}}.$$

The following is the main result of the section. It shows that under Assumption E, after a short burn-in period of $d^{u-\ell} \log(d)$, the gradient’s nuclear rank is lower-bounded by the dimension $\text{nr}(\nabla\mathcal{L}(W_t)) \gtrsim d$ until iteration $t = Cd^u$ where C is an arbitrary numerical constant.⁴ In particular, in the setting $\ell = u$ the burn-in period is of logarithmic size $\log(d)$ while the time-window of the

⁴Note in this statement, we choose $C > 0$ first and then let d tend to infinity.

large nuclear ranks is linear in d . To get a better sense of the scaling, recall that gradient descent will find an ε -optimal solution to the problem after order $d^u \log(\frac{d}{\varepsilon})$ many steps. Thus, if we treat the accuracy ε as being constant, the time window when the nuclear rank of the gradient is large (order d) is shorter than the full run of the algorithm only by a $\log(d)$ factor.

Theorem 6.6 (Multi-step gradient descent). *Suppose that Assumption E holds. Fix $\eta = \frac{1}{c\|B\|_{\text{op}}}$ for any constant $c \geq 1$ and suppose that $\|W_{\sharp}\|_{\text{op}} \lesssim 1$. Let $\bar{M} \in \mathbf{R}^{k \times (k-r)}$ be the matrix consisting of the last $k-r$ columns of the matrix product $W_{\sharp}U$, where $U \in \mathbf{R}^{k \times k}$ is the orthogonal factor in the (decreasing) ordered eigenvalue decomposition of B . Then there exists a constant $C_1 > 0$ such that for any constant $C_2 > 0$ the two estimates hold:*

$$\begin{aligned} \|\nabla \mathcal{L}(W_t)\|_* &\gtrsim \|\bar{M}\|_* - r \\ \|\nabla \mathcal{L}(W_t)\|_F &\lesssim \|\bar{M}\|_F + \sqrt{r}. \end{aligned} \tag{6.11}$$

for any t satisfying $C_1 d^{u-\ell} \log(d) \leq t \leq C_2 d^u$. In particular, if W_{\sharp} has iid Gaussian entries $\mathcal{N}(0, \frac{1}{d})$ independent of A , then in the regime $m = k = d$ there exists a constant C_3 such that conditionally on the realizations of A , with probability tending to one as d tends to infinity, the estimate

$$\text{nr}(\mathcal{L}(W_t)) \geq C_3 d \quad \text{holds for any } t \text{ satisfying } C_1 d^{u-\ell} \log(d) \leq t \leq C_2 d^u.$$

Proof. The eigenvalues of $T_{\eta,t}$ have the form $\lambda_i \left(1 - \frac{\lambda_i}{c\lambda_1}\right)^t$ where λ_i is the i 'th largest eigenvalue of B . Let us next describe the asymptotic growth of the eigenvalues of B . Clearly, we have $\lambda_1(B) \lesssim d^u$ and the condition $B \succeq S$ ensures $\lambda_r(B) \gtrsim \lambda_r(S) \gtrsim d^{\ell}$. Now the rank r interlacing theorem show that for every j with $1 \leq j \leq k-r$ we have

$$\lambda_{j+r}(\Sigma) \leq \lambda_j(B) \leq \lambda_{j-r}(\Sigma).$$

In particular, we deduce $\lambda_{r+1}(B) \leq \lambda_1(\Sigma) \lesssim 1$. Moreover, the condition $B \succeq \Sigma$ ensures $\lambda_k(B) \geq \lambda_k(\Sigma) \gtrsim 1$. Summarizing, we have

$$d^{\ell} \lesssim \lambda_i(B) \lesssim d^u \quad \forall i \in [1 : r] \quad \text{and} \quad c_1 \leq \lambda_i(B) \leq c_2 \quad \forall i \in [r+1 : k].$$

Let us now look at how the eigenvalues of T_{η} depend on the iteration counter t . For any $i \in [1 : r]$, using the standard inequality $1 - x \leq \exp(-x)$, we have

$$\lambda_i \left(1 - \frac{\lambda_i}{c\lambda_1}\right)^t \leq e^{u \log(d) - t\Omega(d^{\ell-u})} \tag{6.12}$$

Consequently, as soon as $t \geq cd^{u-\ell} \log(d)$ for a sufficiently large constant c , the right side of (6.12) is bounded by a numerical constant uniformly over all $i \in [1 : r]$. Now for all $i \in [r+1 : k]$, using the inequality $1 - x \geq \exp(-2x)$ for $x \in [0, 0.8]$, we have the lower bound

$$\lambda_i \left(1 - \frac{\lambda_i}{c\lambda_1}\right)^t \geq c_1 e^{-O(2td^{u-\ell})}. \tag{6.13}$$

Consequently, as long as $t \leq Cd^u$ for any constant C , the right side of (6.13) is lower bounded by a positive numerical constant uniformly over all $i \in [r+1 : k]$. Let us now form an eigenvalue decomposition of $T_{\eta} = U\Lambda U^{\top}$ where the diagonal matrix Λ contains the eigenvalues of T_{η} according

to the increasing order of λ_i . We now decompose U as $U = [U_1 \ U_2]$ where U_1 has r columns and U_2 has $k - r$. Similarly we decompose Λ into two diagonal matrices Λ_1 and Λ_2 . We then compute

$$\begin{aligned} \|W_{\sharp}T_{\eta}\|_* &\geq \|W_{\sharp}U_2\Lambda_2U_2^{\top}\|_* - \|W_{\sharp}U_1\Lambda_1U_1^{\top}\|_* \\ &\gtrsim \|W_{\sharp}U_2\Lambda_2\|_* - \|U_1\Lambda_1U_1^{\top}\|_* \\ &\gtrsim \|W_{\sharp}U_2\Lambda_2\|_* - r \\ &\gtrsim \|W_{\sharp}U_2\|_* - r. \end{aligned}$$

Similarly we compute

$$\|W_{\sharp}T_{\eta}\|_F \leq \|W_{\sharp}U_2\Lambda_2U_2^{\top}\|_F + \|W_{\sharp}U_1\Lambda_1U_1^{\top}\|_F \lesssim \|W_{\sharp}U_2\|_F + \sqrt{r}.$$

Suppose now that W_{\sharp} has iid Gaussian entries $\mathcal{N}(0, \frac{1}{d})$ independent of A . Note that $\bar{M} \in \mathbf{R}^{k \times r}$ has iid Gaussian entries $\mathcal{N}(0, \frac{1}{d})$ and therefore conditionally on realizations of A we have $\|\bar{M}\|_{\text{op}} = O_{d,\mathbb{P}}(1)$, $\|\bar{M}\|_F = O_{d,\mathbb{P}}(\sqrt{d})$, and $\|\bar{M}\|_* = \Omega_{d,\mathbb{P}}(d)$. The result follows. \square

Remark 1 (Extending the window to $d^u \log d$). In Theorem 6.6 we showed that, under Assumption E and the Gaussian ground-truth model for W_{\sharp} , there exist constants $C_1, C_2, C_3 > 0$ such that with probability tending to one,

$$\text{nr}(\nabla \mathcal{L}(W_t)) \geq C_3 d \quad \text{for all } t \in [C_1 d^{u-\ell} \log d, C_2 d^u].$$

Thus on this window the gradient nuclear rank is actually linear in d .

The same bulk-versus-spike analysis used in the proof of Theorem 6.6 yields a slightly larger window (by a logarithmic factor) of large nuclear ranks. Namely, for any $\varepsilon > 0$ there exist constants c_0 and $c = c(\varepsilon) > 0$ such that, with probability tending to one as $d \rightarrow \infty$, we have

$$\text{nr}(\nabla \mathcal{L}(W_t)) \geq d^{1-\varepsilon} \quad \text{for all } t \in [c_0 d^{u-\ell} \log d, c d^u \log d].$$

The only required modification to the proof is to realize that by setting the end horizon to be $c d^u \log(d)$ for a sufficiently small constant $c(\varepsilon)$, we can be sure that the right side of (6.13) is lower bounded by $d^{-\varepsilon}$. The rest of the proof proceeds unchanged.

6.2 Random feature model II

Next, we consider a modification of the random feature model (6.1) corresponding to a “teacher-student setup”:

$$\min_{W \in \mathbb{R}^{m \times k}} \mathcal{L}(W) := \frac{1}{2n} \|WA - Y\|_F^2 \quad \text{where} \quad Y = \bar{W}\bar{A}, \quad \bar{A} = \sigma(\bar{V}X), \quad A = \sigma(VX). \quad (6.14)$$

Here, the dimensions of the involved matrices are $W, \bar{W} \in \mathbf{R}^{m \times k}$ and $V, \bar{V} \in \mathbf{R}^{k \times d}$ and $X \in \mathbf{R}^{d \times n}$. Problem (6.1) corresponds exactly to the setting $V = \bar{V}$, that is when the first layer weights have been learned perfectly and only the second layer weights need to be trained. As in the previous section, we will be interested in the proportional regime

$$k \asymp d \quad \text{as} \quad d \rightarrow \infty.$$

Analogously to Assumption D, we will assume that both matrices $\frac{1}{n}AA^{\top}$ and $\frac{1}{n}\bar{A}\bar{A}^{\top}$ follow a spiked model in the sense of Assumption F. Note that we stipulate that the spike for both matrices has the same right singular vector.

Assumption F (Spiked model). Suppose that we may write

$$\frac{1}{n} A A^\top = uu^\top + \Gamma \quad \text{and} \quad \frac{1}{n} \bar{A} \bar{A}^\top = vu^\top + \Sigma, \quad (6.15)$$

for some vector $u, v \in \mathbf{R}^k$ satisfying $\|v\|_2 \asymp \|u\|_2 \asymp \sqrt{d}$ and matrices $\Gamma, \Sigma \in \mathbf{R}^{k \times k}$. Suppose moreover:

- Γ is symmetric and for some constants $0 < c_1 \leq c_2 < \infty$, we have $c_1 I_k \preceq \Gamma \preceq c_2 I_k$,
- there exists $r \asymp d$ satisfying $c_2 \geq s_1(\Sigma) \geq s_r(\Sigma) \geq c_1$.

In particular, as we have already seen, the rank one interlacing theorem [21, Chapter 4] implies separation of eigenvalues

$$\lambda_1\left(\frac{1}{n} A A^\top\right) \asymp d \quad \text{and} \quad \lambda_i\left(\frac{1}{n} A A^\top\right) \in [c_1, c_2] \quad \forall i \geq 2.$$

Weyl inequality [21, 7.3.P16] and the interlacing theorem for singular values [50, Theorem 1] imply:

$$\begin{aligned} s_1\left(\frac{1}{n} \bar{A} \bar{A}^\top\right) &\asymp d \\ s_i\left(\frac{1}{n} \bar{A} \bar{A}^\top\right) &\in [c_1, c_2] \quad \forall i \in [2 : r]. \end{aligned}$$

The main example of spiked data matrices for us is the post-activation matrix generated from random data. This is the content of the following section.

6.2.1 ReLU post-activation matrices follow the spiked model

Consider the matrices $A = \sigma(VX)$ and $\bar{A} = \sigma(\bar{V}X)$, where the matrices $V, \bar{V} \in \mathbf{R}^{k \times d}$ have iid Gaussian entries $\mathcal{N}(0, \frac{1}{d})$ and $X \in \mathbf{R}^{d \times n}$ has iid standard Gaussian entries $\mathcal{N}(0, 1)$. Recall as before σ is the ReLU activation function. We will show that Assumption F indeed holds with probability tending to one in the proportionate regime $d \asymp k$. Since the requisite properties of AA^\top have already been established in Theorem 6.4, it only remains to analyze $\bar{A} \bar{A}^\top$. To this end, we first focus on the expectation of $\bar{A} \bar{A}^\top$. Define $a := \sigma(Vx)$ and $\bar{a} := \sigma(\bar{V}x)$ where $x \sim \mathcal{N}(0, I_d)$ is a standard Gaussian random vector. Then, we may write

$$\mathbb{E}_x \left[\frac{1}{n} \bar{A} \bar{A}^\top \right] = \mathbb{E}_x [\bar{a} \bar{a}^\top] = \mu \nu^\top + \Sigma,$$

where we define

$$\nu := \mathbb{E}_x [\bar{a}], \quad \mu = \mathbb{E}_x [a] \quad \text{and} \quad \Sigma := \mathbb{E}_x (\bar{a} - \mu)(a - \nu)^\top.$$

Letting v_i and \bar{v}_i denote the rows of V and \bar{V} , respectively, a standard computation shows the explicit formulas:

$$\begin{aligned} \mu &= \frac{1}{2\pi} \begin{bmatrix} \|v_1\|_2 & \dots & \|v_k\|_2 \end{bmatrix}^\top, \\ \nu &= \frac{1}{2\pi} \begin{bmatrix} \|\bar{v}_1\|_2 & \dots & \|\bar{v}_k\|_2 \end{bmatrix}^\top, \\ \Sigma_{ij} &= \frac{\|\bar{v}_i\|_2 \|v_j\|_2}{2\pi} \varphi \left(\frac{\langle \bar{v}_i, v_j \rangle}{\|\bar{v}_i\|_2 \|v_j\|_2} \right), \end{aligned}$$

where we set $\varphi(t) = (\sqrt{1-t^2} + (\pi - \arccos t)t - 1)$; see Figure 18a for an illustration of φ . The next theorem establishes the asymptotics of Σ in the proportionate regime $k \asymp d$ as $d \rightarrow \infty$. Although, this result can be directly proved using the seminar work of [11, 29], we provide a short self-contained argument here based on the hypercontractivity of Gaussian random vectors.

Theorem 6.7 (Asymptotics). *Consider the regime where k and d tend to infinity with $\sqrt{k}/d \rightarrow 0$. Assume that V and \bar{V} are matrices with iid Gaussian entries with variance $1/d$. Then for any $\epsilon > 0$ it holds:*

$$\|\Sigma - \left(\frac{1}{2\pi} \bar{V}V^\top + \frac{1}{d}\mathbf{1}\mathbf{1}^\top\right)\|_{\text{op}} = O_{d,\mathbb{P}}\left(\frac{k^{\frac{1}{2}+\epsilon}}{d}\right).$$

Proof. The proof begins in the same way as the proof of Theorem 6.2. Namely, we write

$$\Sigma = \frac{1}{2\pi} \bar{\Lambda} K \Lambda$$

where the entries of K are $K_{ij} = \varphi\left(\frac{\langle \bar{v}_i, v_j \rangle}{\|\bar{v}_i\|_2 \|v_j\|_2}\right)$ and $\bar{\Lambda}$ and Λ are diagonal matrices with $\bar{\Lambda}_{ii} = \|\bar{v}_i\|$ and $\Lambda_{ii} = \|v_i\|$, respectively. We define $\bar{U} \in \mathbf{R}^{k \times d}$ to be a matrix whose i 'th row is the normalized vector $\bar{v}_i/\|\bar{v}_i\|_2$ and similarly we define $U \in \mathbf{R}^{k \times d}$ to be a matrix whose i 'th row is the normalized vector $v_i/\|v_i\|_2$. We will treat K first and deal with $\Lambda, \bar{\Lambda}$ at the end of the argument. Performing the same Taylor expansion as in the proof of Theorem 6.2 we arrive at the expression

$$K = \frac{\pi}{2} \bar{U}U^\top + \frac{1}{2}(\bar{U}U^\top)^{\odot 2} + \frac{1}{4!} D \odot (\bar{U}U^\top)^{\odot 4}, \quad (6.16)$$

where the entries of D and of $\bar{U}U^\top$ are bounded in absolute value by $c_1 \sqrt{\frac{\log k}{d}}$ with probability at least $1 - \frac{c_2}{k}$. In this event, using Lemma 6.1 (Item 1), we may bound the last term in (6.16) as

$$\|D \odot (\bar{U}U^\top)^{\odot 4}\|_{\text{op}} \leq \max_{ij} |D_{ij}| \cdot \|(\bar{U}U^\top)^{\odot 4}\|_F \lesssim k \log^2(k) d^{-2}.$$

Next, we deal with the term $(\bar{U}U^\top)^{\odot 2}$ in (6.16). To this end, let us first estimate $(\bar{V}V^\top)^{\odot 2}$. We compute $\mathbb{E}(\bar{V}V^\top)^{\odot 2} = \frac{1}{d}\mathbf{1}\mathbf{1}^\top$. Let z_i be the i 'th row of $(\bar{V}V^\top)^{\odot 2} - \frac{1}{d}\mathbf{1}\mathbf{1}^\top$. Note that conditionally on v_1, \dots, v_k , the vectors z_i are independent and identically distributed. Let \mathbb{E}_v be conditional expectation on v_1, \dots, v_k . Then using [53, Theorem 5.48], we deduce

$$\sqrt{\mathbb{E}_v \|(\bar{V}V^\top)^{\odot 2} - \frac{1}{d}\mathbf{1}\mathbf{1}^\top\|_{\text{op}}^2} \leq \|\Sigma\|_{\text{op}}^{1/2} d^{1/2} + Cm^{1/2} \log^{1/2}(\min\{k, d\})$$

where $\Sigma = \mathbb{E}_v z_i z_i^\top$ is the conditional second moment for any index i and $m = \mathbb{E}_v [\max_{i=1, \dots, k} \|z_i\|_2^2]$. Now a straightforward computation shows that the (j, l) entry of Σ is given by $\frac{\|v_j\|_2^2 \|v_l\|_2^2 + 2\langle v_j, v_l \rangle^2 - \|v_j\|_2^2 - \|v_l\|_2^2 + 1}{d^2}$. Thus we may write

$$\Sigma = \frac{1}{d^2} (2(VV^\top)^{\odot 2} + (q - \mathbf{1})(q - \mathbf{1})^\top),$$

where we define the vector $q = (\|v_1\|_2^2, \dots, \|v_k\|_2^2)$. Thus we deduce

$$\|\Sigma\|_{\text{op}} \leq \frac{2\|(VV^\top)^{\odot 2}\|_{\text{op}} + \|q - \mathbf{1}\|_2^2}{d^2}.$$

Now elementary algebra shows $\mathbb{E}\|q - \mathbf{1}\|^2 = \frac{2k}{d}$. Now we break up $(VV^\top)^{\odot 2}$ into the diagonal and off-diagonal parts:

$$\begin{aligned} (VV^\top)^{\odot 2} &= \|\text{Diag}(q^2) + ((VV^\top)^{\odot 2} - \text{Diag}(q^2))\|_{\text{op}} \\ &\leq \|\text{Diag}(q^2)\|_{\text{op}} + \|((VV^\top)^{\odot 2} - \text{Diag}(q^2))\|_F \\ &\leq \max_i \|v_i\|_2^4 + \sqrt{\sum_{i \neq j} \langle v_i, v_j \rangle^4}. \end{aligned}$$

Now simple algebra shows $\mathbb{E} \sum_{i \neq j} \langle v_i, v_j \rangle^4 \lesssim \frac{k^2}{d^2}$ and a standard concentration argument shows $\mathbb{E} \max_i \|v_i\|_2^4 \lesssim \left(1 + \frac{\log k}{d}\right)^2$. Thus we deduce $\mathbb{E} \|\Sigma\|_{\text{op}} \lesssim \frac{1 + \frac{k}{d}}{d^2}$. Next, we compute

$$m = \mathbb{E}_v \left[\max_{i=1, \dots, k} \|z_i\|_2^2 \right] \leq [\mathbb{E}_v \max_{i=1, \dots, k} \|z_i\|_2^{2p}]^{1/p} \leq [\mathbb{E}_v \sum_{i=1}^k \|z_i\|_2^{2p}]^{1/p} = k^{1/p} (\mathbb{E}_v \|z_i\|_2^{2p})^{1/p}.$$

Observe that $\|z_i\|_2^2$ is a a degree 4 polynomial of a Gaussian and therefore by Gaussian hypercontractivity [37, Chapter 3.2] satisfies $(\mathbb{E}_v \|z_i\|_2^{2p})^{1/p} \leq (p-1)^2 (\mathbb{E}_v \|z_i\|_2^4)^{1/2}$. Taking the expectation now with respect to v_1, \dots, v_k , we deduce $\mathbb{E} m \leq k^{1/p} (p-1)^2 (\mathbb{E} \|z_i\|_2^4)^{1/2} \lesssim k^{1/p} (p-1)^2 \frac{k}{d^2}$. Thus we deduce

$$\mathbb{E} \|(\bar{V}V^\top)^{\odot 2} - \frac{1}{d} \mathbf{1} \mathbf{1}^\top\|_{\text{op}}^2 \lesssim \frac{1 + \frac{k}{d}}{d^2} + k^{2/p} (p-1)^4 \frac{k \log(\min\{k, d\})}{d^2}.$$

Applying Markov's inequality completes the proof. \square

Finally, we pass from the expectation $\mathbb{E}[\bar{A}A^\top]$ to its empirical version $\frac{1}{n} \bar{A}A^\top$.

Corollary 6.8 (Spiked model from Gaussian initialization). *Assume that $V, \bar{V} \in \mathbf{R}^{k \times d}$ are matrices with iid Gaussian entries $\mathcal{N}(0, \frac{1}{d})$ and let $X \in \mathbf{R}^{k \times n}$ be an independent matrix with iid Gaussian entries $\mathcal{N}(0, 1)$. Then in the regime $\frac{k}{d} \rightarrow \gamma \in (1, \infty)$ and $n \geq C_0 d$, with probability tending to one as $d \rightarrow \infty$, Assumption F holds.*

Proof. Let a_i and \bar{a}_i denote the i 'th rows of A and \bar{A} , respectively. We have already seen in Theorem 6.4 that there exist constants $C_0, C_1, C_2 > 0$ such that in the regime $k \asymp d$ and $n \geq C_0 d$, with probability tending to one as $d \rightarrow \infty$, we may write

$$\frac{1}{n} AA^\top = \bar{\mu} \bar{\mu}^\top + \bar{\Sigma},$$

where the empirical mean $\bar{\mu} = \frac{1}{n} \sum_{i=1}^n a_i$ and the empirical covariance $\bar{\Sigma} = \frac{1}{n} \sum_{i=1}^n (a_i - \bar{\mu})(a_i - \bar{\mu})^\top$ satisfy $\|\bar{\mu}\|^2 \asymp d$ and $C_1 I \leq \bar{\Sigma} \leq C_2 I$. Therefore we now focus on $\frac{1}{n} \bar{A}A^\top$. To this end, define the empirical means

$$\bar{\mu} := \frac{1}{n} \sum_{i=1}^n a_i, \quad \bar{\nu} := \frac{1}{n} \sum_{i=1}^n \bar{a}_i,$$

and the empirical cross-covariance

$$\bar{\Sigma} := \frac{1}{n} \sum_{i=1}^n (\bar{a}_i - \bar{\nu})(a_i - \bar{\mu})^\top.$$

A simple expansion shows that

$$\bar{B} = \frac{1}{n} \bar{A}A^\top = \bar{\nu} \bar{\mu}^\top + \bar{\Sigma},$$

so \bar{B} already has the desired rank-one plus bulk structure with right spike vector $\bar{\mu}$.

Exactly as in the proof of Theorem 6.4 (using Gaussian concentration), both a and \bar{a} are subgaussian:

$$\|\langle a - \mathbb{E}a, u \rangle\|_{\psi_2} \lesssim \|u\|_2, \quad \|\langle \bar{a} - \mathbb{E}\bar{a}, u \rangle\|_{\psi_2} \lesssim \|u\|_2 \quad \forall u \in \mathbf{R}^k.$$

Applying the covariance concentration inequality [55, Remark 9.2.3] to the joint vector $(a^\top, \bar{a}^\top)^\top \in \mathbf{R}^{2k}$ and reading off the off-diagonal blocks yields, for $n \geq C_0 d$, the estimate

$$\|\bar{\Sigma} - \Sigma\|_{\text{op}} \lesssim \sqrt{\frac{d}{n}} + \frac{d}{n},$$

with probability at least $1 - 2e^{-d}$. Similarly, by [22, Theorem 1] we obtain

$$\|\bar{\mu} - \mu\|_2 \lesssim \sqrt{\frac{d}{n}}, \quad \|\bar{\nu} - \nu\|_2 \lesssim \sqrt{\frac{d}{n}},$$

so that $\|\bar{\mu}\|_2 \asymp \|\bar{\nu}\|_2 \asymp \sqrt{d}$ whenever $n \geq C_0 d$. Now Theorem 6.7 showed

$$\left\| \Sigma - \left(\frac{1}{2\pi} \bar{V}V^\top + \frac{1}{d} \mathbf{1}\mathbf{1}^\top \right) \right\|_{\text{op}} = o_d(1).$$

Now observe that

$$\left\| \frac{1}{d} \mathbf{1}\mathbf{1}^\top - \frac{1}{d} \bar{\nu} \bar{\mu}^\top \right\|_{\text{op}} \leq \left\| \frac{1}{d} \mathbf{1}\mathbf{1}^\top - \frac{1}{d} \nu \mu^\top \right\|_{\text{op}} + \left\| \frac{1}{d} \nu \mu^\top - \frac{1}{d} \bar{\nu} \bar{\mu}^\top \right\|_{\text{op}} \leq o_d(1) + \sqrt{\frac{d}{n}}.$$

Thus we may write

$$\frac{1}{n} \bar{A}A^\top = (1 + \frac{1}{d}) \bar{\nu} \bar{\mu}^\top + \frac{1}{2\pi} \bar{V}V^\top + E$$

where $\|E\|_{\text{op}} \lesssim o_d(1) + \sqrt{\frac{d}{n}}$. Now observe $\bar{V}V^\top (\bar{V}V^\top)^\top \geq \lambda_d(V^\top V) \bar{V} \bar{V}^\top$. Thus standard results [53, Theorem 4.6.1] on the extremal singular values of tall Gaussian matrices (recall we are in the regime $k/d \rightarrow \gamma \in (1, \infty)$) imply that there exist constants $0 < c_1 \leq c_2 < \infty$ such that with probability tending to one as $d \rightarrow \infty$, we have

$$c_2 \geq s_1(\bar{V}V^\top) \geq s_d(\bar{V}V^\top) \geq c_1. \quad (6.17)$$

Therefore after possibly inflating the constants $c_1, c_2 > 0$ the bulk $Q := \frac{1}{2\pi} \bar{V}V^\top + E$ satisfies

$$c_2 \geq s_1(Q) \geq s_d(Q) \geq c_1 \quad \text{and} \quad s_{d+1} \lesssim o_{d,\mathbb{P}}(1) + O_{d,\mathbb{P}}\left(\sqrt{\frac{d}{n}}\right).$$

Thus the proof is complete. \square

6.2.2 The nuclear rank at initialization is constant.

We now look at the consequences of the spiked model (6.23) on the nuclear rank of the gradient. Namely, consider initializing gradient descent on the problem (6.14) at the all-zero matrix $W_0 = 0$. Then taking into account the expression for the gradient

$$\nabla \mathcal{L}(W) = \frac{1}{n} (WA - \bar{W} \bar{A}) A^\top,$$

we have

$$\nabla \mathcal{L}(W_0) = -\bar{W} \bar{B} \quad \text{where} \quad \bar{B} := \frac{1}{n} \bar{A}A^\top. \quad (6.18)$$

Now suppose that the ground truth matrix \bar{W} does not eliminate the spike in the following sense:

$$\|\bar{W}\|_{\text{op}} \leq C \quad \text{and} \quad \|\bar{W}u\|_2 \geq \kappa \cdot \|u\|_2.$$

This is indeed the case for example if the singular values $s_1(\bar{W})$ and $s_k(\bar{W})$ are bounded from above and below by a numerical constant or is true with high probability if the entries of $\bar{W} \in \mathbf{R}^{m \times k}$ are iid Gaussian $\mathcal{N}(0, \frac{1}{m})$ and $m \gtrsim k$. Then we can estimate the nuclear rank of the gradient as:

$$\sqrt{\text{nr}(\bar{W} \bar{B})} = \frac{\|\bar{W} \bar{B}\|_*}{\|\bar{W} \bar{B}\|_F} \leq \frac{C \|\bar{B}\|_*}{\|\bar{W} u v^\top\|_F - \|\bar{W} \Sigma\|_F} \leq \frac{C \|u\|_2 \|v\|_2 + C \|\Sigma\|_*}{\kappa \|u\|_2 \|v\|_2 - C \|\Sigma\|_F} \lesssim \frac{d}{d - \sqrt{d}} \asymp 1.$$

Thus indeed the nuclear rank of the gradient $\nabla \mathcal{L}(W_0)$ is bounded by a constant.

6.2.3 The nuclear rank after one gradient step scales with dimension.

Let us now analyze what happens after a single gradient step $W_1 = W_0 - \eta \nabla \mathcal{L}(W_0)$. Observe the gradient of the objective function at W_1 is

$$\nabla \mathcal{L}(W_1) = -\bar{W} \underbrace{\bar{B}(I - \eta B)}_{=: T_\eta},$$

where recall that we set $\bar{B} = \frac{1}{n} \bar{A} \bar{A}^\top$ and $B = \frac{1}{n} A A^\top$. We will now show that for any stepsize $\eta = \frac{1}{c + \|B\|_{\text{op}}}$ under natural randomness assumptions, the nuclear rank of $\nabla \mathcal{L}(W_1)$ grows with dimension—the main result of the section.

Theorem 6.9 (Nuclear rank after one iteration grows with dimension). *Suppose that Assumption F holds and fix $\eta = \frac{1}{c + \|B\|_{\text{op}}}$ for any constant $c > 0$. Let $\bar{M} \in \mathbf{R}^{k \times r}$ be the matrix consisting of the first r columns of $\bar{W} \bar{L}$, where $\bar{L} \in \mathbf{R}^{k \times k}$ is the left orthogonal factor in the ordered singular value decomposition of \bar{B} . Then the following estimates hold in the regime $k \asymp d$ for all large d :*

$$\text{nr}(\nabla \mathcal{L}(W_1)) \geq \frac{\|\bar{M}\|_*}{\|\bar{W}\|_F}. \quad (6.19)$$

In particular, if \bar{W}, \bar{V}, V have iid Gaussian entries $\mathcal{N}(0, \frac{1}{d})$, and we are in the regime $m \asymp d$ and $\frac{k}{d} \rightarrow \gamma \in (1, \infty)$, then there exists a constant C such that as long as $n \geq Cd$ we have

$$\text{nr}(\mathcal{L}(W_1)) \geq \Omega_{d, \mathbb{P}}(d). \quad (6.20)$$

Proof. Let us write the singular value decompositions

$$B = L S L^\top \quad \text{and} \quad \bar{B} = \bar{L} \bar{S} \bar{R}^\top,$$

where $S, \bar{S} \in \mathbf{R}^{k \times k}$ are diagonal matrices with non-negative decreasing entries (singular values), and $L, \bar{L} \in \mathbf{R}^{k \times k}$ and $\bar{R} \in \mathbf{R}^{k \times k}$ are orthogonal matrices. We then compute

$$\bar{L}^\top T_\eta L = \bar{S} \bar{R}^\top L (I - \eta S).$$

The goal is now to show that the product $\bar{R}^\top L$ nearly has a block form. To this end, let us write

$$\bar{R} = [r_0 \quad R_0] \quad \text{and} \quad L = [\ell_0 \quad L_0]$$

for some vectors $r_0, \ell_0 \in \mathbf{R}^k$. Now the Davis-Kahan Theorem [15] applied to the two matrices AA^\top and uu^\top shows that the corresponding top eigenvectors are close

$$\underset{q \in \{\pm 1\}}{\text{argmin}} \|\hat{u} - q\ell_0\|_2 \lesssim \frac{1}{d}, \quad (6.21)$$

where we set $\hat{u} = u/\|u\|_2$. Without loss of generality, we may assume the optimal orientation is $q = 1$. Similarly, applying the Davis-Kahan theorem for singular values [58] to the right singular vectors of $\bar{A} \bar{A}^\top$ and vu^\top , we deduce

$$\underset{q \in \{\pm 1\}}{\text{argmin}} \|\hat{u} - qr_0\|_2 \lesssim \frac{1}{d}. \quad (6.22)$$

Again without loss of generality, we may assume that $q = 1$ is optimal. Let us now write $\bar{R}^\top L$ in block form:

$$\bar{R}^\top L = \begin{bmatrix} r_0^\top \ell_0 & r_0^\top L_0 \\ R_0^\top \ell_0 & R_0^\top L_0 \end{bmatrix}$$

Now using equations (6.21) and (6.22) we deduce

$$|r_0^\top \ell_0 - 1| \lesssim \frac{1}{d}, \quad \|r_0^\top L_0\|_2 \lesssim \frac{1}{d}, \quad \|R_0^\top \ell_0\|_2 \lesssim \frac{1}{d}.$$

Moreover, by standard principal-angle arguments, the singular values of $R_0^\top L_0$ are the cosines of the principal angles between the subspaces r_0^\perp and ℓ_0^\perp (see, e.g., [6] or [59]). Thus we deduce

$$s_{k-1}(R_0^\top L_0) = |r_0^\top \ell_0| \gtrsim 1 - \frac{1}{d}.$$

Thus writing $S = \text{Diag}(s)$ and $\bar{S} = \text{Diag}(\bar{s})$ for some vectors s and \bar{s} we deduce

$$\bar{S} \bar{R}^\top L (I - \eta S) = \text{Diag}(1, \bar{s}_{\geq 2}) \cdot \underbrace{\begin{bmatrix} \bar{s}_1(1 - \eta s_1)r_0^\top \ell_0 & \bar{s}_1 r_0^\top L_0 (I - \eta \text{Diag}(s_{\geq 2})) \\ (1 - \eta s_1)R_0^\top \ell_0 & R_0^\top L_0 (I - \eta \text{Diag}(s_{\geq 2})) \end{bmatrix}}_{=: Q},$$

where $s_{\geq 2}$ and $\bar{s}_{\geq 2}$ denote, respectively, the vectors s and \bar{s} with the first coordinate removed. Now observe $\bar{s}_1 \asymp d$ and $1 - \eta s_1 \asymp \left(1 - \frac{\|A\|_{\text{op}}^2}{c + \|A\|_{\text{op}}^2}\right) \asymp \frac{1}{d}$. Therefore we may write

$$Q = \begin{bmatrix} a & z^\top \\ 0 & D \end{bmatrix} + E,$$

where $a \asymp 1$, $\|z\|_2 \lesssim 1$, $\|E\|_{\text{op}} \lesssim \frac{1}{d^2}$, and $1 \lesssim s_{k-1}(D) \leq s_1(D) \lesssim 1$. It follows immediately that the operator norm of the blocked matrix is bounded by a constant, while its minimal singular value is bounded away from zero due to the standard linear algebraic Lemma D.1. Thus we deduce

$$1 \lesssim s_k(Q) \lesssim s_1(Q) \lesssim 1.$$

We therefore deduce

$$\text{nr}(\nabla \mathcal{L}(W_1)) = \text{nr}(\bar{W} \bar{L} \bar{L}^\top T_\eta L) = \text{nr}(\bar{W} \bar{L} \text{Diag}(1, \bar{s}_{\geq 2}) Q) \asymp \text{nr}(\bar{W} \bar{L} \text{Diag}(1, \bar{s}_{\geq 2})).$$

Using the linear algebra Lemma D.2 with $P = [1 : r]$ we immediately deduce

$$\|\bar{W} \bar{L} \text{Diag}(1, \bar{s}_{\geq 2})\|_* \gtrsim \|\bar{M}\|_*,$$

while the inequality $\|\bar{W} \bar{L} \text{Diag}(1, \bar{s}_{\geq 2})\|_F \lesssim \|\bar{W}\|_F$ holds trivially. The claimed estimate (6.19) follows immediately.

Suppose now that \bar{W}, V, \bar{V} have iid Gaussian entries $\mathcal{N}(0, \frac{1}{d})$. Then we have already seen in Corollary 6.8 that Assumption F is satisfied with $r = d$. Note that $\bar{M} \in \mathbf{R}^{k \times r}$ has iid Gaussian entries $\mathcal{N}(0, \frac{1}{d})$ and therefore we have $\|\bar{W}\|_F = O_{d, \mathbb{P}}(\sqrt{d})$, $\|\bar{M}\|_* = \Omega_{d, \mathbb{P}}(d)$, and $\|\bar{W}\|_{\text{op}} = O_{d, \mathbb{P}}(1)$. The claimed estimate (6.20) follows immediately. \square

6.2.4 Multi-step and multi-spike for the teacher–student model

Theorem 6.9 shows that, under the rank-one spiked model of Assumption F, the nuclear rank of the gradient in the teacher–student random feature model jumps from $O(1)$ at initialization to order d after a single gradient step. In the realizable model, we further saw in Section 6.1.4 that a similar phenomenon persists for multi-spiked Gram matrices and over many gradient steps (Theorem 6.6). The goal of this section is to develop an analogous multi-step, multi-spike theory in the teacher–student setting. The main technical difference compared to the realizable case is that the gradient now contains the cross-Gram matrix $\bar{B} := \frac{1}{n} \bar{A} A^\top$, rather than the symmetric Gram matrix $B = \frac{1}{n} A A^\top$ alone. As a result, the gradient at time t takes the form $\bar{W} \bar{B}$ multiplied by a polynomial in B , and the relevant spectrum is that of the non-symmetric matrix $\bar{B}(I - \eta B)^t$. We will see, however, that under a natural multi-spiked generalization of Assumption F, the same qualitative picture holds: after a short burn-in period the gradient nuclear rank is of order d for a long time window, so that the spectral-versus-Euclidean advantage is again visible.

We continue to work in the proportional regime $k \asymp d$ as $d \rightarrow \infty$ and we use the same notation as in the rest of this section. In particular,

$$B := \frac{1}{n} A A^\top \in \mathbf{R}^{k \times k}, \quad \bar{B} := \frac{1}{n} \bar{A} A^\top \in \mathbf{R}^{k \times k},$$

and gradient descent on the objective (6.14) satisfies

$$W_{t+1} = W_t - \eta \nabla \mathcal{L}(W_t), \quad \nabla \mathcal{L}(W_t) = \frac{1}{n} (W_t A - \bar{W} \bar{A}) A^\top = W_t B - \bar{W} \bar{B}.$$

We first formulate a multi-spiked analogue of Assumption F. As in the realizable case, we assume that B decomposes into a low-rank “signal” part and a well-conditioned bulk, as in Assumption E, and we impose a compatible structure on the cross-Gram matrix \bar{B} .

Assumption G (Multi-spiked teacher–student model). Suppose that we may write

$$\frac{1}{n} A A^\top = H_1 + \Gamma \quad \text{and} \quad \frac{1}{n} \bar{A} A^\top = H_2 + \Sigma, \quad (6.23)$$

for some matrices $H_1, H_2 \in \mathbf{R}^{k \times k}$. Suppose that the following conditions are true.

- **Spike properties** H_1 and H_2 have rank $p = o(d)$, the matrix H_1 is symmetric positive semidefinite, and the singular values of H_1 and H_2 lie in the interval $[d^\ell, d^u]$ for some constants $u, \ell \in (0, 1]$. Moreover, H_1 and H_2 admit compact singular value decompositions

$$H_1 = U Q U^\top \quad \text{and} \quad H_2 = V \bar{Q} U^\top$$

for orthogonal matrices $U, V \in \mathbf{R}^{k \times p}$ and nonnegative diagonal matrices $Q, \bar{Q} \in \mathbf{R}^{p \times p}$ with non-increasing diagonal entries. Note that the right orthogonal factors of H_1 and H_2 coincide.

- **Bulk properties.** The matrix Γ is symmetric and for some constants $0 < c_1 \leq c_2 < \infty$, we have $c_1 I_k \leq \Gamma \leq c_2 I_k$. Additionally, there exists $r \asymp d$ satisfying $c_2 \geq s_1(\Sigma) \geq s_r(\Sigma) \geq c_1$.

In words, Assumption F ensures that the matrices $\frac{1}{n} A A^\top$ and $\frac{1}{n} \bar{A} A^\top$ decompose into a low-rank *signal* (or “spike”) part H_1, H_2 plus a *bulk* part Γ, Σ . The spike matrices H_1, H_2 have rank $p = o(d)$, so the signal concentrates in a low-dimensional subspace compared to the ambient dimension, and their nonzero singular values grow like a power of d ; moreover, the right singular vectors of H_1 and H_2 in an ordered SVD coincide, so both spikes are aligned in the same latent directions. The bulk matrix Γ is well-conditioned (its eigenvalues are bounded above and below by fixed constants), while

Σ has $r \asymp d$ singular values of constant order. Overall, this is a multi-spike teacher–student model in which a small number of strong signal directions are embedded in an otherwise well-behaved high-dimensional bulk. In particular it is straightforward to check that Assumption F is a strict generalization of the rank-one teacher–student model in Assumption F.

We begin analyzing gradient descent in the multi-spiked student-teacher setting by deriving a simple expression for the gradient of \mathcal{L} along the iterates. This is the content of the following lemma which parallels the realizable case.

Lemma 6.10 (Gradient recursion). *Let $W_{t+1} = W_t - \eta \nabla \mathcal{L}(W_t)$ be the gradient descent iterates on the objective (6.14), initialized at $W_0 = 0$. Then the gradients satisfy*

$$\nabla \mathcal{L}(W_t) = -\overline{W} \overline{B} (I - \eta B)^t \quad \text{for all } t \geq 0.$$

Proof. Recall that $\nabla \mathcal{L}(W) = WB - \overline{W} \overline{B}$. Define $G_t := \nabla \mathcal{L}(W_t)$. Then

$$G_0 = \nabla \mathcal{L}(W_0) = W_0 B - \overline{W} \overline{B} = -\overline{W} \overline{B}.$$

Moreover, using the update $W_{t+1} = W_t - \eta G_t$ we obtain

$$G_{t+1} = W_{t+1} B - \overline{W} \overline{B} = (W_t - \eta G_t) B - \overline{W} \overline{B} = G_t - \eta G_t B = G_t (I - \eta B).$$

By induction this yields $G_t = G_0 (I - \eta B)^t = -\overline{W} \overline{B} (I - \eta B)^t$ for all $t \geq 0$. \square

Thus, the time- t gradient is obtained by multiplying the initial gradient $-\overline{W} \overline{B}$ on the right by the polynomial $(I - \eta B)^t$. In particular, the spectral properties of the family of matrices

$$T_{\eta, t} := \overline{B} (I - \eta B)^t$$

control the evolution of $\nabla \mathcal{L}(W_t)$. We are now ready to estimate the nuclear rank of the gradient after a short burn-in period. This is the content of the following theorem, which closely parallels Theorem 6.6 in the realizable case. Henceforth, for any matrix M we let $M_{i:j}$ denote the submatrix formed by columns i through j .

Theorem 6.11 (Nuclear rank for multi-step GD). *Suppose that Assumption F holds and that $\|\overline{W}\|_{\text{op}} \lesssim 1$. Let \overline{M} consist of the columns $p+1$ through $r-p$ of the matrix $\overline{W} \overline{L}$, where \overline{L} is the left orthogonal factor in the ordered (decreasing) singular values decomposition of \overline{B} . Then for any constants $q, C_3 > 0$ there exists a constant constant $C_1 > 0$ such that the following estimates hold*

$$\begin{aligned} \|\nabla \mathcal{L}(W_t)\|_* &\gtrsim \|\overline{M}\|_* - pd^{u-\ell} - d^{-q} \\ \|\nabla \mathcal{L}(W_t)\|_F &\lesssim \|\overline{W}\|_F + \sqrt{pd^{u-\ell}} + d^{-q}, \end{aligned}$$

for all t in the interval $[C_1 d^{u-\ell} \log(d), C_3 d^u]$.

Proof. First, recall that eigenvalue interlacing directly implies

$$d^\ell \lesssim \lambda_i(B) \lesssim d^u \quad \forall i \in [1 : r] \quad \text{and} \quad c_1 \leq \lambda_i(B) \leq c_2 \quad \forall i \in [r+1 : k].$$

Moreover, interlacing of singular values [50] shows:

$$s_{i+p}(\Sigma) \leq s_i(\overline{B}) \leq s_{i-p}(\Sigma).$$

In particular, we deduce

$$s_i(\overline{B}) \in [c_1, c_2] \quad \forall i \in [p+1, r-p].$$

Let us now write the singular value decompositions

$$B = LSL^\top \quad \text{and} \quad \bar{B} = \bar{L}\bar{S}\bar{R}^\top,$$

where $S, \bar{S} \in \mathbf{R}^{k \times k}$ are diagonal matrices with non-negative decreasing entries (singular values), and $L, \bar{L} \in \mathbf{R}^{k \times k}$ and $\bar{R} \in \mathbf{R}^{k \times k}$ are orthogonal matrices. We then compute

$$\bar{L}^\top T_{\eta,t} L = \bar{S} \bar{R}^\top L (I - \eta S)^t.$$

The goal is now to show that the product $\bar{R}^\top L$ nearly has a block form. To this end, let us write

$$\bar{R} = [R_1 \ R_2] \quad \text{and} \quad L = [L_1 \ L_2]$$

for some matrices $R_1, L_1 \in \mathbf{R}^{k \times p}$ and $R_2, L_2 \in \mathbf{R}^{k \times (k-p)}$. Now the Davis-Kahan Theorem [15] applied to the two matrices AA^\top and UQU^\top shows that

$$\|UU^\top - L_1 L_1^\top\|_{\text{op}} \leq \frac{\|\Gamma\|_{\text{op}}}{d^\ell} \lesssim \frac{1}{d^\ell}, \quad (6.24)$$

Applying the Davis-Kahan theorem for singular values [58] to the right singular vectors of $\bar{A}A^\top$ and $\bar{V}QU^\top$, we deduce

$$\|UU^\top - R_1 R_1^\top\|_{\text{op}} \leq \frac{\|\Sigma\|_{\text{op}}}{d^\ell} \lesssim \frac{1}{d^\ell}. \quad (6.25)$$

Let us now write $\bar{R}^\top L$ in block form:

$$\bar{R}^\top L = \begin{bmatrix} R_1^\top L_1 & R_1^\top L_2 \\ R_2^\top L_1 & R_2^\top L_2 \end{bmatrix}.$$

Let us now partition $S = \begin{bmatrix} S_1 & 0 \\ 0 & S_2 \end{bmatrix}$ and $\bar{S} = \begin{bmatrix} \bar{S}_1 & 0 \\ 0 & \bar{S}_2 \end{bmatrix}$ in the obvious way. Thus we deduce

$$\bar{S} \bar{R}^\top L (I - \eta S)^t = \begin{bmatrix} \bar{S}_1 R_1^\top L_1 (I - \eta S_1)^t & \bar{S}_1 R_1^\top L_2 (I - \eta S_2)^t \\ \bar{S}_2 R_2^\top L_1 (I - \eta S_1)^t & \bar{S}_2 R_2^\top L_2 (I - \eta S_2)^t \end{bmatrix}. \quad (6.26)$$

Now for any constant $a > 0$, we can choose a constant $C > 0$ such that for $t \geq Cd^{u-\ell} \log(d)$ we have $\|(I - \eta S_1)^t\|_{\text{op}} \leq d^{-a}$. Therefore, the first column on the right side of (6.26) is small in operator norm and we may estimate

$$\left\| \bar{S} \bar{R}^\top L (I - \eta S)^t - \begin{bmatrix} 0 & \bar{S}_1 R_1^\top L_2 (I - \eta S_2)^t \\ 0 & \bar{S}_2 R_2^\top L_2 (I - \eta S_2)^t \end{bmatrix} \right\|_{\text{op}} \lesssim d^{-(a-u)}.$$

Recalling the equality $\nabla \mathcal{L}(W_t) = -\bar{W}T_{\eta,t}$, we therefore deduce

$$\left\| \nabla \mathcal{L}(W_t) - \bar{W} \bar{L} \begin{bmatrix} 0 & -\bar{S}_1 R_1^\top L_2 (I - \eta S_2)^t \\ 0 & -\bar{S}_2 R_2^\top L_2 (I - \eta S_2)^t \end{bmatrix} L \right\|_{\text{op}} \lesssim \|\bar{W}\|_{\text{op}} \cdot d^{-(a-u)}.$$

It remains therefore to estimate the nuclear and Frobenius norms of

$$\bar{W} \bar{L} \begin{bmatrix} 0 & -\bar{S}_1 R_1^\top L_2 (I - \eta S_2)^t \\ 0 & -\bar{S}_2 R_2^\top L_2 (I - \eta S_2)^t \end{bmatrix} L \quad \text{or equivalently} \quad \bar{W} \bar{L} \begin{bmatrix} \bar{S}_1 R_1^\top L_2 \\ \bar{S}_2 R_2^\top L_2 \end{bmatrix} (I - \eta S_2)^t.$$

Now observe that as long as $t \leq Cd^u$ for any constant C , the diagonal entries of $(I - \eta S_2)^t$ are bounded from above and below by positive numerical constants. Therefore it remains to estimate the nuclear and Frobenius norms of the matrix

$$M = \bar{W} \bar{L} Q \quad \text{where} \quad Q := \begin{bmatrix} \bar{S}_1 R_1^\top L_2 \\ \bar{S}_2 R_2^\top L_2 \end{bmatrix}.$$

Using (6.24) and (6.25) we have $\|L_1 L_1^\top - R_1 R_1^\top\|_{\text{op}} \lesssim d^{-\ell}$. Now a standard argument based on principal angles shows the estimates

$$\|L_1 L_1^\top - R_1 R_1^\top\|_{\text{op}} = \|R_1^\top L_2\|_{\text{op}} \quad \text{and} \quad s_{k-p}(R_2^\top L_2) = \sqrt{1 - \|L_1 L_1^\top - R_1 R_1^\top\|_{\text{op}}^2}.$$

In particular, we deduce $\|\bar{S}_1 R_1^\top L_2\|_{\text{op}} \lesssim d^{u-\ell}$. Therefore, we obtain the upper bound on the Frobenius norm

$$\begin{aligned} \|Q\|_* &\geq \left\| \bar{W} \bar{L} \begin{bmatrix} 0 \\ \bar{S}_2 R_2^\top L_2 \end{bmatrix} \right\|_* - \left\| \bar{W} \bar{L} \begin{bmatrix} \bar{S}_1 R_1^\top L_2 \\ 0 \end{bmatrix} \right\|_* \\ &\geq \|[\bar{W} \bar{L}]_{p+1:k} \bar{S}_2 R_2^\top L_2\|_* - pd^{u-\ell} \\ &\gtrsim \|[\bar{W} \bar{L}]_{p+1:k} \bar{S}_2\|_* - pd^{u-\ell} \\ &\gtrsim \|[\bar{W} \bar{L}]_{p+1:r-p}\|_* - pd^{u-\ell}, \end{aligned}$$

where the last inequality follows from applying the linear algebraic Lemma D.2 with $P = [p+1 : r-p]$. Similarly, we obtain the bound on the Frobenius norm:

$$\begin{aligned} \|Q\|_F &\leq \left\| \bar{W} \bar{L} \begin{bmatrix} 0 \\ \bar{S}_2 R_2^\top L_2 \end{bmatrix} \right\|_F - \left\| \bar{W} \bar{L} \begin{bmatrix} \bar{S}_1 R_1^\top L_2 \\ 0 \end{bmatrix} \right\|_F \\ &\lesssim \|[\bar{W} \bar{L}]_{p+1:k} \bar{S}_2 R_2^\top L_2\|_F + \sqrt{pd}^{u-\ell} \\ &\lesssim \|[\bar{W} \bar{L}]_{p+1:k} \bar{S}_2\|_F + \sqrt{pd}^{u-\ell} \\ &\lesssim \|\bar{W}\|_F + \sqrt{pd}^{u-\ell}. \end{aligned}$$

The two claimed estimates follow directly. \square

Theorem 6.11 thus shows that after a burn-in of length $d^{u-\ell} \log d$ and up to iteration d^u , the gradient along the iterations satisfies

$$\text{nr}(W_t) \gtrsim \frac{\|[\bar{W} \bar{L}]_{p+1:r-p}\|_*^2}{\|\bar{W}\|_*^2},$$

assuming that the error terms in the numerator and denominator are negligible. Consequently, under a natural incoherence condition

$$\|[\bar{W} \bar{L}]_{p+1:r-p}\|_* \gtrsim \|\bar{W}\|_*,$$

we get the desired conclusion $\text{nr}(W_t) \gtrsim \text{nr}(\bar{W})$. Intuitively, the incoherence condition holds if the spectrum of W_t is well-spread across the columns, and is true for example if \bar{W} has iid Gaussian entries. This is the content of the following Corollary, which is the main result of the section.

Corollary 6.12 (Nuclear rank with multiple spikes). *Suppose that Assumption F holds. Suppose moreover that the entries of \bar{W} are iid Gaussian $\mathcal{N}(1/d)$ and are independent of A and \bar{A} , and we are in the regime $u - \ell < \frac{1}{2}$, $p = o_d(d^{1-2(u-\ell)})$, and $r \asymp d \asymp m \asymp k$ with $k/d \rightarrow \gamma \in (0, \infty)$ as $d \rightarrow \infty$. Then there exist constants $C_1, C_2 > 0$ such that for any constant $C_3 > 0$ the probability conditioned on (A, \bar{A}) of the event*

$$\text{nr}(\nabla \mathcal{L}(W_t)) \gtrsim d \quad \text{holds for all } t \in [C_1 d^{u-\ell} \log(d), C_3 d^u], \quad (6.27)$$

tends to one as d tends to infinity.

Proof. The proof follows immediately from Theorem 6.11 upon noting that the entries of $\bar{M} = [\bar{W} \bar{L}]_{p+1:r-p}$ are iid Gaussian $\mathcal{N}(1/d)$ and therefore standard Gaussian estimates show $\|\bar{W}\|_F = O_{d,\mathbb{P}}(\sqrt{d})$ and $\|\bar{M}\|_* = \Omega_{d,\mathbb{P}}(k(r-2p+1)) = \Omega_{d,P}(d)$. \square

Thus, under a random teacher setting the nuclear rank of $\nabla \mathcal{L}(W_t)$ is linear in d throughout the entire time window $t \in [C_1 d^{u-\ell} \log d, C_3 d^u]$. This confirms that the spectral-versus-Euclidean separation identified in the realizable multi-spike setting persists in the teacher-student regime.

Remark 2. Just as in the realizable case, the window of large nuclear ranks can be extended by a logarithmic factor: Namely, for any $\varepsilon > 0$ there exist constants c_0 and $c = c(\varepsilon) > 0$ such that, with probability tending to one as $d \rightarrow \infty$, we have

$$\text{nr}(\nabla \mathcal{L}(W_t)) \geq d^{1-\varepsilon} \quad \text{for all } t \in [c_0 d^{u-\ell} \log d, c d^u \log d].$$

The only required modification to the proof is to realize that by setting the horizon to be $c d^u \log(d)$ for a sufficiently small constant $c(\varepsilon)$, we can be sure that the diagonal entries of $(I - \eta S_2)^t$ are lower bounded by $d^{-\varepsilon}$. The proof then proceeds similarly, while taking this observation into account.

7 A General Layered Model and Spectral Descent

The theoretical and empirical results in the earlier sections suggest that spectral updates should be particularly effective when the features seen by each block have low stable rank and the corresponding gradients have large nuclear/Frobenius ratios. Until now, this discussion has been framed in terms of specific architectures (e.g., MLPs) and random-feature models. In this section we formulate a general layered model that captures a broad class of architectures and show that, under mild smoothness assumptions, the same spectral-versus-Euclidean descent tradeoff holds for a *full* gradient step. The key ingredient is a layerwise Hessian bound involving a dominant feature term $\sum_\ell \|\Delta W_\ell A_{\ell-1}\|_F^2$ and a smaller parameter-only term $\sum_\ell \|\Delta W_\ell\|_{\text{op}}^2$, and a one-block comparison which pulls in both the stable rank of the incoming features and the stable rank and nuclear rank of the gradient. The model is designed to encompass:

- **Fully-connected networks (MLPs):** each block is a dense matrix W_ℓ , and the activation A_ℓ is obtained by applying a (possibly vector-valued) nonlinearity to the current preactivation X_ℓ and, optionally, combining it with earlier preactivations and activations (residual/skip connections).
- **Convolutional networks:** after flattening, each convolutional or projection layer can be viewed as a matrix W_ℓ acting on an unfolded feature map $A_{\ell-1}$, with A_ℓ produced by pointwise nonlinearities, pooling, and residuals that are smooth functions of (X_1, \dots, X_ℓ) .

- **Transformers and attention-based models:** multihead attention, feedforward sublayers, and output projections are linear maps W_ℓ applied to token/head features $A_{\ell-1}$; the resulting activations A_ℓ are smooth functions of all previous preactivations through attention, normalization, and residual mixing.

In all of these cases, each block is (affine) linear in its parameters W_ℓ , and the nonlinear structure is captured by smooth activation maps Φ_ℓ that depend on the preactivations (X_1, \dots, X_ℓ) . We will show that the curvature of the composite loss can be bounded in a layer-wise fashion by a feature term plus a smaller parameter-only term, and that, once this bound is established, the spectral-versus-Euclidean comparison essentially reduces to the same nuclear-rank versus stable-rank inequality as in the random-feature model, with an additional dependence on the stable rank of the gradient.

7.1 Model and smoothness assumptions

Fix an integer $L \geq 1$. For each layer $\ell = 1, \dots, L$ we have dimensions d_ℓ (output) and $d_{\ell-1}$ (input). We also fix a column dimension n and think of all activations $A_\ell(W) \in \mathbf{R}^{d_\ell \times n}$ as stacking n data points in columns. Let $W_\ell \in \mathbf{R}^{d_\ell \times d_{\ell-1}}$ be the learnable weight matrix at layer ℓ . We denote the collection of all weights by $W = (W_1, \dots, W_L)$.

Preactivations and activations. We define preactivations and activations recursively as follows:

- The input feature $A_0 \in \mathbf{R}^{d_0 \times n}$ is fixed (e.g., the current minibatch).
- For each $\ell = 1, \dots, L$, the preactivation at layer ℓ is

$$X_\ell(W) := W_\ell A_{\ell-1}(W) \in \mathbf{R}^{d_\ell \times n}.$$

- For each $\ell = 1, \dots, L$, the activation at layer ℓ is given by a C^2 -smooth map

$$A_\ell(W) := \Phi_\ell(X_1(W), \dots, X_\ell(W)) \in \mathbf{R}^{d_\ell \times n}.$$

Thus each $A_\ell(W)$ depends only on the previous preactivations $(X_1(W), \dots, X_\ell(W))$, and each $X_\ell(W)$ depends linearly on W_ℓ and on $A_{\ell-1}(W)$.

Outer loss. We assume a C^2 -smooth outer loss

$$f : \mathcal{X}_1 \times \dots \times \mathcal{X}_L \rightarrow \mathbf{R}, \quad \mathcal{X}_\ell = \mathbf{R}^{d_\ell \times n},$$

and define the composite loss

$$\mathcal{L}(W) := f(X_1(W), \dots, X_L(W)).$$

We denote by $G_\ell(W) := \nabla_{W_\ell} \mathcal{L}(W)$ the gradient with respect to block W_ℓ .

7.2 Layerwise Hessian bound

In the previous subsection we introduced the layered model

$$X_\ell(W) = W_\ell A_{\ell-1}(W), \quad A_\ell(W) = \Phi_\ell(X_1(W), \dots, X_\ell(W)), \quad \ell = 1, \dots, L,$$

with A_0 fixed, and the composite loss

$$\mathcal{L}(W) := f(X_1(W), \dots, X_L(W)).$$

We now fix a parameter $W = (W_1, \dots, W_L)$ and study the Hessian quadratic form

$$Q_W(\Delta W) := \langle \Delta W, \nabla^2 \mathcal{L}(W) \Delta W \rangle$$

for perturbations $\Delta W = (\Delta W_1, \dots, \Delta W_L)$. The goal is to show that Q_W is bounded by a feature term $\sum_\ell \|\Delta W_\ell A_{\ell-1}(W)\|_F^2$ and a parameter-only term $\sum_\ell \|\Delta W_\ell\|_{\text{op}}^2$, with constants depending only on local derivative bounds and on the depth L , and *not* on the layer widths.

Notation. At the fixed parameter W , we introduce the following quantities:

$$\begin{aligned} J_{\Phi, \ell} &:= \sup_{\|U\|_F=1} \|D\Phi_\ell(X)[U]\|_F, \\ H_{\Phi, \ell} &:= \sup_{\|U\|_F=1} \|D^2\Phi_\ell(X)[U, U]\|_F, \\ J_\Phi &:= \max_{1 \leq \ell \leq L} J_{\Phi, \ell}, \quad H_\Phi := \max_{1 \leq \ell \leq L} H_{\Phi, \ell}, \\ J_f &:= \|\nabla f(X_1, \dots, X_L)\|_F, \\ H_f &:= \sup_{\|U\|_F=1} |D^2 f(X_1, \dots, X_L)[U, U]|, \\ W_* &:= \max_{1 \leq \ell \leq L} \|W_\ell\|_{\text{op}}, \\ B_\ell &:= \Delta W_\ell A_{\ell-1}(W), \quad \|B^{(\ell)}\|_F^2 := \sum_{i=1}^{\ell} \|B_i\|_F^2, \\ \Gamma &:= \sqrt{2} (1 + 2J_\Phi^2 W_*^2)^{\frac{L}{2}}, \\ \Theta &:= (1 + J_\Phi W_*)^{L-1}. \end{aligned}$$

Here $X = (X_1(W), \dots, X_L(W))$ denotes the collection of preactivations at W .

We parameterize the perturbation along the path $W(t) = W + t\Delta W$ and define

$$X_\ell(t) := X_\ell(W(t)), \quad A_\ell(t) := A_\ell(W(t)).$$

We then write

$$U_\ell := \dot{X}_\ell(0), \quad \tilde{U}_\ell := \ddot{X}_\ell(0), \quad U^{(\ell)} := (U_1, \dots, U_\ell), \quad \tilde{U}^{(\ell)} := (\tilde{U}_1, \dots, \tilde{U}_\ell),$$

and similarly

$$V_\ell := \dot{A}_\ell(0), \quad \tilde{V}_\ell := \ddot{A}_\ell(0).$$

The next two lemmas bound the first and second derivatives of the preactivations in terms of the feature perturbations B_ℓ and the parameter perturbations ΔW_ℓ .

Lemma 7.1 (First-order propagation). *For every $1 \leq \ell \leq L$ we have*

$$\|U^{(\ell)}\|_F \leq \Gamma \|B^{(\ell)}\|_F. \tag{7.1}$$

Proof. Differentiating $X_\ell(t) = W_\ell(t)A_{\ell-1}(t)$ at $t = 0$ yields

$$U_1 = \Delta W_1 A_0 = B_1, \quad U_\ell = B_\ell + W_\ell V_{\ell-1} \quad (\ell \geq 2),$$

where $V_{\ell-1} := \dot{A}_{\ell-1}(0)$. Differentiating $A_\ell(t) = \Phi_\ell(X^{(\ell)}(t))$ at $t = 0$ and using the definition of $J_{\Phi,\ell}$ gives

$$V_\ell = D\Phi_\ell(X)[U^{(\ell)}], \quad \|V_\ell\|_F \leq J_{\Phi,\ell} \|U^{(\ell)}\|_F \leq J_\Phi \|U^{(\ell)}\|_F.$$

Define the quantities

$$S_\ell := \sum_{i=1}^{\ell} \|U_i\|_F^2, \quad b_\ell^2 := \sum_{i=1}^{\ell} \|B_i\|_F^2.$$

Then $S_1 = \|B_1\|_F^2 \leq b_1^2$. For $\ell \geq 2$ we have

$$\|U_\ell\|_F \leq \|B_\ell\|_F + \|W_\ell\|_{\text{op}} \|V_{\ell-1}\|_F \leq \|B_\ell\|_F + W_* J_\Phi \|U^{(\ell-1)}\|_F,$$

and hence

$$\|U_\ell\|_F^2 \leq 2\|B_\ell\|_F^2 + 2W_*^2 J_\Phi^2 S_{\ell-1}.$$

Therefore

$$S_\ell = S_{\ell-1} + \|U_\ell\|_F^2 \leq (1 + 2W_*^2 J_\Phi^2) S_{\ell-1} + 2\|B_\ell\|_F^2.$$

Setting $a := 1 + 2W_*^2 J_\Phi^2$ and iterating from $\ell = 1$ gives $S_\ell \leq 2a^{\ell-1} b_\ell^2 \leq 2a^{L-1} b_L^2$. Thus, we deduce

$$\|U^{(\ell)}\|_F = \sqrt{S_\ell} \leq \sqrt{2} a^{L/2} \|B^{(\ell)}\|_F = \Gamma \|B^{(\ell)}\|_F,$$

as claimed. \square

Lemma 7.2 (Second-order propagation). *The following estimate holds:*

$$\|\tilde{U}^{(L)}\|_F \leq 2\Theta J_\Phi \Gamma \sqrt{L} \left(\sum_{\ell=1}^L \|\Delta W_\ell\|_{\text{op}}^2 \right)^{\frac{1}{2}} \|B^{(L)}\|_F + \Theta W_* H_\Phi \Gamma^2 L \|B^{(L)}\|_F^2. \quad (7.2)$$

Proof. Differentiating $X_\ell(t) = W_\ell(t)A_{\ell-1}(t)$ twice at $t = 0$ gives

$$\tilde{U}_1 = 0, \quad \tilde{U}_\ell = 2\Delta W_\ell V_{\ell-1} + W_\ell \tilde{V}_{\ell-1} \quad (\ell \geq 2),$$

where $V_\ell := \dot{A}_\ell(0)$ and $\tilde{V}_\ell := \ddot{A}_\ell(0)$. For $A_\ell(t) = \Phi_\ell(X^{(\ell)}(t))$, the second-order chain rule yields

$$\tilde{V}_\ell = D^2\Phi_\ell(X)[U^{(\ell)}, U^{(\ell)}] + D\Phi_\ell(X)[\tilde{U}^{(\ell)}].$$

By the definitions of $H_{\Phi,\ell}$ and $J_{\Phi,\ell}$, we have

$$\|D^2\Phi_\ell(X)[U^{(\ell)}, U^{(\ell)}]\|_F \leq H_{\Phi,\ell} \|U^{(\ell)}\|_F^2 \leq H_\Phi \|U^{(\ell)}\|_F^2,$$

and

$$\|D\Phi_\ell(X)[\tilde{U}^{(\ell)}]\|_F \leq J_{\Phi,\ell} \|\tilde{U}^{(\ell)}\|_F \leq J_\Phi \|\tilde{U}^{(\ell)}\|_F.$$

Using the triangle inequality, we obtain

$$\|\tilde{V}_\ell\|_F \leq H_\Phi \|U^{(\ell)}\|_F^2 + J_\Phi \|\tilde{U}^{(\ell)}\|_F \quad \text{for all } \ell. \quad (7.3)$$

Define now $M_\ell := \|\tilde{U}^{(\ell)}\|_F$ for $\ell = 1, \dots, L$. Then $M_1 = \|\tilde{U}_1\|_F = 0$. For $\ell \geq 2$ we have

$$M_\ell = \|\tilde{U}^{(\ell)}\|_F \leq \|\tilde{U}^{(\ell-1)}\|_F + \|\tilde{U}_\ell\|_F = M_{\ell-1} + \|\tilde{U}_\ell\|_F.$$

Using the expression for \tilde{U}_ℓ and the bound (7.3) for $\tilde{V}_{\ell-1}$ yields

$$\begin{aligned} \|\tilde{U}_\ell\|_F &\leq 2\|\Delta W_\ell\|_{\text{op}}\|\tilde{V}_{\ell-1}\|_F + \|W_\ell\|_{\text{op}}\|\tilde{V}_{\ell-1}\|_F \\ &\leq 2\|\Delta W_\ell\|_{\text{op}}\|\tilde{V}_{\ell-1}\|_F + W_*(H_\Phi\|U^{(\ell-1)}\|_F^2 + J_\Phi\|\tilde{U}^{(\ell-1)}\|_F), \end{aligned}$$

and hence

$$M_\ell \leq (1 + W_*J_\Phi)M_{\ell-1} + 2\|\Delta W_\ell\|_{\text{op}}\|\tilde{V}_{\ell-1}\|_F + W_*H_\Phi\|U^{(\ell-1)}\|_F^2.$$

From Lemma 7.1 we have $\|\tilde{V}_{\ell-1}\|_F \leq J_\Phi\Gamma\|B^{(\ell-1)}\|_F$ and $\|U^{(\ell-1)}\|_F \leq \Gamma\|B^{(\ell-1)}\|_F$, so

$$M_\ell \leq (1 + W_*J_\Phi)M_{\ell-1} + 2J_\Phi\Gamma\|\Delta W_\ell\|_{\text{op}}\|B^{(\ell-1)}\|_F + W_*H_\Phi\Gamma^2\|B^{(\ell-1)}\|_F^2.$$

Unrolling this recursion from $\ell = 2$ to $\ell = L$ and using $M_1 = 0$ and $(1 + W_*J_\Phi)^{L-k} \leq \Theta$ for all k gives

$$M_L \leq \Theta \sum_{k=2}^L \left(2J_\Phi\Gamma\|\Delta W_k\|_{\text{op}}\|B^{(k-1)}\|_F + W_*H_\Phi\Gamma^2\|B^{(k-1)}\|_F^2 \right).$$

We bound the two sums separately. First,

$$\sum_{k=2}^L \|B^{(k-1)}\|_F^2 = \sum_{k=2}^L \sum_{i \leq k-1} \|B_i\|_F^2 = \sum_{i=1}^{L-1} (L-i)\|B_i\|_F^2 \leq L \sum_{i=1}^L \|B_i\|_F^2 = L\|B^{(L)}\|_F^2.$$

Second, by Cauchy–Schwarz,

$$\sum_{k=2}^L \|\Delta W_k\|_{\text{op}}\|B^{(k-1)}\|_F \leq \sqrt{L} \left(\sum_{\ell=1}^L \|\Delta W_\ell\|_{\text{op}}^2 \right)^{\frac{1}{2}} \|B^{(L)}\|_F.$$

Substituting these bounds into the expression for M_L gives

$$\|\tilde{U}^{(L)}\|_F = M_L \leq 2\Theta J_\Phi\Gamma\sqrt{L} \left(\sum_{\ell=1}^L \|\Delta W_\ell\|_{\text{op}}^2 \right)^{\frac{1}{2}} \|B^{(L)}\|_F + \Theta W_*H_\Phi\Gamma^2 L \|B^{(L)}\|_F^2,$$

which is exactly (7.2). \square

We can now state the layerwise Hessian bound, which is the main conclusion of this subsection.

Proposition 7.3 (Layerwise Hessian bound). *Let W be fixed and consider the layered model and loss \mathcal{L} described above. Then there exist finite constants $C_F(W), C_{\text{op}}(W) > 0$, depending only on J_Φ, H_Φ, J_f, H_f , on the block operator norms $\|W_\ell\|_{\text{op}}$ (through W_*), and on the depth L , such that for every perturbation $\Delta W = (\Delta W_1, \dots, \Delta W_L)$, we have*

$$|\langle \Delta W, \nabla^2 \mathcal{L}(W) \Delta W \rangle| \leq C_F(W) \sum_{\ell=1}^L \|\Delta W_\ell A_{\ell-1}(W)\|_F^2 + C_{\text{op}}(W) \sum_{\ell=1}^L \|\Delta W_\ell\|_{\text{op}}^2. \quad (7.4)$$

Moreover, one can take for example

$$C_F(W) := \Gamma^2 H_f + J_f \Theta W_* H_\Phi \Gamma^2 L + J_f^2 \Theta \Gamma^2 L, \quad C_{\text{op}}(W) := \Theta J_\Phi^2. \quad (7.5)$$

Proof. Along the path $W(t) = W + t\Delta W$, the chain rule for $\mathcal{L}(W(t)) = f(X_1(t), \dots, X_L(t))$ gives

$$\frac{d^2}{dt^2} \Big|_{t=0} \mathcal{L}(W(t)) = D^2 f(X)[U^{(L)}, U^{(L)}] + \langle \nabla f(X), \tilde{U}^{(L)} \rangle.$$

By the definitions of H_f and J_f , we have

$$|\langle \Delta W, \nabla^2 \mathcal{L}(W) \Delta W \rangle| \leq H_f \|U^{(L)}\|_F^2 + J_f \|\tilde{U}^{(L)}\|_F. \quad (7.6)$$

Lemma 7.1 yields $\|U^{(L)}\|_F \leq \Gamma \|B^{(L)}\|_F$, and Lemma 7.2 yields

$$\|\tilde{U}^{(L)}\|_F \leq 2\Theta J_\Phi \Gamma \sqrt{L} \left(\sum_{\ell=1}^L \|\Delta W_\ell\|_{\text{op}}^2 \right)^{\frac{1}{2}} \|B^{(L)}\|_F + \Theta W_* H_\Phi \Gamma^2 L \|B^{(L)}\|_F^2.$$

Substituting these bounds into (7.6) and collecting terms gives

$$|\langle \Delta W, \nabla^2 \mathcal{L}(W) \Delta W \rangle| \leq A_B(W) \|B^{(L)}\|_F^2 + 2C_c(W) a b,$$

where

$$A_B(W) := \Gamma^2 H_f + J_f \Theta W_* H_\Phi \Gamma^2 L, \quad C_c(W) := J_f \Theta J_\Phi \Gamma \sqrt{L},$$

and

$$a := \left(\sum_{\ell=1}^L \|\Delta W_\ell\|_{\text{op}}^2 \right)^{\frac{1}{2}}, \quad b := \|B^{(L)}\|_F.$$

Using the inequality

$$2C_c(W) a b \leq A a^2 + B b^2 \quad \text{for any } A, B > 0 \text{ with } AB \geq C_c(W)^2,$$

and choosing, for instance,

$$A = \Theta J_\Phi^2, \quad B = \frac{C_c(W)^2}{A} = J_f^2 \Theta \Gamma^2 L,$$

we obtain

$$|\langle \Delta W, \nabla^2 \mathcal{L}(W) \Delta W \rangle| \leq (A_B(W) + B) \|B^{(L)}\|_F^2 + A \sum_{\ell=1}^L \|\Delta W_\ell\|_{\text{op}}^2.$$

Since equality $\|B^{(L)}\|_F^2 = \sum_{\ell=1}^L \|\Delta W_\ell A_{\ell-1}(W)\|_F^2$ holds, this is exactly (7.4) with $C_F(W)$ and $C_{\text{op}}(W)$ as in (7.5). \square

Scaling with the number of samples. For averaged losses such as the squared loss $f(X_1, \dots, X_L) = \frac{1}{2n} \|X_L - Y\|_F^2$, we have

$$J_f = \|\nabla f(X)\|_F = \frac{1}{n} \|X_L - Y\|_F, \quad H_f = \frac{1}{n},$$

as we will verify below. If, in addition, the average loss f remains $O(1)$ along training so that typically $\|X_L - Y\|_F^2 = O(n)$, then $J_f = O(1/\sqrt{n})$ and $H_f = O(1/n)$. A completely analogous scaling holds for softmax cross-entropy: the per-example gradients are uniformly bounded, so for the averaged loss one has $J_f = O(1/\sqrt{n})$ and $H_f = O(1/n)$ regardless of the size of the prediction errors. These factors appear only in $C_F(W)$, which multiplies the feature term $\sum_\ell \|\Delta W_\ell A_{\ell-1}(W)\|_F^2$. Since $\|A_{\ell-1}(W)\|_F^2$ is of order n when $A_{\ell-1}$ stacks n data points in columns, the resulting curvature contribution is of order one in n . In particular, the constants $C_F(W)$ and $C_{\text{op}}(W)$ in Proposition 7.3 do not grow with the number of samples n , nor with the layer widths.

7.2.1 Derivative constants for MLPs and transformer blocks

To interpret the layerwise Hessian bound in concrete architectures, it is useful to understand the size of the derivative constants $J_{\Phi,\ell}, H_{\Phi,\ell}$ and J_f, H_f . In this subsubsection we sketch how these constants are instantiated in multilayer perceptrons and transformer blocks. Throughout, all implicit constants depend only on the choice of nonlinearities and loss, and not on the dimensions d_ℓ or n .

MLPs. Consider a fully-connected network with layers

$$X_1 = W_1 A_0, \quad A_1 = \sigma(X_1), \quad X_2 = W_2 A_1, \quad A_2 = \sigma(X_2), \quad \dots,$$

and a fixed elementwise activation $\sigma : \mathbf{R} \rightarrow \mathbf{R}$. In the layered notation above, the nonlinear map at layer ℓ is simply

$$\Phi_\ell(X_1, \dots, X_\ell) = \sigma(X_\ell) \quad (\text{applied entrywise}).$$

Assume that σ is C^2 -smooth with

$$\sup_{t \in \mathbf{R}} |\sigma'(t)| \leq L_1, \quad \sup_{t \in \mathbf{R}} |\sigma''(t)| \leq L_2.$$

Then for the Jacobian we have

$$D\Phi_\ell(X)[U] = \sigma'(X_\ell) \odot U, \quad \|D\Phi_\ell(X)[U]\|_F \leq L_1 \|U\|_F.$$

Therefore we deduce

$$J_{\Phi,\ell} \leq L_1 \quad \text{and hence} \quad J_\Phi = \max_\ell J_{\Phi,\ell} \leq L_1.$$

Similarly, the second derivative takes the form

$$D^2\Phi_\ell(X)[U, U] = \sigma''(X_\ell) \odot U \odot U,$$

and

$$\|D^2\Phi_\ell(X)[U, U]\|_F \leq L_2 \|U \odot U\|_F \leq L_2 \|U\|_F^2,$$

Therefore, we deduce

$$H_{\Phi,\ell} \leq L_2, \quad H_\Phi \leq L_2.$$

Thus, for MLPs with a fixed smooth activation, the activation-side constants $J_{\Phi,\ell}, H_{\Phi,\ell}$ are controlled entirely by scalar bounds on σ', σ'' and do not depend on width.

For the outer loss f , the squared loss and softmax cross-entropy examples in the scaling paragraph above already show that J_f and H_f inherit only the $1/n$ factors coming from the averaging in the loss, and do not introduce any additional dependence on the layer widths.

Transformer blocks and the layered model. We now make the structure of a single decoder block explicit in the layered notation. Fix a block input $X^{(0)} \in \mathbf{R}^{d_{\text{model}} \times T}$ (hidden dimension d_{model} , sequence length T). We enumerate the trainable matrices inside the block as

$$W_1 = W_Q, \quad W_2 = W_K, \quad W_3 = W_V, \quad W_4 = W_O, \quad W_5 = W_1, \quad W_6 = W_2,$$

corresponding to the attention projections and MLP weights. Following the layered model convention $X_\ell(W) = W_\ell A_{\ell-1}(W)$ and $A_\ell(W) = \Phi_\ell(X_1(W), \dots, X_\ell(W))$, we introduce the following internal variables and maps.

Block structure. Define first the RMS-normalized input

$$A_0(W) := A^{\text{rms}}(W) := \text{RMSNorm}(X^{(0)}(W)),$$

so that the first three preactivations are

$$X_1(W) = W_1 A_0(W) = W_Q A^{\text{rms}}, \quad X_2(W) = W_2 A_0(W) = W_K A^{\text{rms}}, \quad X_3(W) = W_3 A_0(W) = W_V A^{\text{rms}}.$$

Next, we form the scaled attention scores and probabilities

$$S(W) := d_{\text{model}}^{-1/2} X_2(W)^\top X_1(W), \quad P(W) := \text{softmax}(S(W)) \quad (\text{columnwise}),$$

and the value aggregation

$$H(W) := X_3(W) P(W).$$

The output projection preactivation is

$$X_4(W) = W_4 H(W) = W_O H(W),$$

and the attention residual is

$$X^{\text{att}}(W) := X^{(0)}(W) + X_4(W).$$

We then RMS-normalize X^{att} as

$$A_4(W) := A_{\text{mlp}}^{\text{rms}}(W) := \text{RMSNorm}(X^{\text{att}}(W)),$$

and form the MLP preactivations

$$X_5(W) = W_5 A_4(W) = W_1 A_{\text{mlp}}^{\text{rms}}, \quad X_6(W) = W_6 B(W) = W_2 B(W),$$

where

$$B(W) := \sigma(X_5(W))$$

is the pointwise MLP activation. Finally, the block output is

$$X^{(+)}(W) := X^{\text{att}}(W) + X_6(W).$$

In this notation, the preactivations are $X_\ell(W) = W_\ell A_{\ell-1}(W)$ for $\ell = 1, \dots, 6$, with $A_{-1}(W) = X^{(0)}(W)$ and $A_0(W), A_4(W), B(W)$ as above. The corresponding activation maps

$$A_\ell(W) = \Phi_\ell(X_1(W), \dots, X_\ell(W)), \quad \ell = 0, \dots, 6,$$

collect the nonlinear operations that produce the data matrices feeding each linear map; for example

$$\Phi_0(X^{(0)}) = \text{RMSNorm}(X^{(0)}),$$

$$\Phi_3(X_1, X_2, X_3) = A^{\text{rms}}(W) \quad (\text{the attention inputs, reused for } W_Q, W_K, W_V),$$

$$\Phi_4(X_1, \dots, X_4) = \text{RMSNorm}(X^{(0)} + X_4) = A_{\text{mlp}}^{\text{rms}}(W),$$

$$\Phi_5(X_1, \dots, X_5) = \sigma(X_5), \quad \Phi_6(X_1, \dots, X_6) = X^{(+)} = X^{\text{att}} + X_6.$$

Derivative bounds. With this structure in hand, the derivative constants $J_{\Phi, \ell}$ and $H_{\Phi, \ell}$ for the transformer block can be bounded by combining the primitive bounds for RMSNorm, softmax, and the MLP nonlinearity. As before, we assume that the MLP activation σ satisfies

$$\sup_{t \in \mathbf{R}} |\sigma'(t)| \leq L_1, \quad \sup_{t \in \mathbf{R}} |\sigma''(t)| \leq L_2.$$

For the RMS normalization, a direct computation of the Jacobian and Hessian shows that, as long as the rescaled squared norms $d_{\text{model}}^{-1} \|X^{(0)}\|_F^2$ and $d_{\text{model}}^{-1} \|X^{\text{att}}\|_F^2$ remain in a fixed compact interval, there exist constants $C_{\text{rms},1}, C_{\text{rms},2}$ (depending only on the RMSNorm hyperparameters) such that

$$\|D(\text{RMSNorm})(\cdot)[U]\|_F \leq C_{\text{rms},1} \|U\|_F, \quad \|D^2(\text{RMSNorm})(\cdot)[U, U]\|_F \leq C_{\text{rms},2} \|U\|_F^2.$$

For the softmax, viewed columnwise on $S \in \mathbf{R}^{T \times T}$, there exist constants $C_{\text{sm},1}, C_{\text{sm},2}$ such that

$$\|D(\text{softmax})(S)[U]\|_F \leq C_{\text{sm},1} \|U\|_F, \quad \|D^2(\text{softmax})(S)[U, U]\|_F \leq C_{\text{sm},2} \|U\|_F^2$$

for all S, U . The linear projections $W_\ell A_{\ell-1}$ always contribute their spectral norms:

$$\|D(W_\ell A_{\ell-1})[U]\|_F \leq \|W_\ell\|_{\text{op}} \|U\|_F, \quad D^2(W_\ell A_{\ell-1})[\cdot, \cdot] \equiv 0.$$

Combining these primitive estimates through the chain rule, one finds that the constants $J_{\Phi,\ell}, H_{\Phi,\ell}$ are bounded above by expressions of the form

$$J_{\Phi,\ell} \leq C_1 \prod_{\ell' \in \mathcal{N}(\ell)} \|W_{\ell'}\|_{\text{op}}, \quad H_{\Phi,\ell} \leq C_2 \left(1 + \sum_{\ell' \in \mathcal{N}(\ell)} \|W_{\ell'}\|_{\text{op}}^2 \right),$$

where $\mathcal{N}(\ell)$ denotes the (finite) collection of projection matrices whose outputs feed into the nonlinearities affecting $A_{\ell-1}$, and C_1, C_2 depend only on the scalar nonlinearities (RMSNorm, softmax, σ) and not on d_{model} or T . In particular, these bounds show that J_Φ and H_Φ remain bounded as the width and sequence length vary.

7.3 From feature metric to blockwise Lipschitz constants

The mixed Hessian bound of Proposition 7.3 controls the curvature of \mathcal{L} in terms of the feature perturbations $\Delta W_\ell A_{\ell-1}(W)$ and the operator norms $\|\Delta W_\ell\|_{\text{op}}$:

$$\langle \Delta W, \nabla^2 \mathcal{L}(W) \Delta W \rangle \leq C_F(W) \sum_{\ell=1}^L \|\Delta W_\ell A_{\ell-1}(W)\|_F^2 + C_{\text{op}}(W) \sum_{\ell=1}^L \|\Delta W_\ell\|_{\text{op}}^2.$$

The feature term in this inequality plays exactly the same role as in the random-feature model: it yields blockwise curvature constants that are determined by the activations $A_{\ell-1}(W)$. The parameter-only term $C_{\text{op}}(W) \sum_\ell \|\Delta W_\ell\|_{\text{op}}^2$ contributes an extra, geometry-independent correction which we will account for in the descent comparison, but it does not affect which activation matrices are relevant for each block or the stable-rank ratio.

In many architectures of interest, and in particular in the multilayer and transformer examples discussed in Section 1.2.1, each activation $A_{\ell-1}(W)$ admits a natural factorization

$$A_{\ell-1}(W) = M_{\ell,\text{left}}(W) \tilde{A}_{\ell-1}(W) M_{\ell,\text{right}}(W), \quad (7.7)$$

where:

- $\tilde{A}_{\ell-1}(W)$ is the *core activation* feeding block ℓ (for example, the post-activation $A_{\ell-1}$ in an MLP, or an RMS-normalized activation or MLP post-activation in a transformer block as in Section 1.2.1); and
- $M_{\ell,\text{left}}(W)$ and $M_{\ell,\text{right}}(W)$ are fixed linear operators (at the current W) capturing the surrounding linear structure: projections, attention kernels, residual maps, etc.

The dependence on W is smooth but, crucially, these matrices are independent of ΔW . Using submultiplicativity of the operator norm, we obtain the Frobenius and operator bounds, for each block ℓ , given by

$$\begin{aligned}\|\Delta W_\ell A_{\ell-1}(W)\|_F &\leq \|\Delta W_\ell\|_F \|A_{\ell-1}(W)\|_{\text{op}}, \\ \|\Delta W_\ell A_{\ell-1}(W)\|_F &\leq \|\Delta W_\ell\|_{\text{op}} \|A_{\ell-1}(W)\|_F.\end{aligned}$$

Using the factorization (7.7) once more, we obtain

$$\begin{aligned}\|A_{\ell-1}(W)\|_{\text{op}} &\leq \|M_{\ell,\text{left}}(W)\|_{\text{op}} \|\tilde{A}_{\ell-1}(W)\|_{\text{op}} \|M_{\ell,\text{right}}(W)\|_{\text{op}}, \\ \|A_{\ell-1}(W)\|_F &\leq \|M_{\ell,\text{left}}(W)\|_{\text{op}} \|\tilde{A}_{\ell-1}(W)\|_F \|M_{\ell,\text{right}}(W)\|_{\text{op}}.\end{aligned}$$

Combining these inequalities with the feature part of the Hessian bound, we obtain feature-based blockwise curvature constants

$$\begin{aligned}L_\ell^F(W) &:= C_F(W) \|M_{\ell,\text{left}}(W)\|_{\text{op}}^2 \|\tilde{A}_{\ell-1}(W)\|_{\text{op}}^2 \|M_{\ell,\text{right}}(W)\|_{\text{op}}^2, \\ L_\ell^{\text{op}}(W) &:= C_F(W) \|M_{\ell,\text{left}}(W)\|_{\text{op}}^2 \|\tilde{A}_{\ell-1}(W)\|_F^2 \|M_{\ell,\text{right}}(W)\|_{\text{op}}^2,\end{aligned}\tag{7.8}$$

for which the feature term in the Hessian satisfies

$$\langle \Delta W, \nabla^2 \mathcal{L}(W) \Delta W \rangle_{\text{feature}} \leq \sum_{\ell=1}^L L_\ell^F(W) \|\Delta W_\ell\|_F^2,\tag{7.9}$$

$$\langle \Delta W, \nabla^2 \mathcal{L}(W) \Delta W \rangle_{\text{feature}} \leq \sum_{\ell=1}^L L_\ell^{\text{op}}(W) \|\Delta W_\ell\|_{\text{op}}^2.\tag{7.10}$$

By construction, the ratio of these two constants depends only on the stable rank of the *core* activation $\tilde{A}_{\ell-1}(W)$, while the surrounding linear maps cancel:

$$\frac{L_\ell^{\text{op}}(W)}{L_\ell^F(W)} = \frac{\|\tilde{A}_{\ell-1}(W)\|_F^2}{\|\tilde{A}_{\ell-1}(W)\|_{\text{op}}^2} = \text{st}(\tilde{A}_{\ell-1}(W)).\tag{7.11}$$

In words, the feature-based curvature in the spectral geometry is larger than that in the Frobenius geometry by a factor equal to the stable rank of the core activation.

Two special cases are worth highlighting.

- **Fully-connected networks.** For standard MLPs, we may take $M_{\ell,\text{left}}(W) = I$ and $M_{\ell,\text{right}}(W) = I$, so that $\tilde{A}_{\ell-1}(W) = A_{\ell-1}(W)$ is exactly the layerwise post-activation introduced in (4.1). In this case, L_ℓ^F and L_ℓ^{op} are proportional to $\|A_{\ell-1}\|_{\text{op}}^2$ and $\|A_{\ell-1}\|_F^2$, and their ratio is the stable rank $\text{st}(A_{\ell-1})$.
- **Transformer blocks.** In transformer architectures, the effective feature matrices $A_{\ell-1}(W)$ entering each block factor as in Section 1.2.1: the core activation $\tilde{A}_{\ell-1}$ is one of the RMS-normalized hidden states or MLP post-activations, while $M_{\ell,\text{left}}$ and $M_{\ell,\text{right}}$ collect attention kernels, projection matrices, and residual maps. The expressions (7.8)–(7.11) then show that the feature-based curvature is governed, up to fixed operator-norm factors, by the stable rank of the corresponding RMS or MLP activations.

The full Hessian bound of Proposition 7.3 adds the parameter-only term $C_{\text{op}}(W) \sum_\ell \|\Delta W_\ell\|_{\text{op}}^2$ to the right-hand side of (7.9)–(7.10). This term does not depend on the activations and therefore does not change which feature matrices are relevant for a given block or the stable-rank ratio (7.11); it will appear only as a small, blockwise correction in the one-step descent analysis below.

7.4 Descent bounds and spectral-vs.-Euclidean comparison

We now use the blockwise constants from (7.8)–(7.11) together with the full Hessian bound of Proposition 7.3 to compare one-step decreases under Euclidean (Frobenius) and spectral updates acting on all matrix blocks. We write $G_\ell(W) := \nabla_{W_\ell} \mathcal{L}(W)$ for the block gradients, and let $\mathcal{S} \subseteq \{1, \dots, L\}$ denote the subset of matrix-valued blocks on which we intend to apply spectral updates (for example, the internal MLP and attention weights in a transformer stack, as in Section 1.2.1). For notational brevity, we fix W and write G_ℓ , L_ℓ^F , L_ℓ^{op} , C_F , and C_{op} .

Taylor model. Expanding \mathcal{L} around W in the direction $\Delta W = (\Delta W_1, \dots, \Delta W_L)$ yields

$$\mathcal{L}(W + \Delta W) = \mathcal{L}(W) + \sum_{\ell=1}^L \langle G_\ell, \Delta W_\ell \rangle + \frac{1}{2} \langle \Delta W, \nabla^2 \mathcal{L}(W) \Delta W \rangle + R(\Delta W), \quad (7.12)$$

where $R(\Delta W)$ collects third and higher order terms. Combining the feature-based bounds (7.9)–(7.10) with the additional parameter term in Proposition 7.3, we obtain the Frobenius-geometry bound

$$\langle \Delta W, \nabla^2 \mathcal{L}(W) \Delta W \rangle \leq \sum_{\ell} L_\ell^F \|\Delta W_\ell\|_F^2 + C_{\text{op}}(W) \sum_{\ell} \|\Delta W_\ell\|_{\text{op}}^2, \quad (7.13)$$

valid for all ΔW . For mixed Euclidean/spectral updates that use spectral geometry only on the subset \mathcal{S} , we will also use the corresponding mixed bound

$$\langle \Delta W, \nabla^2 \mathcal{L}(W) \Delta W \rangle \leq \sum_{\ell \in \mathcal{S}} L_\ell^{\text{op}} \|\Delta W_\ell\|_{\text{op}}^2 + \sum_{\ell \notin \mathcal{S}} L_\ell^F \|\Delta W_\ell\|_F^2 + C_{\text{op}}(W) \sum_{\ell} \|\Delta W_\ell\|_{\text{op}}^2,$$

which is obtained by applying the spectral feature bound on blocks in \mathcal{S} , the Frobenius feature bound on blocks not in \mathcal{S} , and the same parameter-only term on all blocks.

Definition of the GD and spectral updates. We now define a full Euclidean (Frobenius) gradient step and a mixed spectral step by choosing blockwise step sizes that are natural for the quadratic model (7.12) under the mixed Hessian bounds above.

For the Euclidean step we set, for each block ℓ ,

$$a_{\text{GD},\ell} := L_\ell^F + \frac{C_{\text{op}}(W)}{\text{st}(G_\ell)}, \quad \text{st}(G_\ell) := \frac{\|G_\ell\|_F^2}{\|G_\ell\|_{\text{op}}^2},$$

and define

$$W_\ell^{\text{GD}} := W_\ell - \frac{1}{a_{\text{GD},\ell}} G_\ell, \quad \Delta W_\ell^{\text{GD}} := W_\ell^{\text{GD}} - W_\ell = -\frac{1}{a_{\text{GD},\ell}} G_\ell,$$

so that $W^{\text{GD}} := (W_1^{\text{GD}}, \dots, W_L^{\text{GD}})$ is the full GD update.

For the spectral step we set, for each $\ell \in \mathcal{S}$,

$$a_{\text{Spec},\ell} := L_\ell^{\text{op}} + C_{\text{op}}(W),$$

and define

$$W_\ell^{\text{Spec}} := W_\ell - \frac{\|G_\ell\|_*}{a_{\text{Spec},\ell}} \text{polar}(G_\ell), \quad \Delta W_\ell^{\text{Spec}} := W_\ell^{\text{Spec}} - W_\ell = -\frac{\|G_\ell\|_*}{a_{\text{Spec},\ell}} \text{polar}(G_\ell),$$

where $\text{polar}(G_\ell)$ is the orthogonal factor in the polar decomposition of G_ℓ . For blocks $\ell \notin \mathcal{S}$ we simply set $W_\ell^{\text{Spec}} := W_\ell^{\text{GD}}$. In this way $W^{\text{Spec}} := (W_1^{\text{Spec}}, \dots, W_L^{\text{Spec}})$ is the full mixed update which uses spectral geometry on blocks in \mathcal{S} and Euclidean geometry on the others.

One-step bound for the Euclidean step. For the Euclidean update, the linear term in (7.12) is

$$\langle G_\ell, \Delta W_\ell^{\text{GD}} \rangle = -\frac{1}{a_{\text{GD},\ell}} \|G_\ell\|_F^2.$$

For the quadratic term we use (7.13) together with

$$\|\Delta W_\ell^{\text{GD}}\|_F^2 = \frac{1}{a_{\text{GD},\ell}^2} \|G_\ell\|_F^2, \quad \|\Delta W_\ell^{\text{GD}}\|_{\text{op}}^2 = \frac{1}{a_{\text{GD},\ell}^2} \|G_\ell\|_{\text{op}}^2 = \frac{1}{a_{\text{GD},\ell}^2} \frac{\|G_\ell\|_F^2}{\text{st}(G_\ell)}.$$

Thus the contribution of block ℓ to the quadratic term is bounded by

$$\frac{1}{2} \left(L_\ell^{\text{F}} \frac{\|G_\ell\|_F^2}{a_{\text{GD},\ell}^2} + C_{\text{op}}(W) \frac{\|G_\ell\|_F^2}{a_{\text{GD},\ell}^2 \text{st}(G_\ell)} \right) = \frac{a_{\text{GD},\ell}}{2} \frac{\|G_\ell\|_F^2}{a_{\text{GD},\ell}^2} = \frac{1}{2a_{\text{GD},\ell}} \|G_\ell\|_F^2.$$

Plugging ΔW^{GD} into (7.12) and summing over ℓ gives

$$\mathcal{L}(W^{\text{GD}}) \leq \mathcal{L}(W) - \sum_{\ell=1}^L \frac{1}{a_{\text{GD},\ell}} \|G_\ell\|_F^2 + \frac{1}{2} \sum_{\ell=1}^L \frac{1}{a_{\text{GD},\ell}} \|G_\ell\|_F^2 + R(\Delta W^{\text{GD}}),$$

so the quadratic model predicts the total decrease

$$\Delta_{\text{GD}} := \mathcal{L}(W) - \mathcal{L}(W^{\text{GD}}) \geq \frac{1}{2} \sum_{\ell=1}^L \frac{\|G_\ell\|_F^2}{a_{\text{GD},\ell}} = \frac{1}{2} \sum_{\ell=1}^L \frac{\|G_\ell\|_F^2}{L_\ell^{\text{F}} + C_{\text{op}}(W)/\text{st}(G_\ell)}. \quad (7.14)$$

One-step bound for the spectral step. For the spectral update on $\ell \in \mathcal{S}$ we have

$$\langle G_\ell, \Delta W_\ell^{\text{Spec}} \rangle = -\frac{\|G_\ell\|_*^2}{a_{\text{Spec},\ell}}, \quad \|\Delta W_\ell^{\text{Spec}}\|_{\text{op}}^2 = \frac{\|G_\ell\|_*^2}{a_{\text{Spec},\ell}^2},$$

and for $\ell \notin \mathcal{S}$ the update coincides with the Euclidean one, so the contribution to the linear and quadratic terms on those blocks is exactly the same as in the GD case. Using the mixed Hessian bound (spectral geometry on \mathcal{S} , Frobenius geometry on its complement), the contribution of block $\ell \in \mathcal{S}$ to the quadratic term is bounded by

$$\frac{1}{2} \left(L_\ell^{\text{op}} \frac{\|G_\ell\|_*^2}{a_{\text{Spec},\ell}^2} + C_{\text{op}}(W) \frac{\|G_\ell\|_*^2}{a_{\text{Spec},\ell}^2} \right) = \frac{a_{\text{Spec},\ell}}{2} \frac{\|G_\ell\|_*^2}{a_{\text{Spec},\ell}^2} = \frac{1}{2a_{\text{Spec},\ell}} \|G_\ell\|_*^2.$$

Proceeding as above and summing over all blocks, we obtain the total decrease guarantee

$$\begin{aligned} \Delta_{\text{Spec}} := \mathcal{L}(W) - \mathcal{L}(W^{\text{Spec}}) &\geq \frac{1}{2} \sum_{\ell \in \mathcal{S}} \frac{\|G_\ell\|_*^2}{a_{\text{Spec},\ell}} + \frac{1}{2} \sum_{\ell \notin \mathcal{S}} \frac{\|G_\ell\|_F^2}{a_{\text{GD},\ell}} \\ &= \frac{1}{2} \sum_{\ell \in \mathcal{S}} \frac{\|G_\ell\|_*^2}{L_\ell^{\text{op}} + C_{\text{op}}(W)} + \frac{1}{2} \sum_{\ell \notin \mathcal{S}} \frac{\|G_\ell\|_F^2}{L_\ell^{\text{F}} + C_{\text{op}}(W)/\text{st}(G_\ell)}. \end{aligned} \quad (7.15)$$

Nuclear-rank vs. stable-rank condition. Comparing the global guarantees (7.14) and (7.15), we see that whenever we keep the GD update on blocks $\ell \notin \mathcal{S}$, the total spectral decrease is guaranteed to be at least as large as the Euclidean decrease provided that, for every $\ell \in \mathcal{S}$,

$$\frac{\|G_\ell\|_*^2}{L_\ell^{\text{op}} + C_{\text{op}}(W)} \geq \frac{\|G_\ell\|_F^2}{L_\ell^{\text{F}} + C_{\text{op}}(W)/\text{st}(G_\ell)} \iff \frac{\|G_\ell\|_*^2}{\|G_\ell\|_F^2} \geq \frac{L_\ell^{\text{op}} + C_{\text{op}}(W)}{L_\ell^{\text{F}} + C_{\text{op}}(W)/\text{st}(G_\ell)}.$$

Using the feature-based ratio (7.11), we may rewrite the right-hand side in terms of the stable rank of the core activation feeding block ℓ . Setting

$$s_\ell := \text{st}(\tilde{A}_{\ell-1}(W)) = \frac{L_\ell^{\text{op}}}{L_\ell^{\text{F}}}, \quad \alpha_\ell := \frac{C_{\text{op}}(W)}{L_\ell^{\text{F}}},$$

we have

$$\frac{L_\ell^{\text{op}} + C_{\text{op}}(W)}{L_\ell^{\text{F}} + C_{\text{op}}(W)/\text{st}(G_\ell)} = \frac{s_\ell + \alpha_\ell}{1 + \alpha_\ell/\text{st}(G_\ell)}.$$

Thus the per-block condition for the spectral update on block $\ell \in \mathcal{S}$ to improve upon the Euclidean update on that block is

$$\text{nr}(G_\ell) := \frac{\|G_\ell\|_*^2}{\|G_\ell\|_F^2} \geq \frac{\text{st}(\tilde{A}_{\ell-1}(W)) + \alpha_\ell}{1 + \alpha_\ell/\text{st}(G_\ell)}. \quad (7.16)$$

The right-hand side of (7.16) is increasing in the denominator parameter $\text{st}(G_\ell)$. Since $\text{st}(G_\ell) \leq \text{nr}(G_\ell)$ by definition, we may therefore replace $\text{st}(G_\ell)$ by $\text{nr}(G_\ell)$ in the denominator, which only *increases* the right-hand side and yields a stronger (more conservative) but still sufficient condition for the spectral update to dominate GD. With this replacement, (7.16) is implied by

$$\text{nr}(G_\ell) \geq \frac{\text{st}(\tilde{A}_{\ell-1}(W)) + \alpha_\ell}{1 + \alpha_\ell/\text{nr}(G_\ell)}. \quad (7.17)$$

A simple algebraic rearrangement shows that the stronger inequality (7.17) is in fact *equivalent* to the bare inequality

$$\text{nr}(G_\ell) \geq \text{st}(\tilde{A}_{\ell-1}(W)). \quad (7.18)$$

Indeed, writing $r := \text{nr}(G_\ell)$, $s := \text{st}(\tilde{A}_{\ell-1}(W))$ and $\alpha := \alpha_\ell$, the inequality $r \geq (s + \alpha)/(1 + \alpha/r)$ is equivalent to $r(1 + \alpha/r) \geq s + \alpha$, i.e. $r + \alpha \geq s + \alpha$, hence $r \geq s$.

Summing over all blocks, it follows that whenever the sufficient condition (7.18) holds for every $\ell \in \mathcal{S}$, the quadratic model guarantees that the full mixed spectral update $W \mapsto W^{\text{Spec}}$ (spectral on \mathcal{S} , Euclidean elsewhere) achieves at least as much decrease as the full Euclidean update $W \mapsto W^{\text{GD}}$ (up to the common remainder term $R(\Delta W)$). This is precisely the same rule that emerged in our random-feature analysis: spectral updates are most advantageous on those blocks whose incoming core activations $\tilde{A}_{\ell-1}(W)$ have low stable rank while the corresponding gradients G_ℓ have large nuclear rank.

7.5 Extension: diagonal RMS-normalization weights

In the layered model, the blocks W_ℓ were arbitrary matrices, and the spectral step used the full polar factor of $\nabla_{W_\ell} \mathcal{L}(W)$. The RMS-normalization layers are more structured: their weights are diagonal, and in this case the spectral steepest-descent step reduces to a “signSGD”-type update on the RMSNorm weights, with a corresponding ℓ_1/ℓ_2 analogue of the nuclear-rank condition. We record this diagonal case here.

Each RMSNorm layer carries weights $\gamma \in \mathbf{R}^d$ and acts on a hidden state $X \in \mathbf{R}^{d \times n}$ as

$$\text{RMSNorm}_\gamma(X) = \text{Diag}(\gamma) \tilde{A}^{\text{rms}}(X), \quad A := \tilde{A}^{\text{rms}}(X) \in \mathbf{R}^{d \times n},$$

where $\tilde{A}^{\text{rms}}(X)$ is the parameter-free RMS-normalized activation. In our notation we write $\Gamma := \text{Diag}(\gamma)$ and regard it as a diagonal block with incoming activations A . A perturbation of the RMSNorm weights has the form $\Delta\Gamma = \text{Diag}(\delta\gamma)$ and appears in the same feature term $\|\Delta\Gamma A\|_F^2$ as any other block in the Hessian bound.

For diagonal $\Delta\Gamma$ we have

$$\|\Delta\Gamma A\|_F \leq \|\Delta\Gamma\|_F \|A\|_{\text{op}} = \|\delta\gamma\|_2 \|A\|_{\text{op}}, \quad \|\Delta\Gamma A\|_F \leq \|\Delta\Gamma\|_{\text{op}} \|A\|_F = \|\delta\gamma\|_\infty \|A\|_F.$$

Thus, at the level of the feature term, the RMSNorm block has the same two curvature constants as any matrix block,

$$L_{\text{rms}}^F(W) = C_F(W) \|A\|_{\text{op}}^2, \quad L_{\text{rms}}^{\text{op}}(W) = C_F(W) \|A\|_F^2,$$

and their ratio is

$$\frac{L_{\text{rms}}^{\text{op}}(W)}{L_{\text{rms}}^F(W)} = \frac{\|A\|_F^2}{\|A\|_{\text{op}}^2} = \text{st}(A).$$

Let $g := \nabla_\gamma \mathcal{L}(W) \in \mathbf{R}^d$ be the gradient with respect to the RMSNorm weights. At the level of matrix blocks, this corresponds to the diagonal matrix $G_{\text{diag}} := \text{Diag}(g)$, whose Frobenius and operator norms are

$$\|G_{\text{diag}}\|_F^2 = \|g\|_2^2, \quad \|G_{\text{diag}}\|_{\text{op}}^2 = \|g\|_\infty^2.$$

The analogue of the stable rank of the gradient in this diagonal setting is therefore

$$\text{st}_{\text{diag}}(g) := \frac{\|G_{\text{diag}}\|_F^2}{\|G_{\text{diag}}\|_{\text{op}}^2} = \frac{\|g\|_2^2}{\|g\|_\infty^2}.$$

For this diagonal block we can repeat exactly the one-step analysis from Section 7.4, now with the gradient represented by G_{diag} and curvature constants $L_{\text{rms}}^F(W)$ and $L_{\text{rms}}^{\text{op}}(W)$. In particular, in analogy with (7.14)–(7.15), we define blockwise step sizes

$$a_{\text{GD,rms}} := L_{\text{rms}}^F(W) + \frac{C_{\text{op}}(W)}{\text{st}_{\text{diag}}(g)}, \quad a_{\text{Spec,rms}} := L_{\text{rms}}^{\text{op}}(W) + C_{\text{op}}(W),$$

and consider the two updates

$$\gamma_{\text{GD}}^+ := \gamma - \frac{1}{a_{\text{GD,rms}}} g, \quad \gamma_{\text{Spec}}^+ := \gamma - \frac{\|g\|_1}{a_{\text{Spec,rms}}} \text{sign}(g).$$

For the Euclidean update, the same quadratic-model calculation as in (7.14) (with G_ℓ replaced by G_{diag} and L_ℓ^F by L_{rms}^F) gives the one-step bound

$$\Delta_{\text{GD,rms}} \geq \frac{\|g\|_2^2}{2(L_{\text{rms}}^F(W) + C_{\text{op}}(W)/\text{st}_{\text{diag}}(g))}.$$

For the spectral update, the same argument as in (7.15) (using that $\|\text{Diag}(\text{sign}(g))\|_{\text{op}} = 1$ and $\|\text{Diag}(\text{sign}(g))A\|_F \leq \|A\|_F$) yields

$$\Delta_{\text{Spec,rms}} \geq \frac{\|g\|_1^2}{2(L_{\text{rms}}^{\text{op}}(W) + C_{\text{op}}(W))}.$$

Thus, at the level of the quadratic model, the spectral update dominates the Euclidean update on this diagonal block whenever

$$\frac{\|g\|_1^2}{L_{\text{rms}}^{\text{op}}(W) + C_{\text{op}}(W)} \geq \frac{\|g\|_2^2}{L_{\text{rms}}^{\text{F}}(W) + C_{\text{op}}(W)/\text{st}_{\text{diag}}(g)}.$$

Using $L_{\text{rms}}^{\text{op}}/L_{\text{rms}}^{\text{F}} = \text{st}(A)$ and defining

$$s_A := \text{st}(A) = \frac{\|A\|_F^2}{\|A\|_{\text{op}}^2}, \quad \alpha_{\text{rms}} := \frac{C_{\text{op}}(W)}{L_{\text{rms}}^{\text{F}}(W)},$$

we can rewrite this condition exactly as in (7.16):

$$\frac{\|g\|_1^2}{\|g\|_2^2} \geq \frac{s_A + \alpha_{\text{rms}}}{1 + \alpha_{\text{rms}}/\text{st}_{\text{diag}}(g)}.$$

The right-hand side is increasing in $\text{st}_{\text{diag}}(g)$. On the other hand, for any nonzero g we have the scalar inequality

$$\frac{\|g\|_1^2}{\|g\|_2^2} \geq \frac{\|g\|_2^2}{\|g\|_{\infty}^2} = \text{st}_{\text{diag}}(g),$$

so it is sufficient to impose the stronger condition obtained by replacing $\text{st}_{\text{diag}}(g)$ in the denominator by $\|g\|_1^2/\|g\|_2^2$. This gives

$$\frac{\|g\|_1^2}{\|g\|_2^2} \geq \frac{s_A + \alpha_{\text{rms}}}{1 + \alpha_{\text{rms}}\|g\|_2^2/\|g\|_1^2}.$$

A short algebraic manipulation shows that this is equivalent to

$$\frac{\|g\|_1^2}{\|g\|_2^2} \geq s_A.$$

In other words, the ℓ_1/ℓ_2 ‘‘nuclear rank’’ of the RMSNorm gradient must exceed the (low) stable rank of the incoming RMS-normalized activation matrix A . This is the exact diagonal analogue of the matrix-level condition $\text{nr}(G_{\ell}) \geq \text{st}(\tilde{A}_{\ell-1}(W))$ from (7.18), with the role of $\text{nr}(G_{\ell})$ played by the scalar $\|g\|_1^2/\|g\|_2^2$ and the role of $\text{st}(A_{\ell-1})$ played by $\text{st}(A)$.

References

- [1] Jinho Baik, Gérard Ben Arous, and Sandrine Péché. Phase transition of the largest eigenvalue for nonnull complex sample covariance matrices. 2005.
- [2] Lucas Benigni and Sandrine Péché. Largest eigenvalues of the conjugate kernel of single-layered neural networks. *arXiv preprint arXiv:2201.04753*, 2022.
- [3] Jeremy Bernstein and Laker Newhouse. Old optimizer, new norm: An anthology. *arXiv preprint arXiv:2409.20325*, 2024.
- [4] Jeremy Bernstein and Laker Newhouse. Modular duality in deep learning. In *Proceedings of the 42nd International Conference on Machine Learning*, volume 267, pages 3920–3930. PMLR, 2025.

[5] Rajendra Bhatia. *Positive Definite Matrices*. Princeton University Press, Princeton, NJ, 2007. Thm. 1.4.1 (“Norm of the Schur product”) gives $\|S_A\| = \max_i a_{ii}$ when $A \succeq 0$; Sec. 1.2 states the Schur product theorem.

[6] Åke Björck and Gene H. Golub. Numerical methods for computing angles between linear subspaces. *Mathematics of Computation*, 27(123):579–594, 1973.

[7] Valentyn Boreiko, Zhiqi Bu, and Sheng Zha. Towards understanding orthogonalization in muon. In *Proceedings of the 42nd International Conference on Machine Learning*, volume 267 of *Proceedings of Machine Learning Research*, 2025.

[8] David Carlson, Volkan Cevher, and Lawrence Carin. Stochastic spectral descent for restricted boltzmann machines. In *International Conference on Artificial Intelligence and Statistics*, pages 111–119, 2015.

[9] David E Carlson, Edo Collins, Ya-Ping Hsieh, Lawrence Carin, and Volkan Cevher. Preconditioned spectral descent for deep learning. *Advances in neural information processing systems*, 28, 2015.

[10] David E. Carlson, Edward Collins, Cho-Jui Hsieh, Lawrence Carin, and Volkan Cevher. Preconditioned spectral descent for deep learning. In *Advances in Neural Information Processing Systems*, volume 28, 2015.

[11] Xiuyuan Cheng and Amit Singer. The spectrum of random inner-product kernel matrices. *Random Matrices: Theory and Applications*, 2(04):1350010, 2013.

[12] Youngmin Cho and Lawrence K. Saul. Kernel methods for deep learning. In *Advances in Neural Information Processing Systems 22 (NIPS 2009)*, 2009.

[13] Hadi Daneshmand, Jonas Kohler, Francis Bach, Thomas Hofmann, and Aurelien Lucchi. Batch normalization provably avoids ranks collapse for randomly initialised deep networks. *Advances in Neural Information Processing Systems*, 33:18387–18398, 2020.

[14] Amit Daniely, Roy Frostig, and Yoram Singer. Toward deeper understanding of neural networks: The power of initialization and a dual view on expressivity. In *Advances in Neural Information Processing Systems 29 (NIPS 2016)*, 2016.

[15] Chandler Davis and William Morton Kahan. The rotation of eigenvectors by a perturbation. iii. *SIAM Journal on Numerical Analysis*, 7(1):1–46, 1970.

[16] John Duchi, Elad Hazan, and Yoram Singer. Adaptive subgradient methods for online learning and stochastic optimization. *Journal of Machine Learning Research*, 12(61):2121–2159, 2011.

[17] Essential AI. Layer sharding for large-scale training with Muon. Blog post, May 2025. Available at <https://www.essential.ai/blog/infra>.

[18] Behrooz Ghorbani, Shankar Krishnan, and Ying Xiao. An investigation into neural net optimization via hessian eigenvalue density. In *Proceedings of the 36th International Conference on Machine Learning*, volume 97 of *Proceedings of Machine Learning Research*, pages 2232–2241. PMLR, 2019.

[19] Vineet Gupta, Tomer Koren, and Yoram Singer. Shampoo: Preconditioned stochastic tensor optimization. In *Proceedings of the 35th International Conference on Machine Learning (ICML)*, volume 80 of *Proceedings of Machine Learning Research*, pages 1842–1850, Stockholm, Sweden, 2018. PMLR.

[20] Guy Gur-Ari, Daniel A. Roberts, and Ethan Dyer. Gradient descent happens in a tiny subspace. *arXiv preprint arXiv:1812.04754*, 2018.

[21] Roger A. Horn and Charles R. Johnson. *Matrix Analysis*. Cambridge University Press, Cambridge, 2nd edition, 2013. See Sec. 5.6; in particular eq. (5.6.0.2) for $\|A\|_F^2 = \sum_i \sigma_i(A)^2$ and $\|A\|_{\text{op}} = \sigma_1(A)$.

[22] Daniel Hsu, Sham Kakade, and Tong Zhang. A tail inequality for quadratic forms of subgaussian random vectors. 2012.

[23] Daniel Hsu, Sham M. Kakade, and Tong Zhang. A tail inequality for quadratic forms of subgaussian random vectors. *Electronic Communications in Probability*, 17(52):1–6, 2012.

[24] Minyoung Huh, Hossein Mobahi, Richard Zhang, Brian Cheung, Pulkit Agrawal, and Phillip Isola. The low-rank simplicity bias in deep networks. *Transactions on Machine Learning Research*, 2023.

[25] Sergey Ioffe and Christian Szegedy. Batch normalization: Accelerating deep network training by reducing internal covariate shift. In *International conference on machine learning*, pages 448–456. pmlr, 2015.

[26] Iain M Johnstone. On the distribution of the largest eigenvalue in principal components analysis. *The Annals of statistics*, 29(2):295–327, 2001.

[27] Keller Jordan and collaborators. Modded-nanogpt (july 18 2025 snapshot). <https://github.com/KellerJordan/modded-nanogpt/tree/0d20074260664590e2a1686b9371936944a3ddff>, 2025. Commit 0d20074260664590e2a1686b9371936944a3ddff.

[28] Keller Jordan, Yuchen Jin, Vlado Boža, Jiacheng You, Franz Cesista, Laker Newhouse, and Jeremy Bernstein. Muon: An optimizer for hidden layers in neural networks. <https://kellerjordan.github.io/posts/muon/>, 2024.

[29] Noureddine El Karoui. The spectrum of kernel random matrices. *The Annals of Statistics*, pages 1–50, 2010.

[30] Jordan Keller, Larry Dial, and contributors. modded-nanogpt. <https://github.com/KellerJordan/modded-nanogpt>, 2025. GitHub repository, accessed 31 Oct 2025.

[31] Ahmed Khaled, Kaan Ozkara, Tao Yu, Mingyi Hong, and Youngsuk Park. Muonbp: Faster muon via block-periodic orthogonalization, 2025.

[32] Diederik P. Kingma and Jimmy Ba. Adam: A method for stochastic optimization. In *International Conference on Learning Representations (ICLR)*, 2015.

[33] Vladimir Koltchinskii and Karim Lounici. Concentration inequalities and moment bounds for sample covariance operators. *Bernoulli*, 23(1):110–133, 2017.

[34] Arun Kumar Kuchibhotla and Abhishek Chakrabortty. Moving beyond sub-gaussianity in high-dimensional statistics: Applications in covariance estimation and linear regression. *Information and Inference: A Journal of the IMA*, 11(4):1389–1456, 2022.

[35] Tim Large, Yang Liu, Minyoung Huh, Hyojin Bahng, Phillip Isola, and Jeremy Bernstein. Scalable optimization in the modular norm. In *Advances in Neural Information Processing Systems*, 2024. arXiv:2405.14813.

[36] Béatrice Laurent and Pascal Massart. Adaptive estimation of a quadratic functional by model selection. *Annals of Statistics*, 28(5):1302–1338, 2000.

[37] Michel Ledoux and Michel Talagrand. *Probability in Banach Spaces: isoperimetry and processes*. Springer Science & Business Media, 2013.

[38] James Martens and Roger Grosse. Optimizing neural networks with kronecker-factored approximate curvature. In *Proceedings of the 32nd International Conference on Machine Learning (ICML)*, volume 37 of *Proceedings of Machine Learning Research*, pages 2408–2417, Lille, France, Jul 2015. PMLR.

[39] Ryan O’Donnell. *Analysis of Boolean Functions*. Cambridge University Press, 2014.

[40] Vardan Papyan. The full spectrum of deepnet Hessians at scale: Dynamics with sgd training and sample size. *arXiv preprint arXiv:1811.07062*, 2018.

[41] Jeffrey Pennington and Pratik Worah. Nonlinear random matrix theory for deep learning. *Advances in neural information processing systems*, 30, 2017.

[42] Thomas Pethick, Weijia Xie, Konstantinos Antonakopoulos, Zhenyu Zhu, Alberto Silveti-Falls, and Volkan Cevher. Training deep learning models with norm-constrained LMOs. *arXiv preprint arXiv:2502.07529*, 2025.

[43] Ali Rahimi and Benjamin Recht. Random features for large-scale kernel machines. In *Advances in Neural Information Processing Systems 20 (NIPS 2007)*, 2007.

[44] Ali Rahimi and Benjamin Recht. Weighted sums of random kitchen sinks: Replacing minimization with randomization in learning. In *Advances in Neural Information Processing Systems 21 (NIPS 2008)*, 2008.

[45] Alessandro Rudi and Lorenzo Rosasco. Generalization properties of learning with random features. In *Advances in Neural Information Processing Systems 30 (NIPS 2017)*, 2017.

[46] Levent Sagun, Léon Bottou, and Yann LeCun. Eigenvalues of the hessian in deep learning: Singularity and beyond. *arXiv preprint arXiv:1611.07476*, 2016.

[47] Wei Shen, Ruichuan Huang, Minhui Huang, Cong Shen, and Jiawei Zhang. On the convergence analysis of muon. *CoRR*, abs/2505.23737, 2025.

[48] Rishi Sonthalia, Michael Murray, and Guido Montúfar. Low rank gradients and where to find them. *arXiv preprint arXiv:2510.01303*, 2025.

[49] Nikhil Srivastava and Roman Vershynin. Covariance estimation for distributions with $2 + \varepsilon$ moments. *Annals of Probability*, 41(5):3081–3111, 2013.

- [50] Robert C Thompson. The behavior of eigenvalues and singular values under perturbations of restricted rank. *Linear Algebra and its Applications*, 13(1-2):69–78, 1976.
- [51] Tijmen Tieleman and Geoffrey Hinton. Lecture 6.5—rmsprop: Divide the gradient by a running average of its recent magnitude. Coursera: Neural Networks for Machine Learning, 2012. Lecture slides.
- [52] Joel A. Tropp. User-friendly tail bounds for sums of random matrices. *Foundations of Computational Mathematics*, 12(4):389–434, 2012.
- [53] Roman Vershynin. Introduction to the non-asymptotic analysis of random matrices. *arXiv preprint arXiv:1011.3027*, 2010.
- [54] Roman Vershynin. How close is the sample covariance matrix to the actual covariance matrix? *Journal of Theoretical Probability*, 25(3):655–686, 2012.
- [55] Roman Vershynin. *High-dimensional probability: An introduction with applications in data science*, volume 47. Cambridge university press, 2018.
- [56] Shuche Wang, Fengzhuo Zhang, Jiaxiang Li, Cunxiao Du, Chao Du, Tianyu Pang, Zhuoran Yang, Mingyi Hong, and Vincent YF Tan. Muon outperforms adam in tail-end associative memory learning. *arXiv preprint arXiv:2509.26030*, 2025.
- [57] Zhichao Wang, Denny Wu, and Zhou Fan. Nonlinear spiked covariance matrices and signal propagation in deep neural networks. In *The Thirty Seventh Annual Conference on Learning Theory*, pages 4891–4957. PMLR, 2024.
- [58] Per-Åke Wedin. Perturbation bounds in connection with singular value decomposition. *BIT Numerical Mathematics*, 12(1):99–111, 1972.
- [59] Yi Yu, Tengyao Wang, and Richard J. Samworth. A useful variant of the davis–kahan theorem for statisticians. *Biometrika*, 102(2):315–323, 2015.
- [60] Jiawei Zhao, Zhenyu Zhang, Beidi Chen, Zhangyang Wang, Anima Anandkumar, and Yuan-dong Tian. GaLore: Memory-efficient LLM training by gradient low-rank projection. In *International Conference on Learning Representations*, 2024.

A Sparse Regression and SwiGLU activations

We now return to the sparse regression setup of Figure 1 and replace the squared-ReLU activation by SwiGLU. The architecture and target remain unchanged: we train a four-layer feedforward network on the cubic $f(x) = x_1 x_2 x_3$ from Gaussian inputs using full-batch GD and SpecGD, applying spectral updates only to the hidden layers as in Section 1.2.1. Our aim is to examine how the change in activation affects the stable rank of the post-activations and, in turn, the relative behavior of Euclidean and spectral updates.

Figure 19 reports the stable rank of the post-activation matrices at initialization as a function of batch size. In contrast with the ReLU and squared-ReLU experiments, the stable ranks now grow noticeably with the batch size, reflecting the fact that SwiGLU is approximately centered and therefore does not induce a large mean spike in the hidden-layer Gram matrices.

To see how this change in stable rank interacts with training dynamics, Figure 20 compares the training loss of GD and SpecGD for two batch sizes. For the smaller batch ($n = 512$, left panel), the network is still in a mildly low-stable-rank regime and SpecGD enjoys a visible early advantage, much as in the ReLU case. For the larger batch ($n = 8196$, right panel), the initialization stable ranks of the hidden layers are substantially higher, and the performance of GD and SpecGD becomes similar. As the batch size grows, the inequality $\text{nr}(\nabla \mathcal{L}(W_\ell)) \gtrsim \text{st}(A_{\ell-1})$ is no longer strongly activated, and the structural advantage of spectral updates predicted in Section 1.2 is correspondingly reduced.

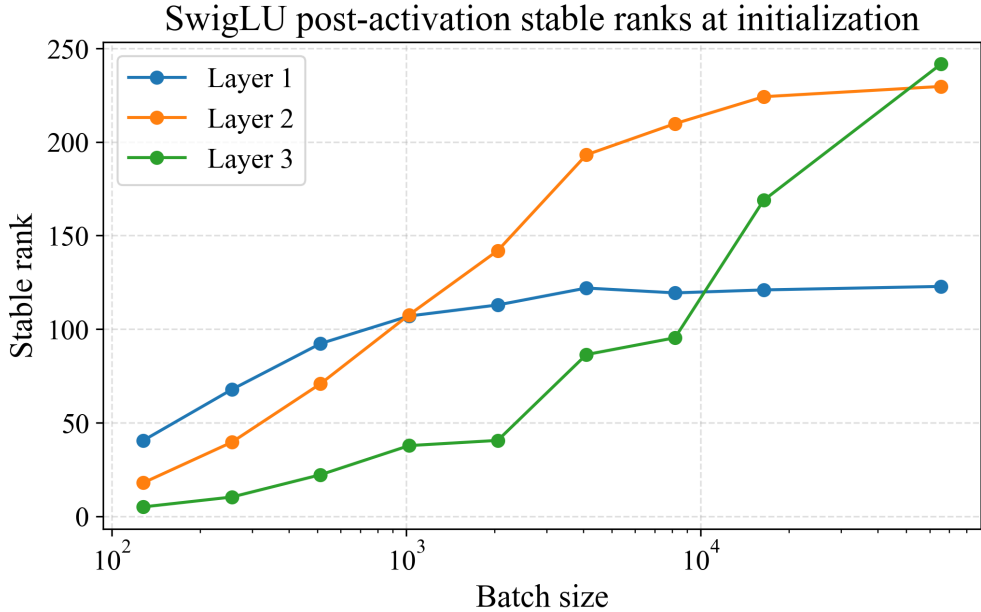


Figure 19: Stable rank at initialization of the post-activation matrices in the sparse regression network with SwiGLU activations, as a function of batch size. For small batches the hidden layers remain only moderately high-stable-rank, but as the batch size increases the stable ranks grow toward their ambient dimension, in contrast with the ReLU and squared-ReLU experiments where the mean-induced spike keeps $\text{st}(A_\ell)$ essentially constant.

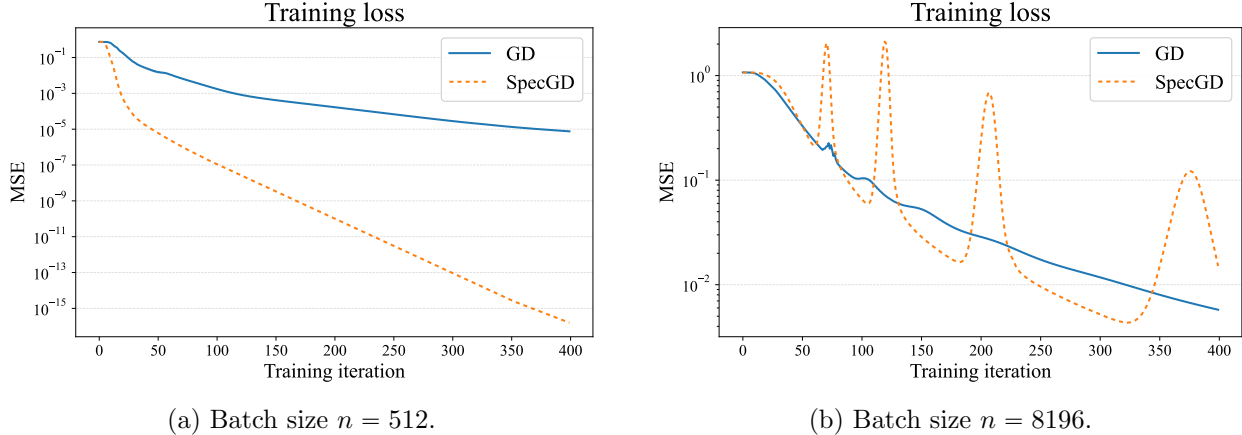


Figure 20: Sparse regression with SwiGLU activations: training loss for gradient descent (GD) and spectral gradient descent (SpecGD) at two batch sizes. For $n = 512$ (left) the methods behave similarly to the ReLU experiment, with SpecGD exhibiting a faster initial decrease in loss. For $n = 8196$ (right), where the initialization stable ranks of the hidden layers are much larger (Figure 19), the trajectories of GD and SpecGD essentially coincide. In both runs, the stable ranks of the first two hidden layers remain close to their initialization values, while the third layer drops rapidly to stable rank ≈ 3 ; this drop occurs in the final scalar-output layer, where the weights form a vector and no spectral update is applied in SpecGD.

B NanoGPT with SwiGLU activations

We repeat the NanoGPT-scale run from Figures 2–9, but replace the squared-ReLU MLP non-linearity by SwiGLU. The figures below report the same stable-rank and gradient nuclear-rank diagnostics, and are meant as direct pointwise analogues of the corresponding modded-NanoGPT plots in the main text.

C Trace and operator-norm bounds for the sample second moment under sub-Gaussian tails

In this section, we derive a few basic deviation inequalities between the operator/Frobenius norms of the sample and population second-moment matrices. There is a rich literature on bounds of this type, notably [23, 33, 36, 49, 52, 54]. Our notation will closely follow the text [55]. In particular, $\|\cdot\|_{\psi_2}$ will denote the sub-Gaussian norm, while the sub-exponential norm will be denoted by $\|\cdot\|_{\psi_1}$. More generally, the quasinorm $\|z\|_{\psi_\theta}$ for any $\theta > 0$ is the infimum over all constants $K > 0$ satisfying $\mathbb{E} \exp(|z|/K)^\theta \leq 2$.

Theorem C.1 (Trace bound). *Consider a sequence of random vectors $z_1, \dots, z_n \in \mathbf{R}^d$ and define $S := \sum_{i=1}^n z_i z_i^\top$. Suppose that for each $i \in [n]$, there exists $K_i < \infty$ satisfying*

$$\|\langle z_i, u \rangle\|_{\psi_2}^2 \leq K_i^2 \mathbb{E} \langle z_i, u \rangle^2 \quad \forall u \in \mathbf{R}^d. \quad (\text{C.1})$$

Then there exists a constant $c < \infty$ such that for any $\varepsilon \geq 0$, the estimate $|\text{tr}(S) - \text{tr}(\mathbb{E}S)| \leq \varepsilon \text{tr}(\mathbb{E}S)$ holds with probability at least $1 - 2 \exp \left(-c \left(\frac{\varepsilon^2 \text{tr}(S)^2}{\sum_{i=1}^n (K_i^2 \text{tr}(M_i))^2} \wedge \frac{\varepsilon \text{tr}(S)}{\max_{i=1,\dots,n} K_i^2 \text{tr}(M_i)} \right) \right)$.

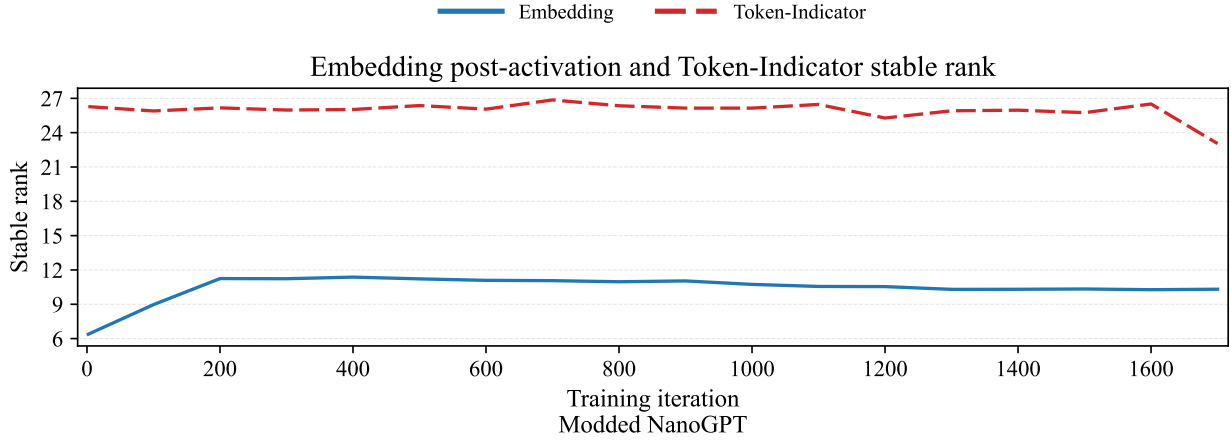


Figure 21: Embedding post-activation and token-indicator stable ranks in the SwiGLU run. This is the SwiGLU analogue of Figure 10. As expected, these curves are essentially unchanged by the MLP activation swap: the token-indicator stable rank stays near $1/p_{\max}$ (here ≈ 26), and the embedding stable rank remains ≈ 10 throughout training.

Proof. Set $\mu_i = \mathbb{E}z_i$ and write $z_i = \mu_i + \tilde{z}_i$ with \tilde{z}_i i.i.d., mean zero. Then we can write:

$$\text{tr}(S) - \text{tr}(\mathbb{E}S) = \sum_{i=1}^n (\|z_i\|_2^2 - \mathbb{E}\|z_i\|_2^2) = 2 \underbrace{\sum_{i=1}^n \langle \tilde{z}_i, \mu_i \rangle}_{=: A_n} + \underbrace{\sum_{i=1}^n (\|\tilde{z}_i\|_2^2 - \mathbb{E}\|\tilde{z}_i\|_2^2)}_{=: B_n}.$$

We bound A_n and B_n in order. First, by (C.1), $\langle \tilde{z}_i, \mu_i \rangle$ is sub-Gaussian with $\|\langle \tilde{z}_i, \mu_i \rangle\|_{\psi_2}^2 \leq K_i^2 \mu_i^\top M_i \mu_i \leq K_i^2 \|M_i\|_{\text{op}} \|\mu_i\|_2^2 \leq K_i^2 \|M_i\|_{\text{op}}^2$, where we set $M_i := \mathbb{E}z_i z_i^\top$. Therefore, Hoeffding inequality [55, Theorem 2.2.1], implies that for all $u > 0$, the estimate $A_n \leq \frac{1}{4}u \text{tr}(S)$, holds with probability at least $1 - 2 \exp\left(-c\left(\frac{t^2 \text{tr}(S)^2}{\sum_{i=1}^n K_i^2 \|M_i\|_{\text{op}}^2}\right)\right)$.

Next applying (C.1) with $u = e_j$ we see that the j 'th coordinate of \tilde{z}_i is $K_i(M_i)_{jj}^{1/2}$ sub-Gaussian, and therefore its square is $K_i^2(M_i)_{jj}$ sub-exponential [55, Lemma 2.8.5]. Therefore by the triangle inequality, $\|\tilde{z}_i\|_2^2$ is sub-exponential with parameter $K_i^2 \text{tr}(M_i)$. Applying Bernstein's inequality [55, Theorem 2.9.1], we deduce that for any $u \geq 0$ the estimate $|B_n| \leq u \text{tr}(S)$ holds with probability at least $1 - 2 \exp\left(-c\left(\frac{u^2 \text{tr}(S)^2}{\sum_{i=1}^n (K_i^2 \text{tr}(M_i))^2} \wedge \frac{u \text{tr}(S)}{\max_{i=1,\dots,n} K_i^2 \text{tr}(M_i)}\right)\right)$, thus completing the proof. \square

Theorem C.2 (Lower tail for the operator norm for non-iid data). *Let $g_1, \dots, g_n \in \mathbb{R}^d$ be independent random vectors and define*

$$M_i := \mathbb{E}[g_i g_i^\top], \quad S := \sum_{i=1}^n g_i g_i^\top, \quad M := \mathbb{E}S = \sum_{i=1}^n M_i.$$

Assume there exist $K_i \geq 1$ such that for every $u \in \mathbb{R}^d$, we have

$$\|\langle u, g_i \rangle\|_{\psi_2} \leq K_i \sqrt{u^\top M_i u}, \quad i = 1, \dots, n, \quad (\text{C.2})$$

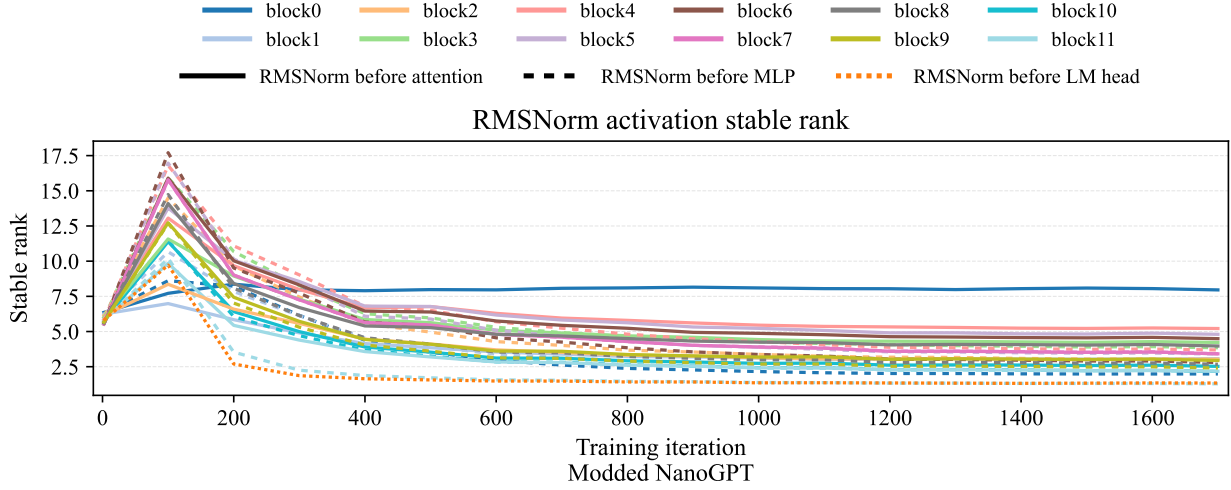


Figure 22: Stable rank of RMS-normalized activations A^{rms} , A^{mlp} , A^{final} in the SwiGLU run. This is the SwiGLU analogue of Figure 6. The RMS features remain low-stable-rank (typically single digits after burn-in), but their stable ranks are systematically larger than in the squared-ReLU run, with a more pronounced early transient before settling.

Then there exists an absolute constant $c > 0$ such that for any $\varepsilon \in (0, 1)$, we have

$$\mathbb{P}(\|S\|_{\text{op}} \leq (1 - \varepsilon)\|M\|_{\text{op}}) \leq \exp\left(-c \min\left\{\frac{\varepsilon^2 \|M\|_{\text{op}}^2}{\sum_{i=1}^n K_i^4 \|M_i\|_{\text{op}}^2}, \frac{\varepsilon \|M\|_{\text{op}}}{\max_{1 \leq i \leq n} K_i^2 \|M_i\|_{\text{op}}}\right\}\right). \quad (\text{C.3})$$

Proof. Let $v \in \mathbb{R}^d$ be a unit eigenvector of M associated with $\|M\|_{\text{op}}$ and set

$$a_i := v^\top M_i v = \mathbb{E}(v^\top g_i)^2.$$

Clearly, we have $\|S\|_{\text{op}} \geq v^\top S v = \sum_{i=1}^n (v^\top g_i)^2$. The sub-Gaussian assumption (C.2) shows

$$\|\langle v, g_i \rangle^2 - \mathbb{E}\langle v, g_i \rangle^2\|_{\psi_1} \lesssim \|\langle v, g_i \rangle^2\|_{\psi_1} \asymp \|\langle v, g_i \rangle\|_{\psi_2}^2 = K_i^2 a_i,$$

where the first inequality follows from [55, Exercise 2.44] while the first equality follows from [55, Lemma 2.8.5]. Applying the Bernstein inequality [55, Theorem 2.9.1] gives the estimate

$$\mathbb{P}\left\{\sum_{t=1}^n ((v^\top g_i)^2 - \mathbb{E}(v^\top g_i)^2) \leq -s\right\} \leq \exp\left(-c \min\left\{\frac{s^2}{\sum_{t=1}^n (K_i^2 a_i)^2}, \frac{s}{\max_i (K_i^2 a_i)}\right\}\right),$$

for all $s \geq 0$, with an absolute constant $c > 0$. Setting $s = \varepsilon \|M\|_{\text{op}}$ completes the proof of (C.3). \square

Lemma C.3 (Lower-bounding the operator norm). *Let $v_1, \dots, v_n \in \mathbb{R}^d$ be independent realizations of a random vector v in \mathbb{R}^d and suppose that for some values $K, \theta < \infty$ the estimate holds:*

$$\|\langle v - \mathbb{E}v, u \rangle\|_{\psi_\theta} \leq K \|u\|_2 \quad \forall u \in \mathbb{R}^d.$$

Define the sum $S = \sum_{i=1}^n v_i v_i^\top$. Let $V \in \mathbb{R}^{n \times d}$ be a matrix whose rows are v_1, \dots, v_n and define the second-moment matrix $M := \mathbb{E}vv^\top$. Then there exists a numerical constant c that depends only on θ such that for any $\varepsilon \in (0, 1)$ the estimate $\|S\|_{\text{op}} \geq (1 - \varepsilon)\|\mathbb{E}S\|_{\text{op}}$ holds with probability at least

$$1 - 2 \exp\left(-c \left(\frac{n\varepsilon^2 \|M\|_{\text{op}}^2}{K^4} \wedge n^{1 \wedge \frac{\theta}{2}} \left(\frac{\varepsilon \|M\|_{\text{op}}}{K^2}\right)^{\theta/2}\right)\right) - 2 \exp\left(-c \left(\frac{n\varepsilon^2 \|M\|_{\text{op}}}{K^2} \wedge n^{1 \wedge \theta} \left(\frac{\varepsilon \sqrt{\|M\|_{\text{op}}}}{K}\right)^\theta\right)\right).$$

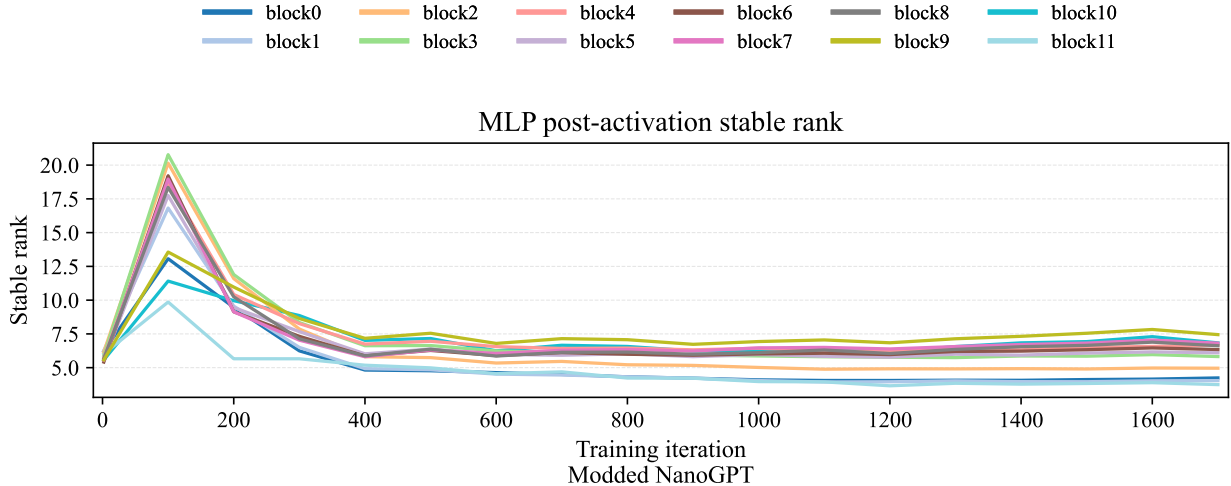


Figure 23: Stable rank of MLP post-activations in the SwiGLU run. This is the SwiGLU analogue of Figure 2 (modded-NanoGPT with squared ReLU). The maximal possible stable rank is 3072, and the observed values remain far below this ceiling throughout training. Compared to Figure 2, the post-activation stable ranks are noticeably larger (typically $\approx 5\text{--}8$ after burn-in, versus $\approx 2\text{--}3$ in the squared-ReLU run), consistent with the absence of a large mean-induced spike under SwiGLU.

Proof. Let $V \in \mathbf{R}^{n \times d}$ be a matrix whose rows are v_1, \dots, v_n and define the second-moment matrix $M := \mathbb{E}vv^\top$. Define the matrix $M_n = \frac{1}{n}V^\top V$ and note $\mathbb{E}[M_n] = M$. Fix a unit length vector $u \in \mathbf{R}^d$ satisfying

$$\|M\|_{\text{op}} = u^\top Mu = \mathbb{E}\langle v, u \rangle^2.$$

Define now $\mu := \mathbb{E}v$ and $z_i := \langle v_i - \mu, u \rangle$. We may then write

$$\begin{aligned} \frac{1}{n}\|V^\top V\|_{\text{op}} &\geq \frac{1}{n}u^\top V^\top Vu = \frac{1}{n}\|Vu\|_2^2 = \frac{1}{n}\sum_{i=1}^n \langle v_i, u \rangle^2 \\ &= \frac{1}{n}\sum_{i=1}^n (z_i^2 - \mathbb{E}z_i^2) + 2\langle \mu, u \rangle \cdot \frac{1}{n}\sum_{i=1}^n z_i + \|M\|_{\text{op}}, \end{aligned} \quad (\text{C.4})$$

where the last equality follows from algebraic manipulations. We now bound the first two terms on the right side of (C.4). Using basic properties of Orlitz quasi-norms we have

$$\|z_i^2 - \mathbb{E}z_i^2\|_{\psi_{\theta/2}} \lesssim \|z_i^2\|_{\psi_{\theta/2}} \asymp \|z_i\|_{\psi_\theta}^2 \leq K^2.$$

Therefore Bernstein's inequality [34, Theorem 3.1] yields for any $t \geq 0$ the estimate:

$$\mathbb{P}\left(\left|\frac{1}{n}\sum_{i=1}^n z_i^2 - \mathbb{E}z_i^2\right| \geq t\right) \leq 2 \exp\left(-c\left(n\frac{t^2}{K^4} \wedge n^{1 \wedge \frac{\theta}{2}}\left(\frac{t}{K^2}\right)^{\theta/2}\right)\right).$$

Another application of Bernstein's inequality [34, Theorem 3.1] implies for any $s \geq 0$ the estimate

$$\mathbb{P}\left(\left|\frac{1}{n}\sum_{i=1}^n z_i\right| \geq s\right) \leq 2 \exp\left(-c\left(\frac{ns^2}{K^2} \wedge n^{1 \wedge \theta}\left(\frac{s}{K}\right)^\theta\right)\right).$$

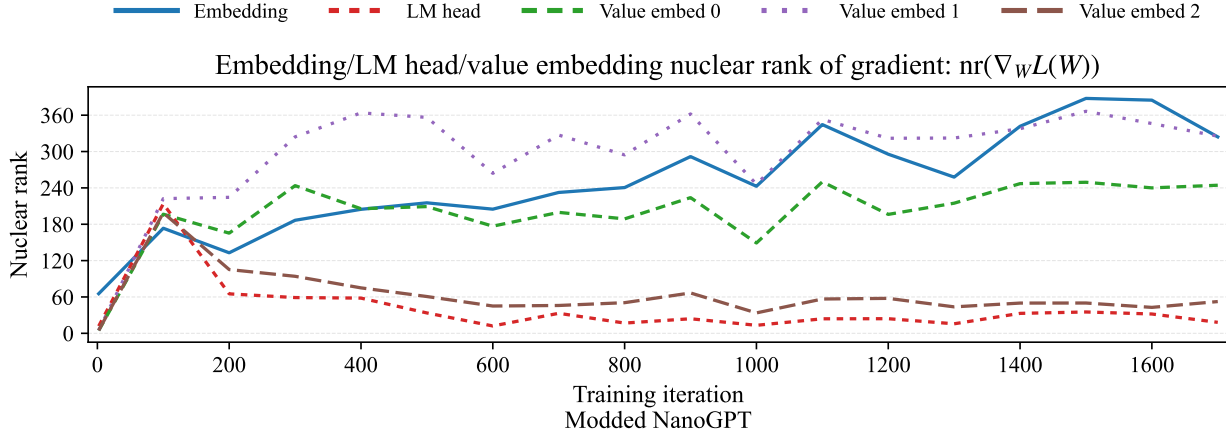


Figure 24: Gradient nuclear ranks for the token embedding and language-model head parameters in the SwiGLU run, together with the value-embedding parameters tracked by the same logging code. This is the SwiGLU analogue of Figure 7. The embedding gradient nuclear rank grows to the hundreds while the LM-head nuclear rank remains in the tens after burn-in; unlike the squared-ReLU run, the LM-head curve exhibits a larger early transient before relaxing.

Note moreover that we may write the second moment as $M = \mu\mu^\top + \text{Cov}(v)$ and therefore $|\langle \mu, u \rangle| \leq \|\mu\|_2 \leq \sqrt{\|M\|_{\text{op}}}$. Thus setting $s := \frac{\varepsilon\sqrt{\|M\|_{\text{op}}}}{4}$ and $t := \frac{\varepsilon}{2}\|M\|_{\text{op}}$ and taking a union bound over the two events we deduce that the lower bound $\frac{1}{n}\|V^\top V\|_{\text{op}} \geq (1 - \varepsilon)\|M\|_{\text{op}}$ with probability at least

$$1 - 2 \exp \left(-c \left(\frac{n\varepsilon^2\|M\|_{\text{op}}^2}{K^4} \wedge n^{1 \wedge \frac{\theta}{2}} \left(\frac{\varepsilon\|M\|_{\text{op}}}{K^2} \right)^{\theta/2} \right) \right) - 2 \exp \left(-c \left(\frac{n\varepsilon^2\|M\|_{\text{op}}}{K^2} \wedge n^{1 \wedge \theta} \left(\frac{\varepsilon\sqrt{\|M\|_{\text{op}}}}{K} \right)^\theta \right) \right),$$

which completes the proof. \square

D Auxiliary linear algebraic results.

Lemma D.1 (Minimal singular value of blocked matrices). *Let $a \in \mathbf{R}$, let $z \in \mathbf{R}^p$, and let $D \in \mathbf{R}^{(q-1) \times p}$ with $q-1 \leq p$. Define*

$$M := \begin{bmatrix} a & z^\top \\ 0 & D \end{bmatrix} \in \mathbf{R}^{q \times (p+1)}.$$

Then assuming $a \neq 0$, we have $\sigma_q(M) \geq \frac{\min\{|a|, \sigma_{q-1}(D)\}}{1 + \|z\|_2/|a|}$.

Proof. We may write $M = AN$, where

$$A = \begin{bmatrix} a & 0 \\ 0 & D \end{bmatrix}, \quad N = \begin{bmatrix} 1 & a^{-1}z^\top \\ 0 & I_p \end{bmatrix}.$$

Clearly we have

$$\sigma_q(M) \geq \sigma_q(A) \sigma_q(N). \quad (\text{D.1})$$

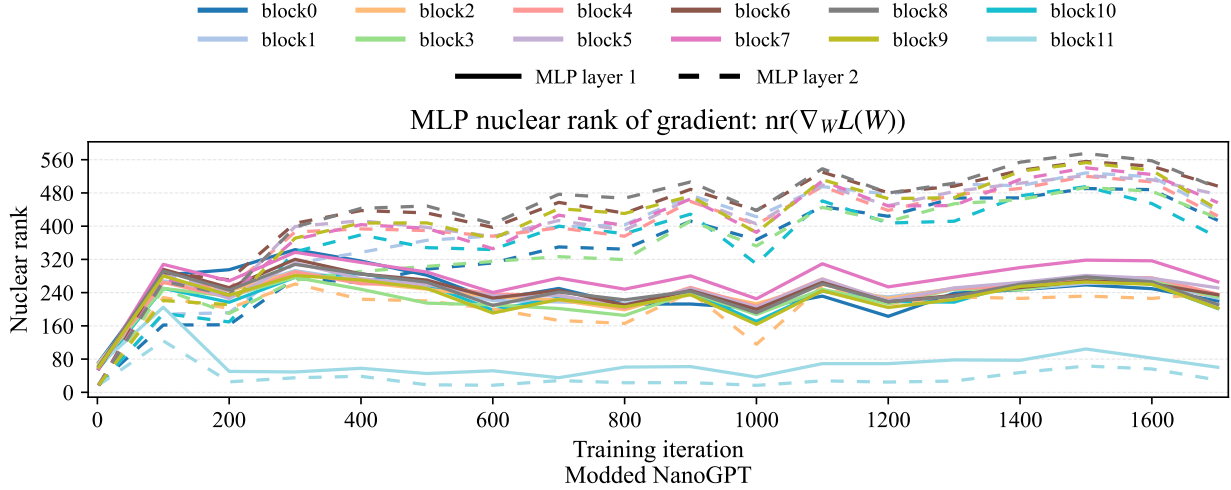


Figure 25: MLP gradient nuclear ranks in the SwiGLU run (solid: W_1 ; dashed: W_2). This is the SwiGLU analogue of Figure 5. As in the squared-ReLU run, nuclear ranks for the MLP gradients remain large (hundreds) throughout training, with the W_2 blocks typically larger than the W_1 blocks.

Because A is block diagonal, we have

$$\sigma_q(A) = \min\{|a|, \sigma_{q-1}(D)\}. \quad (\text{D.2})$$

The matrix N is invertible with

$$N^{-1} = \begin{bmatrix} 1 & -a^{-1}z^\top \\ 0 & I_p \end{bmatrix} = I_{p+1} + E, \quad \text{where we set} \quad E := \begin{bmatrix} 0 & -a^{-1}z^\top \\ 0 & 0 \end{bmatrix}.$$

Hence $\|N^{-1}\|_{\text{op}} \leq 1 + \frac{\|z\|_2}{|a|}$ and therefore $\sigma_q(N) = \|N^{-1}\|_{\text{op}}^{-1} \geq \frac{1}{1 + \|z\|_2/|a|}$. Substituting (D.2) and this bound for $\sigma_q(N)$ into (D.1) yields the claimed result. \square

Lemma D.2 (Lower bound on the nuclear rank). *Consider a matrix $M \in \mathbf{R}^{m \times d}$ and a vector $v \in \mathbf{R}^d$. Then for any subset $P \subset [d]$ the estimate holds:*

$$\|M \text{Diag}(v)\|_* \geq \left(\min_{i \in P} |v_i| \right) \cdot \|M_P\|_*,$$

where $M_P \in \mathbf{R}^{m \times |P|}$ is the submatrix of M formed by columns indexed by P .

Proof. Let $e_P \in \mathbf{R}^d$ denote the vector with ones in all coordinates indexed by P and zeros elsewhere and set $q := \min_{i \in P} |v_i|$. Then observe

$$M \text{Diag}(v) \text{Diag}(v)^\top M^\top \geq q^2 \cdot M e_P e_P^\top M^\top = q^2 \cdot M_P M_P^\top.$$

Taking matrix square roots of both sides and taking the trace completes the proof. \square

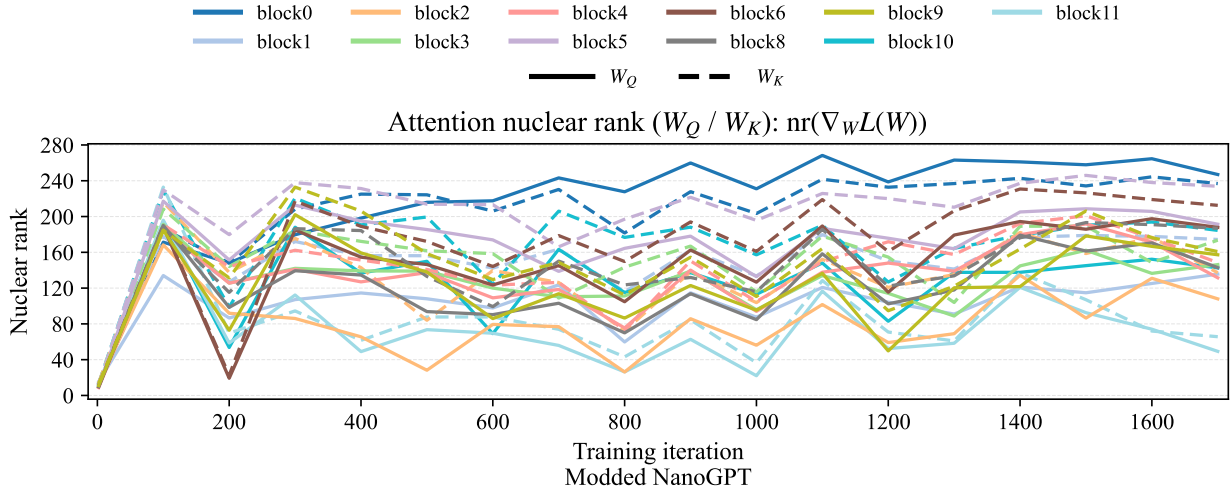


Figure 26: Gradient nuclear ranks for the attention parameters W_Q, W_K in the SwiGLU run. This is the SwiGLU analogue of Figure 8. Many of the nuclear ranks remain in the hundreds across blocks with modest variation over training.

E Shardwise SpecGD and distributed orthogonalization

Large training runs typically store parameters, gradients, and optimizer states *sharded across devices*. For a single matrix-shaped tensor, this means the gradient (or EMA gradient) matrix $G \in \mathbf{R}^{P \times Q}$ is available only as S disjoint shards across a device group. SpecGD-style updates orthogonalize G by applying a polar-factor map; the systems question is how to implement this orthogonalization when G is sharded. Any method that targets the *global* polar factor must move information across devices in order to realize the requisite matrix products (e.g. to form GG^\top and apply a polynomial in GG^\top to G), even if no device ever materializes the full matrix.

There are several standard ways to organize this global computation (all-gather, distributed matmuls inside the Newton–Schulz loop, or resharding along a batch-like axis such as layers). This section focuses on an *alternative strategy*: instead of computing the global polar factor, one can apply the same polar-factor map independently to each local shard. Variants of this strategy under, e.g., tensor parallelism appear in [7, 31]. When the sharding splits the dimension that governs the Newton–Schulz cost, this shardwise option has two immediate quantitative features: (i) it introduces no *incremental* optimizer communication, and (ii) it reduces the *per-device* orthogonalization work by a factor S relative to any method that computes a global polar factor with ideal $1/S$ parallel scaling. The quadratic model at the end of the section makes this locality explicit by identifying a blockwise polar step as the exact minimizer of a block-separable upper model. Before turning to that calculation, we briefly fix the minimal distributed vocabulary used in the cost comparison (shards and the two standard reshuffling primitives) and recall why Newton–Schulz governs the arithmetic cost.

Communication primitives and sharded matrices. Assume $G \in \mathbf{R}^{P \times Q}$ is sharded across S devices. For concreteness, consider row-sharding: each device $s \in [S]$ stores a disjoint block of rows $G^{(s)} \in \mathbf{R}^{(P/S) \times Q}$, and $\{G^{(s)}\}_{s \in [S]}$ partitions G . Two group-wide communication primitives recur below:

- an *all-gather* broadcasts shards so that every device can access all of the distributed data

(often materializing it locally);

- an *all-to-all* permutes shards so that each device ends with a different slice (a *resharding*).

Any group-wide operation of this type is called a *collective*. When we say *incremental optimizer communication*, we mean collectives that are introduced solely to implement the orthogonalization step, beyond whatever communication the baseline training step already requires.

Why Newton–Schulz enters and what it costs. For a matrix M , write $\text{polar}(M)$ for the polar factor (equivalently, UV^\top when $M = U\Sigma V^\top$ is an SVD). Muon applies (or approximates) $\text{polar}(G)$ to a gradient- or momentum-like matrix G [28]. A standard practical route computes $\text{polar}(G)$ via an inverse square root of a Gram matrix, e.g. $\text{polar}(G) = (GG^\top)^{-1/2}G$ when $Q \geq P$, and approximates $(GG^\top)^{-1/2}$ with a fixed small number of Newton–Schulz iterations using only matrix multiplications and additions [17, 28]. In the regime $Q \geq P$, each iteration is dominated by multiplying a $P \times P$ matrix by a $P \times Q$ matrix, so the per-iteration arithmetic cost is on the order of $\Theta(P^2Q)$ flops (up to constant factors and the fixed iteration count).

Three ways to orthogonalize a sharded matrix (global) and their costs. When G is row-sharded across S devices, there are three natural ways to obtain the *global* polar factor $\text{polar}(G)$:

1. All-gather then orthogonalize locally. Perform an all-gather so every device can access (and typically materialize) G , then compute $\text{polar}(G)$ independently on each device. This uses one collective, but it duplicates the full $\Theta(P^2Q)$ orthogonalization work across all S devices.
2. Keep G sharded and distribute the Newton–Schulz algebra. Keep G row-sharded and implement the Newton–Schulz multiplications as distributed matmuls. This avoids duplicating compute, but the loop requires repeated synchronization of intermediate results across devices. Concretely, each Newton–Schulz iteration induces one or more collectives, so the communication cost scales with the iteration count.
3. Reshard to make the orthogonalization local, then reshards back. If there is an additional batch-like axis indexing many independent matrices (e.g. the layer axis in a deep network), one can temporarily reshards so that each device holds full $P \times Q$ matrices for a subset of that axis, orthogonalize locally, then all-to-all back [17]. This yields a fixed number of reshuffles (two all-to-alls), rather than one collective per Newton–Schulz iteration.

How sharding arises in large-scale training. Sharding of a single matrix-shaped tensor typically reduces to a partition of its rows and/or columns:

- *Tensor parallelism (TP)* splits matrix multiplications across devices; weights are commonly sharded by rows or columns.
- *Fully-sharded data parallelism (FSDP/ZeRO)* shards parameters and optimizer states across data-parallel ranks; for matrix-shaped tensors this again induces a row/column partition after flattening/packing.
- *Pipeline parallelism (PP)* partitions layers across devices; this creates a layer index that can act as the batch-like axis exploited by the resharding strategy above.
- *Expert parallelism (EP)* in MoE models partitions experts across devices; within any single expert matrix, the effective sharding is still row/column.

In what follows we treat the sharding as a partition of matrix coordinates, and we emphasize row/column partitions since they are the canonical sharding patterns for a single matrix.

Shardwise SpecGD: orthogonalize only the local shard. As an alternative to the global strategies above, one can define a *shardwise* direction by applying the same polar-factor map to each local shard:

$$\widetilde{\text{polar}}(G) := \begin{bmatrix} \text{polar}(G^{(1)}) \\ \vdots \\ \text{polar}(G^{(S)}) \end{bmatrix}.$$

This introduces *no incremental optimizer communication*: each device computes $\text{polar}(G^{(s)})$ from its locally stored shard. If $Q \geq P$ and the sharding splits the contracted dimension P (as in row-sharding above), then the Newton–Schulz work is also reduced. A global orthogonalization has cost $\Theta(P^2Q)$ in total and hence $\Theta(P^2Q/S)$ per device under ideal $1/S$ scaling. In contrast, shardwise orthogonalization costs

$$\Theta((P/S)^2Q) = \Theta(P^2Q/S^2) \quad \text{per device,}$$

which is a factor- S reduction in per-device orthogonalization flops relative to any globally orthogonalizing method with ideal $1/S$ scaling. The tradeoff is structural: $\widetilde{\text{polar}}(G)$ enforces orthogonality only *within* each shard and does not coincide with $\text{polar}(G)$.

Summary of incremental cost (row-sharded G). Let $|G|$ denote the number of matrix entries (so communication scales in bytes like $|G|$ up to datatype size). The table records *incremental* optimizer communication beyond the baseline training loop.

method	extra communication per update	per-device orthog flops
all-gather then local orthog	one all-gather moving $\Theta(G)$ entries	$\Theta(P^2Q)$
distributed Newton–Schulz	$\Theta(\# \text{iters})$ collectives	$\Theta(P^2Q/S)$
reshard \rightarrow local orthog \rightarrow reshard	two all-to-alls	$\Theta(P^2Q/S)$
shardwise SpecGD	none	$\Theta(P^2Q/S^2)$

We now return to the quadratic-model viewpoint from Section 1.2 and record the blockwise majorization calculation underlying the shardwise polar step. In this calculation, the partition \mathcal{P} should be read as the coordinate partition induced by device shards (or any other block structure).

Quadratic model and a blockwise operator geometry. Fix $A \in \mathbf{R}^{k \times n}$ and $Y \in \mathbf{R}^{m \times n}$ and consider

$$\mathcal{L}(W) := \frac{1}{2n} \|WA - Y\|_F^2, \quad G := \nabla \mathcal{L}(W) = \frac{1}{n}(WA - Y)A^\top. \quad (\text{E.1})$$

Let \mathcal{P} be a partition of the coordinate set $[m] \times [k]$. For each $p \in \mathcal{P}$ let $\Pi_p : \mathbf{R}^{m \times k} \rightarrow \mathbf{R}^{m \times k}$ be the associated coordinate projection (so $\Pi_p \Pi_q = 0$ for $p \neq q$ and $\sum_{p \in \mathcal{P}} \Pi_p = \text{Id}$), and set

$$W_p := \Pi_p W, \quad U_p := \Pi_p U, \quad G_p := \Pi_p G.$$

Write the row/column footprints of block p as

$$R_p := \{i \in [m] : \exists j \in [k] \text{ with } (i, j) \in p\}, \quad C_p := \{j \in [k] : \exists i \in [m] \text{ with } (i, j) \in p\},$$

and define the overlap multiplicities

$$\nu_{\mathcal{P}} := \max_{i \in [m]} |\{p \in \mathcal{P} : i \in R_p\}|, \quad \mu_{\mathcal{P}} := \max_{j \in [k]} |\{p \in \mathcal{P} : j \in C_p\}|, \quad \kappa_{\mathcal{P}} := \min\{\mu_{\mathcal{P}}, \nu_{\mathcal{P}}\}.$$

Finally, define the blockwise seminorm

$$\|U\|_{\mathcal{P}}^2 := \sum_{p \in \mathcal{P}} \|U_p\|_{\text{op}}^2.$$

Lemma E.1 (Partitioned spectral majorization). *For all $U \in \mathbf{R}^{m \times k}$,*

$$\mathcal{L}(W + U) \leq \mathcal{L}(W) + \sum_{p \in \mathcal{P}} \langle G_p, U_p \rangle + \frac{L_{\mathcal{P}}}{2} \|U\|_{\mathcal{P}}^2, \quad L_{\mathcal{P}} := \frac{\kappa_{\mathcal{P}} \|A\|_F^2}{n}. \quad (\text{E.2})$$

In particular, $\kappa_{\mathcal{P}} = 1$ for row partitions ($\nu_{\mathcal{P}} = 1$) and for column partitions ($\mu_{\mathcal{P}} = 1$).

Proof. The identity

$$\mathcal{L}(W + U) = \mathcal{L}(W) + \langle G, U \rangle + \frac{1}{2n} \|UA\|_F^2$$

is exact and $\langle G, U \rangle = \sum_{p \in \mathcal{P}} \langle G_p, U_p \rangle$. It remains to show $\|UA\|_F^2 \leq \kappa_{\mathcal{P}} \|A\|_F^2 \sum_{p \in \mathcal{P}} \|U_p\|_{\text{op}}^2$.

Row-overlap bound. Write $UA = \sum_{p \in \mathcal{P}} U_p A$ and set $X_p := U_p A$. Each X_p is supported only on rows in R_p , hence

$$\begin{aligned} \|UA\|_F^2 &= \left\| \sum_{p \in \mathcal{P}} X_p \right\|_F^2 = \sum_{i=1}^m \left\| \sum_{p: i \in R_p} (X_p)_{i:} \right\|_2^2 \leq \sum_{i=1}^m \nu_{\mathcal{P}} \sum_{p: i \in R_p} \|(X_p)_{i:}\|_2^2 \\ &= \nu_{\mathcal{P}} \sum_{p \in \mathcal{P}} \|X_p\|_F^2 \leq \nu_{\mathcal{P}} \sum_{p \in \mathcal{P}} \|U_p\|_{\text{op}}^2 \|A\|_F^2. \end{aligned}$$

Column-overlap bound. For each p , the block U_p uses only columns in C_p , hence $U_p A = U_p A_{C_p:}$. Therefore

$$\begin{aligned} \|UA\|_F &= \left\| \sum_{p \in \mathcal{P}} U_p A_{C_p:} \right\|_F \leq \sum_{p \in \mathcal{P}} \|U_p A_{C_p:}\|_F \leq \sum_{p \in \mathcal{P}} \|U_p\|_{\text{op}} \|A_{C_p:}\|_F \\ &\leq \left(\sum_{p \in \mathcal{P}} \|U_p\|_{\text{op}}^2 \right)^{1/2} \left(\sum_{p \in \mathcal{P}} \|A_{C_p:}\|_F^2 \right)^{1/2}. \end{aligned}$$

Moreover,

$$\sum_{p \in \mathcal{P}} \|A_{C_p:}\|_F^2 = \sum_{p \in \mathcal{P}} \sum_{j \in C_p} \|A_{j:}\|_2^2 \leq \sum_{j=1}^k \mu_{\mathcal{P}} \|A_{j:}\|_2^2 = \mu_{\mathcal{P}} \|A\|_F^2,$$

so $\|UA\|_F^2 \leq \mu_{\mathcal{P}} \|A\|_F^2 \sum_{p \in \mathcal{P}} \|U_p\|_{\text{op}}^2$. Taking the minimum of the row- and column-overlap bounds yields the claim. \square

Corollary E.2 (Blockwise polar step and one-step decrease). *Define $W^+ := W + U^*$ by*

$$U_p^* := -\frac{1}{L_{\mathcal{P}}} \|G_p\|_* \text{polar}(G_p), \quad p \in \mathcal{P},$$

where $\text{polar}(M)$ is the polar factor of M . Then U^* minimizes the right-hand side of (E.2) over U , and hence

$$\mathcal{L}(W) - \mathcal{L}(W^+) \geq \frac{1}{2L_{\mathcal{P}}} \sum_{p \in \mathcal{P}} \|G_p\|_*^2 = \frac{n}{2\kappa_{\mathcal{P}} \|A\|_F^2} \sum_{p \in \mathcal{P}} \|G_p\|_*^2. \quad (\text{E.3})$$

Proof. The bound (E.2) is a quadratic upper model in the variables $\{U_p\}_{p \in \mathcal{P}}$, and it decouples across p . For fixed p , minimizing $\langle G_p, U_p \rangle + \frac{L_{\mathcal{P}}}{2} \|U_p\|_{\text{op}}^2$ over U_p yields the steepest-descent direction $-\text{polar}(G_p)$ with optimal step length $\|G_p\|_*/L_{\mathcal{P}}$. Summing the optimal values over p gives (E.3). \square

Comparison to Euclidean GD. Let $L_F := \|A\|_{\text{op}}^2/n$ be the Frobenius smoothness constant of $\mathcal{L}(\cdot)$ in (E.1). The GD step $W_{\text{GD}} := W - \frac{1}{L_F}G$ satisfies

$$\mathcal{L}(W) - \mathcal{L}(W_{\text{GD}}) \geq \frac{1}{2L_F} \|G\|_F^2 = \frac{n}{2\|A\|_{\text{op}}^2} \|G\|_F^2. \quad (\text{E.4})$$

Combining (E.3) and (E.4), the blockwise polar step achieves at least as much one-step decrease as GD whenever

$$\text{nr}_{\mathcal{P}}(G) \geq \text{st}_{\mathcal{P}}(A), \quad \text{nr}_{\mathcal{P}}(G) := \frac{\sum_{p \in \mathcal{P}} \|G_p\|_*^2}{\|G\|_F^2}, \quad \text{st}_{\mathcal{P}}(A) := \frac{L_{\mathcal{P}}}{L_F} = \kappa_{\mathcal{P}} \frac{\|A\|_F^2}{\|A\|_{\text{op}}^2} = \kappa_{\mathcal{P}} \text{st}(A).$$

For row and column partitions, $\kappa_{\mathcal{P}} = 1$ and the threshold is $\text{st}(A)$, matching the criterion in the main text. In the notation of Section 1.2, the deciding metric is the comparison between a (blockwise) nuclear-rank proxy for the gradient and a (partition-weighted) stable rank of the incoming features: when $\text{nr}_{\mathcal{P}}(G)$ exceeds $\text{st}_{\mathcal{P}}(A)$, the blockwise spectral geometry promises at least as much one-step decrease as the Euclidean geometry.

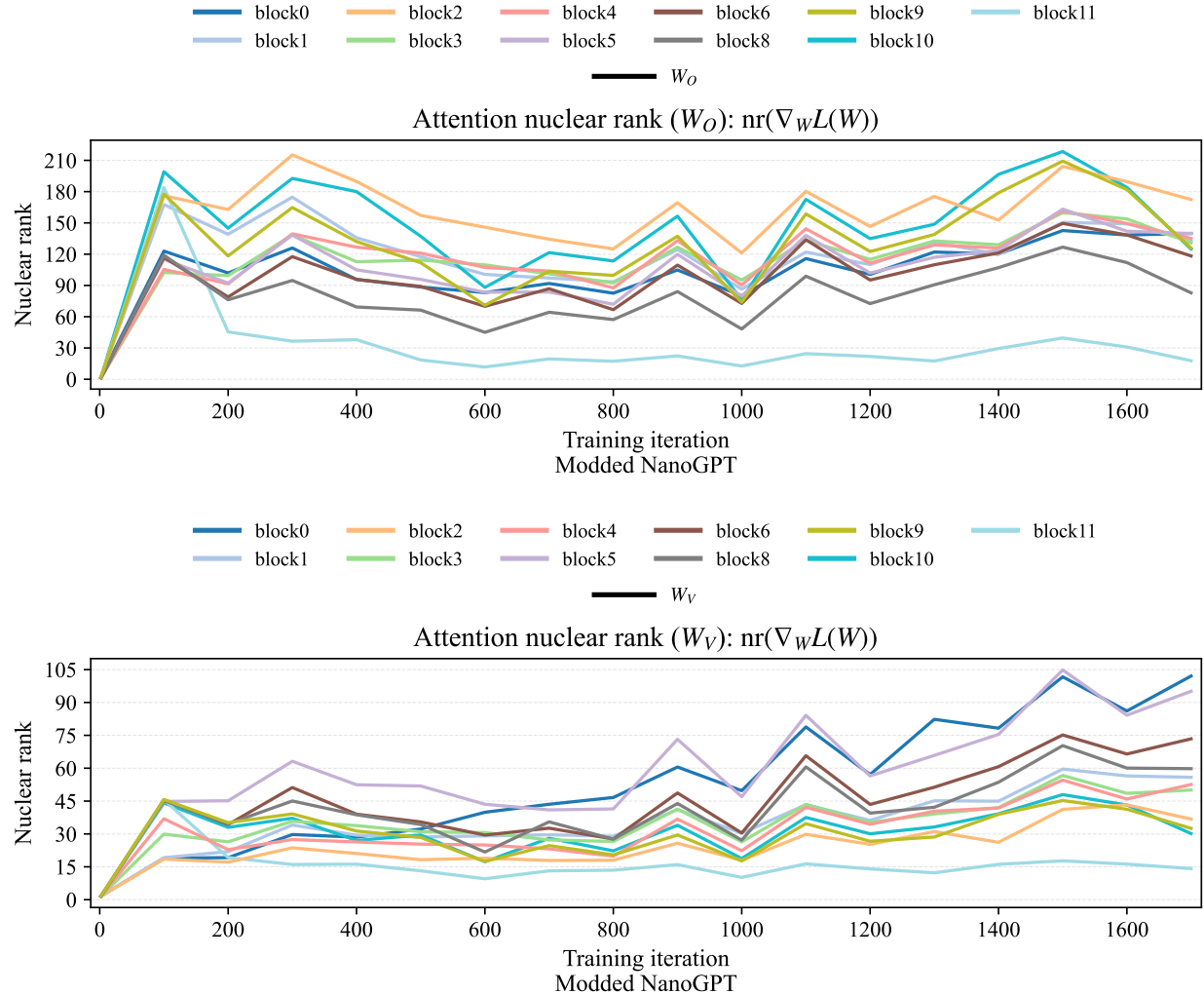


Figure 27: Gradient nuclear ranks for the attention parameters W_O (top) and W_V (bottom) in the SwiGLU run. This is the SwiGLU analogue of Figure 9. As in the squared-ReLU run, W_O typically has larger nuclear rank than W_V , while both remain well above the single-digit stable ranks of the corresponding RMS inputs (Figure 22).

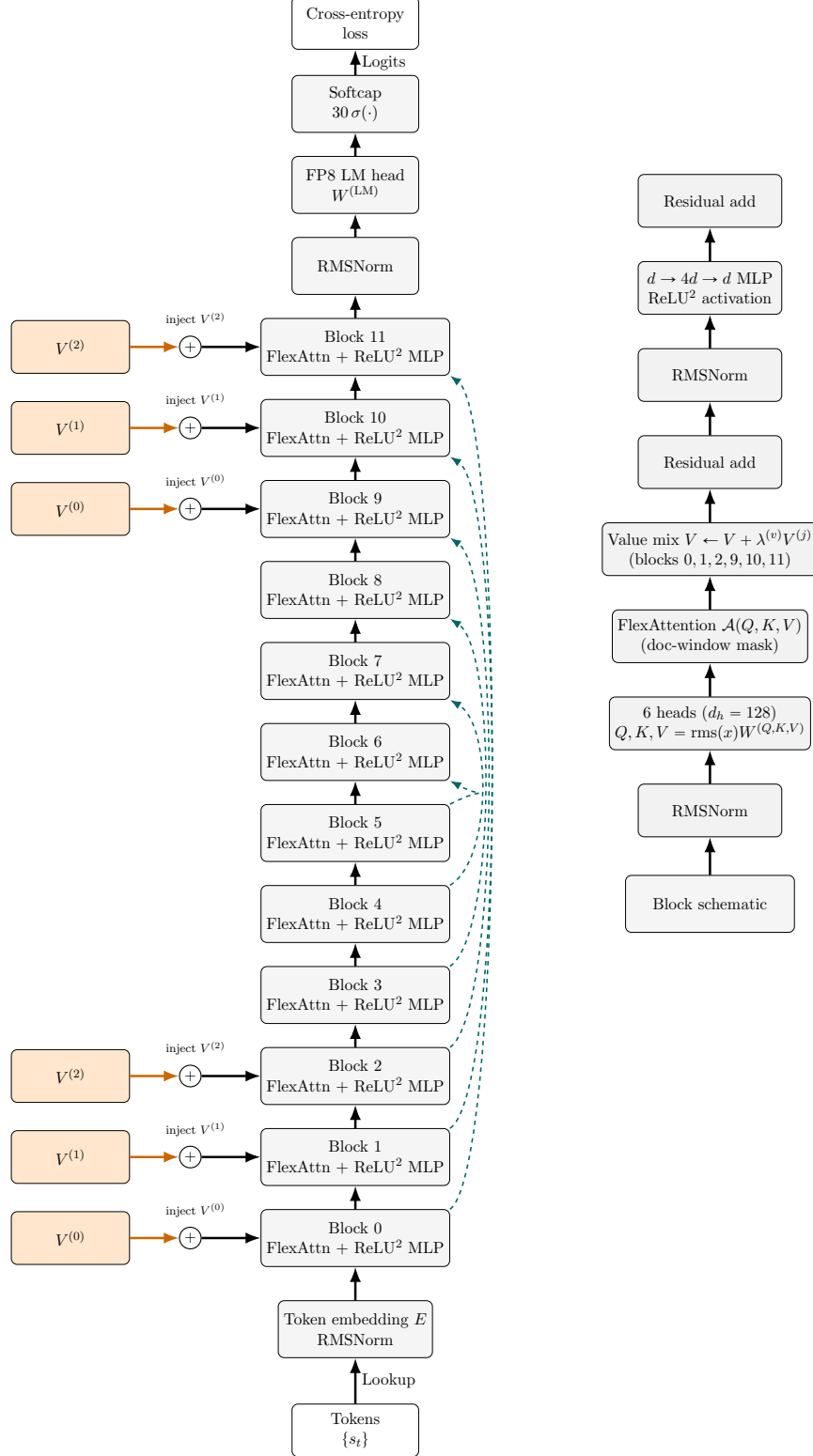


Figure 28: The `train_gpt.py` architecture of snapshot [30]. Value embeddings $V^{(0)}, V^{(1)}, V^{(2)}$ enter through explicit addition nodes in blocks 0, 1, 2 and 9, 10, 11, while the block schematic (right) shows the RMS normalisations, six-head FlexAttention, and two-layer ReLU-squared MLP shared across the stack. Teal skip arcs connect block k to block $11 - k$, indicating the pop step $x^{(i+1)} = \tilde{x}^{(i+1)} + \kappa_i s^{(i)}$.